

# The Application of Solid Phase Extraction in Organic Synthesis Using Fluorous Derivatised Metal Catalysts

**Thesis submitted for the degree of  
Doctor of Philosophy  
At the University of Leicester**

by

**Ben Croxtall MChem (Hons.)  
Department of Chemistry  
Faculty of Science  
University of Leicester**

**June 2003**



UMI Number: U493827

All rights reserved

INFORMATION TO ALL USERS

The quality of this reproduction is dependent upon the quality of the copy submitted.

In the unlikely event that the author did not send a complete manuscript and there are missing pages, these will be noted. Also, if material had to be removed, a note will indicate the deletion.



UMI U493827

Published by ProQuest LLC 2013. Copyright in the Dissertation held by the Author.  
Microform Edition © ProQuest LLC.

All rights reserved. This work is protected against  
unauthorized copying under Title 17, United States Code.



ProQuest LLC  
789 East Eisenhower Parkway  
P.O. Box 1346  
Ann Arbor, MI 48106-1346

## Statement

The experimental work in this thesis has been carried out by the author in the Department of Chemistry at the University of Leicester between October 1999 and October 2002. The work has not been submitted, and is not presently being submitted, for any other degree at this or any other university.

Signed:



Date:

11/8/03

Department of Chemistry

University of Leicester

University Road

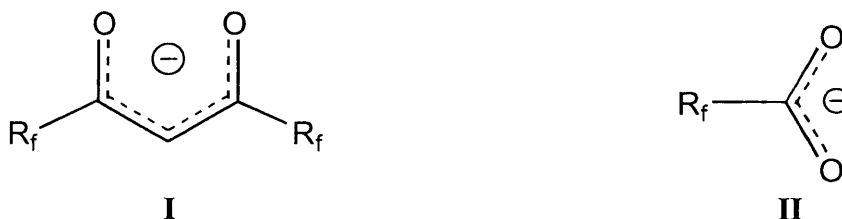
Leicester

LE1 7RH

England

## Abstract

This thesis describes the synthesis, characterisation and coordination chemistry of a variety of fluorinated  $\beta$ -diketonate ligands (I) and carboxylate ligands (II), the catalytic activity of the resultant metal complexes for oxidation and C-C bond forming reactions, and an evaluation of fluorous methodologies for catalyst / product separation.



Chapter 1 introduces the concept and application of fluorous methodologies, including fluorous biphasic catalysis and fluorous reverse phase silica gel (FRPSG), as alternative approaches to product / catalyst separation in homogeneous catalysis. A review of the current state of the literature in fluorous chemistry is included, followed by an outline of the aims and objectives of the work in this project.

Chapter 2 describes the synthesis and characterisation, in some cases by X-ray diffraction, of the fluorinated  $\beta$ -diketonate ligands and an evaluation of the influence of the perfluoroalkyl groups on the coordination of these ligands to a variety of transition metals including copper, nickel, palladium and zinc.

Chapter 3 outlines attempts to use fluorous nickel  $\beta$ -diketonate complexes for the oxidation of sulfides. The results indicate that a metal catalyst is not necessary for oxidation in this system although the veracity of catalyst separation using FRPSG was established. This chapter also describes the investigation of a fluorous molybdenum  $\beta$ -diketonate complex for the oxidation of alkenes, although the extreme moisture sensitivity of the complex negated any attempts at recovery and recycling.

The scope of Lewis acid catalysed coupling of  $\beta$ -diketones with cyanofornates and the ability to reuse and recycle the fluorinated  $\beta$ -diketonate catalysts is described in chapter 4.

Chapter 5 describes attempts to extend this efficient separation procedure to the C-C bond forming reactions of rhodium carboxylate dimers. Although catalysis was observed, catalyst / product separation using FRPSG was unsuccessful.

Chapter 6 summarises all the experimental details and spectroscopic data, whilst a CD-rom includes all of the crystallographic data.

## Contents

Title	i
Statement	ii
Abstract	iii
Contents	iv
Abbreviations	xii
Acknowledgements	xiv

## Chapter One: Introduction

1.1. Introduction	1
1.1.1. Separation and Purification	1
1.1.2. Homogeneous and Heterogeneous Catalysis	2
1.2. Aqueous Heterogenisation of Homogeneous Catalysis	5
1.2.1. Aqueous Biphasic Catalysis	6
1.2.2. Supported Aqueous Phase Catalysis	10
1.3. Ionic Liquids	11
1.4. Fluorous Biphasic Catalysis	15
1.4.1. The Introduction of Fluorine	15
1.4.2. Fluorous Biphasic Catalysis	17
1.4.3. Phosphorus and Nitrogen Donor Ligands	17
1.4.4. Oxygen Donor Ligands	25
1.5. Alternative fluorous phase systems	31
1.5.1. Supercritical Fluids	32
1.5.2. Fluorous Solid Phase Separation (and 'Light Fluorous Synthesis')	33
1.6. Miscellaneous Fluorous Chemistry	37
1.6.1. Fluorous Triphasic Reactions	38
1.6.2. Fluorous Nanoparticles	39
1.6.3. Fluorous Reagents	40
1.7. Objectives	41
1.8. References for Chapter One	43

## Chapter Two: Fluorinated Beta-Diketones – Synthesis and Coordination Chemistry

2.1. Introduction	48
2.2. Ligand Synthesis	50
2.2.1. Synthesis of $C_6F_{13}C(O)CHC(O)C_6F_{13}$ (IV)	50
2.2.2. Synthesis of $[CF_3C(O)CHC(O)C_6F_{13}]$ (V) and $[C_7F_{15}C(O)CHC(O)C_7F_{15}]$ (I)	54
2.2.3. Characterisation of Copper $\beta$ -diketonate intermediates $[Cu(R_fC(O)CHC(O)R_f)_2(OH_2)_2]$ (VIa-c)	55
2.3. Coordination Chemistry	58
2.3.1. Palladium $\beta$ -diketonates	58
2.3.2. Nickel $\beta$ -diketonates	61
2.3.3. Zinc $\beta$ -diketonates	63
2.3.4. Vanadyl and Molybdenum $\beta$ -diketonates	64
2.3.5. Coordination to other systems	68
2.4. Separation Science	71
2.5. References for Chapter Two	73

## Chapter Three: Oxidation Reactions Catalysed by Perfluoroalkylated Metal Catalysts

3.1. Introduction	75
3.2. Nickel Catalysed Sulfide Oxidations	76
3.2.1. Introduction	76
3.2.2. Results and Discussion	80
3.3. Molybdenum Catalysed Alcohol Oxidations	87
3.3.1. Introduction	87
3.3.2. Results and Discussion	89
3.4. Conclusions	91
3.5. References for Chapter Three	93

## Chapter Four: Carbon – Carbon Bond Forming Reactions Catalysed by Perfluoroalkylated Metal Complexes

4.1. Introduction	94
4.1.1. Carbon-carbon bond forming reactions between <i>β</i> -dicarbonyls and nitriles	94
4.2. Enaminodione reactions	100
4.2.1. Catalysis using fluorous derivatised <i>β</i> -diketonates – Preliminary investigations	100
4.2.2. Catalysis using perfluoroalkylated zinc <i>β</i> -diketonates – Recovery and Recycling	104
4.2.3. Catalysis using perfluoroalkylated nickel <i>β</i> -diketonates	105
4.3. Catalysis using fluorous derivatised <i>β</i> -diketonates – Alternative Substrates	113
4.3.1. Catalysis using fluorous derivatised <i>β</i> -diketonates – Alternative <i>β</i> -dicarbonyls	114
4.3.2. Catalysis using fluorous derivatised <i>β</i> -diketonates – Alternative Nitriles	122
4.3.3. Catalysis using fluorous derivatised <i>β</i> -diketonates – Reaction Profiling	127
4.3.4. Conclusion	132
4.4. References for Chapter Four	134

## Chapter Five: Fluorinated Carboxylates

5.1. Introduction	135
5.1.1. Carboxylate ligands	135
5.1.2. Fluorinated Carboxylates	136
5.2. Catalysis Using Carboxylates	138
5.2.1. Dirhodium Tetraacetate	138
5.2.2. Cobalt Acetate	143

5.2.3. Manganese Acetate	144
5.3. Ligand Synthesis and Coordination Chemistry	145
5.3.1. Fluorinated Carboxylic Acids	145
5.3.2. Fluorous Carboxylate Rhodium Dimers	146
5.3.3. Fluorous Cobalt Carboxylates	149
5.3.4. Fluorous Manganese Carboxylates	152
5.3.5. Fluorous Zinc Carboxylates	154
5.4. Catalysis Using Fluorinated Rhodium Carboxylates	157
5.4.1. Separation Science	157
5.4.2. Catalytic Reactions	160
5.5. Catalysis Using Fluorinated Cobalt Carboxylates	162
5.5.1. Separation Science	162
5.5.2. Catalytic Reactions	163
5.6. Conclusions	164
5.7. References for Chapter Five	165

## **Chapter Six: Experimental Procedures**

6.1. General Experimental Procedures	167
6.1.1. NMR spectroscopy	167
6.1.2. Infra-red Spectroscopy	168
6.1.3. Mass Spectrometry	168
6.1.4. Elemental analysis	168
6.1.5. X-Ray Crystallography	168
6.2. Anhydrous Solvents	169
6.3. Starting Materials and Reagents	170
6.4. Laboratory Apparatus	171
6.4.1. Schlenk Line	171
6.4.2. Glassware	171
6.4.3. Faircrest Dry-box and Nitrogen Flush-box	171
6.5. Experimental Procedures	172
6.5.1. 3,3,4,4,5,5,6,6,7,7,8,8,8-Tridecafluoro-octan-2-one	172

<b>6.5.2.</b> 3,3,4,4,5,5,6,6,7,7,8,8,9,9,9-Pentadecafluoro-nonan-2-one	173
<b>6.5.3.</b> 1,1,1,5,5,6,6,7,7,8,8,9,9,10,10,10-Hexadecafluoro-decane-2,4-dione ( <b>V</b> ).	173
<b>6.5.4.</b> 1,1,1,2,2,3,3,4,4,5,5,6,6,10,10,11,11,12,12,13,13,-14,14,15,15,15-Hexacosafuoro-pentadecane-7,9-dione ( <b>IV</b> )	174
<b>6.5.5.</b> 1,1,1,2,2,3,3,4,4,5,5,6,6,7,7,11,11,12,12,13,13,14,14,-15,15,16,16,17,17,17-Triacontafluoro-heptadecane-8,10-dione ( <b>I</b> )	176
<b>6.5.6.</b> Copper <i>bis</i> (1,1,1,5,5,6,6,7,7,8,8,9,9,10,10,10-hexadecafluorodecane-2,4-dionate) ( <b>VIa</b> )	177
<b>6.5.7.</b> Copper <i>bis</i> (1,1,1,2,2,3,3,4,4,5,5,6,6,10,10,11,11,12,12,-13,13,14,14,15,15,15-hexacosafuoropentadecane-7,9-dionate) ( <b>VIb</b> )	177
<b>6.5.8.</b> Copper <i>bis</i> (1,1,1,2,2,3,3,4,4,5,5,6,6,7,7,11,11,12,12,-13,13,14,14,15,15,16,16,17,17,17-triacontafluoroheptadecane-8,10-dionate) ( <b>VIc</b> )	178
<b>6.5.9.</b> Palladium <i>bis</i> (1,1,1,5,5,6,6,7,7,8,8,9,9,10,10,10-hexadecafluoro-decane-2,4-dionate) ( <b>VIIa</b> )	178
<b>6.5.10.</b> Palladium <i>bis</i> (1,1,1,2,2,3,3,4,4,5,5,6,6,10,10,11,11,-12,12,13,13,14,14,15,15,15-hexacosafuoro-pentadecane-7,9-dionate) ( <b>VIIb</b> )	179
<b>6.5.11.</b> Palladium <i>bis</i> (1,1,1,2,2,3,3,4,4,5,5,6,6,7,7,11,11,12,12,-13,13,14,14,15,15,16,16,17,17,17-triacontafluoro-heptadecane-8,10-dionate) ( <b>VIIc</b> )	179
<b>6.5.12.</b> Nickel <i>bis</i> (1,1,1,5,5,6,6,7,7,8,8,9,9,10,10,10-hexadecafluoro-decane-2,4-dionate) ( <b>VIIIa</b> )	180
<b>6.5.13.</b> Nickel <i>bis</i> (1,1,1,2,2,3,3,4,4,5,5,6,6,10,10,11,11,12,12,-13,13,14,14,15,15,15-hexacosafuoro-pentadecane-7,9-dionate) ( <b>VIIIb</b> )	180
<b>6.5.14.</b> Nickel <i>bis</i> (1,1,1,2,2,3,3,4,4,5,5,6,6,7,7,11,11,12,12,-13,13,14,14,15,15,16,16,17,17,17-triacontafluoro-heptadecane-8,10-dionate) ( <b>VIIIc</b> )	181
<b>6.5.15.</b> Zinc <i>bis</i> (1,1,1,5,5,6,6,7,7,8,8,9,9,10,10,10-hexadecafluoro-decane-2,4-dionate) ( <b>IXa</b> )	181
<b>6.5.16.</b> Zinc <i>bis</i> (1,1,1,2,2,3,3,4,4,5,5,6,6,10,10,11,11,12,12,-13,13,14,14,15,15,15-hexacosafuoro-pentadecane-7,9-dionate) ( <b>IXb</b> )	182

<b>6.5.17.</b> Zinc <i>bis</i> (1,1,1,2,2,3,3,4,4,5,5,6,6,7,7,11,11,12,12,- 13,13,14,14,15,15,16,16,17,17,17-triacontafuoro-heptadecane- 8,10-dionate) ( <b>IXc</b> )	182
<b>6.5.18.</b> Vanadyl <i>bis</i> (acetylacetonate) ( <b>Xa</b> )	183
<b>6.5.19.</b> Vanadyl <i>bis</i> (hexafluoroacetylacetonate) ( <b>Xb</b> )	183
<b>6.5.20.</b> Attempted synthesis of vanadyl <i>bis</i> (1,1,1,2,2,3,3,4,4,- 5,5,6,6,10,10,11,11,12,12,13,13,14,14,15,15,15-hexacosafuoro- pentadecane-7,9-dionate) ( <b>Xc</b> )	184
<b>6.5.21.</b> Dioxo <i>bis</i> (acetylacetonate) molybdenum (VI) ( <b>XIa</b> )	184
<b>6.5.22.</b> Attempted synthesis of Dioxo <i>bis</i> (hexafluoro- acetylacetonate) molybdenum (VI) ( <b>XIb</b> )	185
<b>6.5.23.</b> Dioxo <i>bis</i> (1,1,2,2,3,3,4,4,5,5,6,6,10,10,11,11,12,12,- 13,13,14,14,15,15,15-hexacosafuoro-pentadecane-7,9-dionate) molybdenum (VI) ( <b>XIc</b> )	185
<b>6.5.24.</b> Copper <i>bis</i> (triphenylphosphine)(1,1,1,2,2,3,3,4,4,5,5,6,6,- 10,10,11,11,12,12,13,13,14,14,15,15,15-hexacosafuoro- pentadecane-7,9-dionate) ( <b>XIIa</b> )	186
<b>6.5.25.</b> Copper <i>bis</i> (triphenylphosphine)(1,1,1,2,2,3,3,4,4,5,5,6,6,- 7,7,11,11,12,12,13,13,14,14,15,15,16,16,17,17,17-triacontafuoro- heptadecane-8,10-dionate) ( <b>XIIb</b> )	186
<b>6.5.26.</b> Attempted synthesis of rhodium dichloride pentamethyl- cyclopentadienyl(1,1,1,2,2,3,3,4,4,5,5,6,6,10,10,11,11,12,12,13,13,- 14,14,15,15,15-hexacosafuoro-pentadecane-7,9-dionate) ( <b>XIIIa</b> )	187
<b>6.5.27.</b> General procedure for nickel catalysed sulfide (thioanisole) oxidations	187
<b>6.5.28.</b> General procedure for molybdenum catalysed alcohol oxidations	188
<b>6.5.29.</b> Enaminodione procedures: 2,4-Pentanedione and Ethyl Cyanofornate	188
<b>6.5.30.</b> Enaminodione procedures: Methylacetoacetate and Ethyl Cyanofornate	189
<b>6.5.31.</b> Enaminodione procedures: Dimethylmalonate and Ethyl Cyanofornate	189

<b>6.5.32.</b> Enaminodione procedures: Benzoylacetone and Ethyl Cyanofornate	190
<b>6.5.33.</b> Enaminodione procedures: Dibenzoylmethane and Ethyl Cyanofornate	190
<b>6.5.34.</b> Enaminodione procedures: Tetramethyl-3,5-heptanedione and Ethyl Cyanofornate	191
<b>6.5.35.</b> Enaminodione procedures: 2,4-Pentanedione and Benzoyl cyanide	191
<b>6.5.36.</b> Enaminodione procedures: 2,4-Pentanedione and Malonitrile	191
<b>6.5.37.</b> Enaminodione procedures: 2,4-Pentanedione and Trichloroacetonitrile	192
<b>6.5.38.</b> 2 <i>H</i> ,2 <i>H</i> ,3 <i>H</i> ,3 <i>H</i> -perfluorononanoic acid, C <sub>6</sub> F <sub>13</sub> CH <sub>2</sub> CH <sub>2</sub> CO <sub>2</sub> H	192
<b>6.5.39.</b> Preparation of tetrakis(μ-perfluoroheptanato-O:O') dirhodium [Rh <sub>2</sub> (O <sub>2</sub> CC <sub>6</sub> F <sub>13</sub> ) <sub>4</sub> ], ( <b>XIVa</b> )	193
<b>6.5.40.</b> Preparation of tetrakis(μ-perfluorononanato-O:O') dirhodium [Rh <sub>2</sub> (O <sub>2</sub> CC <sub>8</sub> F <sub>17</sub> ) <sub>4</sub> ], ( <b>XIVb</b> )	194
<b>6.5.41.</b> Preparation of tetrakis[μ-3-(perfluorohexyl) propionato-O:O'] dirhodium [Rh <sub>2</sub> (O <sub>2</sub> CCH <sub>2</sub> CH <sub>2</sub> C <sub>6</sub> F <sub>13</sub> ) <sub>4</sub> ], ( <b>XIVc</b> )	194
<b>6.5.42.</b> Preparation of cobalt (II) <i>bis</i> (perfluoroheptanate) [Co(O <sub>2</sub> CC <sub>6</sub> F <sub>13</sub> ) <sub>2</sub> ]( <b>XVa</b> )	195
<b>6.5.43.</b> Preparation of cobalt (II) <i>bis</i> (perfluorononanate) [Co(O <sub>2</sub> CC <sub>8</sub> F <sub>17</sub> ) <sub>2</sub> ] ( <b>XVb</b> )	195
<b>6.5.44.</b> Preparation of cobalt (II) <i>bis</i> (2 <i>H</i> ,2 <i>H</i> ,3 <i>H</i> ,3 <i>H</i> - perfluorononanate) [Co(O <sub>2</sub> CCH <sub>2</sub> CH <sub>2</sub> C <sub>6</sub> F <sub>13</sub> ) <sub>2</sub> ] ( <b>XVc</b> )	196
<b>6.5.45.</b> Preparation of manganese (II) <i>bis</i> (perfluoroheptanate) [Mn(O <sub>2</sub> CC <sub>6</sub> F <sub>13</sub> ) <sub>2</sub> ]( <b>XVIa</b> )	196
<b>6.5.46.</b> Preparation of manganese (II) <i>bis</i> (perfluorononanate) [Mn(O <sub>2</sub> CC <sub>8</sub> F <sub>17</sub> ) <sub>2</sub> ]( <b>XVIb</b> )	197
<b>6.5.47.</b> Preparation of manganese (II) 2 <i>H</i> ,2 <i>H</i> ,3 <i>H</i> ,3 <i>H</i> - perfluorononanate [Mn(O <sub>2</sub> CCH <sub>2</sub> CH <sub>2</sub> C <sub>6</sub> F <sub>13</sub> ) <sub>2</sub> ] ( <b>XIVc</b> )	197
<b>6.5.48.</b> Attempted synthesis of manganese (III) <i>tris</i> (perfluorononanate) [Mn(O <sub>2</sub> CC <sub>8</sub> F <sub>17</sub> ) <sub>3</sub> ] - ligand exchange method.	198

6.5.49. Attempted synthesis of manganese (III) <i>tris</i> (perfluoroheptanate) $[\text{Mn}(\text{O}_2\text{CC}_6\text{F}_{13})_3]$ - oxidation method	198
6.5.50. Preparation of zinc (II) <i>bis</i> (perfluoroheptanate) $[\text{Zn}(\text{O}_2\text{CC}_6\text{F}_{13})_2]$ (XVIIa)	198
6.5.51. Preparation of zinc (II) <i>bis</i> (perfluorononate) $[\text{Zn}(\text{O}_2\text{CC}_8\text{F}_{17})_2]$ (XVIIb)	199
6.5.52. Synthesis of 1-diazo-3-phenyl-5-hexen-2-one	199
6.5.53. Transition metal catalysed decomposition of 1-diazo- 3-phenyl-5-hexen-2-one using $[\text{Rh}_2(\text{O}_2\text{CC}_3\text{F}_7)_4]$	200
6.5.54. Transition metal catalysed decomposition of 1-diazo- 3-phenyl-5-hexen-2-one using $[\text{Rh}_2(\text{O}_2\text{CCH}_2\text{CH}_2\text{C}_6\text{F}_{13})_4]$	200
6.6. References for Chapter Six	201

## Appendices

Appendix One: Crystal Data and Structure Refinements	204
Appendix Two: ICP Data	211
Appendix Three: Courses, Lectures and Conferences Attended	212

## Abbreviations

$\delta$	Chemical Shift
$\nu$	Stretching Frequency
acac	Acetylacetonato
Ar	Aryl Fragment
BTF	Benzotrifluoride
CDCl <sub>3</sub>	Deuterated chloroform
C <sub>6</sub> D <sub>6</sub>	Deuterated benzene
COD	1,5-Cyclooctadiene
Cp*	Pentamethylcyclopentadienyl
d	Doublet
dd	Doublet of doublets
ddd	Doublet of doublet of doublets
DMSO	Dimethyl sulfoxide
EI	Electron Impact
ES	Electrospray
Et	Ethyl fragment
FAB	Fast atom bombardment
FRPSG	Fluorous reverse phase silica gel
hfacac	Hexafluoroacetylacetonato
HSAB	Hard/Soft Acid/Base
Hz	Hertz
IR	Infrared
<i>J</i>	Coupling constant
m	Multiplet
M	Parent Ion
Me	Methyl fragment
MHz	Megahertz
mp	Melting point
NMR	Nuclear magnetic resonance
Ph	Phenyl

PP3	Perfluoro-1,3-dimethylcyclohexane
ppm	Parts per million
q	Quartet
R	Undefined molecular fragment
R <sub>f</sub>	Undefined fluorinated molecular fragment
RT	Room temperature
s	Singlet
t	Triplet
TMS	Tetramethylsilane
um	Unresolved multiplet

## Acknowledgements

Firstly I would like to thank my parents, Dawn and Jon for their unreserved love and support throughout my life. I could not have accomplished any of this without you both – thank you so much. I would also like to thank my Grandparents, Do and Ray for all their love and guidance.

At the University of Leicester, my studies at both undergraduate and postgraduate levels have been helped tremendously by so many people and I thank them all. However, I would especially like to thank my supervisors Prof. Eric Hope and Dr. Alison Stuart for all their ideas and discussions throughout my Ph.D. In this regard, I also owe a debt of gratitude to Dr. Dai Davies for all of his suggestions and conversations during the past three years. I have also had the pleasure of working alongside three excellent Post-Doctoral research fellows; Dr. Dave Adams, Dr. David Birdsall and Dr. Howard Clark who have all contributed enormously to my understanding of chemistry. I would also like to thank Dr. David Gudmunsen, James Sherrington, Andy West and Dr. Dan Wood and all other members of the fluorine group, both past and present, for making my stay in the fluorine lab so enjoyable.

On the technical side, I would like to thank Dr. Graham Eaton, Dr. John Fawcett, Dr. Gerry Griffiths, Anne Crane, Mick Lee and Kuldip Singh.

At GlaxoSmithKline laboratories I would like to thank my industrial supervisor, Dr. Dean Edney and also Barney Squires for all their input into this thesis and also for making my stay at the Dartford plant so pleasurable.

I am also enormously grateful to my friends Dr. Heidi French, David Hook, Dr. Neesha Patel and Joseph Wright – thanks for putting up with me!

Finally, these acknowledgements would not be complete without mentioning my dog Will, who kept me sane whilst writing this thesis with his constant requests for a game of ball or a walk in the park, when really I should have been typing!

My sincerest thanks to you all and best wishes for the future.

## 1.1. Introduction

### 1.1.1. Separation and Purification

The common goal of all chemical processes is to obtain the desired compound in the highest yield and purity possible. The requirement to maximise efficiency is paramount throughout the chemical community, whether the procedure is catalytic or synthetic. Whilst historically, purification focussed exclusively upon isolating the final product, the impetus of modern chemistry is striving toward a more environmentally-friendly approach to both laboratory and industrial-scale synthesis with the ultimate goal being to minimise solvent and reagent waste for disposal by the development of recovery and recycling technologies.

The necessity for pure chemicals, especially in the pharmaceutical industry, has enhanced separation science over the past fifty years. Following the tragic consequences of the use of a racemic mixture of Thalidomide, in which one of the enantiomers was teratogenic, new pharmaceuticals are subject to more stringent tests prior to general medical implementation. In many respects, technology has advanced accordingly with the demands of modern synthetic chemistry; there are many more spectroscopic and analytical techniques to elucidate structures and to assess purity, whilst the advent of automated organic synthesis is beginning to enable a vast array of compounds to be synthesised in a relatively short time.<sup>1</sup> However, the eventual means for isolating the product have not altered significantly during the same period and in many respects the ‘work-up’ procedures for many reactions have remained the same.<sup>2</sup> Unfortunately, many of the established isolation techniques, such as crystallisation, distillation and chromatography, result in significant product loss due to the inherent problem of compromising yield in order to achieve perfect separation, although there have been notable improvements in chromatographic techniques over the past twenty years.<sup>2</sup>

Although the complexity of many chemical processes will inevitably increase with the utilisation of more intricate species, such as macromolecular and enzymatic systems, separation science will aspire towards simpler systems which are cost effective and easily implemented on an industrial scale. Hopefully these advances will enable the use of more varied systems, expanding the range of

elements available for industrial applications. For example, heavy metal systems that were once considered *taboo* for fine chemical and pharmaceutical synthesis may be utilised if total recovery is established.

Perhaps the most important area of all the synthetic procedures where separation is a significant stage of the process, is that of metal-based catalytic reactions; particularly *homogeneous* and *heterogeneous* catalysis.<sup>3</sup> The development of these two contrasting methodologies has provided the focus for both academic and industrial chemists alike. It is for this reason that the key principles of these two regimes will form the basis for this work and as a consequence it is necessary to introduce the two techniques.

### 1.1.2. Homogeneous and Heterogeneous Catalysis

Prior to 1938 the science of *catalysis* was synonymous with large-scale, industrial processes such as the Haber cycle (ammonia synthesis), Fischer-Tropsch synthesis (hydrocarbons), coal hydrogenation, fat hardening and mineral oil processing, *i.e.* reactions based upon heterogeneous catalysis.<sup>4</sup> All of these processes deal with the ‘bulk’ phase chemistry of necessity materials and as a consequence the catalysts involved have to be durable and / or cheap. These are two of the key characteristics of heterogeneous catalysis, although the most important feature is that a solid catalyst is used which is exposed to a gaseous or liquid substrate. As a consequence, the reaction occurs at the interface between the two phases (or throughout the solid if a porous material is used), which thus enables facile product isolation at the end of the reaction. Due to these properties, heterogeneous catalysis has found many industrial applications where high throughput catalysis of bulk materials is required. Unfortunately, however, there are many disadvantages associated with this type of catalysis. Harsh conditions of both temperature and pressure are required in order to obtain satisfactory levels of conversion. Often, this is due to the fact that the activity of the solid phase catalyst is variable over specific ‘regions’ and ‘domains’ distributed on the surface of the material. As a consequence the selectivity of the ‘catalyst’ also varies accordingly across the surface, which in turn, often negates the possibility of achieving a full mechanistic understanding of the reaction pathway.<sup>5</sup>

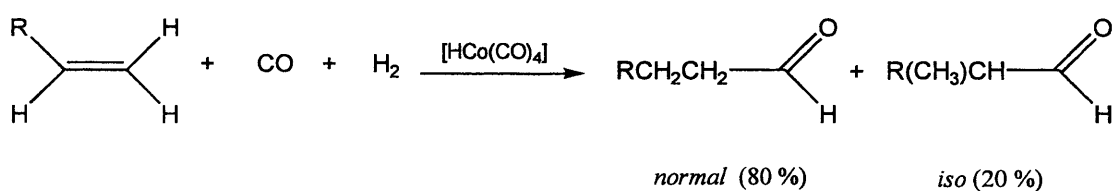
In direct contrast, homogeneous catalysis is normally better understood from a mechanistic viewpoint because a distinct compound or metal complex is used to perform the catalytic process in the same phase as the reactant/s. This has provided chemists with a means of ‘fine tuning’ the catalyst to a specific substrate or process and as a consequence, the mechanism can often be elucidated from experimental evidence.<sup>4</sup> For this reason homogeneous catalysis is often associated with the synthesis of ‘fine-grade’ compounds where selectivity is important, for example, the hydroformylation of alkenes in the fragrance industry. The fact that a discrete molecule is utilised to perform the catalysis results in high activity and often milder conditions than those used for heterogeneous catalysis. However, in many cases, the species employed are expensive due to the fact that precious metals, such as platinum and rhodium, generate the most efficient catalysts. Unfortunately, the lifetime of the catalysts can be quite low due to the difficulties associated with product / catalyst isolation when the two components are in the same phase.

The difficulties associated with catalyst / product separation have limited the industrial implementation of many homogeneous processes. Although higher levels of activity can often be obtained due to the increased levels of mass transport obtained with a monophasic system, the associated difficulties of liberating the final product often render the process unviable. Separation techniques, such as distillation or extraction with a second solvent system, are often not possible due to the sensitivity of the catalyst to heat and / or moisture, leading to progressive degradation of the system after several cycles. Hence, the recycling of homogeneous catalysts is both problematical and expensive, although in many cases essential to offset the initial expenditure of the precious metal centres.

The re-use of heterogeneous catalysts is comparatively straightforward. In many examples, the stationary phase is simply re-exposed to more substrate/s or in most cases, continually exposed to a gaseous feed, such as syngas (hydrogen and carbon monoxide) in the Fischer-Tropsch hydroformylation of olefins.<sup>6</sup> The only problem arises through ‘catalyst-poisoning’ due to the accumulation of surface particulates that block the catalytic sites, decreasing activity over time. However, taking into account the low cost of many industrially used heterogeneous catalysts, recycling is often not necessary. The obvious advantages of heterogeneous catalysis has led to the large difference in industrial implementation and for the mineral oil

processing industry, the relative ratio to homogeneous processes is approximately 85 : 15.<sup>7</sup>

Since many heterogeneous catalysts only give poor selectivity, this negates their use in applications where precise single product synthesis is required. Unfortunately, to a certain extent, it is impossible to modify an existing heterogeneous system due to the ill-defined nature of the active species. By comparison, homogeneous catalysts are quite easily adapted or ‘fine-tuned’ to favour either selectivity or activity and it is this feature that has led to the expansion of this form of catalysis in the past sixty-five years.<sup>4</sup> The advantage of utilising a well-defined molecule, especially a metal coordination compound, is that the ligands surrounding the cation can be substituted to impart different characteristics on the catalytic mechanism. In certain cases, the metal centre can be exchanged to allow alternative reaction pathways altogether. This is exemplified by the development of the hydroformylation of alkenes, where initially, a simple cobalt hydrido-carbonyl complex  $[\text{HCo}(\text{CO})_4]$  was utilised, yielding aldehydes with an *n:i* (*normal:iso*) ratio of 80:20 (**Scheme 1.1**).<sup>4</sup> By exchanging one of the carbonyl ligands with an alkyl phosphine, i.e.  $[\text{HCo}(\text{CO})_3(\text{PR}_3)]$ , the catalyst was modified to generate alcohol products, rather than aldehydes, and further still, by exchanging the metal centre and the ligands, a similar rhodium complex can be employed to generate aldehydes with *n:i* ratios of >95:<5.<sup>4</sup>



**Scheme 1.1**

Neither form of catalysis offers an ideal solution, and it is for this reason that a variety of methodologies have been proposed which attempt to combine the advantages of the two techniques. It is not surprising that the problem has mainly been approached through ‘heterogenising’ homogeneous catalysis. The key to achieving this goal is to incorporate a ‘biphasic’ liquid component into the

homogeneous system to facilitate product / catalyst separation. Ideally, this would occur between the reactant phase and a product phase, negating any additional separation procedures by simply decanting the insoluble product. Unfortunately, examples of insoluble product phases are quite rare, although this methodology was successfully employed by Shell in the “Higher Olefins Process” (SHOP), which was designed by Keim *et al.*<sup>4,8</sup> In the process, a nickel catalyst is used to catalyse the oligomerisation of propylene in a polar media of 1,4-butanediol at 80 – 120 °C and 70 – 140 bar. The catalyst is rendered soluble in the alcohol by substitution with a polar aryl phosphine [ $\text{Ph}_2\text{P}(\text{CH}_2\text{CO}_2\text{H})$ ] and, upon completion of the reaction, the products form a second distinct phase above the diol allowing facile separation. This regime has been employed successfully on an industrial scale and illustrates the obvious advantage of combining homogeneous and heterogeneous catalysis. As mentioned earlier, a separate product phase is quite rare, and even in this example, a secondary washing procedure is necessary to remove traces of the nickel catalyst which contaminate the olefin.

The heterogenisation of homogeneous catalysis has become a constantly expanding area of modern chemistry with a variety of contrasting routes employed to achieve, what is after all, a common goal. The majority of these techniques utilise distinct phase boundaries or interfaces at which reaction can occur, examples include “Aqueous Biphasic Catalysis”, “Supported Aqueous Phase Catalysis”, “Solid-Support (or tethered) Catalysis”, “Ionic Liquids” and “Fluorous Biphasic Catalysis”. As yet, none of the techniques offers a universal solution to the problem of product / catalyst separation. However, the merits and limitations of each of these different methodologies will now be discussed, with an emphasis towards how they attempt to isolate the products of the reaction from the catalyst.

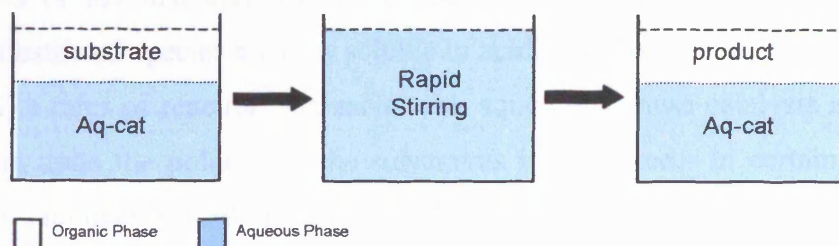
## 1.2. Aqueous Heterogenisation of Homogeneous Catalysis

The immiscibility of a variety of common organic solvents with water has provided chemists with a valuable means of purification and extraction throughout history. When combined with the fact that water is an environmentally friendly (and biologically benign) solvent, it is not surprising that chemists have sought to utilise aqueous media in biphasic catalyst systems. Obviously, the system will

impose the restriction that the organic substrate/s and product/s will be preferentially soluble in the organic phase, and as a consequence this area of research is dominated by water-soluble metal complexes, or rather, the synthesis of hydrophilic ligands which modify the polarity of the central metal cation.<sup>9</sup>

### 1.2.1. Aqueous Biphasic Catalysis

Aqueous biphasic catalysis offers many of the advantages of homogeneous catalysis combined with the ability to separate the catalyst from the product/s. In general, a homogeneous catalyst is substituted with hydrophilic ligands of suitable size and number in order to procure selective solubility in the aqueous phase. A top phase consisting of an immiscible organic solvent containing the substrate/s is then introduced and the biphasic stirred rapidly. This allows the catalyst to become exposed to the reagents, allowing the catalytic process to occur at the interface, or in the aqueous phase in certain cases. Upon completion of the reaction, simple phase separation allows for the facile removal of the organic layer by decantation. In this regard, the catalyst is both immobilised and heterogenised by the aqueous environment, yet able to perform a typically homogeneous catalytic process (**Scheme 1.2**).<sup>4,9</sup>



**Scheme 1.2**

Although many ligand classes are available for modification in order to achieve aqueous phase solubility, phosphines offer the greatest versatility in terms of their coordination chemistry and established catalytic reactivity.<sup>10</sup> The introduction of a variety of polar functional groups have been used to achieve preferential solubility in water; including sulfonate (SO<sub>3</sub>H), carboxylate (CO<sub>2</sub>H), amine (NH<sub>2</sub>) and hydroxyl groups (OH), or the salts of all of these moieties. Two

examples are shown below, triphenylphosphine trisulfonate (TPPTS) and 2-(diphenylphosphino)-N,N,N-trimethylethanaminium iodide (amphos) (Figure 1.1).<sup>9</sup>

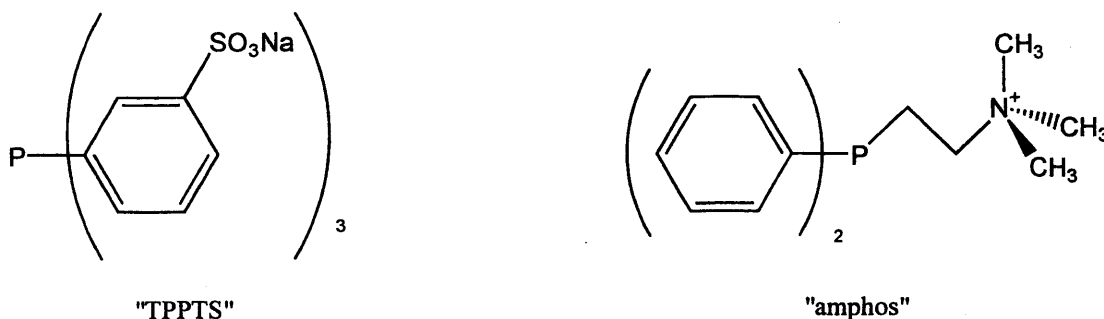


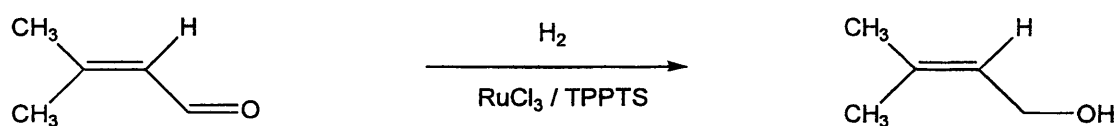
**Figure 1.1**

By varying the number of polar moieties and the conditions used, the degree of hydrophilic and hydrophobic characteristics can be adjusted specifically to the individual requirements of the chosen catalyst. This is illustrated by the sulfonatophenylphosphines, where the incorporation of one, two or three sulfonate groups increases the hydrophilicity of the phosphine and corresponding metal complexes. Analogously, the polarity and acidity of the aqueous phase can exert similar effects, whereas sulfonatophenylphosphines dissolve in aqueous media regardless of the pH, carboxy-derivatised ligands require basic conditions, and amino-substituted species are only soluble in acidic media.

The rates of reaction attainable with aqueous biphasic catalysis are strongly dependent upon the polarity of the substrate/s investigated. In certain cases, this limits the applicability of the technique, especially for higher molecular weight aliphatic hydrocarbons (approximately  $> C_8$ ) where the immiscibility of the substrate in aqueous media decreases mass transport to the catalyst, preventing reaction. However, for 'smaller' molecules, the rates of reaction have been shown to be comparable in terms of activation energy to an equivalent homogeneous process; this is exemplified by the hydroformylation of propene in an aqueous biphasic system utilising a water-soluble rhodium catalyst  $[HRh(CO)(TPPTS)_3]$ .<sup>11,12</sup> However, when the substrate is changed to 1-hexene the rate-determining step becomes dependent on mass transport. In such cases, it is possible to modify the biphasic system by the addition of co-solvents, or to tailor the ligands of the metal catalyst

to incorporate surfactant or solubilising properties to increase the solubility of the substrate in the biphasic media. Overall, however, the slight decrease in rate is often more than compensated for by the ease of product / catalyst separation.

During the early and rapid advances in aqueous biphasic technology, the hydrogenation of carbon-carbon multiple bond and carbon-oxygen unsaturated compounds provided a ‘benchmark’ against which to compare existing catalytic reduction protocols. However, due to the solubility issues raised earlier, it soon became apparent that only equivalent or poorer rates were obtainable and, in the majority of cases, the addition of a co-solvent detracted slightly from the original ideal biphasic design. The true value of aqueous phase catalysts was only realised when the selective reduction of  $\alpha,\beta$ -unsaturated aldehydes to unsaturated alcohols was investigated by Grosselin and co-workers, using a ruthenium triphenylphosphine trisulfonate complex (Scheme 1.3).<sup>13</sup>

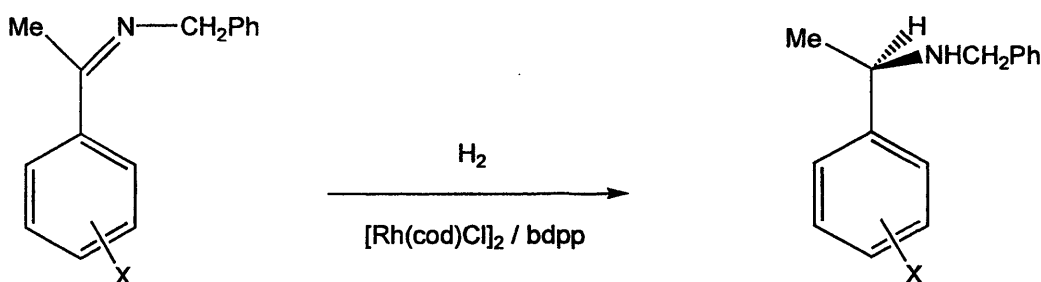


**Scheme 1.3**

The catalyst, formed *in situ*, reduces 3-methyl-2-butenal to 3-methyl-2-buten-1-ol with 96 % selectivity and up to 99 % conversion. The system tolerates a variety of unsaturated aldehydes, with comparable levels of conversion and high selectivity ( $\geq 97$  %). By exchanging the metal centre for rhodium, the alternative selectivity can be achieved whereby the C=C bond is reduced instead of the C=O. Crucially however, the recycled aqueous phases exhibit the same levels of conversion and selectivity when reused following separation from the organic product phase.<sup>12</sup>

In a logical progression considerable attention was focused upon the hydrogenation of prochiral substrates with aqueous phase soluble rhodium catalysts. For certain systems the implementation of this strategy has proved to be very successful, although for the majority, the conversions and enantiomeric excesses (e.e.) are lower than the ‘parent’ homogeneous catalysts.<sup>9</sup> One system, analysed by Sinou *et al.*, is the asymmetric hydrogenation of imines.<sup>14</sup> Using a rhodium

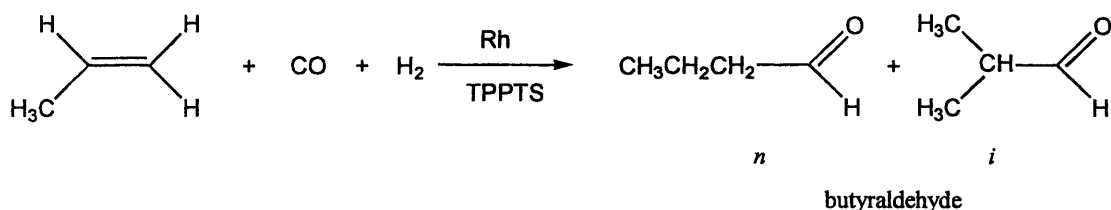
complex, substituted by “sulfonated bdpp” ((2*S*,4*S*)-*bis*-(diphenylphosphino)pentane, almost complete enantioselectivity was obtained (>90 %) for the reduction of a number of substrates (**Scheme 1.4**). Relatively mild conditions were employed (70 bar H<sub>2</sub>, 20 °C, 6 hours), and almost quantitative conversions of the imines were obtained upon separation of the organic phase.



X = H, 4-OMe, 3-OMe, 2-OMe

**Scheme 1.4**

The examination of carbon-carbon coupling reactions with water-soluble catalysts has spawned numerous pilot plants and eventually several industrial scale processes. Many reactions have been investigated and these include: diene hydrodimerisation; alkylation of CH-acidic compounds; addition reactions to alkenes (including hydroamination and hydroformylation<sup>12</sup>) and carbonylation of allylic systems.<sup>9</sup> Of all of these processes, the hydroformylation of olefins (see earlier example) demonstrates the most successful transition into an aqueous biphasic regime. The Ruhrchemie / Rhône-Poulenc process utilises a TPPTS modified rhodium catalyst in an aqueous biphasic system for the hydroformylation of propene. It is estimated that two operational plants now generate in excess of 300, 000 tonnes per annum of butyraldehyde, with an *n:i* ratio of 95 : 5 and yields approaching 99 % depending on the quality of the propene feedstock (**Scheme 1.5**).<sup>15</sup>

**Scheme 1.5**

The plant design incorporates a ‘phase separator’ which is maintained at an ideal temperature to ensure efficient partition between the two phases generating minimal levels of rhodium leaching into the product phase.<sup>9</sup> The aqueous phase is then recycled back into the reactor to undergo progressive cycles. During the development of this methodology, numerous patent applications were made for virtually all aspects of the process, from ligand design to catalyst recovery, a trend which still continues to the present day. The development of new catalysts with higher activities, increased *n:i* ratios and improved long term stability continues to be the focus of considerable research.

### 1.2.2. Supported Aqueous Phase Catalysis

One of the drawbacks of water-based catalytic systems is the problem of solubilising hydrophobic substrates in an aqueous environment. In response to this impediment, Davis *et al.* devised ‘Supported Aqueous Phase Catalysts’ (SAPC’s) in an attempt to hydroformylate higher olefins in a hybrid aqueous biphasic medium.<sup>16</sup> Essentially, the system consists of a thin film of an aqueous solution of a water-soluble catalyst, dispersed over a hydrophilic porous support that possesses a high internal surface area, such as surface modified silica. The SAPC can then be placed into a solution of the desired substrate dissolved in an organic solvent. The ligands of the catalyst are derivatised with polar sulfonate groups (e.g. TPPTS), to ensure preferential aqueous phase solubility. However, the crucial difference is that these catalysts act at the interface, rather than in the bulk solution. Consequently, the substrate and catalyst remain isolated in the two phases, allowing facile separation upon completion of the reaction, by simple filtration of the supported phase from the reaction mixture.

Supported aqueous phase catalysts have been investigated for hydroformylation and hydrogenation involving high molecular weight substrates, for example oleyl alcohol, octene and dicyclopentadiene.<sup>16</sup> A number of studies have been carried out with the hydrido rhodium complex  $[\text{HRh}(\text{CO})(\text{P}[m\text{-C}_6\text{H}_4\text{SO}_3\text{Na}]_3)_3]$  and although excellent yields have been obtained, the activity is highly dependent upon the experimental conditions. For example, the hydroformylation of 1-octene demonstrates a decrease in activity if the water content of the support is too high ( $> 8 \text{ wt } \%$ ).<sup>9</sup> It has been postulated that the increased amount of water allows for greater mobility of the catalyst, promoting decomposition reactions. Conversely, a similar decrease is observed if the water content of the support becomes too low, or if the porosity of the stationary phase is reduced. Within these extremes, there is an optimum water content at which the highest reactivity is obtained. Initially, the rate increases as the volume of water is increased due to the large surface area generated over which reaction can occur. However, once the maximum is achieved, the addition of further water lowers the rate of reaction as the support becomes saturated and the system approaches an aqueous biphasic system. Unfortunately, this sensitivity has limited the industrial application of SAPC's, although work continues in this area as the leaching levels obtained upon phase separation are excellent; for the hydroformylation reaction detailed above, the levels of rhodium in the organic phase are virtually undetectable ( $< 1 \text{ ppb}$ ).

### 1.3. Ionic Liquids

The development of catalytic reactions carried out in ionic liquids has provided an alternative means of heterogenising homogeneous catalysis. By exploiting the unique properties of these room temperature molten salts, various authors have investigated a range of reactions from early simple hydroformylation reactions through to complex enzyme systems functioning as 'biocatalysts'.<sup>17</sup> As well as product / catalyst separation, ionic liquids offer the possibility of replacing standard hydrocarbon solvents (volatile organic compounds VOC's), and for this reason, have attracted considerable interest from the 'green chemistry' community.<sup>18</sup>

Ionic liquids are often characterised by properties general associated with regular solvents, *i.e.* free-flowing, low viscosity, colourless and easily handled at room temperature and pressures. They are composed of the salts of large, bulky organic cations, such as, tetraalkylammonium, tetraalkylphosphonium, *N*-alkylpyridinium, 1,3-dialkylimidazolium and trialkylsulfonium cations (**Figure 1.2**).<sup>19</sup>

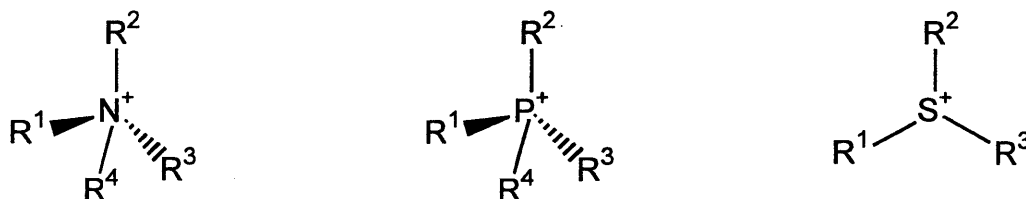


**Figure 1.2**

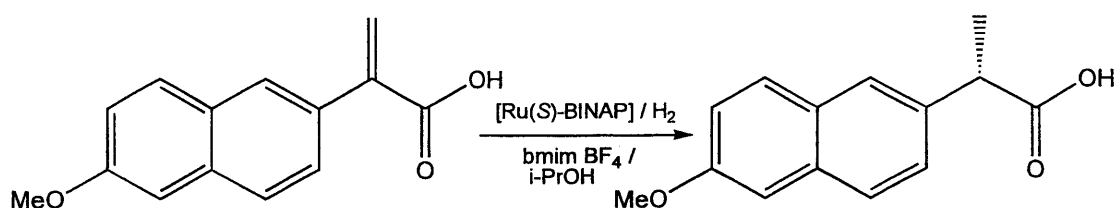
To ensure that the cation / anion pair is liquid at room temperature, interactions between corresponding ions must be reduced, for this reason the most effective cations contain inequivalent R groups to minimise symmetry and thus intermolecular interactions. The anion also influences the melting point, and in most cases, a balanced charge distribution over both ions is essential to reduce dipolar interactions.

Ionic liquids exhibit many properties that render them attractive as an alternative media in which to conduct homogeneous catalysis:

- They have no vapour pressure making them easy to contain, thus reducing losses to the environment
- They have the ability to solvate a range of organic, inorganic and organometallic compounds
- They can be considered to be “Designer solvents” – due to the ability to alter the anion and cation, the solvent properties can be adjusted to an individual reaction
- Their thermal stability ranges between 300 – 400 °C
- High gas solubilities can be achieved for selected ionic liquids, making them attractive for hydrogenations, carbonylations and hydroformylations.

The platinum catalysed hydroformylation of ethene by Parshall in 1972 demonstrated the first example of a homogeneous transition-metal based reaction in an ionic liquid.<sup>20</sup> At the time, the reaction media was considered to be a molten salt (tetraethylammonium trichlorostannate), and unfortunately passed by with little attention until two decades later. However, there are now numerous, elegant processes carried out in ionic liquids, which exploit the unique properties of these novel media. In parallel with the aqueous biphasic systems, many of the reactions investigated take advantage of the variation in solubility obtainable at both elevated and reduced temperatures to allow facile product / catalyst separation.

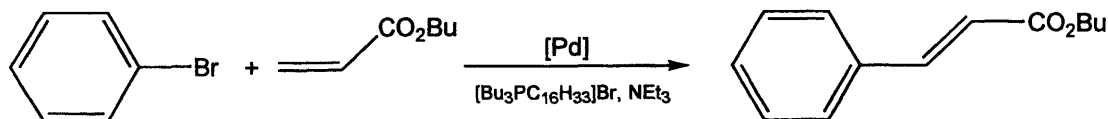
Hydrogenations have been investigated extensively in various biphasic ionic liquid systems. In general these reactions are particularly amenable to this approach due to the reasonable solubility of hydrogen and numerous alkene substrates in ionic liquids, but also due to the miscibility gap with the final saturated reaction product enabling facile isolation from the catalyst. Recently this approach has been extended to enantioselective hydrogenations, with the aim of recycling the metal complexes of expensive chiral ligands. Dupont and co-workers demonstrated this principle by using a ruthenium based catalyst for the asymmetric hydrogenation of 2-(6-methoxy-2-naphthyl)acrylic acid to the anti-inflammatory drug, (*S*)-naproxen in 80 % ee (Scheme 1.6).<sup>21</sup> The biphasic system of isopropyl alcohol and butylmethylimidazolium tetrafluoroborate enables facile separation, enabling quantitative product isolation. The ionic liquid containing the catalyst can then be recycled several times with no significant change in activity or selectivity.



**Scheme 1.6**

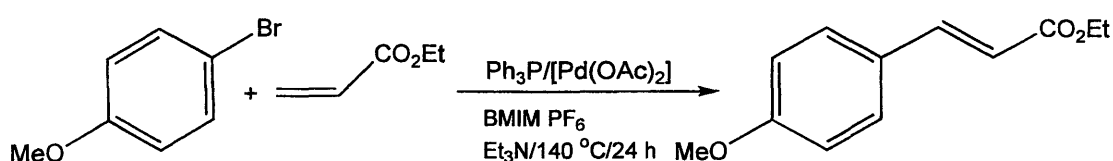
The palladium-catalysed Heck reaction has also been investigated in ionic liquids and the first example was described by Kaufmann in 1996.<sup>22</sup> The reaction of

bromobenzene with butylacrylate was carried out directly in molten tetraalkylammonium or tetraalkylphosphonium bromide salts (**Scheme 1.7**).



**Scheme 1.7**

The ionic liquid appears to impart a stabilising effect upon the palladium catalyst as no elemental palladium was observed. The butyl *trans*-cinnamate was isolated by distillation from the ionic liquid in excellent yield. A recent development of the Heck reaction was developed by Seddon and co-workers, who employed a three-phase work-up system of an ionic liquid ([BMIM]PF<sub>6</sub>), water and hexane.<sup>23</sup> The aim was to retain the catalyst [(BMIM)<sub>2</sub>PdCl<sub>4</sub>] in the ionic liquid, extract the product into the organic phase, whilst removing the salt ([Hbase]<sup>+</sup>X<sup>-</sup>), formed as a by-product of the reaction, *via* the aqueous layer. The success of this regime was demonstrated in the coupling reaction between 4-bromoanisole and ethyl acrylate (**Scheme 1.8**). The product, ethyl 4-methoxycinnamate was isolated in 98 % yield from the hexane layer, whilst the catalyst was retained by the ionic liquid.



**Scheme 1.8**

Whilst catalysis in ionic liquids is an expanding area of chemistry, the implementation on an industrial scale is currently limited by the prohibitive cost of these systems. Furthermore, the fact that a secondary solvent is often used to extract the product often appears to be somewhat paradoxical to the original hypothesis. Whilst this may be useful for situations where a very hazardous solvent is replaced by an ionic liquid, to be followed by extraction with a comparatively benign solvent, the relative advantages do not balance the increased expenditure in

comparison to aqueous biphasic systems. However, for reactions involving hydrophobic substrates or moisture sensitive catalysts, ionic liquids offer an excellent alternative to standard organic solvents, particularly where a biphasic system is formed upon completion of the reaction.

## 1.4. Fluorous Biphasic Catalysis

### 1.4.1. The Introduction of Fluorine

The extreme reactivity of elemental fluorine is in direct contrast to the stability imparted upon compounds which contain a degree of fluorination.<sup>24</sup> This has been exploited throughout numerous areas of research; for example, perfluorinated solvents have been shown to be ideal environments for liquid ventilation.<sup>25</sup> Due to the high oxygen solubility of these liquids and their inert characteristics, it is predicted that premature babies, whose lungs are not capable of aerobic ventilation, may be kept alive by immersing them in the oxygen-bubbled liquid. Similarly, the extremely inert nature of Teflon, a fully fluorinated polymer, has enabled numerous applications where hard wear and long life-time mechanical stability are required. This is exemplified by the utilisation of Teflon hip replacement joints and replacement heart valves.<sup>26</sup>

However, until recently, the utilisation of perfluorinated solvents and reagents had not been widely exploited. In 1994, Horváth and Rábai published their seminal paper delineating the use of a “fluorous biphasic” system as an alternative to aqueous biphasic systems for product / catalyst separation.<sup>27</sup> The term ‘fluorous’ was coined to describe highly fluorinated alkane, ether and tertiary amine solvents, such as perfluoro-1,3-dimethylcyclohexane or “PP3” (**Figure 1.3**).

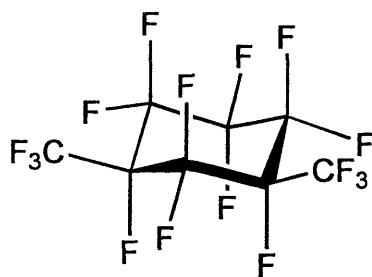


Figure 1.3

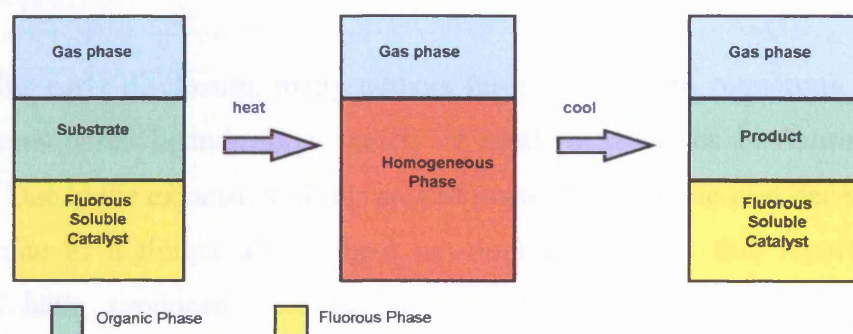
However, the adjective now applies to a vast array of chemistry including silicas; reagents; catalysts and, in certain cases, products. The expansion of this concept has led to a precise definition of the term *fluorous* in a recent article by Gladysz and Curran.<sup>28</sup>

*“of, relating to, or having the characteristics of highly fluorinated saturated organic materials, molecules or molecular fragments. Or, more simply (but less precisely), ‘highly fluorinated’ or ‘rich in fluorines’ and based upon  $sp^3$ -hybridised carbons”*

In this area of chemistry the incorporation of fluorine is used to impart solubility in highly fluorinated media. This is then used to enable separation *via* biphasic processes due to the immiscibility of fluorous solvents with many organic solvents. The term ‘*similia similibus solvuntur*’ or ‘*like dissolves like*’ has been used to describe the high affinity of fluorinated molecules for the fluorous phase.<sup>5</sup> However, numerous other properties contribute toward the unique nature of this novel reaction medium. Fluorinated solvents are thermally more stable than their organic counterparts, when combined with the chemical inertness of these species, it is clearly apparent that they represent ideal reaction media for recovery and recycling. Fluorous solvents also have higher gas solubilities than many organic solvents, which has led to many potential applications involving gaseous feedstocks. However, perhaps the most significant feature arises *via* the miscibility of fluorous solvents with certain organic solvents at elevated temperatures. As a consequence, this enables a homogeneous monophasic system to be formed, a feature which has been exploited in ‘fluorous biphasic catalysis’.<sup>5</sup>

### 1.4.2. Fluorous Biphasic Catalysis

In many respects the fluorous biphasic system is analogous to the aqueous biphasic system, as it relies upon the contrasting properties of two immiscible media. The catalysts are dissolved in the lower fluorous phase, whilst the organic substrates and / or products reside in the organic phase. Whereas polar ionic groups are required to confer aqueous phase solubility, for preferential fluorous phase solubility, several non-polar, highly fluorinated moieties are attached. An intermediate homogeneous phase is generated upon heating, given the correct choice of solvent pair, allowing the catalyst to become exposed to the substrate and thus reaction to occur. Upon cooling at the end of the reaction, the two phases are re-established, enabling product / catalyst separation *via* simple decantation of the upper organic phase (Scheme 1.9).<sup>27</sup>



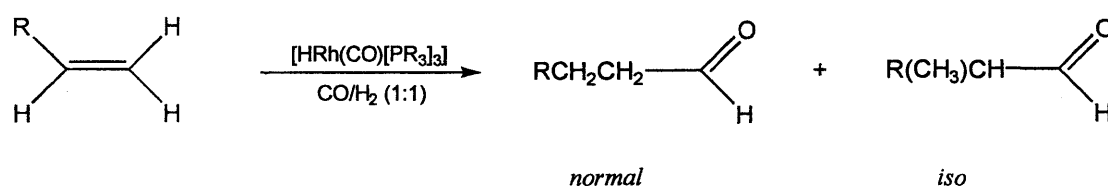
Scheme 1.9

The most convenient method of introducing these fluorous side chains, or *ponytails* as they have been termed, is through ligand modification procedures. Following the disclosure of the fluorous biphasic methodology by Horváth and Rábai, a variety of fluorous ligands have been prepared and coordinated to numerous metal centres in order to generate fluorous catalysts.

### 1.4.3. Phosphorus and Nitrogen Donor Ligands

In order to render a metal catalyst soluble in perfluorocarbon solvents, approximately 60 % total fluorine content is considered to be the literature standard,<sup>5,29</sup> although this issue is slightly contentious with several factors such as

polarity, chain geometry and temperature all exerting considerable influence.<sup>30</sup> However, to fulfil this criterion, the modification of phosphorus (III) ligands provides a facile and flexible means of incorporating fluorous character in much the same way as in aqueous phase soluble catalysts. This was realised by Horváth and Rábai who utilised a rhodium catalyst, substituted with phosphine ligands bearing perfluoroalkyl chains ( $\text{P}[\text{C}_2\text{H}_4\text{C}_6\text{F}_{13}]_3$ ), in the first example of a fluorous biphasic hydroformylation system (**Scheme 1.10**).<sup>27</sup>



**Scheme 1.10**

Since this early disclosure, many authors have investigated numerous fluorinated phosphorus based ligands for a variety of catalytic reactions in fluorous biphasic media. Due to the expansion of this area of research during the past decade, it is not appropriate to highlight all of these developments within this report. Several authors have produced detailed reviews describing both the genesis and development of these techniques.<sup>5,31</sup> Within the confines of this introduction, emphasis will be placed upon highlighting the most recent developments and emerging methodologies.

Continuing Horváth and Rábai's original premise, hydroformylation under fluorous biphasic conditions has been developed considerably during this period. Recently, Hope and co-workers have demonstrated the application of this regime to long chain alkenes.<sup>32</sup> As indicated earlier, the hydroformylation of higher olefins is problematical in aqueous biphasic systems due to the poor solubility of the substrates (see section 1.2.1). However, these authors have shown that long chain alkenes, such as oct-1-ene, are sufficiently soluble in fluorous solvents under reaction conditions ( $\geq 60$  °C, 20 bar  $\text{CO}/\text{H}_2$ ), to enable reaction to occur. In effect, the system designed is almost a hybrid biphasic system, which eliminates any need for a

conventional organic solvent. The fluoros solvent used was PP3, and upon completion of the reaction, the product forms a discrete phase which is in a “substantially pure state”, negating the requirement of a post-reaction distillation procedure.<sup>32</sup> The catalyst design was also improved, enhancing the economic and environmental viability of industrial scale synthesis. Currently, the hydroformylation of higher olefins are carried out using cobalt catalysts, modified by tertiary phosphines. Due to the harsh conditions employed, large amounts of alcohol by-product are formed, whilst the *n:i* ratio of the aldehyde component is biased toward the branched chain isomer which is of less commercial value. By exchanging the metal centre for rhodium, milder conditions could be employed, preventing further reaction. Under these conditions more strategically designed ligand systems can be used to improve the *n:i* ratio, and ultimately to raise the atom efficiency of the process. Unfortunately, one of the drawbacks of Horváth and Rábai’s initial system was that high concentrations of the expensive fluoros ligand  $[P(CH_2CH_2C_6F_{13})_3]$  were required to obtain satisfactory selectivity. Previous investigations have revealed that triarylphosphines yield greater *n:i* ratios and consequently, by utilising a fluoros analogue of triphenylphosphine (**Figure 1.4**), the authors demonstrated that high yields of the straight chain aldehyde could be obtained under mild fluoros biphasic conditions *n:i* ratio = 4:1.

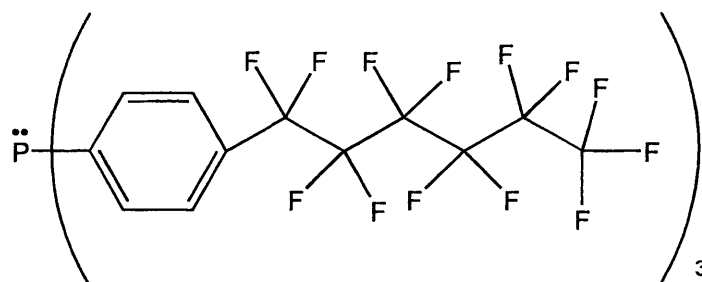


**Figure 1.4**

The search for effective hydrogenation regimes has seen considerable developments *via* the implementation of fluoros biphasic techniques. Initial studies focused upon an analogue of Wilkinson’s catalyst  $[RhCl(PR_3)_3]$  modified by fluoros phosphine ligands  $[P(CH_2CH_2C_6F_{13})_3]$ .<sup>33</sup> The catalyst generated was found

to be active for the hydrogenation of cyclododecene and recycling of the fluoros phase was demonstrated. In an attempt to minimise leaching of the fluoros catalysts, a number of authors have synthesised fluoros analogues of chelating diphosphines, unfortunately, the catalytic activity of the resultant catalysts was found to be low.<sup>34</sup> In a new approach to chelating phosphines, Deelman and co-workers have synthesised a range of compounds incorporating silicon spacer groups (or ‘branching points’), enabling up to twelve fluoros ponytails to be attached to the phosphine backbone (Figure 1.5).<sup>35</sup>

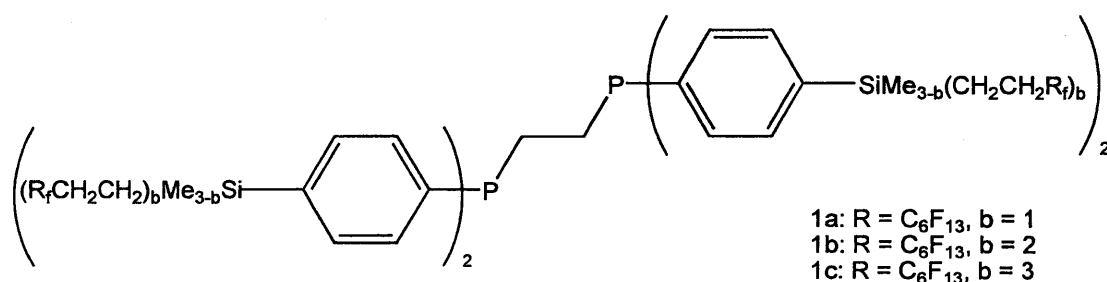


Figure 1.5

The incorporation of silicon spacer groups was first documented as an alternative to ethylene and aryl spacers in monodentate phosphines.<sup>36</sup> The aim was to utilise the positive inductive effect of the silicon atoms to counteract the powerful electron withdrawing effect of the fluorinated groups. A range of monodentate phosphines were prepared and interestingly, the optimum fluorophilicity under biphasic conditions was still obtained at 63 wt % fluorine (Figure 1.6).

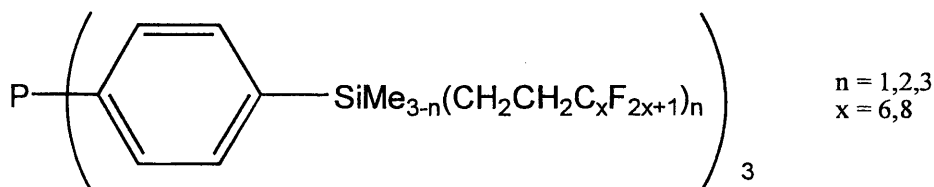
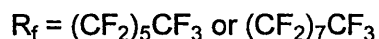
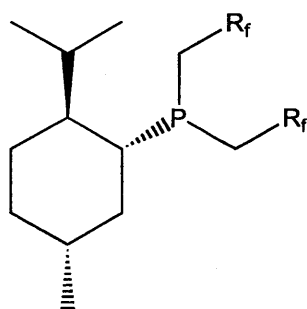


Figure 1.6

For the longer chain *tris*-substituted phosphines, the fluoros phase solubility decreased with increasing molecular weight. Evidently, this trend is echoed in the chelating diphosphines and the resultant catalytic complexes. The authors

investigated the hydrogenation of alkenes and alkynes under fluororous biphase conditions using a rhodium based species  $[\text{Rh}(\text{COD})(\text{L-L})][\text{BF}_4]$ .<sup>35</sup> Due to the contrasting solubilities of the diphosphines, varying solvent systems were used and an unconventional biphase of acetone and  $\text{PP}_3$  was employed for the highly fluorinated species. As a consequence, direct comparison of the catalysts is virtually impossible although under homogeneous conditions, the activity of the ‘fully’ fluorinated (“1c”) diphosphine catalyst was comparable to non-fluorous  $[\text{Rh}(\text{COD})(\text{dppe})][\text{BF}_4]$ . Significantly though, the levels of rhodium leaching were very low; in a FC75 (perfluoro(2-*n*-butyltetrahydrofuran) / hexane biphase system, lower than 1 ppm was detected, although in the  $\text{PP}_3$  / acetone system, the value was higher at 36 ppm. The implication of this almost total recovery is enhanced by excellent recycling data, thus overcoming the problems associated with ligand dissociation and subsequent leaching in monodentate phosphine systems.

The implementation of fluororous biphase regimes in enantioselective transformations appears to be a logical and obvious application, considering the often prohibitive cost of chiral catalysts on an industrial scale. However, a recent review by Pozzi indicates there has been a relative dearth of research in this potentially lucrative area.<sup>37</sup> The first example of a fluorinated chiral phosphine was reported by Gladysz (**Figure 1.7**), although no catalytic applications were described.<sup>38</sup>



**Figure 1.7**

The second ligand was synthesised by Pozzi and co-workers and is an analogue of the MOP ligand and binaphthyl (**Figure 1.8**).<sup>39</sup> The feasibility of this system was

evaluated in the Pd(0) catalysed asymmetric allylic alkylation of 1,3-diphenyl-2-propenyl acetate (**Scheme 1.11**). The reactions were carried out in toluene or benzotrifluoride affording good enantioselectivities of up to 87 % e.e. Upon completion of the reaction, liquid-liquid extraction by perfluorooctane liberated the fluorinated ligand and the palladium containing species. Unfortunately, however, the recovered material had lost its catalytic activity, negating the possibility of recycling the fluoruous phase.

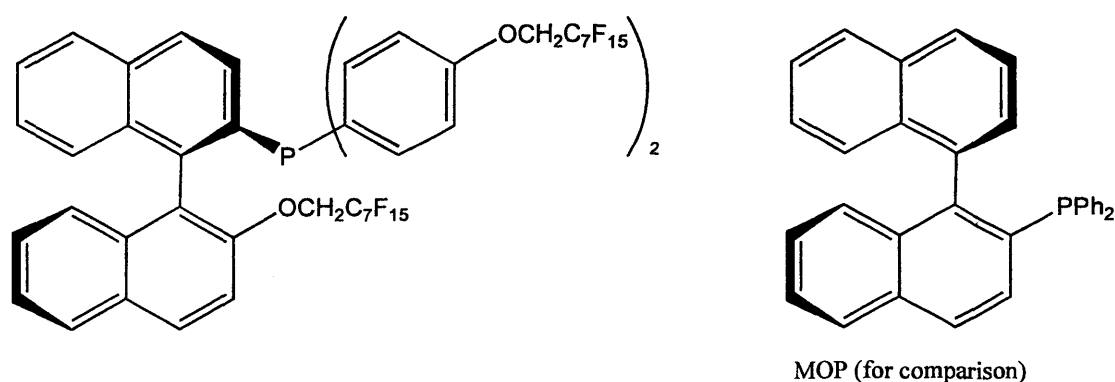
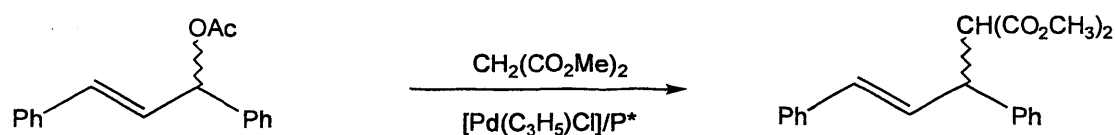


**Figure 1.8**



**Scheme 1.11**

Recently, Hope *et al.* have also investigated a series of perfluoroalkyl substituted *R*-BINAP ligands (**Figure 1.9**), with the aim of evaluating the ruthenium catalysed asymmetric hydrogenation of dimethyl itaconate.<sup>40</sup> The ligands were designed for use in traditional fluoruous solvents and also in *sc*CO<sub>2</sub>, although preliminary investigations were carried out in methanol. The results obtained were promising with very high stereoselectivities recorded that were comparable to the parent Ru-*(R)*-BINAP system. However, the authors discovered that the perfluorohexyl moieties needed to be insulated in order to obtain satisfactory conversions; for the

ethylene spacer derived ligand, the yield was approximately double that of the analogous directly bound  $C_6F_{13}$  ligand (83 and 42 % respectively).

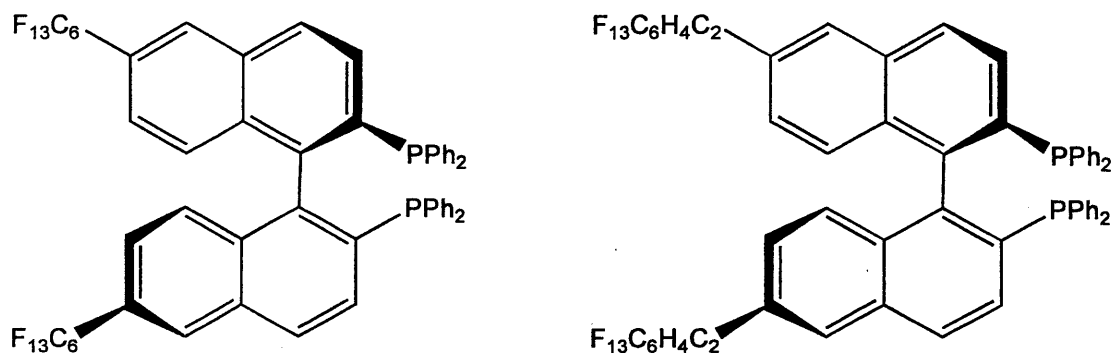


Figure 1.9

In comparison, the development of chiral nitrogen donor ligands is considerably more advanced with several systems documented.<sup>37</sup> The first example was an optically active (salen)-manganese (III) complex bearing perfluoroalkyl ponytails (**Figure 1.10**), that was examined as a catalyst for the asymmetric epoxidation of indene under fluoruous biphasic conditions.<sup>41</sup> Although the activity of these so-called ‘first generation’ salen complexes was high (both in terms of yield and enantioselectivity), they proved to be compound specific, yielding poor conversions for substrates other than indene. The development of ‘second generation’ salen ligands based upon a biaryl framework, allowed greater variation in the substrate molecule, whilst also incorporating bulky *tert*-butyl groups to increase steric hindrance (**Figure 1.10**).<sup>42</sup> These improvements led to more versatile catalysts that also yielded high e.e.’s under fluoruous biphasic conditions (perfluorooctane/ $CH_3CN$ ). Significantly, the catalysts were recyclable and the yields of epoxide were high.

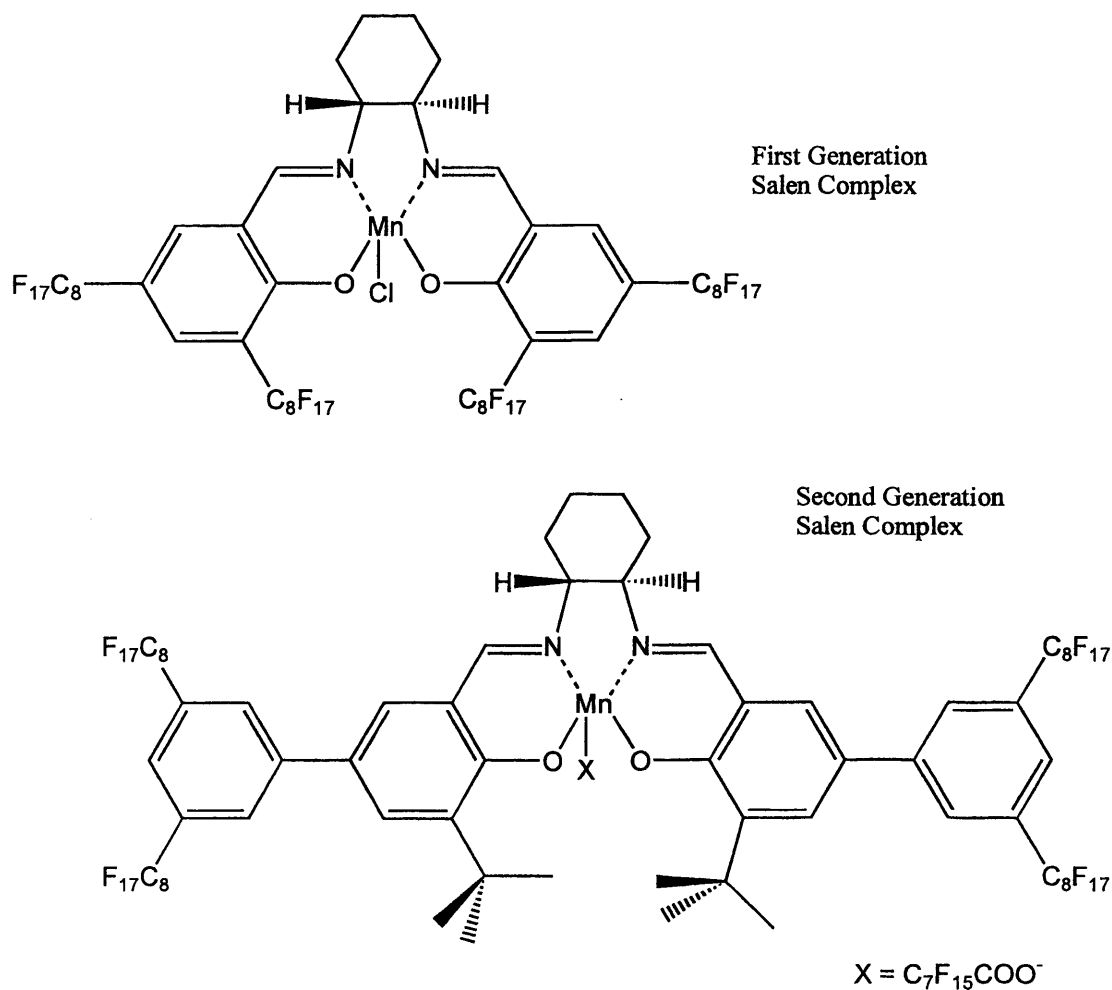


Figure 1.10

Recently, this area of research has been extended to the asymmetric hydrogen transfer reduction of ketones using iridium based salen complexes,<sup>43</sup> and also the hydrolytic kinetic resolution of terminal epoxides using analogous cobalt species.<sup>44</sup>

The development of fluorinated nitrogen donor ligands has been dominated by macrocyclic systems, particularly substituted porphyrins.<sup>45</sup> A range of catalytic oxidation reactions have been investigated and recently these have been extended to the oxidation of sulfides under fluorous biphasic conditions.<sup>46</sup> Pozzi *et al.* have investigated the cobalt complexes of two macrocyclic ligands; the previously reported tetraarylporphyrin,<sup>45</sup> and the novel perfluoroalkyl-substituted phthalocyanine (Figure 1.11).

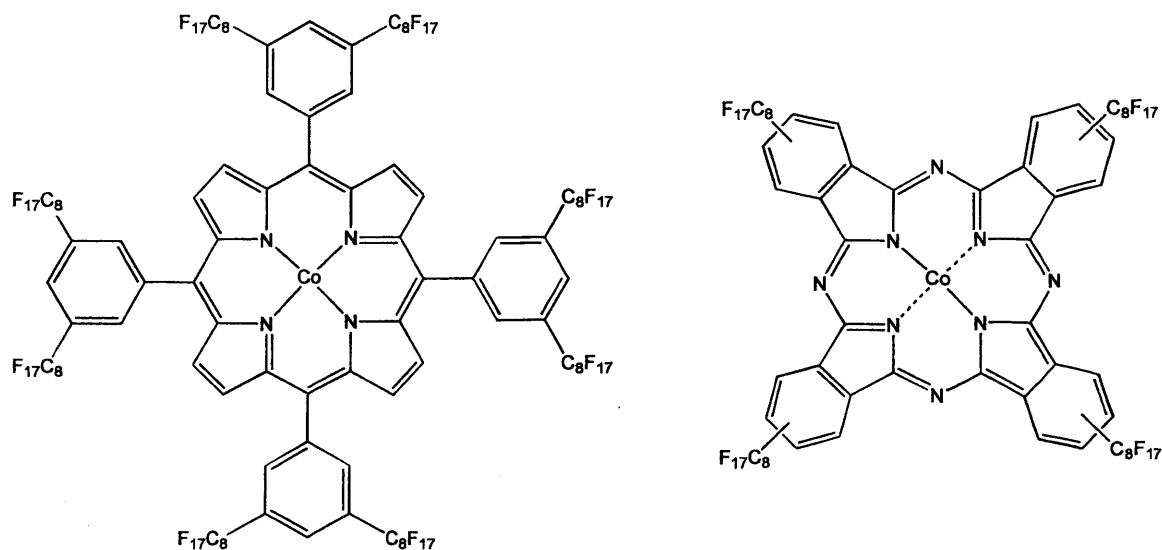


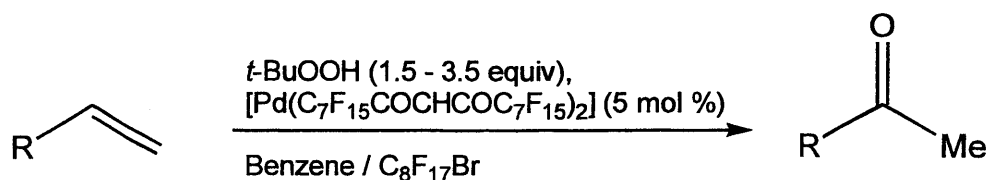
Figure 1.11

The catalytic oxidation of methyl *p*-tolyl sulfide was examined in a fluorous biphasic system of dichloromethane and perfluorooctane at 20 °C. The reactions were carried out in the dark, under an atmosphere of oxygen and required the presence of *iso*-butyraldehyde. Initially, it was found that the cobalt tetraarylporphyrin complex was an efficient and selective catalyst for sulfide oxidation, achieving 94 % conversion to the sulfoxide in four hours. However, when the fluorous phase was recycled, the selectivity decreased dramatically, with 100 % conversion to the sulfone observed after just three cycles. This appears to indicate that the nature of the catalytic species is being significantly altered during the catalytic cycles. A similar investigation was carried out for the phthalocyanine cobalt complex. Overall, selectivity towards formation of the sulfoxide was very high, although unfortunately, the conversion was significantly lower, initially at 40 %, decreasing markedly to 11 % in the second cycle.

#### 1.4.4. Oxygen Donor Ligands

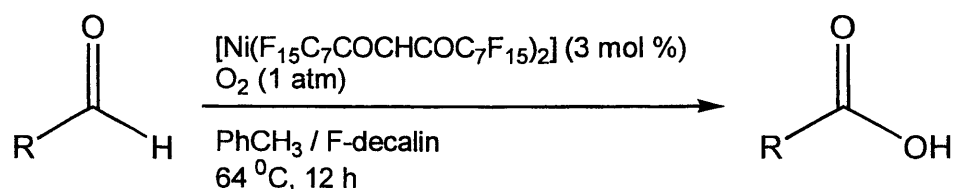
Although there are fewer examples of perfluorinated oxygen donor ligands, the breadth of reactions is equally as large as those encompassed by the phosphine and nitrogen species. One of the first species investigated were the fluorinated  $\beta$ -diketones, which have been examined for oxidation reactions and various

oligomerisation processes. As mentioned earlier, the high gas solubilities of perfluorinated solvents renders them attractive as oxidation media. The 1,1,1,2,2,3,3,4,4,5,5,6,6,7,7,11,11,12,12,13,13,14,14,15,15,16,16,17,17,17-triacontafuoro-heptadecane-8,10-dione, has been coordinated to palladium, nickel and ruthenium metal centres to generate highly efficient, fluorous soluble catalysts.<sup>47,48</sup> The palladium complex,  $[\text{Pd}(\text{F}_{15}\text{C}_7\text{COCHCOC}_7\text{F}_{15})_2]$ , catalyses the oxidation of alkenes to the corresponding methyl ketones using *tert*-butyl hydroperoxide.<sup>47</sup> The reaction is carried out in a benzene / bromoperfluorooctane biphase which becomes monophasic at *ca.* 60 °C allowing the substrate to become exposed to the catalyst (**Scheme 1.12**).



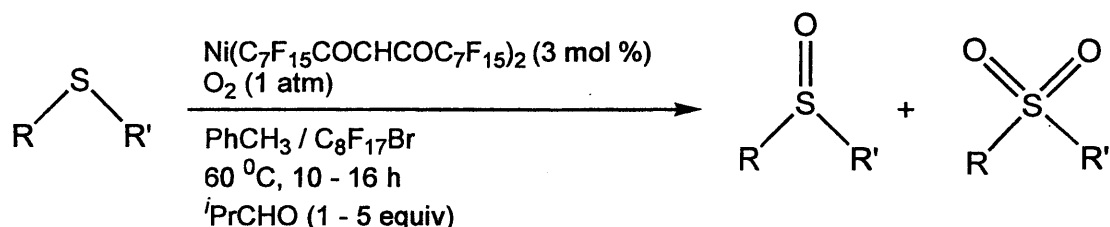
Scheme 1.12

The system tolerates a variety of alkene functionalities from simple aromatic compounds (for example, styrene), to long chain esters and ethers. With one or two exceptions, the yields are universally high ( $\geq 70\%$ ) and the catalyst could be reused several times, but progressively longer reaction times were required. The nickel analogue is also an oxidation catalyst, and the very high solubility of molecular oxygen in fluorous solvents was exploited to effect the conversion of aliphatic and aromatic aldehydes and ketones to the corresponding acids (**Scheme 1.13**).<sup>48</sup>



Scheme 1.13

Significantly, no leaching of the catalyst is observed and after six catalytic cycles the product yield still remained high at 70 %. This catalyst system can also be used for the oxidation of sulfides to sulfoxides and sulfones, although the process requires the presence of *iso*-butyraldehyde (**Scheme 1.14**).



**Scheme 1.14**

In direct contrast, Carlini and co-workers have attempted to carry out propylene oligomerisation under fluoruous biphasic conditions using similar nickel  $\beta$ -diketonates.<sup>49</sup> In this type of reaction, the active species is generated *via* reaction with methyl aluminoxane (MAO), and the obvious difficulty arises through diffusion of this species from the non-polar fluoruous phase into the organic (product) phase. To counteract this problem, the authors introduced a number of fluorinated phosphine ligands and also a borane co-catalyst  $[\text{B}(\text{C}_6\text{F}_5)_3]$ , which increase the fluorophilicity of the active species. Two nickel  $\beta$ -diketonates were investigated (**Figure 1.12**), and both were found to be active for the dimerisation of propylene to 2,3-dimethylbutenes in a conventional organic solvent.

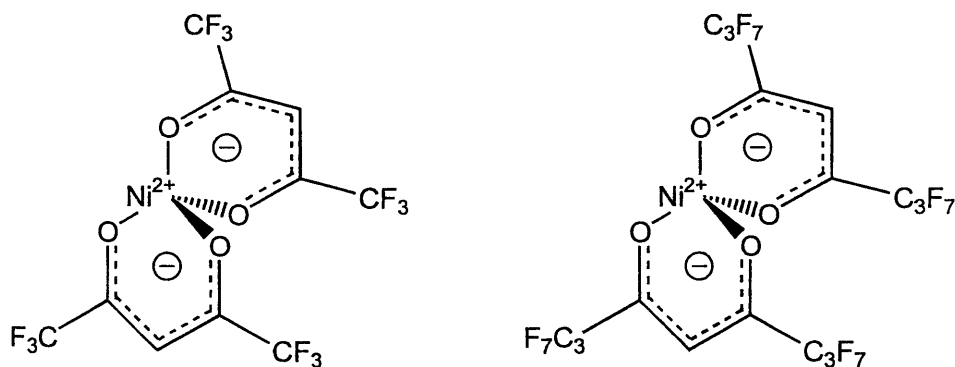


**Figure 1.12**

Unfortunately, progressive migration of the fluorinated catalyst to the organic phase occurred when the reactions were analysed using a toluene / perfluorohexane biphase, and the authors were forced to concede that propylene dimerisation represents a “very severe test” to the fluorous biphase methodology due to the affinity of the polar intermediate for the organic phase.

Considerable interest has been shown in utilising perfluorinated carboxylates in the fluorous biphase system. Perhaps the motivation for investigating these systems arises through the commercial availability of perfluorinated carboxylic acids and their relatively facile coordination chemistry to a wide variety of metals. However, due to the polarity of the carboxylate group, which is exacerbated by the electron withdrawing effect of the perfluoroalkyl ponytail, the majority of the species studied have incorporated spacer functionalities to counteract this effect.<sup>50</sup> Unfortunately, solubility in fluorinated media remains difficult to achieve, prompting one group recently to synthesize a branched chain carboxylic acid in order to increase the fluorophilicity (**Figure 1.13**).<sup>50</sup>

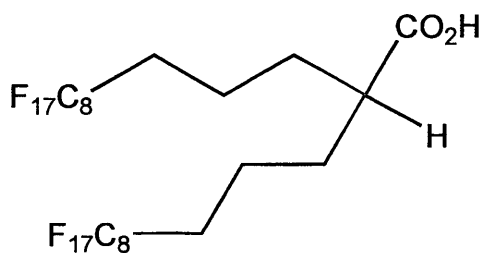


**Figure 1.13**

Even though this ligand contains 65.9 % fluorine, the resultant manganese and cobalt complexes required the presence of small amounts of THF to achieve fluorous phase solubility. Employing a second class of fluorous ligand to render the carboxylates soluble in such a non-polar media can overcome this problem. Fish and co-workers utilised a perfluoroalkyl-substituted triazocyclononane (**Figure 1.14**), to achieve this aim when exploring the oxidation of alkanes and alkenes.<sup>51</sup> The tridentate amine is rendered fluorous soluble by functionalisation with three C<sub>3</sub>H<sub>6</sub>C<sub>8</sub>F<sub>17</sub> chains and added to [Mn<sup>2+</sup>(O<sub>2</sub>C{CH<sub>2</sub>}<sub>2</sub>C<sub>8</sub>F<sub>17</sub>)<sub>2</sub>] and [Co<sup>2+</sup>(O<sub>2</sub>C{CH<sub>2</sub>}<sub>2</sub>C<sub>8</sub>F<sub>17</sub>)<sub>2</sub>] to generate the fluorous soluble complexes.

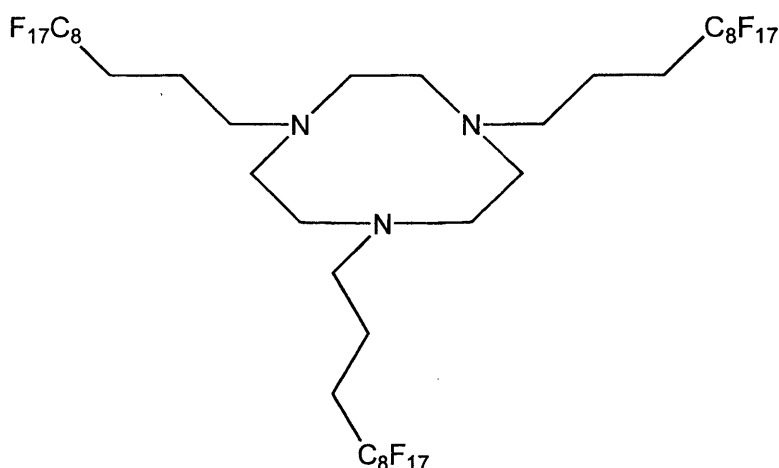


Figure 1.14

In the presence of *tert*-butyl hydroperoxide and 1 atm. of oxygen, the complexes function as alkene oxidation catalysts. In this case the organic substrate was actually used as the organic phase of the catalytic system, whilst the catalyst was dissolved in perfluoroheptane. The yields of alcohols and ketones were reasonable, and significantly, the product / catalyst separation was extremely efficient.

The rhodium dimers of perfluorinated carboxylates have also recently been the focus of investigation in fluoruous biphasic systems.<sup>52</sup> However, the chemistry of these ligands was quite extensive prior to this current interest. In particular, dirhodium (II) tetrakis(perfluorobutyrate)  $[\text{Rh}_2(\text{pfb})_4]$ , has been used as a catalyst for carbenoid reactions of diazo compounds,<sup>53</sup> hydrosilylation of alkenes,<sup>54</sup> and silycarbonylation of alkynes.<sup>55</sup> Some of these reactions have been investigated with long chain fluoruous analogues (**Figure 1.15**), with varying levels of success. A more detailed description of these catalytic processes are given in Chapter 5.

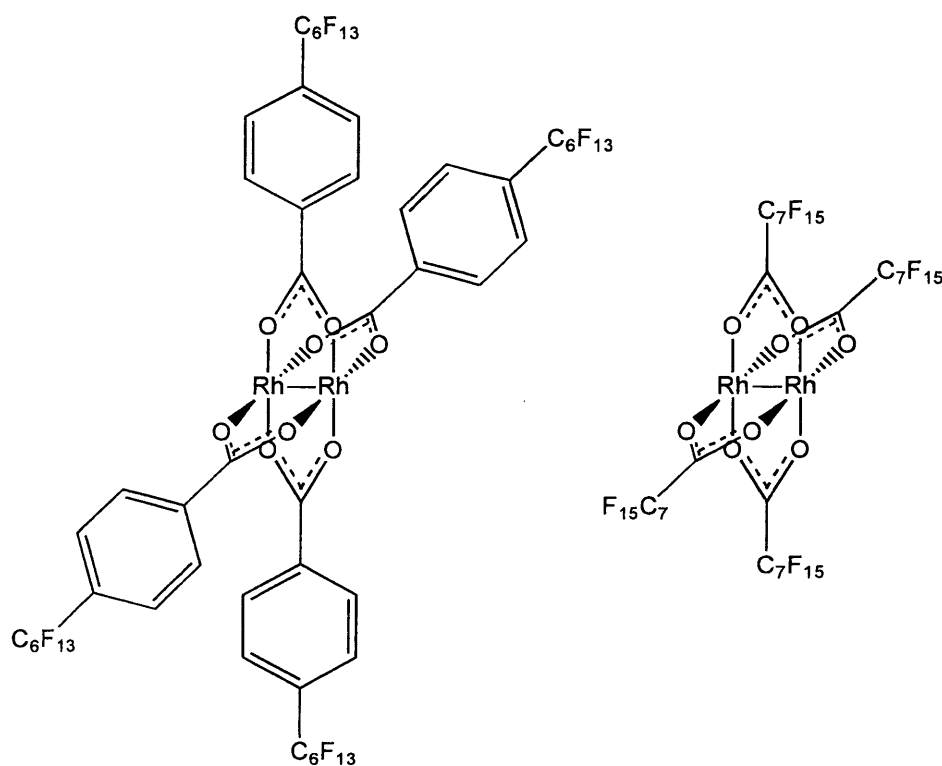
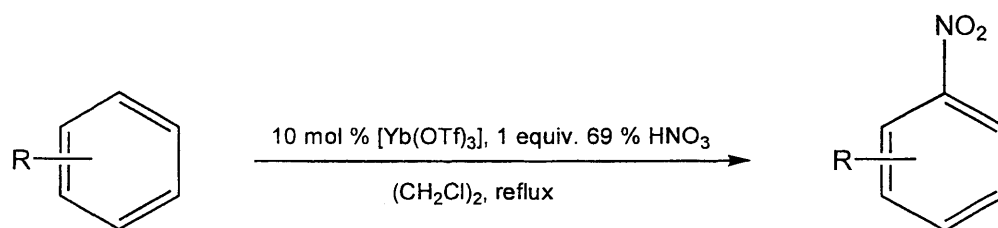


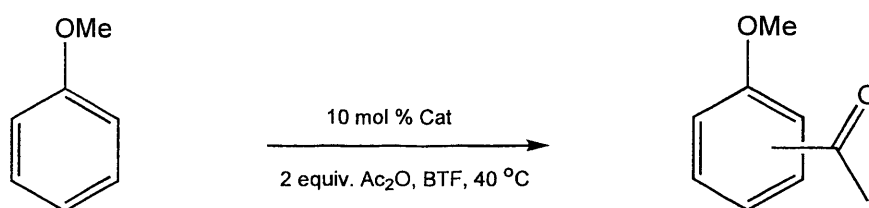
Figure 1.15

In an attempt to create an “atom efficient” aromatic nitration process, Braddock *et al.* have investigated a variety of commercially available lanthanide triflates as potential catalysts for this important industrial process.<sup>56</sup> Ytterbium triflate [ $\text{Yb}(\text{OTf})_3$ ] was found to be an efficient catalyst for a variety of aromatic substrates (**Scheme 1.15**). The only by-product from the reaction is water and the catalyst can be recycled and retained similar activity.



Scheme 1.15

The scope of the system has been extended to the nitration of fluoroaromatics by utilising lanthanide ‘triflides’, such as ytterbium (III) triflido [Yb(CTf<sub>3</sub>)<sub>3</sub>]. Fluoroaromatics are difficult to nitrate due to the elimination of hydrogen fluoride which results from the harsh conditions usually employed (*i.e.* HNO<sub>3</sub> / H<sub>2</sub>SO<sub>4</sub>). However, by utilising the increased Lewis acidity of lanthanide triflides, nitration of these compounds has been achieved as well as in other deactivated systems. For example, *o*-nitrotoluene can be nitrated to dinitrotoluene (93 %) in twenty-four hours, whereas [Yb(OTf)<sub>3</sub>] is essentially ineffective with this substrate.<sup>56</sup> Subsequently, the authors have expanded the triflido ligands to long chain perfluorinated homologues, having recently demonstrated the first fluoros phase Friedel-Crafts acylation of arenes.<sup>58,59</sup> Ytterbium (III) tris(perfluoroalkanesulfonyl) methides function as effective catalysts, under fluoros biphasic conditions, for the acylation of a variety of aromatic compounds. Furthermore, the complexes can be recycled *via* extraction with perfluoromethyldecalin and subsequently recycled with similarly high levels of conversion (**Scheme 1.16**).

**Scheme 1.16**

### 1.5. Alternative fluoros phase systems

Throughout the development of the fluoros biphasic paradigm, several concurrent evolutionary paths have been followed which attempt to expand upon the original premise. One reoccurring theme is the elimination of perfluorocarbon solvents in an attempt to render the process more economically viable on an industrial scale. Several approaches are described below and compared with conventional fluoros biphasic systems.

### 1.5.1. Supercritical Fluids

Supercritical carbon dioxide (scCO<sub>2</sub>), has long been vaunted as an environmentally benign solvent for chemical syntheses although in reality, the decaffeination of coffee remains the most significant application. Although the many advantages of scCO<sub>2</sub> are desirable for homogeneous catalysis, including low toxicity, non-flammability and ease of separation from the reaction mixture, the often prohibitive feature is the low polarity of the medium.<sup>60</sup> As a consequence, many metal based catalyst molecules will not dissolve. Although a variety of compounds can be added to alter the polarity, so called ‘polar modifiers’, the presence of these species belies the true aim of generating a clean reaction system due to the difficulty of re-isolating these species from the catalyst / product. The second drawback of modifying additives is the unknown effect which can lead to undesired by-products and as a result, many applications are prohibited unless the substrate itself can act as a co-solvent to solubilise the catalyst.<sup>61</sup>

However, the non-polarity of scCO<sub>2</sub> is, to a certain degree, similar to perfluorinated solvents and consequently, by substituting the catalytic species with fluorinated sidechains solubility in this unusual environment can be achieved. It is thought that interactions between the relatively electron rich C-F bonds and the electron poor carbon dioxide molecules contribute towards dissolving the catalyst.<sup>62</sup> Several groups have explored this area, often in parallel to conventional fluororous biphasic systems resulting in similar fluorinated ligand systems. Leitner and co-workers have investigated a number of fluororous derivatised mono- and bi-dentate phosphine and phosphite ligands in conjunction with the catalyst precursor [ $\{\text{COD}\}\text{Rh}(\text{hfacac})$ ].<sup>61</sup> The rhodium catalyst generated was found to be active for the hydroformylation of oct-1-ene to isomeric aldehydes in scCO<sub>2</sub>. Holmes and Carroll have also demonstrated that carbon-carbon bond forming reactions can be carried out using fluorinated palladium catalysts in scCO<sub>2</sub>,<sup>63</sup> whilst similar species were employed by Tumas and colleagues to effect Heck and Stille couplings.<sup>64</sup> Other reactions investigated utilising fluororous ligands include hydrogenation,<sup>65</sup> hydrovinylation<sup>66</sup> and polymerisation,<sup>67</sup> but despite the success of these systems in terms of reactivity, the recovery and re-use of the catalyst remains difficult to

achieve. This has recently prompted Kani *et al*, to generate a polymer supported catalyst which was analysed for the hydrogenation of oct-1-ene (**Figure 1.16**).<sup>60</sup>

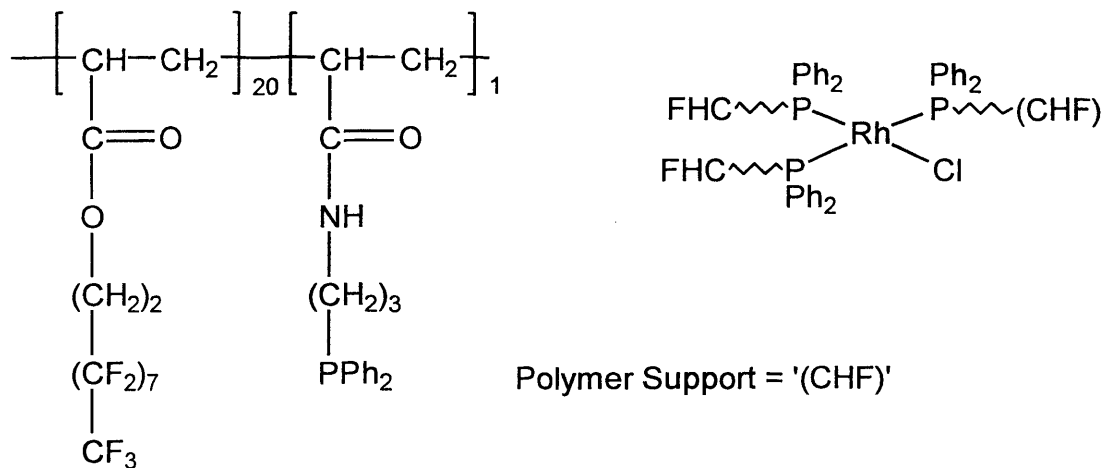


**Figure 1.16**

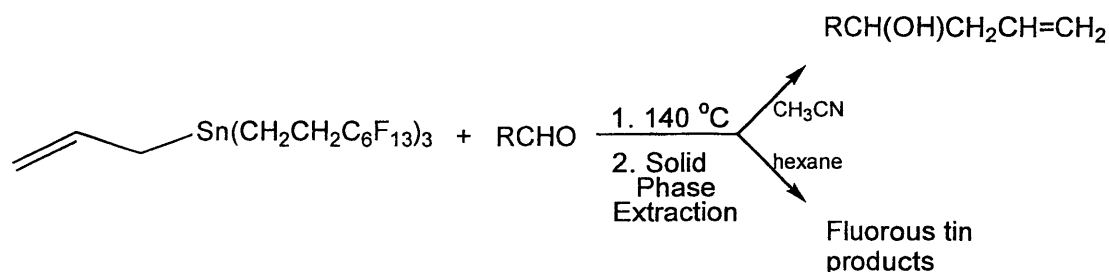
Hydrocarbon polymers can be solubilised in  $\text{scCO}_2$  by attaching fluorinated sidechains such as perfluorooctylacetates, as demonstrated by Hsiao *et al*.<sup>68</sup> Using this approach, a variety of Wilkinson's catalyst analogues were attached *via* the phosphine donor atoms to generate the catalytic polymers. Conversions of up to 70 % were observed for the hydrogenation of oct-1-ene and although "duplicate" experiments were carried out, detailed recovery and re-use was unfortunately not documented. However, the solubility of the polymer species was high and clearly represents a significant advance towards catalyst recovery in  $\text{scCO}_2$  systems.

### 1.5.2. Fluorous Solid Phase Separation (and 'Light Fluorous Synthesis')

Chromatography is an effective method of separation that is used to isolate and purify compounds, often of similar chemical composition. Essentially, the process relies upon the different extent to which the components of a mixture of compounds adhere to a stationary phase, usually alumina or silica gel. By passing the mixture down a column of the finely divided adsorbent, molecules of higher polarity are retained to a greater extent than non-polar compounds. Effective separation is achieved by tailoring the polarity of the liquid phase (eluent), in order to carry the components of the mixture down the column at different rates.

Recently, a new technique has been developed, termed ‘fluorous solid phase extraction’. This uses a modified stationary phase which is silylated with  $\text{ClSi}(\text{Me})_2\text{CH}_2\text{CH}_2\text{C}_6\text{F}_{13}$ .<sup>69</sup> Consequently, the affinity of the column towards organic components is completely reversed and since fluorinated molecules interact with the modified surface these are retained selectively.

Applications of fluorous reverse phase silica gel are still emerging, but essentially there are two types; the separation of fluorinated metal components and ‘fluorous tagged reagents / products’ from reaction mixtures. The first method has been used in the allylation of aldehydes to allylic alcohols by the fluorinated allyl tin reagent (**Scheme 1.17**).<sup>70</sup>



**Scheme 1.17**

The crude reaction mixture is loaded directly onto the fluorous column where the organic products are eluted with acetonitrile, and then a non-polar solvent, *i.e.* hexane (or a fluorous solvent), is used to elute the fluorinated tin by-products. A variety of aldehydes have been investigated to analyse their compatibility with this methodology and compared to the results obtained using a liquid-liquid biphasic extraction. In all cases, the yield was higher, but the percentage purity varied with different substrates. In most of the reactions the values were comparable, whilst some exhibited a distinct enhancement ( $\text{PhCH}_2\text{CH}_2\text{CHO} = 100\%$ , *c.f.* 88% for liquid-liquid extraction).

In a development of fluorous reverse phase silica gel chemistry, Curran has investigated the separation of a variety of fluorinated phosphines and the derived phosphine oxides. A range of linear chain and branched chain fluorinated phosphines were analysed (**Figure 1.17**).<sup>71</sup>

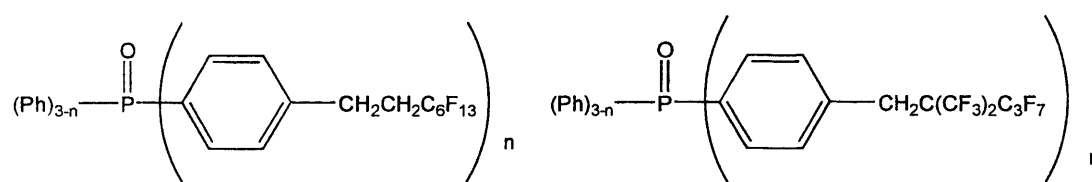
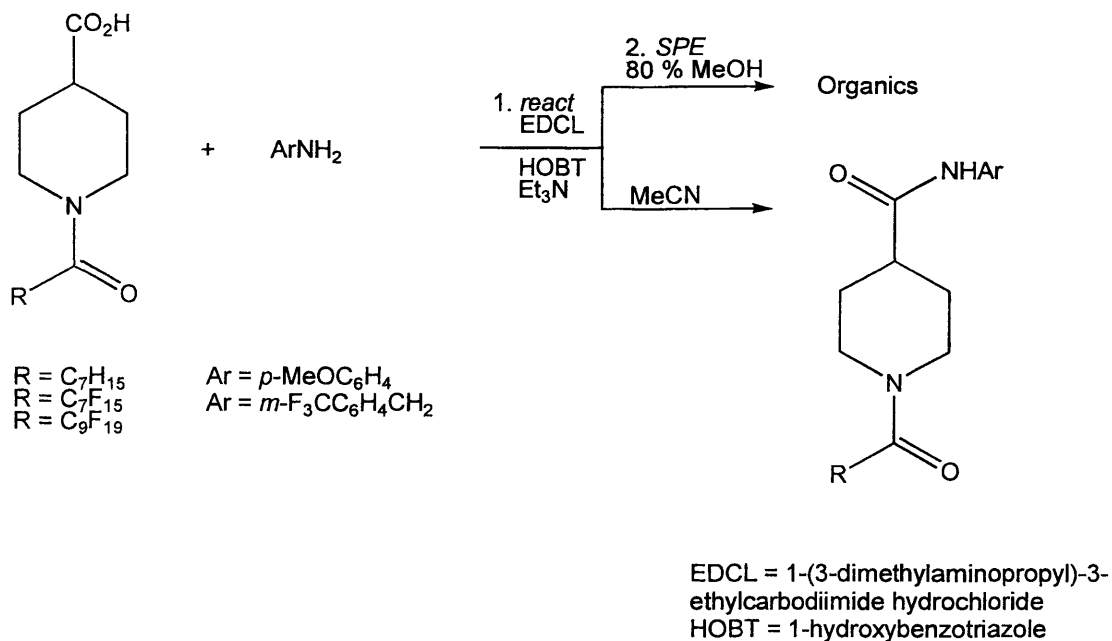


Figure 1.17

By implementing a solvent gradient beginning with 80 % MeOH / H<sub>2</sub>O and increasing to 100 % MeOH, followed by a second gradient of 90 % MeOH / THF, the authors were able to selectively elute the compounds on the basis of increasing fluorine content. The phosphine oxides were eluted, on average, 1-3 minutes before the analogous phosphines due to the higher polarity of the initial solvent mixture. Analysis of the results, however, leads to the inevitable conclusion that the compounds are being separated upon the basis of their polarity, as much as the total fluorine content, a feature which the authors concede may be “*probably more important*”. A simple investigation reveals that many of the fluorine phosphine oxides, especially the highly fluorinated compounds are virtually insoluble in the eluting mixture of MeOH / H<sub>2</sub>O. As a consequence, certain aspects of the separations detailed are simply filtrations. However, the results clearly demonstrate the efficiency of the process, attaining separation between very similar fluorine derivatised-phosphines, which would not be possible using standard non-fluorinated silica gel.

The second form of solid phase separation has been termed ‘Light Fluorine Synthesis’ and involves tagging an organic substrate with a perfluoroalkyl substituent (termed *fluorine tags*) to enable separation of the resultant product by fluorine reverse phase silica gel.<sup>72</sup> Potentially this type of extraction has many advantages over standard fluorine biphasic catalysis. The fluorinated tags do not need to be as large (or as great in number) as the fluorinated ponytails required to produce solubility in fluorine solvents, as the moiety is simply used as an anchor to attach to the fluorine surface. Consequently, the technique avoids the use of costly perfluorocarbon solvents and in fact, the tagged molecules have little or no solubility in these media. They are, however, soluble in common organic solvents, and this widens the synthetic scope of this methodology.

Once again, synthetic examples of this new ‘Light Fluorine Synthesis’ are still emerging. A recent example highlights the facile fluororous / organic separation achievable with common laboratory solvents.<sup>73</sup> The coupling of tagged acids with amines to generate amides was investigated and compared to an analogous hydrocarbon system (**Scheme 1.18**).

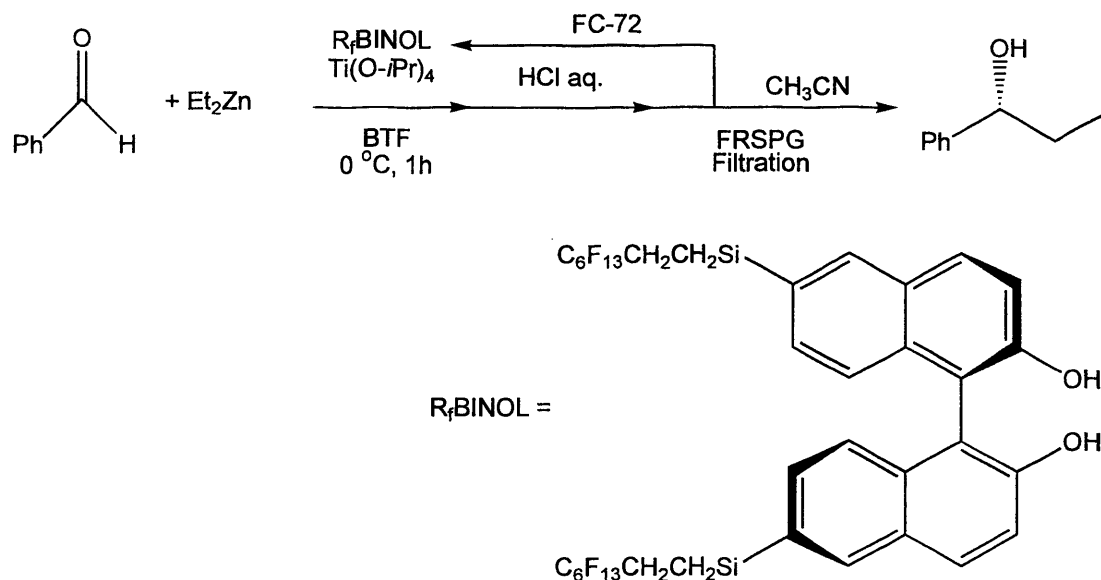


**Scheme 1.18**

When the reaction was carried out with the hydrocarbon tagged-reagents, the solid phase extraction (SPE) proved to be ineffective, with the product, excess reagents and reagent by-products all contained in the aqueous methanol fraction. When the fluorine-tagged reagents were used, however, the coupled product had been retained selectively by the stationary phase and was consequently eluted from the column by acetonitrile. From the results obtained with this preliminary system, Curran synthesised a library of amide products, achieving high yields and, in most cases, excellent purities.

Curran and Pozzi have recently addressed the development of this approach toward catalytic processes in two separate publications. Curran has investigated the recovery and re-use of fluororous chiral BINOL ligands for the asymmetric addition of diethylzinc to aromatic aldehydes.<sup>74</sup> The reactions were carried out in

benzotrifluoride (BTF), a fluorous hybrid solvent, to enable both the fluorous and organic components to dissolve (**Scheme 1.19**).



**Scheme 1.19**

The crude reaction mixture was loaded onto a FRPSG column, where elution with acetonitrile yielded the chiral product. A second elution by perfluorohexane enables the ligand to be recovered, which could be recycled into successive reactions without further purification. This procedure is, in many respects, an extension of the light fluorous synthesis / tagged reagent approach. In an attempt to isolate and recycle a discrete catalyst molecule, Pozzi has recently explored the retention of a fluorous derivatised [Co(salen)] complex on FRPSG.<sup>44</sup> Unfortunately, although the catalyst was selectively isolated, elution was difficult to achieve, with just 50 % recovery obtained for the best solvent (toluene). Elemental analysis proved that the cobalt complex remained on the column, which therefore negated the possibility of re-using the catalyst.

## 1.6. Miscellaneous Fluorous Chemistry

Several novel approaches to fluorous phase chemistry have been documented which are either specific or unique to a certain area of chemistry.

Ultimately, the underlying principles of efficient separation and recovery are similar to the systems documented above. However, they are discussed here to illustrate the breadth of chemistry in this rapidly expanding area of research.

### 1.6.1. Fluorous Triphasic Reactions

In an extension to his pioneering ‘Light Fluorous Synthesis’ approach, Curran has recently disclosed the application of a three phase system, which aims to reduce the loss of fluorous solvents, and also minimise the degree of fluorination required to achieve efficient separation.<sup>75</sup> The triphase employed consists of two organic phases separated by a fluorous solvent partition at the base of a U-tube (Figure 1.17). The concept is that substrates are added to one of the organic phases and eventually collected, pure, in the second organic phase following diffusion through the lower fluorous phase. Curran highlights the utilisation of this method for the removal of a fluorous tag from a precursor, whilst simultaneously isolating undesired organic impurities from the final substrate. By adding a reaction mixture and a detagging reagent to the first organic phase, migration of the tagged reagent into the fluorous phase subsequently occurs. Removal of the tag then takes place at the interface with the second organic phase, at which point the product is no longer soluble in the fluorous phase. Decantation of the second organic phase liberates the desired product.

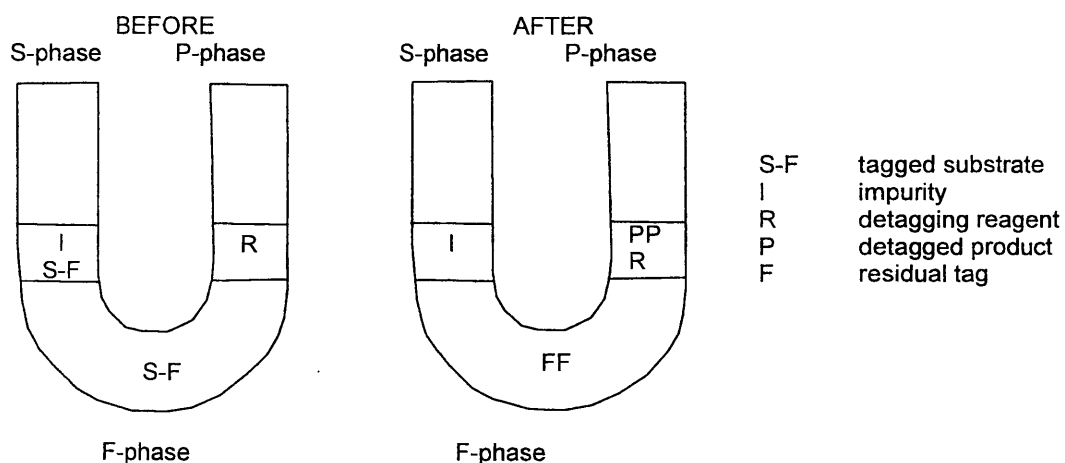
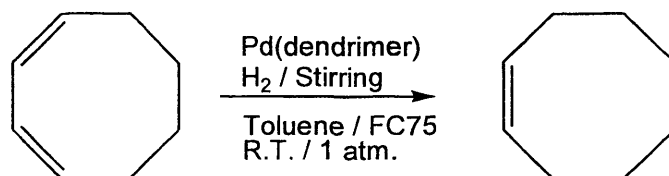


Figure 1.18

Curran postulated that the detagging reaction drives the non-equilibrium across through the fluoruous phase. Investigations into this novel regime are still in progress.

### 1.6.2. Fluorous Nanoparticles

Recently, the boundary between homogeneous and heterogeneous catalysis has been further diminished by the advent of fluorous-soluble dendrimer-encapsulated palladium nanoparticles.<sup>76</sup> Due to the increase in surface area with decreasing particle size, nanoparticles are the most efficient type of heterogeneous catalysis.<sup>77</sup> However, colloidal particles are difficult to isolate from the reaction mixture and are, therefore, limited in terms of their re-use in catalytic processes. The introduction of non-covalently modified perfluoropolyethers into the catalyst-carrying dendrimer [poly(amidoamine) – PAMAM], renders the particles preferentially soluble in the fluorous phase of a toluene / perfluoro-2-butyltetrahydrofuran (FC-75) biphase. The catalytic activity of this system was investigated for the hydrogenation of a variety of alkenes (**Scheme 1.20**).

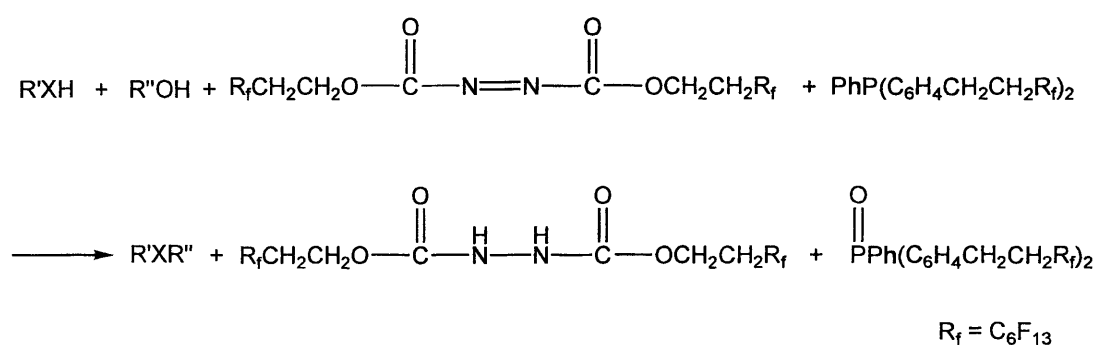


**Scheme 1.20**

The product yields obtained were an order of magnitude lower than those reported for a polymer supported Pd(0) catalyst. However, the catalytic viability of the system was clearly demonstrated by the fact that the fluorous phase could be recycled many times (twelve times with minimal loss of activity), and no leaching of the catalyst was observed.

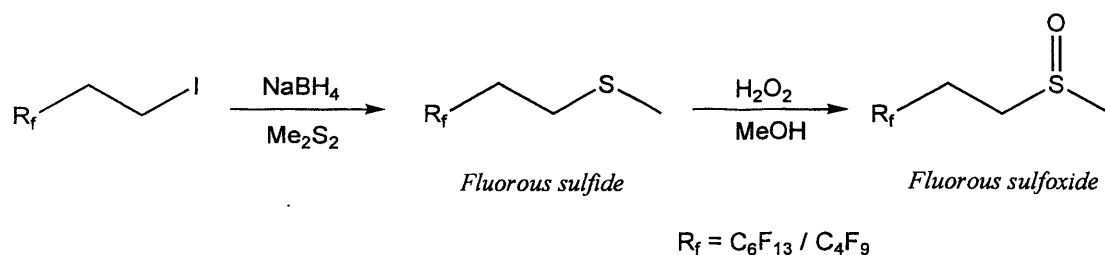
### 1.6.3. Fluorous Reagents

Several protocols for the development of organic reagents have been described recently. These include Swern,<sup>78</sup> Corey Kim<sup>78</sup> and Mitsunobu reagents.<sup>79</sup> With the Mitsunobu reagents, Curran has built upon the existing chemistry of fluorinated phosphines (see section 1.4.3.), and utilised these in combination with a new fluorous azodicarboxylate to perform the coupling reaction between an acidic pronucleophile and an alcohol (**Scheme 1.21**).<sup>79</sup>



**Scheme 1.21**

The reagents are isolated *via* a FRPSG filtration and then regenerated by a relatively straightforward procedure. The Swern and Corey Kim reactions both utilise fluorous substituted sulfur compounds to effect oxidation reactions. In the Swern reaction, dimethyl sulfoxide is used to convert primary and secondary alcohols to aldehydes and ketones. Unfortunately, the by-product of this process is the stoichiometric generation of dimethyl sulfide. As a consequence, the large-scale implementation of this reaction has been negated due to the environmental hazard arising from this toxic compound. To improve the viability of this process, Crich and Neelamkavil synthesised a fluorous analogue of DMSO by reacting 1*H*,1*H*,2*H*,2*H*-perfluorooctyl iodide with dimethyl disulfide in the presence of base (**Scheme 1.22**).<sup>78</sup>



Scheme 1.22

Under standard Swern reaction conditions, the fluorosulfoxide was found to function as an efficient oxidant for a variety of aldehydes and ketones. Upon completion of the reaction, the reagent was extracted into a fluorosolvent (FC72), re-oxidised by hydrogen peroxide and then re-used. In a similar fashion, the authors have also investigated a range of Corey Kim oxidations in which alcohols are converted to aldehydes and ketones.<sup>78</sup> However, this reaction utilises the sulfide rather than the sulfoxide, in the presence of isothiocyanate (NCS). Once again, excellent conversions were observed, although care was required to ensure stoichiometric quantities of the fluorosulfide and NCS were used to prevent oxidation to the sulfoxide, which could not be recovered by the fluorosolvent extraction due to its higher polarity.

### 1.7. Objectives

The aims of this research encompass many aspects of organic synthesis, from synthetic strategies to the final purification of the product. Each phase of the work will attempt to exploit the advantages of modern technology to achieve more efficient synthesis on both a laboratory and industrial scale. The main features that have been targeted are:

- ❖ **The ability to separate catalysts / metal reagents from organic products utilising fluorosolvent separation technology (liquid / liquid extraction and solid phase extraction)**

- ❖ **The potential to incorporate highly specific and / or reactive metals and reagents which are currently *taboo* for fine chemical and pharmaceutical synthesis**
- ❖ **The enhancement of reactivity and / or selectivity of catalysts as a consequence of the powerful electron withdrawing effect of fluorine containing moieties**
- ❖ **The maximisation of catalyst activity, turnover rates and recovery by virtue of recycling the fluororous phase over repeated catalytic cycles**

At the core of this project was the investigation of three, related groups of ligands with perfluoroalkyl side chains:

- ❖ **Perfluorinated carboxylates** –  $\text{CF}_3(\text{CF}_2)_n\text{COO}^-$  ( $n = 3 - 16$ )
- ❖ **2H,2H,3H,3H-Perfluorinated carboxylates** -  
 $\text{CF}_3(\text{CF}_2)_n\text{CH}_2\text{CH}_2\text{COO}^-$  ( $n = 5 - 9$ )
- ❖ **Fluorous-derivatised  $\beta$ -diketonate ligands** –  $\text{CF}_3(\text{CF}_2)_n\text{C}(\text{O})\text{CH}-$   
 $\text{C}(\text{O})(\text{CF}_2)_n\text{CF}_3^-$

These ligands were chosen on the basis of the wide range of processes that are catalysed by the resulting complexes of the hydrocarbon analogues. In certain cases, an extensive fluororous chemistry is already established; in these systems, the existing work will be built upon and enhanced. Where possible the novel technologies will be used, in order to facilitate catalyst recovery / re-use and / or product / by-product separation.

## 1.8. References for Chapter 1

- [1] J.S. Früchtel and G. Jung, *Angew. Chem. Int. Ed. Engl.*, 1996, **35**, 17.
- [2] D.P. Curran, *Angew. Chem. Int. Ed. Engl.*, 1998, **37**, 1174.
- [3] D.F. Shriver, P.W. Atkins and C. H. Langford. ‘Inorganic Chemistry’, (second edition). 1992. Oxford.
- [4] B. Cornils and W.A. Herrmann. ‘Applied Homogeneous Catalysis with Organometallic Compounds’, 2000. Wiley-VCH.
- [5] I.T. Horváth, *Acc. Chem. Res.*, 1998, **31**, 641.
- [6] H.H. Storch, N. Golombic and R.B. Anderson, ‘The Fischer-Tropsch and Related Syntheses, Wiley, Chapman and Hall, New York, London, 1951.
- [7] G.W. Parshall and R.E. Putscher, *J. Chem. Educ.*, 1986, **63**, 189.
- [8] Shell Dev. Co. (S.R. Baur, H. Chung, P.W. Glockner, W. Keim and H. van Zwet), US 3.635.937 (1972).
- [9] W.A. Herrmann and C.W. Kohlpainter, *Angew. Chem. Int. Ed. Engl.*, 1993, **32**, 1524.
- [10] K.V. Katti, H. Gali, C.J. Smith and D.E. Berning, *Acc. Chem. Res.*, 1999, **32**, 9.
- [11] W.A. Herrmann, C.W. Kohlpainter, H. Bahrmann and W. Konkol, *J. Mol. Catal.*, 1992, **73**, 191.
- [12] B. Cornils and E. Kuntz, *J. Organomet. Chem.*, 1995, **502**, 177.
- [13] J.M. Grosselin, C. Mercier, G. Allmang and F. Grass, *Organometallics*, 1991, **10**, 2126.
- [14] J. Bakos, A. Orosz, B. Heil, M. Laghmari, P. Lhoste and D. Sinou, *Chem. Commun.*, 1991, 1684; C. Lensink and J. de Vries, *Tetrahedron Asymmetry*, 1992, **3**, 235.
- [15] H. Bahrmann and H. Bach, *Phosphorus, Sulfur, Silicon and Relat. Elem.*, 1987, **30**, 611.
- [16] J.P. Arhancet, M.E. Davis, J.S. Merola and B.E. Hanson, *Nature*, 1989, **339**, 454.
- [17] J.D. Holbrey and K.R. Seddon, *Clean Products and Processes*, 1999, **1**, 223; P. Wasserscheid and W. Keim, *Angew. Chem. Int. Ed. Engl.*, 2000, **39**, 3772.
- [18] M.J. Earle and K.R. Seddon, *Pure Appl. Chem.*, 2000, **7**, 1391.

- [19] R. Sheldon, *Chem. Commun.*, 2001, 2399.
- [20] G.W. Parshall, *J. Am. Chem. Soc.*, 1972, **94**, 8716.
- [21] A.L. Monteiro, F.K. Zinn, R.F. de Souza and J. Dupont, *Tetrahedron Asymmetry*, 1997, **8**, 177.
- [22] D.E. Kaufmann, M. Nouroozian and H. Henze, *Synlett*, 1996, 1091.
- [23] A.J. Carmichael, M.J. Earle, J.D. Holbrey, P.B. M<sup>c</sup>Cormac and K.R. Seddon, *Org. Lett.*, 1999, **1**, 997.
- [24] G.E. May, *Chemistry in Britain*. 1997, **8**, 34.
- [25] L.C. Clark. “Perfluorinated Liquids in Biology and Medicine.” Applications of Organic Fluorine Compounds II, American Chemical Society, 1995, pp.1138-1142.
- [26] A.E. Feiring. “Fluoroplastics”, Chapter 15, pp.339-371. ‘Organofluorine Chemistry: Principles and Commercial Applications’, R.E. Banks. Plenum Press, New York, 1994.
- [27] I.T. Horváth and J. Rábai, *Science*, 1994, **266**, 72.
- [28] J.A. Gladysz and D.P. Curran, *Tetrahedron*, 2002, **58**, 3823.
- [29] L.P. Barthel-Rosa and J.A. Gladysz, *Coord. Chem. Rev.*, 1999, **190-192**, 587.
- [30] E.L. Kiss, I. Kövesdi and J. Rábai, *J. Fluorine Chem.*, 2001, **108**, 95; F.T.T. Huque, K. Jones, R.A. Saunders and J. A. Platts, *J. Fluorine Chem.*, 2002, **115**, 119.
- [31] R.H. Fish, *Chem. Eur. J.*, 1999, **5**, 1677; E. de Wolf, G. van Koten and B. Deelman, *Chem. Soc. Rev.*, 1999, **28**, 37; E.G. Hope and A.M. Stuart, *J. Fluorine Chem.*, 1999, **100**, 75; P. Bhattacharyya, B. Croxtall, J. Fawcett, J. Fawcett, D. Gudmunsen, E.G. Hope, R.D.W. Kemmitt, D.R. Paige, D.R. Russell, A.M. Stuart and D.R.W. Wood, *J. Fluorine Chem.*, 2000, **101**, 247.
- [32] D.F. Foster, D. Gudmunsen, D.J. Adams, A.M. Stuart, E.G. Hope, D.J. Cole-Hamilton, G.P. Schwarz and P. Pogorzelec, *Tetrahedron*, 2002, **58**, 3901; D.F. Foster, D. Gudmunsen, D.J. Adams, A.M. Stuart, E.G. Hope and D.J. Cole-Hamilton, *Chem. Commun.*, 2002, 722.
- [33] D. Rutherford, J.J.J. Juliette, C. Rocaboy, I.T. Horváth and J.A. Gladysz, *Catal. Today*, 1998, **42**, 381.

- [34] E.G. Hope, R.D.W. Kemmitt, and A.M. Stuart, *J. Chem. Soc., Dalton Trans.*, 1998, 3765; S. Kainz, D. Koch, W. Baumann and W. Leitner, *Angew. Chem. Int. Ed. Engl.*, 1997, **36**, 1628; E.G. Hope, R.D.W. Kemmitt, D.R. Paige and A.M. Stuart, *J. Fluorine Chem.*, 1999, **99**, 197.
- [35] E. de Wolf, A.L. Spek, B.W.M. Kuipers, A.P. Philpse, J.D. Meeldijk, P.H.H. Bomans, P.M. Frederik, B-J. Deelman and G. van Koten, *Tetrahedron*, 2002, **58**, 3911; E. de Wolf, B. Richter, B-J. Deelman and G. van Koten, *J. Org. Chem.*, 2000, **65**, 5424.
- [36] E. de Wolf, B. Richter, B-J. Deelman and G. van Koten, *J. Org. Chem.*, 2000, **65**, 3887.
- [37] G. Pozzi, M. Cavazzini, S Quici, D. Maillard and D. Sinou, *J. Mol. Catal.*, 2002, **182-183**, 455.
- [38] A. Klose and J.A. Gladysz, *Tetrahedron*, 1999, **10**, 2665.
- [39] M. Cavazzini, S Quici, G. Pozzi, D. Maillard and D. Sinou, *Chem. Comm.*, 2001, 1220.
- [40] D.J. Birdsall, E.G. Hope, A.M. Stuart, W. Chen, Y. Hu and J. Xiao, *Tetrahedron Lett.*, 2001, **42**, 8551.
- [41] G. Pozzi, F. Cinato, F. Montanari and S Quici, *Chem. Comm.*, 1998, 877.
- [42] M. Cavazzini, A. Manfrdi, F. Montanari, S Quici and G. Pozzi, *Chem. Comm.*, 2001, 2171.
- [43] D. Maillard, G. Pozzi, S Quici and D. Sinou, *Tetrahedron*, 2002, **58**, 3971.
- [44] M. Cavazzini, S Quici and G. Pozzi, *Tetrahedron*, 2002, **58**, 3943.
- [45] G. Pozzi, F. Montanari and S. Quici, *Chem. Comm.*, 1997, 69. Y. Kuroda, H. Murase, Y. Suzuki, H. Ogoshi, *Tetrahedron Lett.*, 1989, **30**, 2411.
- [46] S. Colonna, N. Gaggero, F. Montanari, G. Pozzi and S. Quici, *Eur. J. Org. Chem.*, 2001, 181.
- [47] B. Betzemeier, F. Lhermitte and P. Knochel, *Tetrahedron Lett.*, 1998, 6679.
- [48] I. Klement, H. Lutjens and P. Knochel, *Angew. Chem. Int. Ed. Engl.*, 1997, **36**, 1454.
- [49] F. Benvenuti, C. Carlini, M. Marchionna, A.M.R. Galletti and G. Sbrana, *J. Mol. Catal.*, 2002, **178**, 9; F. Benvenuti, C. Carlini, M. Marchionna, A.M.R. Galletti and G. Sbrana, *J. Organomet. Chem.*, 2001, **622**, 286.

- [50] J. Loiseau, E. Fouquet, R.H. Fish, J. Vincent and J. Verlhac, *J. Fluorine Chem.*, 2001, **108**, 195.
- [51] J.M. Vincent, A. Rabion, V.K. Yachandra and R.H. Fish, *Angew. Chem. Int. Ed. Engl.*, 1997, **36**, 2346.
- [52] A. Endres and G. Maas, *Tetrahedron Lett.*, 1999, **40**, 6365; A. Biffis, E. Castello, M. Zecca and M. Basato, *Tetrahedron*, 2001, **57**, 10391; A. Endres and G. Maas, *J. Organomet. Chem.*, 2002, **643-644**, 174; A. Endres and G. Maas, *Tetrahedron*, 2002, **58**, 3999.
- [53] A. Padwa, D.J. Austen, A.T. Price, M.A. Semones, M.P. Doyle, M.N. Protopopova, R. Winchester and A. Tran, *J. Am. Chem. Soc.*, 1993, **115**, 8669.
- [54] M.P. Doyle, G.A. Devora and A.O. Nefedov, *Organometallics*, 1993, **12**, 11.
- [55] M.P. Doyle and M.S. Shanklin, *Organometallics*, 1992, **11**, 549.
- [56] C. Braddock, *Green Chemistry*, 2001, **3**, G26.
- [57] A.G.M. Barrett, D.C. Braddock, R.M. McKinnel and F.J. Waller, *Synlett.*, 1999, 1489.
- [58] A.G.M. Barrett, D.C. Braddock, D. Catterick, D. Chadwick, J.P. Henschke and R.M. McKinnell, *Synlett*, 2000, 847.
- [59] A.G. Barrett, N. Bouloc, D.C. Braddock, D. Catterick, D. Chadwick, A.J.P. White and D.J. Williams, *Tetrahedron*, 2002, **58**, 3835.
- [60] I. Kani, M.A. Omary, M.A. Rawashdeh-Omary, Z.K. Lopez-Castillo, R. Flores, A. Akgerman and J.P. Fackler, Jr., *Tetrahedron*, 2002, **58**, 3923.
- [61] S. Kainz, D. Koch, W. Baumann and W. Leitner, *Angew. Chem. Int. Ed. Engl.*, 1997, **36**, 1628.
- [62] A.V. Yazdi and E.J. Beckman, *Ind. Eng. Chem. Res.*, 1996, **35**, 3644.
- [63] M.A. Carroll and A.B. Holmes, *Chem. Comm.*, 1998, 1395.
- [64] D.K. Morita, D.R. Pesiri, S.A. David, W.H. Glaze and W. Tumas, *Chem. Comm.*, 1998, 1397.
- [65] S. Kainz, A. Brinkmann, W. Leitner and A. Pfaltz, *J. Am. Chem. Soc.*, 1999, **121**, 6421.
- [66] A. Wegner and W. Leitner, *Chem. Comm.*, 1999, 1583.
- [67] H. Hori, C. Six and W. Leitner, *Macromolecules*, 1999, **32**, 3178.

- [68] Y.L. Hsiao, E.E. Maury, J.M. Desimone, S. Mavson and K.P. Jonstan, *Macromolecules*, 1995, **28**, 8159.
- [69] S. Kainz, Z. Luo, D.P. Curran and W. Leitner, *Synthesis*, 1998, 1425. D.P. Curran, *Green Chemistry*, 2001, **3**, G3.
- [70] D.P. Curran S. Hadida and M. He, *J. Org. Chem.*, 1997, **62**, 6714.
- [71] Q. Zhang, Z. Luo and D.P. Curran, *J. Org. Chem.*, 2000, **65**, 8866.
- [72] Q. Zhang, Z. Luo, Y. Oderaotoshi and D.P. Curran, *Science*, 2001, **291**, 1766. D.P. Curran, *Pure Appl. Chem.*, 2000, **72**, 1649.
- [73] D.P. Curran and Z. Luo, *J. Am. Chem. Soc.*, 1999, **121**, 9069.
- [74] Y. Nakamura, S. Takeuchi, K. Okumura, Y. Ohgo and D.P. Curran, *Tetrahedron*, 2002, **58**, 3963.
- [75] Y. Nakamura, B. Linclau and D.P. Curran, *J. Am. Chem. Soc.*, 2001, **123**, 10119.
- [76] V. Chechik and R.M. Crooks, *J. Am. Chem. Soc.*, 2000, **122**, 1243.
- [77] L.N. Lewis, *Chem. Rev.*, 1993, **93**, 2693.
- [78] D. Crich and S. Neelamkavil, *J. Am. Chem. Soc.*, 2001, **123**, 7449. D. Crich and S. Neelamkavil, *Tetrahedron*, 2002, **58**, 3865.
- [79] S. Dandapani and D.P. Curran, *Tetrahedron*, 2002, **58**, 3855.

## 2. Fluorinated Beta-Diketones – Synthesis and Coordination Chemistry

### 2.1. Introduction

$\beta$ -Diketonates are bidentate oxygen donor species, classified as ‘hard’ ligands according to Pearson’s “Hard and Soft Acid and Base Principle”.<sup>1</sup> However, due to the possible delocalisation of charge over three carbon atoms and two oxygen atoms (Figure 2.1),  $\beta$ -diketonates exhibit an extensive coordination chemistry to a wide range of both hard and soft metal centres.<sup>2</sup> In particular, 2,4-pentanedionato (acetylacetonato or ‘acac’) (II), and its partially fluorinated analogue, 1,1,1,3,3,3-hexafluoro-2,4-pentanedionato (hexafluoroacetylacetonato or ‘hfacac’) (III), have been thoroughly investigated, both in terms of the homoleptic and mixed ligand complexes.<sup>3</sup>

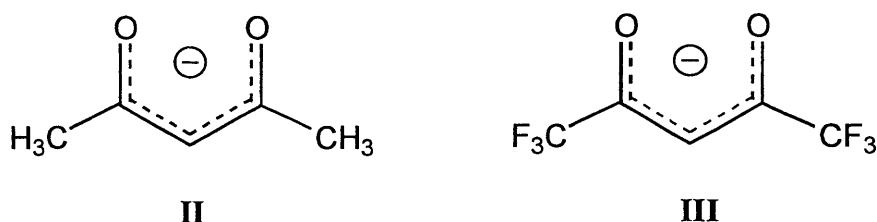


Figure 2.1

A wide range of catalytic processes has been documented for the acac complexes,<sup>4</sup> whilst the hfacac species are used in the chemical vapour phase deposition of a number of metal films. For example, tris(hexafluoroacetylacetonate) iron (III) is used in the deposition of iron oxide films.<sup>5</sup> Hybrid organofluorine ligands have also been exploited in terms of their ability to coordinate to lanthanide ( $\text{Ln}^{3+}$ ) cations.<sup>6</sup> The partially fluorinated  $\beta$ -diketonate 6,6,7,7,8,8,8-heptafluoro-2,2-dimethyl-3,5-octanedionato (fod), (Figure 2.2), affords lanthanide complexes that are soluble in a wide range of organic solvents.

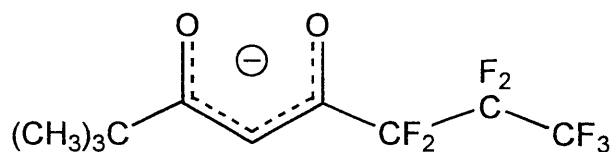


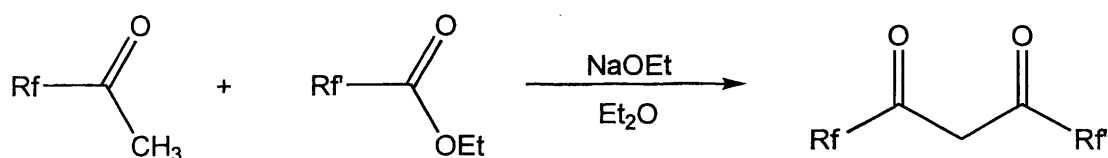
Figure 2.2

Due to the volatility of these species, they are utilised industrially as precursors for the synthesis of lanthanide-containing superconductors. Also, however, their solubility in organic solvents enables them to function as NMR shift reagents. The availability of vacant coordination sites allows ligands to bind to the metal centre and experience the local magnetic field of the paramagnetic lanthanide atom. As a consequence, protons of the ligand that are closest to the donor atom are shifted, thus simplifying complex coupling patterns where signals are overlapping.<sup>6</sup>

Recently, interest has focussed upon rendering metal  $\beta$ -diketonate complexes fluorous soluble for use in biphasic catalytic applications<sup>7,8</sup> and the ligand which has been investigated the most is 1,1,1,2,2,3,3,4,4,5,5,6,6,7,7,-11,11,12,12,13,13,14,14,15,15,16,16,17,17,17-triacontafluoro-heptadecane-8,10-dione  $[\text{F}_{15}\text{C}_7\text{C}(\text{O})\text{CH}_2\text{C}(\text{O})\text{C}_7\text{F}_{15}](\text{I})$ , which was first investigated by Tatlow in 1971.<sup>9</sup> A discussion of the catalytic applications of this ligand is given in Chapter 3. Unfortunately, although complexes incorporating this ligand have been used catalytically, there is little characterisation data for any of them. Consequently, the actual composition of the catalyst / catalyst precursor(s) are unknown and one of the first objectives was to synthesize the new perfluorohexyl ligand  $[\text{F}_{13}\text{C}_6\text{C}(\text{O})\text{CH}_2\text{C}(\text{O})\text{C}_6\text{F}_{13}](\text{IV})$ , in order to investigate the coordination chemistry of these highly fluorinated  $\beta$ -diketones and to fully characterise the resulting complexes. However, the primary aim was to investigate the fluorous phase solubility of these species and to determine the extent of fluorination required to confer preferential solubility in liquid / liquid extraction and retention on FRP silica gel in solid / liquid extraction. To achieve these goals, the ligand synthesis was extended to an unsymmetrical species 1,1,1,5,5,6,6,7,7,8,8,9,9,10,10,10-hexadecafluoro-decane-2,4-dione  $[\text{F}_3\text{CC}(\text{O})\text{CH}_2\text{C}(\text{O})\text{C}_6\text{F}_{13}](\text{V})$ , and the analysis of the coordination chemistry was broadened to include **II** and **III**. The analogous unsymmetrical perfluoroheptyl / trifluoromethyl ligand had been synthesised previously by Tatlow, but no coordination chemistry had been documented, besides the copper complex  $[\text{Cu}(\text{CF}_3\text{C}(\text{O})\text{CHC}(\text{O})\text{C}_7\text{F}_{15})_2]$  which had been generated during the synthetic procedure.<sup>9</sup>

## 2.1. Ligand Synthesis

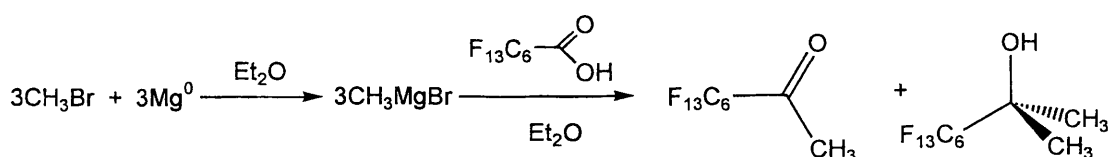
The general synthetic procedure for synthesising fluorinated  $\beta$ -diketones is essentially that described by Massyn, Pastor and Cambon, and is the condensation reaction between a fluorinated methyl ketone and a fluorinated ester, in the presence of base (**Scheme 2.1**):<sup>10</sup>



**Scheme 2.1**

### 2.2.1. Synthesis of C<sub>6</sub>F<sub>13</sub>C(O)CHC(O)C<sub>6</sub>F<sub>13</sub> (IV).

The synthesis of the symmetrical tridecafluorohexyl  $\beta$ -diketone (IV) began with the formation of the perfluorohexyl methyl ketone following the procedure detailed by Kondo and Iwatsuki.<sup>11</sup> The method involved the synthesis of methyl magnesium bromide which was then reacted with perfluoroheptanoic acid (**Scheme 2.2**), but unfortunately, the reaction generated impure products in poor yields. The failure of this initial reaction was attributed, in part, to the volatility of the bromomethane which simply boiled out of solution. For this reason, subsequently commercial methyl magnesium bromide was employed to ensure that the reaction reached completion. It is interesting to note that the perfluorinated carboxylic acid requires a three molar excess of the Grignard reagent in order to generate the ketone. Consequently, the generation of a quantity of the tertiary alcohol is unavoidable, but fortuitously it is readily separable from the final product by vacuum distillation.<sup>11</sup>



**Scheme 2.2**

Following aqueous acidic work-up and vacuum distillation, the product was obtained as a clear colourless liquid in 60 % yield ( $\geq 30$  % tertiary alcohol, white solid). The perfluorohexyl methyl ketone was fully characterised by elemental analysis, mass spectrometry, infrared spectroscopy and NMR spectroscopy ( $^1\text{H}$ ,  $^{19}\text{F}$  and  $^{13}\text{C}$  nuclei). Comparison of the data obtained with the literature values for the analogous perfluoroheptyl derivatised species confirmed the formation of the desired compound.<sup>11</sup> Similarly, the tertiary alcohol by-product was characterised and compared to the literature analogue [ $\text{C}_7\text{F}_{15}\text{C}(\text{CH}_3)_2\text{OH}$ ].<sup>11</sup> Interestingly, the solid formed long needle shaped crystals on standing that enabled the crystal structure to be obtained (**Figure 2.1**). The compound exists as three unique molecules, differing by the arrangement of the perfluorohexyl units. The increased polarity of the alcohol group, imparted by its direct attachment to the fluororous ponytail, enables the molecule to undergo extensive hydrogen bonding throughout the crystal lattice. The O-H---O bonds form a continuous link down the z-axis of the structure, whilst extensive fluorine-fluorine interactions also occur between adjacent molecules. A table of crystal data and structure refinements are given in Appendix 1, whilst a complete collection of data for all the crystal structures contained in this thesis can be found on the accompanying CD-ROM.

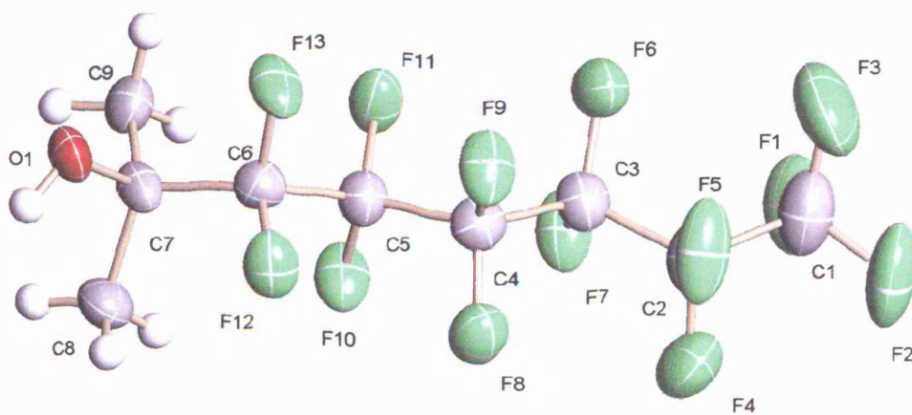
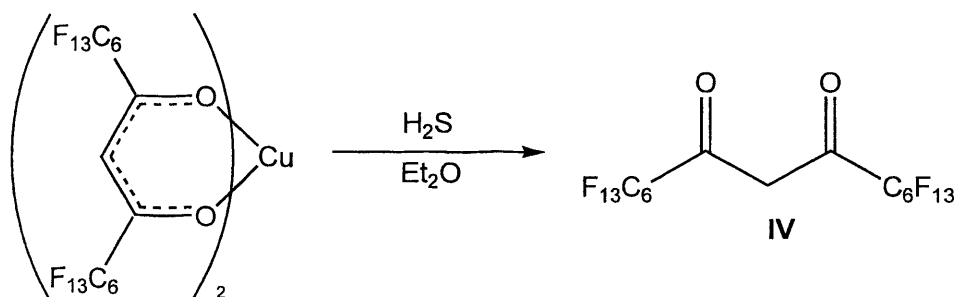


**Figure 2.1.** Crystal Structure of 2-methyl-3,3,4,4,5,5,6,6,7,7,8,8,8-tridecafluorooctan-2-ol.

The tridecafluorohexyl methyl ketone was reacted with commercially obtained ethyl perfluoroheptanoate in the presence of sodium ethoxide at 0 °C, according to **Scheme 2.1**. The reaction was maintained at this temperature for 12 hours, followed by 48 hours at room temperature. The yellow solution that was generated was quenched with dilute ethanoic acid before the addition of copper (II) acetate in order to generate a green copper  $\beta$ -diketonate complex. The motivation for this reaction was that the copper complex facilitated the removal of the ligand from the reaction mixture. It was found that this stage was crucial in purifying the final ligand. In order to proceed to the next stage, it was vital to obtain the copper complex as a very fine, pale green powder, which was only attainable after several washes with water and light petroleum ether. The intermediate was then dried under high vacuum for several hours to remove volatiles. Further discussion of this copper complex (**VIb**) is given in section 2.2.3.

Reaction of the copper intermediate with hydrogen sulfide (**Scheme 2.3**), regenerates the free ligand, which was then further purified by Kugelröhr distillation to yield the desired product as a viscous, colourless oil (34 % yield overall).



**Scheme 2.3**

The product was characterised by elemental analysis, mass spectrometry, infrared spectroscopy and NMR spectroscopy. When the ligand was examined by  $^1H$  NMR spectroscopy, the spectrum revealed that the molecule adopted exclusively the enol conformation in solution ( $CDCl_3$ ), with two signals at 9.21 ppm and 6.45 ppm attributable to the C-OH and C=C-H protons respectively (**Figure 2.2**):<sup>12</sup>

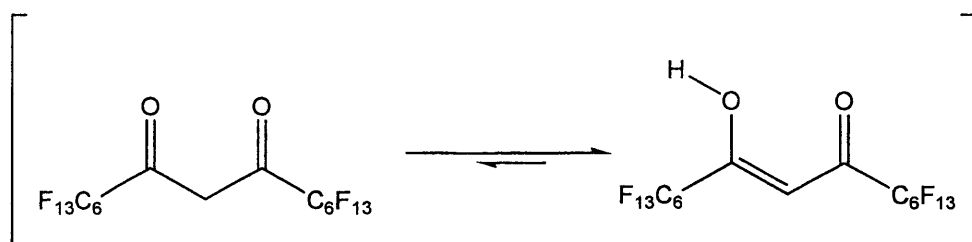


Figure 2.2

The  $^{13}\text{C}\{^1\text{H}\}$  NMR spectrum indicated that there was only one carbonyl carbon environment within the molecule; a triplet at 176.1 ppm due to coupling to the  $\alpha$ - $\text{CF}_2$ 's of the fluoruous ponytails. This can be rationalised by considering the geometry and bonding occurring within the ligand. The rate at which the enol tautomerisation occurs between the two carbonyls will be very fast and as a consequence, the NMR spectrum will observe the average structure of the two equivalent enol structures, which is symmetrical with regard to the carbon atoms, whilst still enabling the two protons to be distinct (Figure 2.3). The spectrum also exhibited resonances for the central 'pseudo-vinylic' carbon at 98.3 ppm, and a mixture of unresolved multiplets generated by the carbons of the fluoruous ponytails.

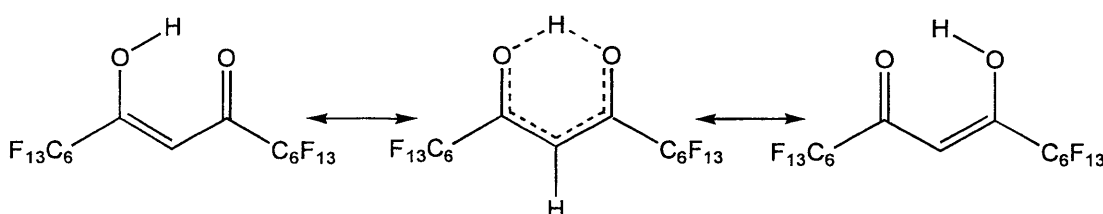


Figure 2.3

When the molecule was analysed by infrared spectroscopy, two signals were observed in the carbonyl region at  $1663\text{ cm}^{-1}$  and  $1616\text{ cm}^{-1}$ . These carbonyl stretching frequencies are quite diagnostic, with very similar values recorded in the literature for the perfluoroheptyl derivatised ligands prepared by Tatlow (see section 2.2.2. Table 2.1).<sup>9</sup> Point group symmetry confirms that two infrared active bands are predicted (the  $A_1$  and  $B_1$ ), due to the irreducible representation arising from the  $C_{2v}$  symmetry of the molecules.

**2.2.2. Synthesis of [CF<sub>3</sub>C(O)CHC(O)C<sub>6</sub>F<sub>13</sub>] (V) and [C<sub>7</sub>F<sub>15</sub>C(O)CHC(O)C<sub>7</sub>F<sub>15</sub>] (I).**

The unsymmetrical ligand [CF<sub>3</sub>C(O)CHC(O)C<sub>6</sub>F<sub>13</sub>] (V), and the perfluoroheptyl derivatised species [C<sub>7</sub>F<sub>15</sub>C(O)CHC(O)C<sub>7</sub>F<sub>15</sub>] (I), were prepared in an analogous fashion to (IV), in similar yields. As expected, the ligands exhibited similar characteristics to (IV); the enol tautomer was the dominant species in the <sup>1</sup>H NMR spectra for both compounds. However, where as (IV) and (V) were obtained as slightly viscous oils, (I) exists as a cream coloured solid. The spectroscopic data obtained for all of the ligands synthesised is summarised in **Table 2.1** below, and is compared to 1,1,1,3,3,3-hexafluoro-2,4-pentanedione and the literature data for the unsymmetrical perfluoroheptyl derivatised species that was reported previously.<sup>9</sup>

**Table 2.1.** Spectroscopic data for fluorinated β-diketonates

R <sup>1</sup> / R <sup>2</sup>	<sup>1</sup> H NMR Chemical Shift / ppm		Carbonyl Stretching Frequency / cm <sup>-1</sup>
	C=C-OH	C=C-H	
CF <sub>3</sub> / CF <sub>3</sub> (III)	12.9	6.35	~
CF <sub>3</sub> / C <sub>6</sub> F <sub>13</sub> (V)	9.95	6.25	1682 & 1622
CF <sub>3</sub> / C <sub>7</sub> F <sub>15</sub> <sup>9</sup>	12.98	6.40	1680 & 1625
C <sub>6</sub> F <sub>13</sub> / C <sub>6</sub> F <sub>13</sub> (IV)	9.21	6.45	1663 & 1616
C <sub>7</sub> F <sub>15</sub> / C <sub>7</sub> F <sub>15</sub> (I)	9.55	6.48	1675 & 1605

The <sup>1</sup>H NMR spectra of the ligands display an obvious similarity, with any variation in the resonances assigned to the enol protons attributable to the concentration variation of this broad diffuse peak.<sup>12</sup> As mentioned earlier, the infrared data are in precise agreement, and it is interesting to observe that the stretching frequencies recorded are very similar between the symmetrical ligands (I and IV), whilst the unsymmetrical derived ligands are virtually identical and at slightly higher frequency. Obviously, these trends arise due to the similar electronic environments of the corresponding ligand pairs and furthermore, it is reasonable to postulate that the higher frequency of the unsymmetrical ligands occurs due to the presence of the

three  $\alpha$ -fluorine atoms of the trifluoromethyl groups. All other spectroscopic data, including mass spectroscopy and elemental analysis, were in accordance with predicted values, confirming the formation of the desired products.

### 2.2.3. Characterisation of Copper $\beta$ -diketonate intermediates $[\text{Cu}(\text{R}_f\text{C}(\text{O})\text{CHC}(\text{O})\text{R}_f)_2(\text{OH}_2)_2]$ (**VIa-c**).

The green copper intermediate for the symmetrical perfluorohexyl  $\beta$ -diketone (**VIb**), was shown, by X-ray structural analysis, to be the *bis*-ligand, *bis*-aquo complex,  $[\text{Cu}(\text{C}_6\text{F}_{13}\text{C}(\text{O})\text{CHC}(\text{O})\text{C}_6\text{F}_{13})_2(\text{OH}_2)_2]$ . In order to obtain full characterisation data, the complex was re-synthesised using the purified ligand. However, although elemental analysis and infrared spectroscopy were recorded, the paramagnetism of the copper metal centre hampered further characterisation by NMR spectroscopy, whilst mass spectrometry data was inconclusive. In the solid state structure, (**Figure 2.4**) the molecule adopts a tetragonally distorted octahedral geometry with two elongated Cu-O bonds to the axial water molecules. This distortion arises due to the Jahn-Teller effect, which is typical for a  $\text{Cu}^{\text{II}}$   $d^9$  metal centre. This observation is in agreement with work previously carried out by Toscano *et al.* who synthesised the similar copper *bis*-1,1,1,2,2,3,3,7,7,8,8,9,9,9-tetradecafluorononane-4,6-dionate *bis* aquo complex  $[\text{Cu}(\text{C}_3\text{F}_7\text{C}(\text{O})\text{CHC}(\text{O})\text{C}_3\text{F}_7)_2(\text{OH}_2)_2]$ .<sup>13</sup>

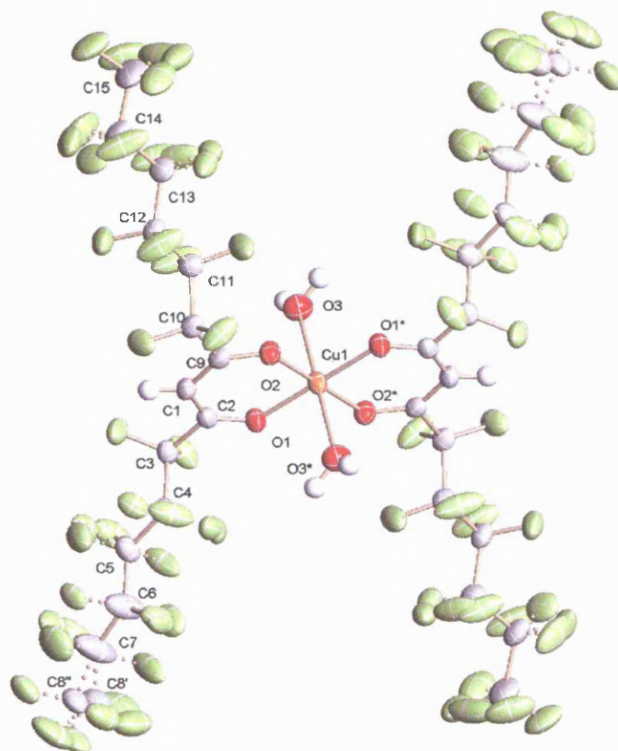


**Figure 2.4.** Crystal Structure of  $[\text{Cu}(\text{C}_6\text{F}_{13}\text{C}(\text{O})\text{CHC}(\text{O})\text{C}_6\text{F}_{13})_2(\text{OH})_2]$  (**VIb**).

All four perfluorohexyl chains exhibit considerable disorder beyond the  $\alpha\text{-CF}_2$  groups, however, due to the quality of the data obtained, it was possible to model the static disorder, which indicated the random distribution of a series of arrangements of the ponytails throughout the crystal lattice rather than the dynamic thermal libration of the  $\text{CF}_2$  units.

In a similar manner, the copper intermediate prepared during the synthesis of the unsymmetrical ligand (**V**) was re-synthesised in order to procure accurate characterisation data. Unfortunately, characterisation of the complex was limited to elemental analysis and infrared spectroscopy due to the paramagnetism of the copper metal centre. However, the data acquired through these techniques indicated the formation of the desired compound, although as for the symmetrical analogue, mass spectroscopy failed to reveal an informative trace. Fortuitously, crystals of the complex grew *via* a layered slow evaporation technique. The crystal structure (**Figure 2.5**) reveals that, in contrast to the symmetrical analogue, the fluorine ponytails adopt a regular linear arrangement in a much more ordered fashion.

However, the  $\alpha$ -CF<sub>3</sub> group is disordered across three sites in a well-recognised “propeller” pattern.

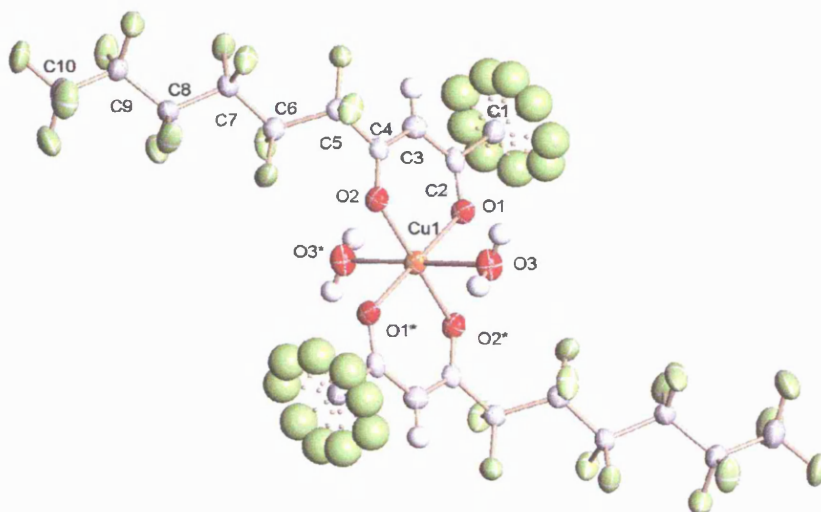


**Figure 2.5.** Crystal Structure of [Cu(CF<sub>3</sub>C(O)CHC(O)C<sub>6</sub>F<sub>13</sub>)<sub>2</sub>(OH<sub>2</sub>)<sub>2</sub>] (**VIa**).

As expected, the coordination geometry of the copper atom is very similar to that for **VIb**. **Table 2.2** reveals the almost identical bond lengths for the two complexes and also, the data for the similar tetradecafluorononane-4,6-dione complex [Cu(tdf)<sub>2</sub>(OH<sub>2</sub>)] is shown for comparison (the Cu-O bonds are labelled in accordance with the conventions in **Figures 2.4** and **2.5**). The Jahn-Teller effect is clearly apparent for all three complexes, indicated by the lengthened Cu-OH<sub>2</sub> bond lengths. The four shorter Cu-O bonds to the fluorinated  $\beta$ -diketonate ligands lie in the equatorial plane, completing the coordination sphere.

**Table 2.2.** Selected bond lengths for fluorinated copper  $\beta$ -diketonate complexes

Bond	<b>VIa</b> / Å	<b>VIb</b> / Å	[Cu(tdf) <sub>2</sub> (OH <sub>2</sub> )] / Å <sup>13</sup>
Cu(1)-O(1)	1.942(3)	1.9567(17)	1.941
Cu(1)-O(2)	1.939(3)	1.9485(16)	1.944
Cu(1)-O(3)(OH <sub>2</sub> )	2.334(3)	2.369(2)	2.363

The crystal-packing diagram for **VIa** also reveals that the molecules are stacked down the b-axis, with adjacent molecules linked by four intermolecular hydrogen bonds from the water hydrogen atoms to the oxygen atoms of the perfluoroalkylated  $\beta$ -diketonates. A similar effect is also observed in the crystal-packing diagram of  $[\text{Cu}\{\text{C}_6\text{F}_{13}\text{C}(\text{O})\text{CHC}(\text{O})\text{C}_6\text{F}_{13}\}_2(\text{H}_2\text{O})_2]$ , but only two hydrogen bonds link the adjacent molecules.

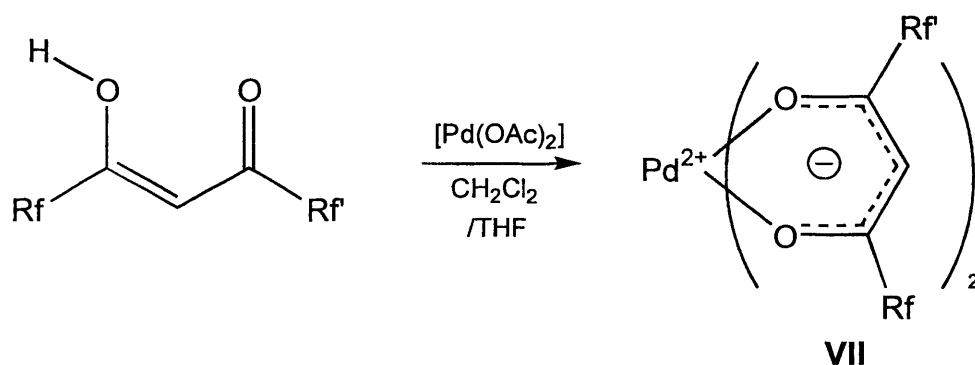
The perfluoroheptyl derivatised copper complex (**VIc**) was similarly re-analysed. The spectroscopic data obtained was comparable to the two earlier complexes, whilst elemental analysis was in agreement with the predicted values. Unfortunately, although attempts were made to grow crystals of the complex, the material obtained did not diffract well, leading to incomplete data. Tables of crystallographic data and structure refinements for both the copper complexes (**VIa** and **XVb**) can be found in Appendix 1, whilst a complete collection of data for all the crystal structures contained in this thesis can be found on the accompanying CD-ROM.

## 2.2. Coordination Chemistry

To investigate the coordination chemistry of the four fluorinated  $\beta$ -diketonate ligands, a variety of complexes were synthesised, in many cases mimicking literature species in order to analyse the spectroscopic changes that occur upon chelation.<sup>7,8</sup> Throughout, comparison is made with the corresponding 2,4-pentanedionato complexes to probe the effect of the fluorinated groups.

### 2.2.1. Palladium $\beta$ -diketonates

The first metal investigated was palladium. The complexes were synthesized by adding palladium (II) acetate to a stirred solution of the  $\beta$ -diketone in an equal mixture of dichloromethane and tetrahydrofuran (**Scheme 2.4**).



**Scheme 2.4**

For the complexes derived from the symmetrical perfluorohexyl and perfluoroheptyl derivatised ligands, the products were isolated by simple suction filtration of the powdery, yellow air-stable solids; **VIIb**, 81.5% and **VIIc**, 82 % respectively. However, the analogous unsymmetrical  $\beta$ -diketonate complex required recrystallisation from refluxing toluene before the final isolation of a yellow, air-stable solid (**VIIa**), (52 %). Unfortunately, characterisation of the molecules was somewhat limited by the lack of spectroscopic changes occurring upon coordination. The most informative change occurred in the  $^1\text{H}$  NMR spectra, where the formation of the anionic ligand and concurrent coordination to the metal centre is indicated by the disappearance of the broad singlets representing the enolic protons. However, the vinylic peak did not shift significantly upon coordination, a trend echoed in all of the complexes synthesised. The unsymmetrical ligand shifted slightly from 6.35 ppm to 6.41 ppm but this is of no significant diagnostic value. To confirm this observation, palladium (II) hexafluoroacetylacetonate was synthesised in order to compare the chemical shift of the vinylic proton to that of the free ligand. The data obtained is given in **Table 2.3**, alongside literature data for the analogous acetylacetonate complex.<sup>14</sup>

**Table 2.3.** Characterisation data for fluorinated palladium  $\beta$ -diketonate complexes

Complex	$\delta$ - C=C-H (free ligand, enol)	$\delta$ - C=C-H (complex)	Carbonyl Stretching frequency / $\text{cm}^{-1}$
$\text{Pd}(\text{acac})_2^{11}$	5.66	5.43	1563
$\text{Pd}(\text{hfacac})_2$	6.41	6.42	1598
$\text{Pd}(\text{C}_6\text{F}_{13} / \text{CF}_3)_2$ ( <b>VIIa</b> )	6.35	6.41	1590
$\text{Pd}(\text{C}_6\text{F}_{13} / \text{C}_6\text{F}_{13})_2$ ( <b>VIIb</b> )	6.45	6.45	1595
$\text{Pd}(\text{C}_7\text{F}_{15} / \text{C}_7\text{F}_{15})_2$ ( <b>VIIc</b> )	6.48	*	1594

\* Insoluble in common deutero solvents.

The overall conclusion from the data depicted above is that there is no significant change in the electronic environment of the enolised  $\beta$ -diketonate upon coordination to the palladium metal centre. One feature that is clearly apparent is the electron withdrawing effect of the fluorine atoms, which shift the pseudo vinylic proton downfield in comparison to that for the non-fluorinated acetylacetone. This trend is mirrored in the resultant complexes which are also shifted downfield, however, in both cases, the degree of fluorination appears to impart no significant effect. Similarly, the single infrared active carbonyl stretching frequencies are all very similar for the fluorinated molecules, but significantly higher than that for the acetylacetonate complex. Once again this indicates the electron withdrawing effect of the fluorine moieties which decrease the ability of the ligands to donate electron density, resulting in the comparatively stronger C=O bond.

Examination of (**VIIa**), by  $^{19}\text{F}$   $\{^1\text{H}\}$  NMR spectroscopy, revealed four resonances in the trifluoromethyl region, from  $-73.31 \delta$  to  $-81.36 \delta$ , indicating that the molecule is adopting a mixture of the *cis* and *trans* isomers in solution (**Figure 2.6**).

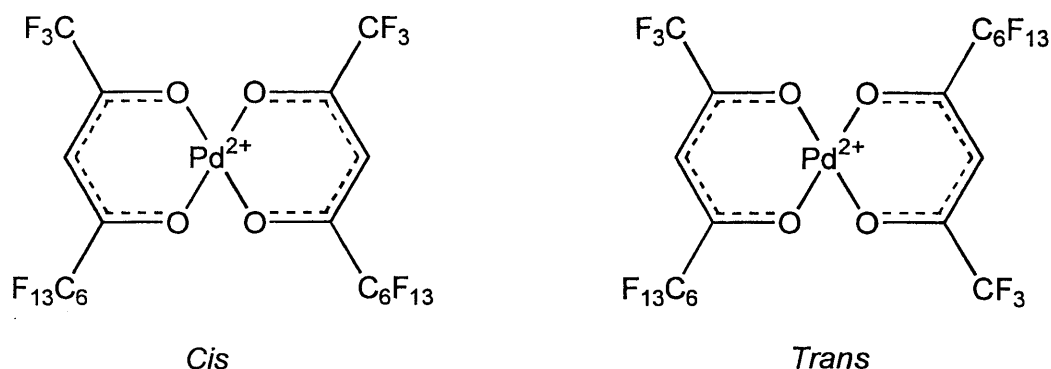
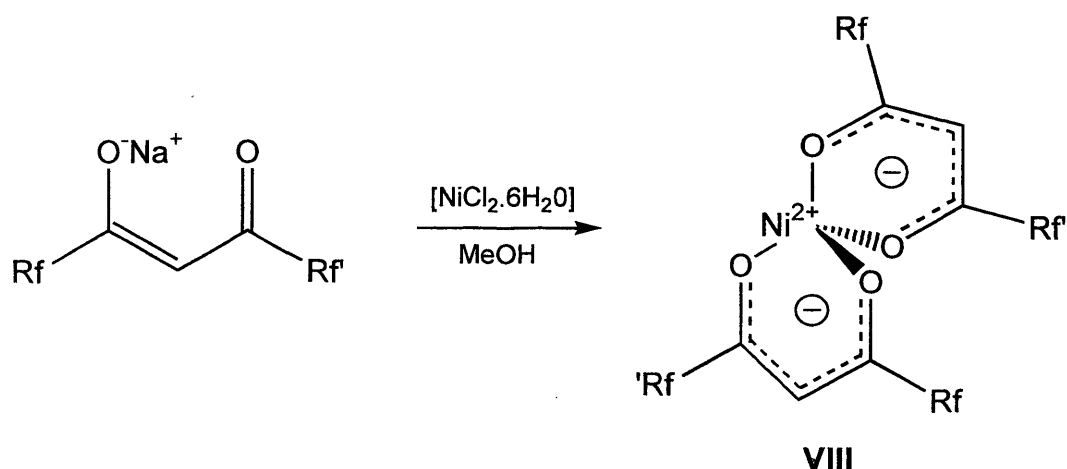


**Figure 2.6**

Two of the signals (-81.2 ppm and -81.3 ppm), are split into triplets due to coupling to the  $\delta$ -CF<sub>2</sub>'s of the fluorinated ponytails, whereas the two signals at -73.4 ppm and -73.6 ppm are singlets generated by the  $\alpha$ -carbonyl CF<sub>3</sub>'s that do not couple to any other fluorine atoms. Two overlapping triplets were observed at -116.9 ppm, which were generated by the  $\alpha$ -CF<sub>2</sub>'s of the two fluorinated ponytails of the *cis* / *trans* isomers. Attempts were made to grow crystals of these complexes but, unfortunately the crystals generated were not of sufficient quality for crystallographic studies. Further characterisation studies were carried out including mass spectroscopy and elemental analysis, all of which confirmed the formation of the coordination compounds. The mass spectrum of **VIIa** was of particular interest due to the occurrence of a distinctive palladium isotopic pattern at 1020 Daltons representing the parent ion.

### 2.2.2. Nickel $\beta$ -diketonates

When the fluorinated  $\beta$ -diketones were coordinated to nickel, pale green, air-stable powdery solids were obtained in very high yields. The reactions were achieved by firstly synthesizing the sodium salt of the ligand, *via* reaction with sodium acetate, before the addition of nickel dichloride hexahydrate (NiCl<sub>2</sub>·6H<sub>2</sub>O) (**Scheme 2.5**).

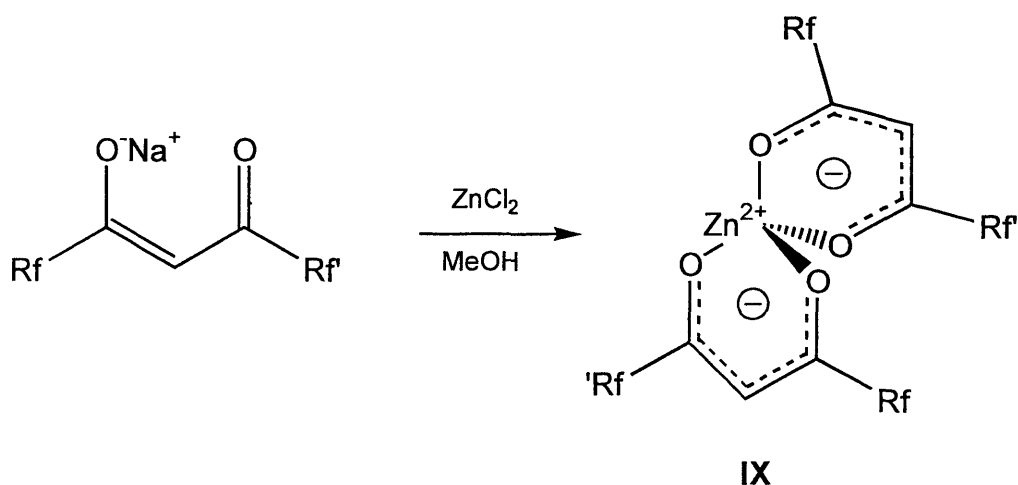


Scheme 2.5

Once again, the perfluorohexyl and perfluoroheptyl ligand species could be isolated by suction filtration (**VIIIb**, 92 % and **VIIIc**, 94 % respectively), and *via* rotary evaporation of the solvent in the case of the unsymmetrical coordination compound (**VIIIa**, 85 %). Characterisation was limited by the fact that the complexes adopt a tetrahedral geometry, owing to the low position of the  $\beta$ -diketonate ligand in the spectrochemical series, and are, therefore, paramagnetic ( $\text{Ni}^{2+}$ ,  $d^8$ ). This was confirmed by the infra-red spectra of the complexes, which reveal two peaks corresponding to the  $B_2$  and  $E$  infra-red active stretches predicted by group theory for the irreducible representation, generated by the  $D_{2d}$  point group to which the nickel species belong. As a consequence, NMR spectroscopy was very badly distorted, although six signals could be identified in the  $^{19}\text{F}\{^1\text{H}\}$  NMR spectrum of **VIIIb**. Further characterisation did, however, confirm the identity of the compounds, with mass spectrometry providing the most diagnostic information, whilst elemental analysis elucidated the composition of the solids. Despite employing various techniques, crystals suitable for X-ray crystallography could not be acquired.

### 2.3.3. Zinc $\beta$ -diketonates

Coordination to zinc was undertaken in order to generate fluorosoluble analogues of the  $[\text{Zn}(\text{acac})_2]$  complex used in the catalytic coupling of cyanoformates to 1,3-dicarbonyl compounds, which is described in detail in Chapter 4.<sup>15</sup> The complexes were prepared analogously to the nickel species described above, except that sodium hydroxide was used to generate the sodium salt of the ligands (**Scheme 2.6**).



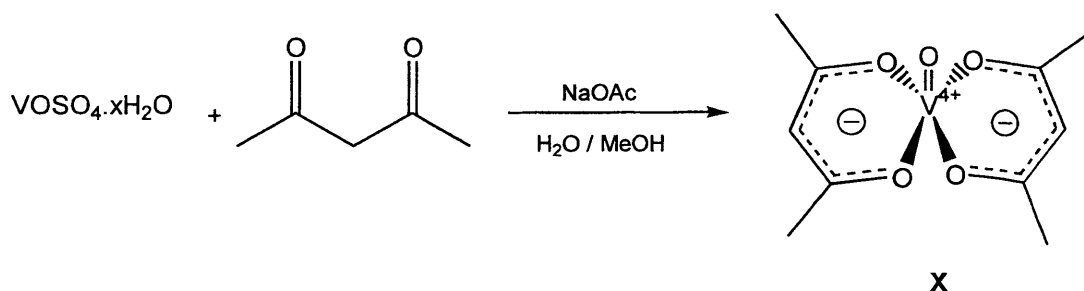
**Scheme 2.6**

White, air-stable solids were obtained in reasonably high yields. Examination of the compounds by  $^1\text{H}$  NMR established that complexation had occurred by the disappearance of the enolic protons. Predictably, the symmetrical perfluorohexyl and perfluoroheptyl derivatised species (**IXb** and **IXc**, respectively), exhibited the required number of peaks in their  $^{19}\text{F}\{^1\text{H}\}$  NMR spectra. Seven signals were observed for the complex of the unsymmetrical ligand (**IXa**) consistent with a tetrahedral geometry. This geometry is present since the complexes are unsolvated as a result of rigorous drying over silica gel under high vacuum. This is in direct contrast to the geometry determined by the  $^{19}\text{F}$  NMR spectroscopic studies, on the closely related tetradecafluorononane-4,5-dionato-zinc (II) complexes reported by Toscano *et al.*<sup>12</sup> The spectra revealed a second order pattern arising from strongly coupled diastereotopic  $\alpha\text{-CF}_2$  fluorine atoms, which indicate a *cis*-octahedral geometry for the aquated  $[\text{Zn}(\text{C}_3\text{F}_7\text{C}(\text{O})\text{CHC}(\text{O})\text{C}_3\text{F}_7)_2(\text{H}_2\text{O})_2]$  species. Once again,

a variety of techniques were used to analyse the molecules, although crystallographic data could not be obtained despite several attempts.

#### 2.3.4. Vanadyl and Molybdenum $\beta$ -diketonates

The coordination chemistry of vanadium and molybdenum with fluorinated  $\beta$ -diketonate ligands was also investigated with the aim of examining the catalytic properties of these higher oxidation state species.<sup>16,17</sup> The first vanadium complex which was analysed was the parent  $\beta$ -diketonate, vanadyl bis (acetylacetonate) [VO{CH<sub>3</sub>C(O)CHC(O)CH<sub>3</sub>}<sub>2</sub>] (**Xa**), which is an easily prepared, air stable solid (**Scheme 2.7**).<sup>18</sup>



**Scheme 2.7**

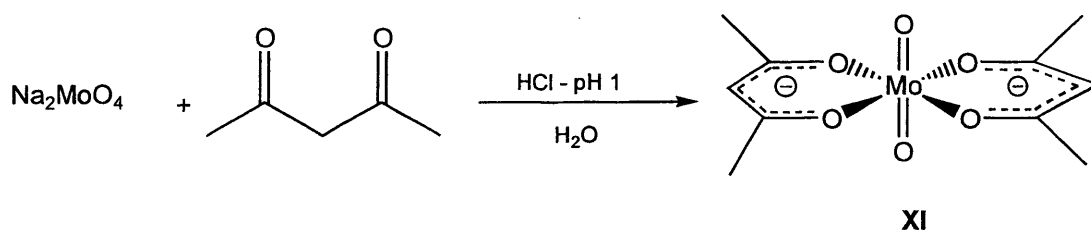
However, upon attempting a similar procedure for the synthesis of vanadyl bis (hexafluoroacetylacetonate) [VO{CF<sub>3</sub>C(O)CHC(O)CF<sub>3</sub>}<sub>2</sub>] (**Xb**), a dark green / black oil was produced, rather than a crystalline solid. This result was attributed to the increased acidity of the fluorinated diketone, which influences the pH of the reaction mixture, thus altering the redox chemistry between the vanadyl and sulfate ions. Essentially, sulfuric acid is eliminated during complex formation and as a consequence, an alternative preparation was sought in which the acidity of the reaction could be controlled. Two methods were employed, which utilised an aqueous solution of base, whilst monitoring the pH.<sup>19,20</sup> Unfortunately, the yields obtained were very poor, even after repeated attempts to optimise the methodology. Furthermore, the vast excess of the commercially available hexafluoroacetylacetone used in the synthesis precluded the implementation of this route for the long chain

fluorinated  $\beta$ -diketones. Several factors were apparent which could possibly have explained these poor results; the first was that vanadyl sulphate is dissolved in water, thus forming a biphasic system upon addition of the ligand that prevented efficient reaction from occurring. Another factor was undoubtedly the solubility of the product in the reaction mixture; although the minimum volume of water was used, the addition of aqueous base increased the total solvent volume, preventing the compound from precipitating out of solution. Attempts were made to remove the remaining product by extraction with alternative solvents and by simple evaporation of the solvent, but on both occasions the product appeared to decompose, generating a brown / black residue.

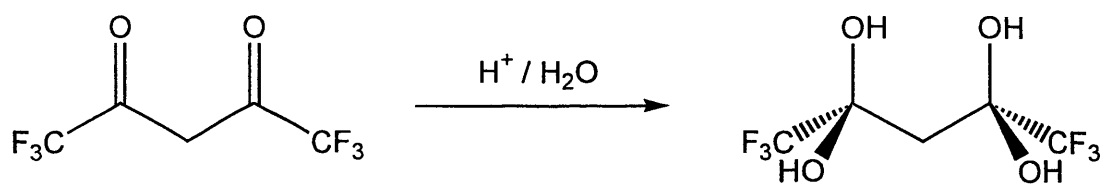
Alternative preparations were attempted in different solvents in order to remove water from the reaction mixture. Methanol and 1,1,1-trifluoroethanol have both been employed with no success, in part due to the insolubility of the vanadyl sulfate in these media. However, by stirring the trifluoroethanol reaction for three days, an olive coloured solution was obtained, possibly indicating that reaction had occurred as the metal salt had been pulled slowly into solution. Once again, however, similar problems were encountered when the solvent was removed by evaporation, as a brown / black tar-like residue was obtained.

Complexes of the hexafluoroacetylacetonate ligand have shown an inherent instability, making them difficult to prepare, this was manifested in both the palladium and zinc complexes described earlier. For this reason, it was decided to attempt the preparation of one of the longer chain fluorosubstituted vanadyl  $\beta$ -diketonate complexes. Following the methodology employed for (**Xb**), attempts were made to synthesise vanadyl *bis*-1,1,1,2,2,3,3,4,4,5,5,6,6,-10,10,11,11,12,12,13,13,14,14,15,15,15-hexacosafluoro-pentadecane-7,9-dionate  $[\text{VO}\{\text{C}_6\text{F}_{13}\text{C}(\text{O})\text{CHC}(\text{O})\text{C}_6\text{F}_{13}\}_2]$  (**Xc**). A blue oil was generated which was preferentially fluorosoluble, but both the  $^1\text{H}$  and  $^{19}\text{F}$  NMR spectra exhibited clearly defined peaks, rather than the distortion expected for the paramagnetic  $\text{V}^{4+}$  central ion. Although the mass spectrum (FAB) indicated that the parent ion might be present, the spectrum was difficult to interpret with any degree of certainty. Unfortunately, a similar result was obtained for the unsymmetrical ligand, and consequently it was decided not to pursue this area of research any further.

A similar approach was undertaken for the synthesis of the molybdenum  $\beta$ -diketonates as described for the vanadyl complexes, initially dioxobis-(acetylacetonato) molybdenum(VI)  $[\text{MoO}_2\{\text{CH}_3\text{C}(\text{O})\text{CHC}(\text{O})\text{CH}_3\}_2]$  (**XIa**), was prepared following the literature route by Gehrke and Veal.<sup>21</sup> Once again, the formation of the complex is pH sensitive, requiring very acidic conditions (**Scheme 2.8**).

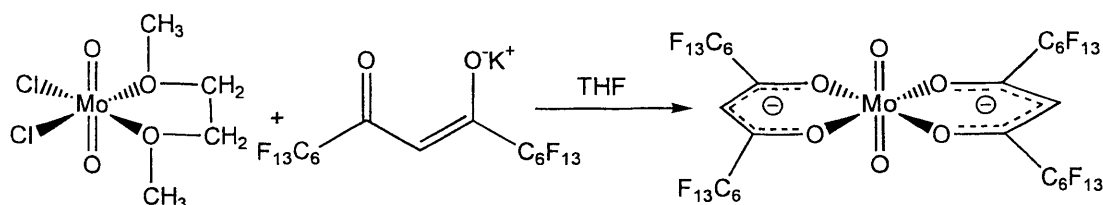
**Scheme 2.8**

The compound was obtained as a fine yellow powder and the characterisation data agreed with literature values. The compound was very sensitive to the solvent that was used to obtain the NMR spectrum, decomposing to a green solution in deuterated chloroform with a blue precipitate after approximately thirty minutes. Following this successful procedure, the synthesis of dioxobis-(hexafluoroacetylacetonato) molybdenum  $[\text{MoO}_2\{\text{CF}_3\text{C}(\text{O})\text{CHC}(\text{O})\text{CF}_3\}_2]$  (**XIb**), was carried out analogously. Initially, the reaction appeared to be successful, with a white crystalline solid obtained in high yield. A singlet was observed in the  $^{19}\text{F}$  NMR spectra, concurrent with the single environment expected for the fluorinated ligands, whilst a broad singlet in the  $^1\text{H}$  NMR spectra at  $7.1 \delta$  was tentatively assigned to the central vinylic proton. However, a single crystal was acquired for X-ray crystallography, which revealed that the compound obtained was actually the tetraol, *i.e.* the hydrolysis product of the ligand (**Scheme 2.9**). This was confirmed by the mass spectrum of the compound, which verified the presence of the alcohol, whilst revealing no trace of the  $\beta$ -diketonate complex. This compound has been described previously by Bouwman *et al*, and can be formed by simply stirring the ligand in water for fifteen minutes.<sup>22</sup> The extreme electrophilicity of the carbonyl groups, generated by the  $\alpha$ - $\text{CF}_3$  groups, allows the formation of the ‘hydrate’ even in the acidic conditions which are used.



**Scheme 2.9**

To confirm that this result was not due to the non-uniform behaviour of hexafluoroacetone, the synthesis of dioxobis 1,1,1,2,2,3,3,4,4,5,5,6,6,10,10,-11,11,12,12,13,13,14,14,15,15,15-hexacosafuoro-pentadecane-7,9-dionato molybdenum (VI)  $[\text{MoO}_2\{\text{C}_6\text{F}_{13}\text{C}(\text{O})\text{CHC}(\text{O})\text{C}_6\text{F}_{13}\}_2]$  (**XIc**), was attempted. The procedure was modified slightly, due to the hydrophobicity of the fluorous diketone, by carrying out the reaction in a water / trifluoroethanol mixture. Regardless of this, and similar procedures with methanol and other solvents, the ligand was recovered unreacted on each occasion, forming a biphase when rapid stirring was halted (there was never any indication of a similar hydrolysis product). For this reason, an alternative route was sought which allowed the reaction to be carried out in an organic media. An organic based molybdenum species was required with a labile ligand to allow replacement by the fluorous  $\beta$ -diketonate. The compound chosen for this role was a dimethoxyethane adduct of dioxomolybdenum (VI) dichloride  $[\text{MoO}_2\text{Cl}_2.\text{dme}]$ .<sup>23</sup> The compound was prepared by literature methods, although rigorous drying was employed at each stage to ensure water was excluded from the complex synthesis. Reaction of this intermediate with two equivalents of the potassium salt of the fluorous ligand (**Scheme 2.10**) yielded a viscous green oil.

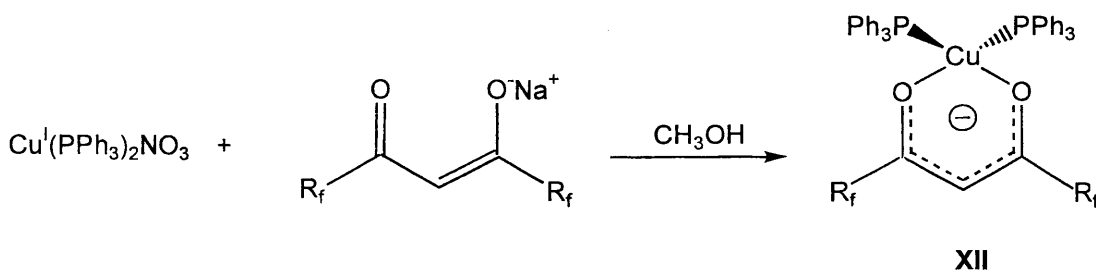


**Scheme 2.10**

The formation of (**XIc**) was indicated by a distinct molybdenum pattern in the FAB mass spectrum corresponding to the parent ion. The  $^{19}\text{F}$  NMR spectrum revealed six multiplets, whilst elemental analysis data was in precise agreement with predicted values, confirming the formation of the desired product. Unfortunately, despite drying under high vacuum, the compound remained amorphous, precluding attempts to grow single crystals for X-ray analysis.

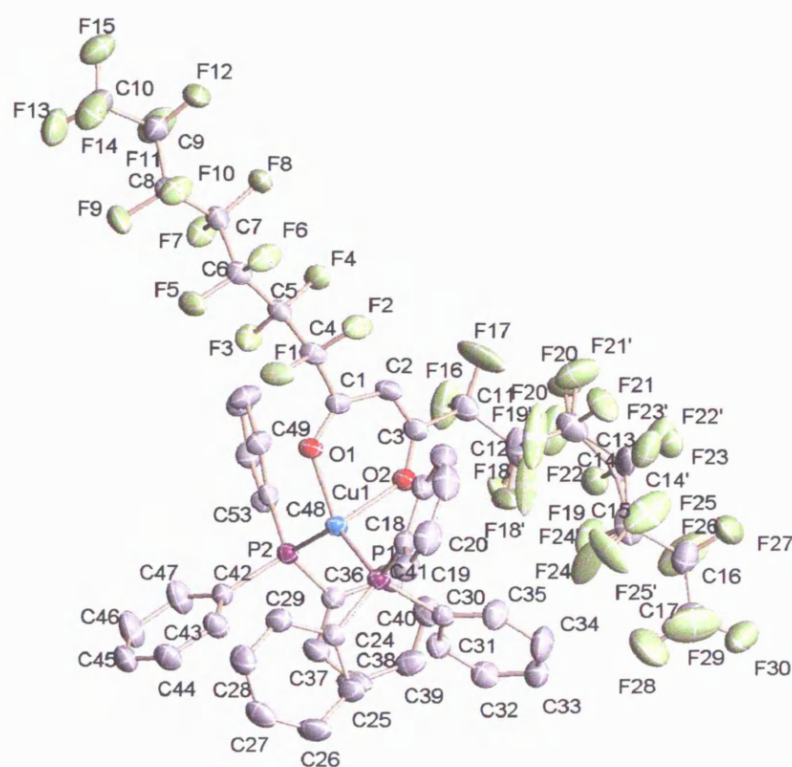
### 2.3.5. Coordination to other systems

Due to the difficulty of analysing the homoleptic  $\beta$ -diketonates, especially with regard to the ambiguous NMR shifts and inability to grow single crystals, attempts were made to synthesize a number of heteroleptic species, with the primary aim of generating informative  $^1\text{H}$  NMR spectra with more than one peak to compare the relative integrations. The first of these complexes was a copper *bis*-triphenylphosphine (**XII**) species where the thirty aromatic protons on the triphenylphosphine ligands offer a means of integrating the single proton of the  $\beta$ -diketonate ligand. Previous work within the group has indicated that similar species with perfluoroalkyl-derivatised dithiocarbamates, provide suitable crystals for crystallographic analysis.<sup>24</sup> Also, however, there have been several reports of similar species with partially fluorinated  $\beta$ -diketonates, including  $[\text{Cu}(\text{PPh}_3)_2(\text{tfac})]$  (*tfac* = trifluoroacetylacetonate),<sup>25</sup> and  $[\text{Cu}(\text{PCy}_3)_2(\text{hfacac})]$  which contains the bulky tricyclohexylphosphine ligand.<sup>26</sup> The complexes were synthesised by reacting the copper (I) nitrate *bis*-triphenylphosphine complex<sup>27</sup> with the sodium salt of the  $\beta$ -diketone in methanol (**Scheme 2.11**).



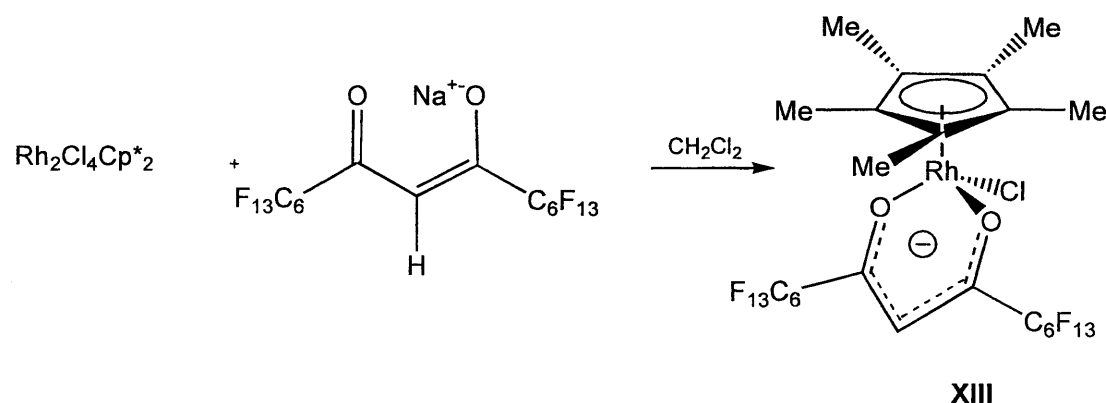
**Scheme 2.11**

The products precipitated out of solution and were isolated by suction filtration, washed with a small amount of cold methanol and dried under vacuum to give pale orange powders, which were air stable (**XIIa**, 95 % yield, and **XIIb**, 92 %). Analysis by  $^1\text{H}$  NMR spectroscopy confirmed that coordination had occurred; in both cases the enolic proton had been removed, but surprisingly, the pseudo vinylic proton had shifted significantly upfield. As expected, the spectra also contained large singlets attributable to the triphenylphosphine ligands with integrations corresponding to 30:1 with respect to the vinylic proton of the diketonate ligands. The  $^{19}\text{F}\{^1\text{H}\}$  NMR spectra produced six and seven signals which mirrored the free ligands, whilst broad singlets were observed in the  $^{31}\text{P}\{^1\text{H}\}$  NMR spectra. However, in accordance with the true intentions of these syntheses, a single crystal of **XIIb** was obtained by slow evaporation from acetone (**Figure 2.7**).



similar P-Cu-P bond angle ( $128^\circ$ ) to that for  $[\text{Cu}(\text{PPh}_3)_2(\text{tfac})]$  ( $127^\circ$ ).<sup>26,25</sup> In the same way as seen in the structural determination of  $[\text{Cu}\{\text{C}_6\text{F}_{13}\text{C}(\text{O})\text{CHC}(\text{O})\text{C}_6\text{F}_{13}\}_2(\text{OH}_2)_2]$  (**Figure 2.4**), one of the perfluoroheptyl ponytails exhibits considerable disorder beyond the  $\alpha\text{-CF}_2$  group and this static disorder was modelled successfully. However, this prevented the identification of genuine short non-bonded F...F contacts, even though fluororous layers are observed in the solid-state packing diagram demonstrating the preference for the fluororous ponytails to align. A table of crystal data and structure refinements are given in Appendix 1, whilst a complete collection of data for all the crystal structures contained in this thesis can be found on the accompanying CD-ROM.

The second heteroleptic system analysed was a rhodium pentamethylcyclopentadiene complex, which it was hoped, would provide similar  $^1\text{H}$  NMR data and possibly solid-state analysis. These familiar ‘piano-stool’ complexes have been used to analyse numerous fluorinated ligands, especially phosphines and phosphites.<sup>24,28</sup> The first synthesis attempted, was of the symmetrical, perfluorohexyl-derivatised ligand (**Scheme 2.12**), to generate **XIII**.



**Scheme 2.12**

The reaction generated an orange tar-like semi-solid, which upon analysis by  $^1\text{H}$  NMR spectroscopy proved to be a complex mixture of products, indicated by multiple signals in the pentamethylcyclopentadienyl region. These could possibly have arisen through the ligand bonding as a mixture of mono- and bi-dentate, but also, *via* a bridging dimeric species. Attempts to isolate the products by fluororous

extraction and fractional recrystallisation all failed. Further attempts to synthesise the complex were not carried out.

### 2.3. Separation Science

The fluorophilicity of the new complexes synthesised was investigated to ascertain the degree of fluorination required in order to generate preferential fluorous phase solubility. Unfortunately, due to the moisture sensitivity of the molybdenum  $\beta$ -diketonates, this analysis was not possible for those compounds, nor were the heteroleptic copper triphenylphosphine complexes analysed, due to the purely synthetic motivation behind their production.

To investigate the fluorous affinity of the  $\beta$ -diketonate complexes in a dichloromethane / perfluoro-1,3-dimethylcyclohexane biphasic system, 0.1 g of the compounds were placed into a sample vial containing 2 cm<sup>3</sup> of each solvent. The mixture was stirred for 30 minutes before the layers were separated and the solvent from each phase evaporated to constant mass. The results obtained provide a clear indication of the fluorophilic nature of all of the complexes (**Table 2.4**). However, although attempts were made to eliminate error wherever possible, these results can only offer a general indication of how well the compounds partition between the two phases.

**Table 2.4.** Gravimetric analysis of fluorous phase affinities for selected  $\beta$ -diketonates complexes

Complex	Complex recovered from the Fluorous Phase (g).	Complex recovered from the Organic Phase (g).
Pd(C <sub>6</sub> F <sub>13</sub> / C <sub>6</sub> F <sub>13</sub> ) <sub>2</sub> <b>VIIa</b>	0.104	0.002
Ni(C <sub>6</sub> F <sub>13</sub> / C <sub>6</sub> F <sub>13</sub> ) <sub>2</sub> <b>VIIIa</b>	0.107	-0.005
Zn(C <sub>6</sub> F <sub>13</sub> / C <sub>6</sub> F <sub>13</sub> ) <sub>2</sub> <b>IXa</b>	0.102	0.003
Pd(CF <sub>3</sub> / C <sub>6</sub> F <sub>13</sub> ) <sub>2</sub> <b>VIIb</b>	0.111	0.004
Ni(CF <sub>3</sub> / C <sub>6</sub> F <sub>13</sub> ) <sub>2</sub> <b>VIIIb</b>	0.105	-0.007
Zn(CF <sub>3</sub> / C <sub>6</sub> F <sub>13</sub> ) <sub>2</sub> <b>IXb</b>	0.099	0.004

*Experimental error = ±2%*

From the data, it is clear that all of the complexes are preferentially fluororous phase soluble. This was quite surprising because of the relatively low percentage fluorine-content of the complexes derived from the unsymmetrical ligand and the initial expectation for these systems was that they would be retained by fluororous reverse phase silica gel, rather than being preferentially fluororous phase soluble.

To test the affinity of the complexes towards fluororous reverse phase silica gel, a 2 cm column of the modified silica was placed into a Pasteur pipette (cotton wool plug), which was charged with solvent, the choice of which proved critical in achieving efficient separation. The compound was then introduced in the same solvent and the retention investigated *via* addition of further solvent. Eventually the complex was recovered from the column, usually with diethyl ether. Of the metal complexes investigated, it was found that the nickel complexes were retained on the FRP silica gel most effectively; both the symmetrical and unsymmetrical molecules could be dissolved in hexane, retained on the column and then finally eluted with diethyl ether. In contrast, the retention of the palladium species was found to be dependent upon the ligands attached. Whilst the palladium *bis*-8H,8H-tridecafluorohexa-7,9-dione was easily retained by the modified silica, the unsymmetrical complex proved more problematic with leaching occurring in a variety of solvents. Similarly, palladium *bis*-hexafluoroacetylacetate was not retained by the column. A wide range of solvents have been investigated to ascertain whether or not the two zinc complexes can be retained by fluororous reverse phase silica gel. Although several solvents appear to show positive results (dichloromethane, toluene and hexane), slight leaching is observed in all cases. Overall, these results are fairly positive and indicate that solid phase extraction can be applied to fluororous-derivatised metal complexes.

## 2.5. References for Chapter 2

- [1] R.G. Pearson, *J. Am. Chem. Soc.*, 1963, **85**, 3533.
- [2] K.C. Joshi and V.N. Pathak, *Coord. Chem. Rev.*, 1977, **22**, 37.
- [3] Encyclopaedia of Reagents for Organic Synthesis John Wiley & Sons, 1995; [Cu(acac)<sub>2</sub>], E.J. Parish, L. Shengrong, **2**, 1311. [Ni(acac)<sub>2</sub>], J. Doyyon, **6**, 3689. [Pd(acac)<sub>2</sub>], J. Tsuji, **6**, 3860. [Mn(acac)<sub>3</sub>], B.B. Snider, **5**, 3226. [In(acac)<sub>3</sub>], S.A. Westcott, **8**, 5424. [Fe(acac)<sub>3</sub>], M.W. Zettler, **8**, 5425.
- [4] See Chapters 3, 4 and 5 for a detailed discussion of the catalytic processes.
- [5] Dictionary of Inorganic Compounds, Chapman and Hall, Chemical Database. IC-008845.
- [6] D.F. Shriver, P.W. Atkins and C. H. Langford. 'Inorganic Chemistry', (second edition). 1992. Oxford.
- [7] B. Betzemeier, F. Lhermitte and P. Knochel, *Tetrahedron Lett.*, 1998, **39**, 6667.
- [8] I. Klement, H. Lutzjens and P. Knochel, *Angew. Chem. Int. Ed. Engl.*, 1997, **36**, 1454.
- [9] A.E. Pedler, R.C. Smith and J.C. Tatlow, *J. Fluorine Chem.*, 1971 / 72, **1**, 433.
- [10] C. Massyn, R. Pastor and A. Cambon, *Bull. Soc. Chim. Fr.*, 1974, **5**, 975.
- [11] A. Kondo and S. Iwatsuki, *J. Fluorine Chem.*, 1984, **26**, 59.
- [12] Bassetti, G. Cerichelli and B. Floris, *Tetrahedron*, 1988, **44**, 2997.
- [13] C. Dettelbacher, E.T. Eisenbraun, D.H. Hunt, A.E. Kaloyeros, N.P. Pavri, P.J. Toscano, J. Waechter and B. Zheng, *J. Coord. Chem.*, 1996, **38**, 319.M.
- [14] S. Okeya, S. Ooi, K. Matsumoto and Y. Nakamura, *Bull. Chem. Soc. Jpn.*, 1981, **54**, 1085.
- [15] A.C. Veronese, V. Gandolfi, B. Longato, B. Corain and M. Basato, *J. Mol. Catal.*, 1989, **54**, 73.
- [16] M.N. Sheng, and N. Zajacek, *J. Org. Chem.*, 1968, **33**, 588; R. Curci, F. Di Furia, R. Testi and G. Modena, *J. Chem. Soc., Perkin 2*, 1974, 752.
- [17] C.Y. Lorber, I. Pauls and J.A. Osborn, *Bull. Soc. Chim. Fr.*, 1996, **133**, 755; S. Maignien, S. Alt-Mohand and J. Muzart, *Synlett.*, 1996, 439.
- [18] E. Hata, T. Takai, T. Yamada and T. Mukaiyama, *Chem. Lett.*, 1994, 1849.

- [19] C.C. Su, J.W. Reed and E.S. Gould, *Inorg. Chem.*, 1973, **12**, 337.
- [20] R.L. Carlin and F.A. Walker, *J. Am. Chem. Soc.*, 1965, **87**, 2128.
- [21] H. Gehrke (Jnr.) and J. Veal, *Inorg. Chim. Acta.*, 1969, **3:4**, 623.
- [22] E. Bouwman, K.G. Caulton, G. Christou, K. Folting, C. Gasser, D.N. Hendrickson, J.C. Huffman, E.B. Lobkovsky, J.D. Martin, P. Michel, H. Tsai and Z. Xue, *Inorg. Chem.*, 1993, **32**, 3463.
- [23] H.T. Chiu, Y.P. Chen, S.H. Chuang, J.S. Jen, G.H. Lee and S.M. Peng, *Chem. Commun.*, 1996, 139.
- [24] D.R.W. Wood. ‘The Synthesis and Characterisation of Novel Fluorinated Compounds Suitable for Evaluation as Oil Additives’, Ph. D. Thesis, University of Leicester, 2002.
- [25] M. Bartlett and J. Palenik, *Acta Crystallogr.* 1969, **Sect. A 25**, s173.
- [26] H. Shin, M.J. Hampden-Smith, E.N. Duesler and T.T. Kodas, *Can. J. Chem.*, 1992, **70**, 2954.
- [27] F.A. Cotton and D.M.L. Goodgame, *J. Chem. Soc.*, 1960, 5267.
- [28] D. Gudmunson, ‘The Synthesis, Coordination Chemistry and Catalytic Applications of Phosphinite, Phosphonite and Phosphite Ligands Containing Perfluoroalkyl Substituents’, Ph.D. Thesis, University of Leicester, 2000.

### 3. Oxidation Reactions Catalysed by Perfluoroalkylated Metal Catalysts

#### 3.1. Introduction

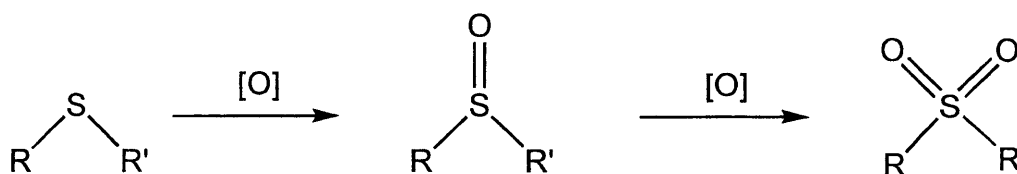
Numerous authors have investigated the implementation of fluoruous biphasic methodologies for oxidation reactions (see Chapter 1). Several features render these reactions particularly attractive to this approach; firstly, the change in polarity of the substrate molecule to the product enables facile separation *via* decantation of the organic phase. Also, perfluorinated solvents are very stable under oxidizing conditions and can dissolve large volumes of oxygen.<sup>1</sup> However, the magnitude of this final point was brought into question by Gladysz *et al.* when the gas solubilities of PP3 were compared to a standard organic solvent (tetrahydrofuran).<sup>2</sup> When expressed in mole fractions (mol O<sub>2</sub>), the solvents varied by a factor of five in favour of the fluoruous species. However, by considering the higher molecular weight of the fluoruous solvent (*ca.* five times greater), the authors revealed that the molal (mol Kg<sup>-1</sup>) concentrations were approximately equal, (0.00453 mol O<sub>2</sub>)/(350.05 g CF<sub>3</sub>C<sub>6</sub>F<sub>11</sub>) and (0.000815 mol O<sub>2</sub>)/(72.11 g THF).<sup>2</sup> Obviously, this questions the much vaunted value of fluoruous solvents as oxidation media, especially when combined with the often prohibitive cost of these liquids on an industrial scale.

In direct contrast, the utilisation of fluorinated catalysts for oxidation procedures remains valid, both in terms of economic and environmental goals. The requirement for cheap oxidation reagents, such as oxygen and hydrogen peroxide, that are activated by easily recyclable and non-polluting catalysts, dominates large areas of chemical research.<sup>3</sup> The aim of the work described within this chapter is to combine the benefits of fluoruous biphasic catalysts with fluoruous reverse phase silica gel for use in the study of a variety of oxidation reactions.

## 3.2. Nickel Catalysed Sulfide Oxidations

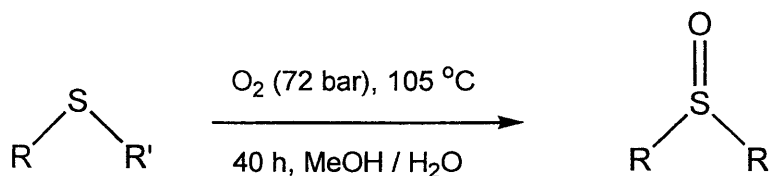
### 3.2.1. Introduction

The oxidation of sulfides (**Scheme 3.1**) is a widely studied process due to the importance of the products, sulfoxides, as intermediates in organic synthesis.<sup>4</sup> The lack of a universally applicable method has generated the large volume of work concentrating on this process and a wide variety of oxidants have been investigated.<sup>5</sup>



**Scheme 3.1**

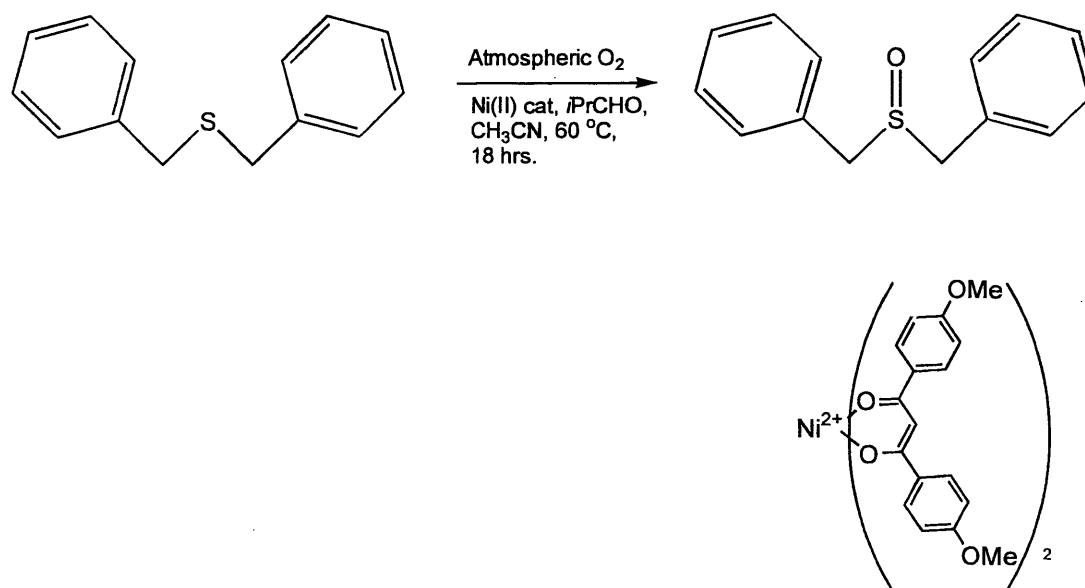
Common oxidants include hydrogen peroxide, peracids,  $\text{NaIO}_4$  and oxaziridines.<sup>6,7</sup> However, the problem of over-oxidation to the sulfone (as illustrated above), competing side reactions and deleterious effects for sensitive substrates has spurred the search for more selective reagents and catalysts. High yields have been obtained utilising molecular oxygen, but high pressures and temperatures are required (**Scheme 3.2**).<sup>8</sup>



**Scheme 3.2**

In an attempt to move away from these harsh reagents and / or reaction conditions, Lion *et al.*<sup>9</sup> utilised a nickel catalyst in the presence of an aldehyde (isobutyraldehyde) to selectively oxidise sulfides to sulfoxides (**Scheme 3.3**). The

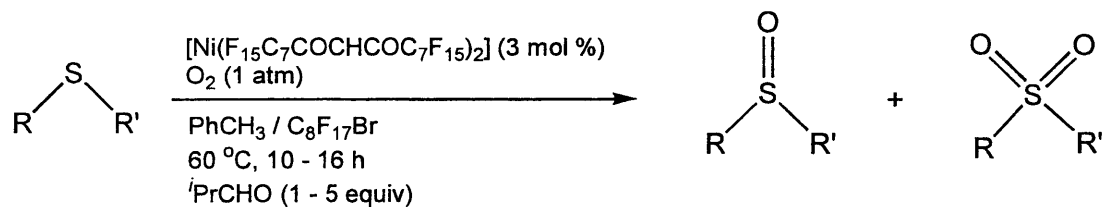
reactions were carried out using atmospheric oxygen, enabling a variety of substrates to be converted to the sulfoxide and, because none of the sulfone was formed, quantitative conversion could be achieved in some cases. The catalyst used was *bis*[1,3-(*p*-methoxyphenyl)-1,3-propanedionato]nickel(II) and was utilised in a 3 mol % ratio relative to the substrate.

**Scheme 3.3**

The authors also examined  $[\text{Ni}(\text{acac})_2]$  under the same conditions. Lower yields were obtained for the oxidation of di-*n*-butyl sulfide even after longer reaction times, suggesting that  $[\text{Ni}(\text{acac})_2]$  is a less effective catalyst. In both cases, however, the product was isolated by column chromatography following an aqueous sodium carbonate work-up; the metal catalysts were not re-used. The high cost of the nickel catalysts has limited the large-scale application of this system and the extreme toxicity of the complexes (carcinogenic, mutagenic and teratogenic) also prohibits their implementation due to the difficulty of disposing of hazardous waste.

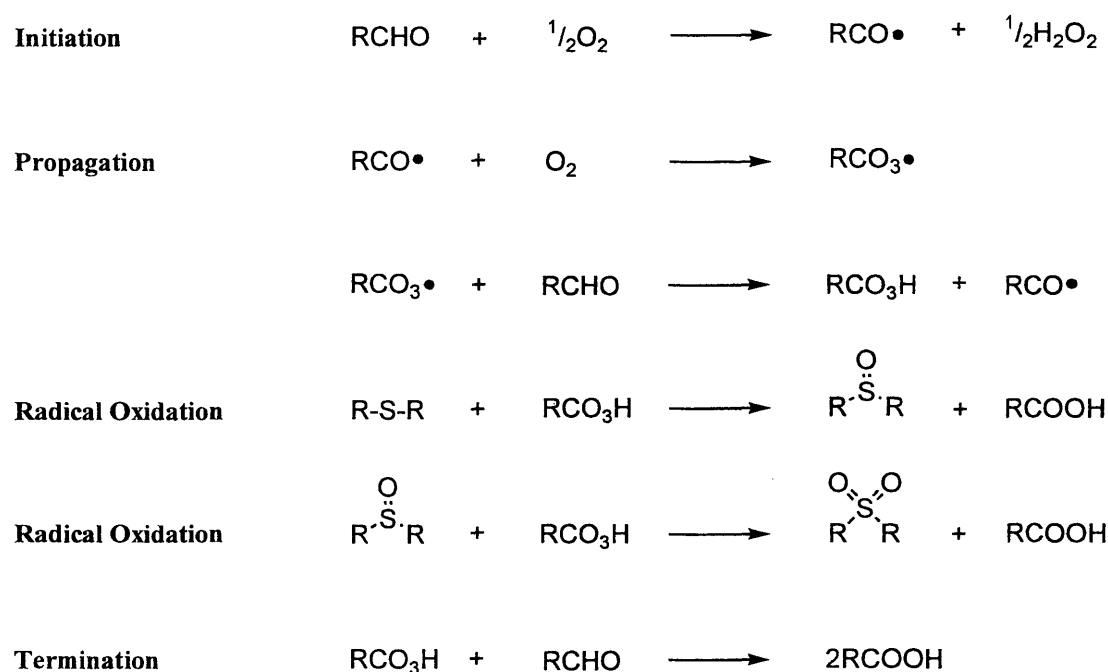
Recently, the application of fluoros biphase technology has improved the viability of this system. By employing the  $[\text{F}_{15}\text{C}_7\text{C}(\text{O})\text{CH}_2\text{C}(\text{O})\text{C}_7\text{F}_{15}](\text{I})$  ligand,<sup>10</sup> Knochel *et al.* have investigated the oxidation of a variety of sulfides to sulfoxides and sulfones in a fluoros biphase medium (Scheme 3.4).<sup>11</sup> However, the reactions

were carried out under an atmosphere of oxygen due to the lower activity of the catalyst.



**Scheme 3.4**

By tailoring the amount of isobutyraldehyde, the system was designed to selectively obtain either the sulfoxide or the sulfone. The role of this sacrificial auxiliary reagent is to reduce the nickel catalyst back to Ni(II) from Ni(III), thus allowing further oxidation of the sulfide / sulfoxide to occur. Analysis of the reaction suggests a radical mechanism involving an acylperoxy intermediate as the active species (**Scheme 3.5**).<sup>12</sup> The process is initiated by an oxygen radical which reacts with the aldehyde to form an acyl radical (RCO $\cdot$ ). Chain propagation continues the generation of this species and also forms the peracid radical (RCO $_3\cdot$ ), both of which can react with the sulfide to form the sulfoxide. With an excess of the auxiliary reagent, the second oxidation can take place to generate the sulfone. Overall, the aldehyde is converted to the corresponding carboxylic acid (2,2-dimethylpropanoic acid):

**Scheme 3.5**

It is postulated that the nickel  $\beta$ -diketonate functions as a mediating species to which both the aldehyde and dioxygen coordinate thus enabling the initiation step to proceed although the exact mechanism occurring is uncertain (see Laszlo and Levart, for a discussion of this stage in the reaction pathway).<sup>12</sup>

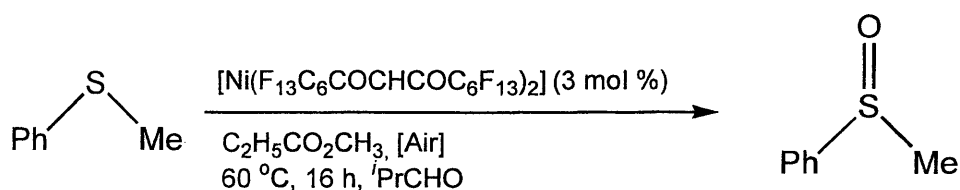
Significantly, however, the implementation of the fluoruous biphasic approach enables the catalyst to be recycled by re-using the lower fluoruous layer, in this case perfluorooctyl bromide. The product and carboxylic acid, along with any unused starting materials can be removed by decantation of the top organic phase (toluene). The catalytic phase can be recycled several times but, unfortunately, longer reaction times are required, indicating either catalyst leaching or degradation. For one system, after six cycles, the activity falls from 87 % to 70 %, which is unacceptable on an industrial scale due to the expense of the fluoruous catalyst and solvent.

The aim of the work described within this section was to combine the benefits of fluoruous biphasic methodology with fluoruous reverse phase silica gel for use in the study of sulfide oxidations. Ultimately, the objective was to remove the fluoruous solvent from the procedure, thus rendering the methodology more commercially viable. After carrying out the oxidation in a standard organic solvent,

the aim was to separate the fluorinated-derivatised catalyst from the product using FRP silica gel. A further aim was to remove the catalyst from the column to allow recovery and recycling to be investigated.

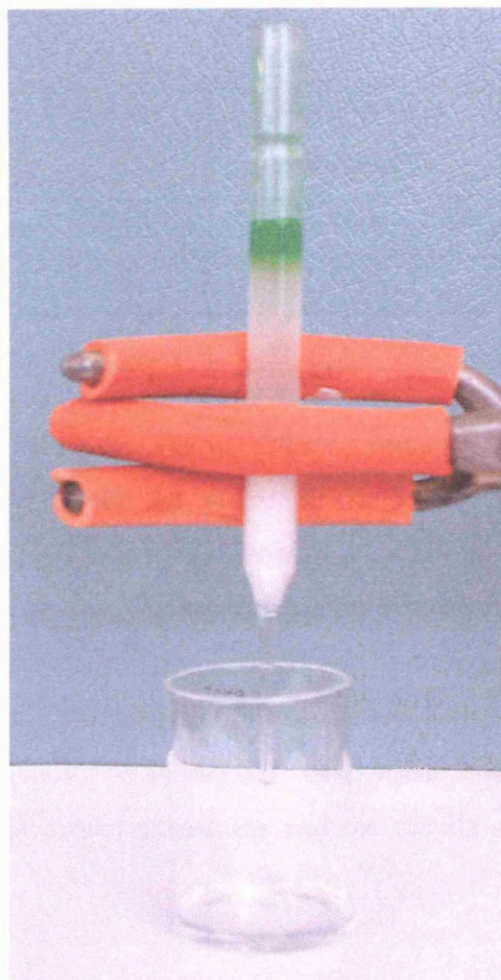
### 3.2.2. Results and Discussion

The oxidation of thioanisole (methyl phenyl sulfide) was chosen due to the ease of following the reaction by  $^1\text{H}$  NMR spectroscopy. Although a variety of catalysts were examined, the  $\text{C}_6\text{F}_{13}/\text{C}_6\text{F}_{13}$  ligand formed the basis of most of the catalytic investigations. Initially, the reaction was carried out under air to analyse the activity of the catalyst, reproducing the conditions employed by Lion *et al* (Scheme 3.6).<sup>9</sup>



Scheme 3.6

Ethyl acetate was used as the solvent because the fluorinated catalyst dissolves readily in the small volume used and had previously been reported to allow excellent results in the *para*-methoxy derivatised ligand system.<sup>9</sup> All reagents and solvents were dried prior to use and unless otherwise stated, reactions were carried out at 60 °C for 16 hours in a Radleys “Reaction Carousel Station” to ensure that exactly the same conditions were maintained throughout. The process has proved to be remarkably adaptable to utilising fluorinated reverse phase silica gel as a means of isolating the catalyst from the product / substrate mixture. The ethyl acetate was removed by evaporation and the residue dissolved in dichloromethane yielding a homogeneous green solution. The solution was then passed down an FRP silica gel column, where the nickel complex was retained selectively (Figure 3.1). Further dichloromethane was then used to elute the substrate / product mixture, during which time, no visible leaching of the catalyst was detected

**Figure 3.1**

Surprisingly, the affinity of the nickel complex for ethyl acetate is sufficiently high to allow the catalyst to be removed from the column once the organic compounds have been eluted, thus regenerating the catalyst system for future oxidations. The dichloromethane phase is washed with an aqueous sodium carbonate solution, prior to drying over anhydrous magnesium sulfate. Evaporation of the solvent yields the substrate / product mixture which is analysed by  $^1\text{H}$  NMR to determine the percentage conversion to the sulfoxide. The yields obtained for the initial investigations are detailed below (**Table 3.1**). The recovered catalyst from the first experiment was recycled to demonstrate the viability of this approach to catalyst / product separation and recycling *i.e.* entries 1 and 2.

**Table 3.1.** Sulfide oxidation reactions carried out under air

Catalyst	<sup>1</sup> PrCHO (mol %)	O <sub>2</sub> / Air	Conversion to sulfoxide %	Conversion to sulfone %
Ni(C <sub>6</sub> F <sub>13</sub> ) <sub>2</sub>	1.6	Air	46.8	0.0
Ni(C <sub>6</sub> F <sub>13</sub> ) <sub>2</sub>	1.6	Air	43.5	0.0
Ni(C <sub>6</sub> F <sub>13</sub> ) <sub>2</sub>	1.6	Air	6.5	0.0

Whilst these results indicated that the catalytic regime (60 °C, 16 h), was effective for the oxidation of thioanisole, the yields obtained were not comparable to the bis[1,3-(*p*-methoxyphenyl)-1,3-propanedionato]nickel complex which promoted the oxidation at 24 °C in 14 hours. However, from the results discussed by Knochel *et al.* for the analogous catalyst incorporating the perfluoroheptyl derivatised ligand, it appears that in order to compensate for the lower activity of the species, the reactions are carried out under an atmosphere of oxygen.<sup>11</sup> As a consequence, these conditions were used for future oxidations and the results are given in **Table 3.2** below.

**Table 3.2.** Sulfide oxidations carried out under O<sub>2</sub> atmosphere

Catalyst	<sup>1</sup> PrCHO (mol %)	O <sub>2</sub> / Air	Conversion to sulfoxide %	Conversion to sulfone %
Ni(C <sub>6</sub> F <sub>13</sub> ) <sub>2</sub>	1.6	O <sub>2</sub>	81.2	1.0
Ni(C <sub>6</sub> F <sub>13</sub> ) <sub>2</sub>	1.6	O <sub>2</sub>	61.2	6.7
Ni(C <sub>6</sub> F <sub>13</sub> ) <sub>2</sub>	1.6	O <sub>2</sub>	49.8	1.0
Ni(C <sub>6</sub> F <sub>13</sub> ) <sub>2</sub>	1.6	O <sub>2</sub>	23.5	0.8

Surprisingly, the conversions varied considerably between the four parallel experiments, a particularly surprising result due to the fact that a literature procedure was followed. The amount of sacrificial aldehyde was varied in two further experiments in an attempt to obtain stoichiometric conversion to the

sulfoxide and to the sulfone (Table 3.3 – shown for comparison is the most efficient 1.6 mol % conversion).

**Table 3.3.** Sulfide oxidations carried out with varying quantities of *iso*-butyraldehyde

Catalyst	<sup>i</sup> PrCHO (mol %)	O <sub>2</sub> / Air	Conversion to sulfoxide %	Conversion to sulfone %
Ni(C <sub>6</sub> F <sub>13</sub> ) <sub>2</sub>	1.6	O <sub>2</sub>	81.2	1.0
Ni(C <sub>6</sub> F <sub>13</sub> ) <sub>2</sub>	2.6	O <sub>2</sub>	1.0	0.0
Ni(C <sub>6</sub> F <sub>13</sub> ) <sub>2</sub>	5.0	O <sub>2</sub>	33.0	67.0

Unfortunately, these two experiments further indicated the unpredictable nature of the reaction rather than elucidating the quantity of sacrificial aldehyde required to obtain quantitative conversion to the sulfoxide or sulfone. The variation in results led to the possibility that a secondary process was occurring. For this reason a number of control reactions were carried out to investigate, individually, the various components of the reaction system (Table 3.4).

**Table 3.4.** Sulfide oxidations – various control experiments

Catalyst	<sup>1</sup> PrCHO (mol %)	O <sub>2</sub> / Air	Temp / °C	Conversion to sulfoxide %	Conversion to sulfone %
-	1.6	O <sub>2</sub>	60	72.7	2.0
-	1.6	O <sub>2</sub>	60	48.7	0.0
-	1.6	O <sub>2</sub>	60	46.2	3.0
-	1.6	O <sub>2</sub>	60	35.5	0.0
-	1.6	O <sub>2</sub>	60	27.5	0.0
-	1.6	O <sub>2</sub>	60	47.9	0.0
-	1.6	Air	60	18.7	0.0
-	1.6	Air	60	18.0	0.0
-	0.00	O <sub>2</sub>	60	0.0	0.0
Ni(C <sub>6</sub> F <sub>13</sub> ) <sub>2</sub>	1.6	O <sub>2</sub>	25	0.0	0.0
Ni(C <sub>6</sub> F <sub>13</sub> ) <sub>2</sub>	0.00	O <sub>2</sub>	60	0.0	0.0
-	1.6	N <sub>2</sub>	60	0.0	0.0

The series of control experiments generated very surprising results, most notably the experiments performed without the catalyst present, which achieved high levels of sulfoxide formation regardless. The fact that the reaction is proceeding auto-catalytically is very surprising due to the harsh conditions required to perform the reaction in the absence of a catalyst.<sup>8</sup> Tests were carried out under atmospheric conditions to ascertain whether the concentration of oxygen affected the reaction. Unfortunately, the reaction still occurred even though the conversion dropped significantly. When the reaction was carried out under nitrogen, no conversion to the sulfoxide was observed. Initially, it was thought that these results indicated that a secondary process was occurring, independent of either the catalyst or the sacrificial aldehyde. However, when the auxiliary reagent was completely removed, no conversion was observed regardless of whether or not the catalyst was present. Theoretically, it is impossible for isobutyraldehyde to catalyse the oxidation of a sulfide to a sulfoxide due to the different spin states of the carbonyl oxygen and molecular oxygen. For this reason, it was postulated that a secondary process was

occurring which converted the aldehyde to the peroxy acid. A radical mechanism appeared unlikely due to the presence of molecular oxygen which is a radical trapping agent; whilst the alternative route would be *via* a photolytic pathway. However, when the reaction was carried out in the dark, even without the catalyst, 22 % conversion to the sulfoxide was still observed. The only remaining possibility was that the solvent was affecting the reaction, although this appeared to be unlikely due to the rigorous conditions employed to dry and de-gas the ethyl acetate prior to use in the reactions. The choice of solvent was limited by the insolubility of the nickel complex in most common laboratory solvents. However, a number of solvents were tested, the results of which are listed in **Table 3.5** below.

**Table 3.5.** Sulfide oxidations – alternative solvent systems

Catalyst	Solvent	<sup>1</sup> PrCHO (mol %)	O <sub>2</sub> / Air	Conversion to sulfoxide %	Conversion to sulfone %
-	PP3	1.6	O <sub>2</sub>	32.0	2.6
Ni(C <sub>6</sub> F <sub>13</sub> ) <sub>2</sub>	PP3	1.6	O <sub>2</sub>	50.0	1.0
Ni(C <sub>6</sub> F <sub>13</sub> ) <sub>2</sub>	Ph-CF <sub>3</sub>	1.6	O <sub>2</sub>	19.4	0.0
Ni(C <sub>6</sub> F <sub>13</sub> ) <sub>2</sub>	Acetone	1.6	O <sub>2</sub>	12.7	0.0

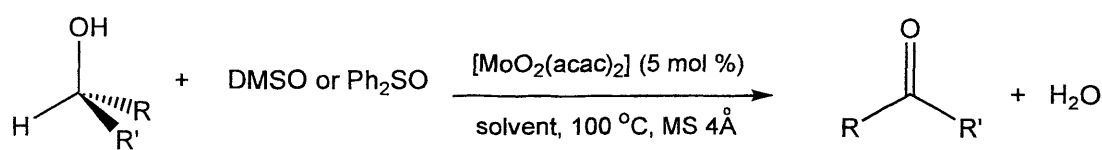
As can be observed from the data, changing the solvent had little effect upon the unpredictable nature of the reaction. Part of the rationale for analysing 1,3-perfluoro-dimethylcyclohexane was that the higher oxygen affinity of this medium, may have aided the conversions, similar to the results obtained in biphasic systems.<sup>11</sup> Clearly this was not the case, as a poor level of conversion was observed irrespective of the presence of the catalyst. Similarly, when the reaction was carried out in a “hybrid” organic / fluoruous solvent (1,1,1-trifluorotoluene, Ph-CF<sub>3</sub>), the conversion languished at only 19.4 %. Finally, as a direct organic comparison to ethyl ethanoate, acetone was examined under similar conditions, although obviously, the temperature was decreased to ~40 °C due to the lower boiling point of the solvent. Unfortunately, once again, the conversion was very low at just 12.7 %. At this point, it was decided not to pursue this system any further due to the capricious nature of the reaction.

In many respects, this investigation was successful, demonstrating that a fluorinated metal catalyst can be separated on fluorous reverse phase silica gel and subsequently removed and recycled. Regrettably, however, the chosen reaction appears to proceed auto-catalytically and even after prolonged investigation, the activating mechanism could not be determined. As a consequence the role of the nickel complex is no longer clear because the reaction pathway is not completely understood. Unfortunately, Knochel *et al.* did not detail any ‘control’ experiments to confirm the role of the catalyst in their report.<sup>11</sup> In some respects it is plausible to suggest that a highly fluorinated nickel  $\beta$ -diketonate complex would be a poor sulfide oxidation catalyst following the results obtained by Lion for nickel *bis*-acetylacetonate. The fluorous complex is similar in terms of geometry, but comparatively electron deficient due to the powerful electron withdrawing effect of the four perfluoroheptyl chains. This is in sharp contrast to the relatively electron donating effect of the four methoxy phenyl groups of the bis[1,3-(*p*-methoxyphenyl)-1,3-propanedionato]nickel system which is a highly effective catalyst even under atmospheric conditions and ambient temperatures (in certain cases). This argument is compounded by the fact that the perfluoroheptyl derivatised nickel complex is “not suitable for the oxidation of olefins”.<sup>11</sup> This is surprising because there is usually a distinct overlap between catalysts which function for the oxidation of sulfides and those which perform alkene epoxidations. This is indicated by the *para*-methoxy derived nickel system which was originally used by Yamada and co-workers for the epoxidation of olefins prior to being used for the oxidation of sulfides.<sup>13</sup> Furthermore, a variety of  $\beta$ -diketonate ligands were examined for alkene epoxidations using nickel catalysts and, alarmingly, the introduction of fluorinated moieties dramatically reduced the rate of reaction.<sup>13</sup> This may indicate that the catalyst is indeed not appropriate for the oxidation of sulfides.

### 3.3. Molybdenum Catalysed Alcohol Oxidations

#### 3.3.1. Introduction

The oxidation of primary and secondary alcohols is one of the most important reactions in synthetic chemistry with a multitude of reagents and catalysts designed to effect the transformation.<sup>14</sup> Some of the most frequently employed species include modified chromate species,  $\text{MnO}_4^-$ ,  $\text{V}_2\text{O}_5$  and high oxidation state ruthenium complexes.<sup>15</sup> In this context, dioxomolybdenum (VI) acetylacetonato  $[\text{MoO}_2(\text{acac})_2]$ , has recently been shown to be an effective catalyst for these reactions.<sup>15,16</sup> This versatile species catalyses a wide range of reactions including sulfide oxidation,<sup>17</sup> alkene epoxidation,<sup>18</sup> methoxymethylation of alcohols,<sup>19</sup> hetero Diels-Alder reactions<sup>20</sup> and the oxidative cleavage of *vic*-diols.<sup>21</sup> However, for the oxidation of alcohols, two methods have been described, the first involves oxygen atom transfer from sulfoxides (**Scheme 3.7**).<sup>15</sup>



**Scheme 3.7**

The catalytic results indicate that the system is most effective for the oxidation of allyl and benzyl alcohols to the corresponding aldehyde / ketones. Significantly, however, the further 'over' oxidation to carboxylic acids was avoided, whilst elimination processes were only encountered when harsher conditions were employed to accelerate the conversion of less reactive substrates, such as aliphatic alcohols. No attempts to recover and recycle the catalyst have been described in this work, although the mechanism postulated by the authors concludes with the regeneration of the Mo(VI) central ion (**Figure 3.2**).<sup>15</sup>

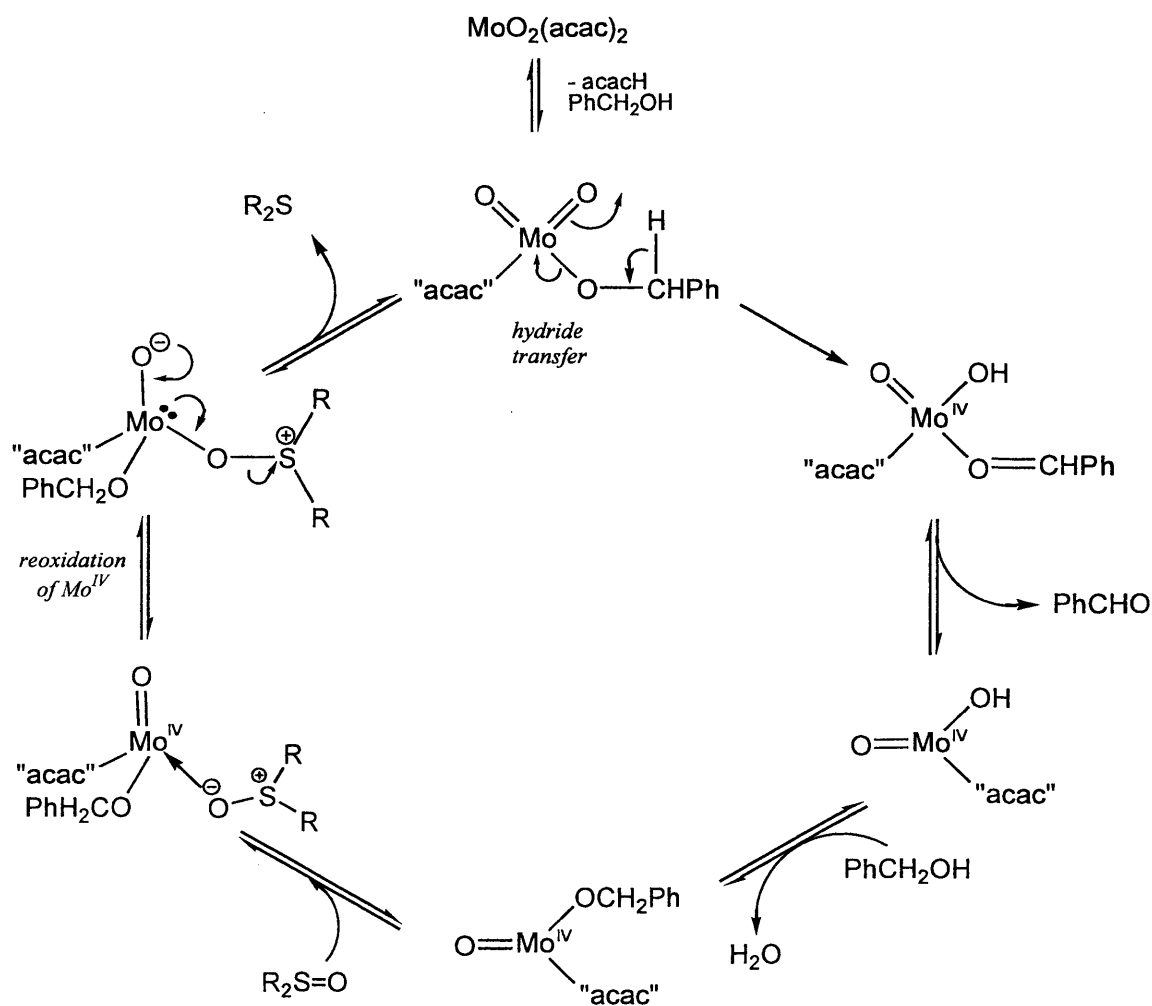
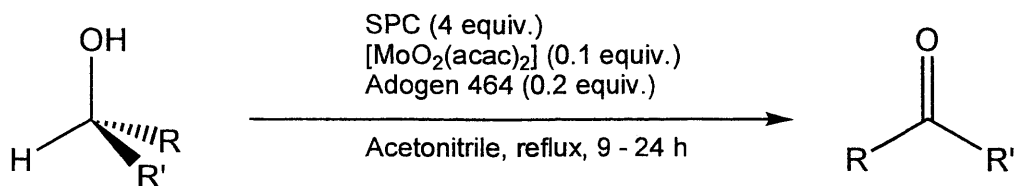


Figure 3.2

The second report of a dioxobis(acetylacetonato) molybdenum catalysed alcohol oxidation utilises sodium percarbonate (SPC) as the oxidising agent and employs a phase transfer catalyst (Adogen 464) to overcome the insolubility of the inorganic salt in organic solvents (Scheme 3.8).<sup>16</sup>



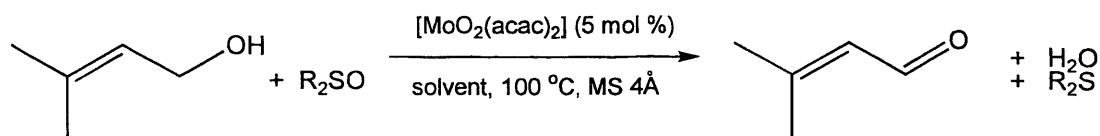
Scheme 3.8

The system generates fair to high yields of the carbonyl product, although for primary alcohols the formation of the corresponding carboxylic acid is observed upon numerous occasions and for allylic alcohols, epoxidation of the double bond was observed during the oxidation of isophorol and cholest-4-en-3-ol. Once again, recovery or re-use of the catalyst has not been described.

The aim of the work detailed within this section was to investigate the catalytic activity of the fluoros molybdenum  $\beta$ -diketonate (**XIc**), for the oxidation of primary and secondary alcohols, whilst also testing the application of fluoros biphasic separation in order to recover and recycle the complex for further reactions. Due to the moisture sensitivity of the fluoros species, the emphasis of the work was targeted toward traditional liquid / liquid biphasic regimes.

### 3.3.2. Results and Discussion

Before investigating the fluoros analogue, the conversions obtained with [MoO<sub>2</sub>(acac)<sub>2</sub>] were assessed using the two alternative methods to establish the more efficient process.<sup>15,16</sup> In order to simplify the analysis of the conversions obtained, a relatively simple substrate was chosen (3-methyl-2-buten-1-ol), which is also reported to yield high conversions (99 %), to the corresponding aldehyde using the sulfoxide oxygen transfer methodology (**Scheme 3.9**).<sup>15</sup>



Scheme 3.9

Unfortunately, the experimental procedures documented are rather ambiguous and it was not possible to repeat the levels of conversion detailed in the paper. Initially dimethyl sulfoxide was used as the oxygen transfer reagent, resulting in only 50 % conversion even though activated molecular sieves and completely anhydrous conditions were used. Attempts to use an alternative oxygen transfer reagent (phenyl sulfoxide,  $\text{Ph}_2\text{S}=\text{O}$ ), were hindered by the large excess required (40 equivalents), which made isolation of the product virtually impossible due to the large amount of solid in comparison to the small volume of liquid product.

The alternative methodology relies upon the *in situ* generation of hydrogen peroxide from sodium percarbonate [ $\text{Na}_2\text{CO}_3 \cdot 1.5\text{H}_2\text{O}_2$ ], to perform the oxidation. The procedure was investigated with cyclohexanol as the substrate, which is documented to proceed to 91 %.<sup>16</sup> Once again, this high level of conversion could not be repeated, but more significantly, the presence of the phase transfer catalyst (Adogen 464), severely complicated the work-up procedure and even after purification, traces remained visible in the  $^1\text{H}$  NMR spectrum. The necessity to incorporate this species arises due to the insolubility of the sodium percarbonate in the reaction mixture, a factor that effectively prohibits the implementation of the fluororous biphasic regime. Due to these complications, the investigation of the fluorinated molybdenum  $\beta$ -diketonate was carried out using the sulfoxide oxygen atom transfer route.

The fluororous molybdenum complex was evaluated following the strategy detailed in **Scheme 3.9**, with all manipulations carried out under a dry nitrogen atmosphere. Upon dissolving the catalyst **XIc**, in anhydrous DMSO the solution changed from dark green to gold. After seven hours at 100 °C the reaction was analysed and revealed a small trace of the aldehyde product, indicated by the distinctive doublet for the aldehyde proton at 9.5 $\delta$  in the  $^1\text{H}$  NMR spectrum. Disappointingly, the spectrum was dominated by the fluororous  $\beta$ -diketone ligand

arising from the decomposition of the molybdenum catalyst, which is extracted into the ether layer upon work-up. Attempts were made to remove the ligand by fluoruous extractions and distillation to determine the exact level of conversion obtained, but this was not possible due to the large excess of the fluorinated species. Unfortunately, it appears evident that the postulated recombination step (see **Figure 3.2**), does not occur readily for the fluorinated catalyst and as a consequence it is simply not compatible with the fluoruous biphasic approach. It is possible that the high dilution of the system, which results from the large excess of DMSO required to perform the oxidation, may contribute to the poor recombination of the catalyst. For this reason, several reactions were carried out using  $[\text{MoO}_2(\text{acac})_2]$  in more concentrated solutions, *i.e.* using a lower volume of DMSO. Unfortunately, however, the yield of the aldehyde decreased considerably, negating the possibility of attempting more concentrated reactions for the fluorinated catalyst. As a consequence, the reaction was not investigated further.

### 3.4. Conclusions

The application of fluoruous reverse phase silica gel technology to the nickel catalysed sulfide oxidations was successful on the basis of the physical isolation of the catalyst and also in the elimination of the need for expensive fluoruous solvents. Unfortunately, the activity of the catalysts was brought in to question during the investigation and overall it appears that nickel  $\beta$ -diketonates are not the species of choice for these reactions and that in certain cases the oxidation appears to proceed auto-catalytically. It was unfortunate that the fluoruous molybdenum  $\beta$ -diketonate was so moisture-sensitive, a factor that precluded the utilisation of FRPSG to separate the species from the reaction mixture. However, it transpired that neither of the reactions chosen to evaluate the catalyst were compatible with the fluoruous biphasic methodology. This was disappointing, especially due to the fact that this catalyst was active for the oxidation of 3-methyl-2-buten-1-ol using the sulfoxide oxygen atom transfer route. However, due to the moisture-sensitivity of the compound and the relatively poor conversions observed with the parent dioxobis(acetylacetonato) molybdenum, it is doubtful whether the yields would be very good, whilst the long-term stability of the catalyst would have to be

questioned, especially considering the harsh reaction conditions of 100 °C for seven hours. Furthermore, the fact that the quantity of DMSO could not be reduced, limits the appeal of the reaction on environmental grounds due to the large amounts of the dimethyl sulfide / sulfoxide mixture, which would have to be either re-oxidised or disposed of in large quantities.

### 3.5. References for Chapter 3

- [1] S. Colonna, N. Gaggero, F. Montanari, G. Pozzi and S. Quici, *Eur. J. Org. Chem.*, 2001, 181.
- [2] L.P. Barthel-Rosa and J.A. Gladsysz, *Coord. Chem. Rev.*, 1999, **190-192**, 587.
- [3] B. Betzemeier, F. Lhermitte and P. Knochel, *Synlett*, 1999, **4**, 489.
- [4] M. Madesclaire, *Tetrahedron*, 1986, **42**, 5459.
- [5] E.G. Mata, *Phosphorus, Sulfur and Silicon*, 1996, **96**, 231.
- [6] Y. Chang, L.L. Szafraniec and W. Beandry, *J. Org. Chem.*, 1990, **55**, 3664.
- [7] D.D. DesMarteau, V.A. Petrov, V.M. Montanari, M. Pregnotato and G. Resnati, *J. Org. Chem.*, 1994, **59**, 2762.
- [8] P.E. Correa and D.P. Riley, *J. Org. Chem.*, 1985, **50**, 1787.
- [9] S. Vincent, C. Lion, M. Hedayatullah, A. Challier, G. Delmas and G. Magnaud, *Phosphorus, Sulfur and Silicon*, 1994, **92**, 189.
- [10] A.E. Pedler, R.C. Smith and J.C. Tatlow, *J. Fluorine Chem.*, 1971 / 72, **1**, 433.
- [11] I. Klement, H. Lutjens and P. Knochel, *Angew. Chem. Int. Ed. Engl.*, 1997, **36**, 1454.
- [12] P. Laszlo and M. Levart, *Tetrahedron Lett.*, 1993, **34**, 1127.
- [13] T. Yamada, T. Takai, O. Rhode and T. Mukaiyama, *Bull. Chem. Soc. Jpn.*, 1991, **64**, 2109.
- [14] J. March, 'Advanced Organic Chemistry', (third edition), 1985. Wiley.
- [15] C.Y. Lorber, I. Pauls and J.A. Osborn, *Bull. Soc. Chim. Fr.*, 1996, **133**, 755.
- [16] S. Maignien, S. Alt-Mohand and J. Muzart, *Synlett*, 1996, 439.
- [17] O. Bortolini, F. Di Furia, G. Modena and C. Scardellato, *J. Mol. Catal.*, 1981, **11**, 107.
- [18] V.N. Sapunov, *J. Mol. Catal.*, 1980, **7**, 149.
- [19] M. Lakshmi Kantam and P. Lakshmi Santhi, *Synlett*, 1993, 429.
- [20] Y. Yamamoto, H. Suzuki and Y. Moro-oka, *Chem. Lett.*, 1986, 73.
- [21] K. Kaneda, K. Morimoto and T. Imanaka, *Chem. Lett.*, 1988, 1295.

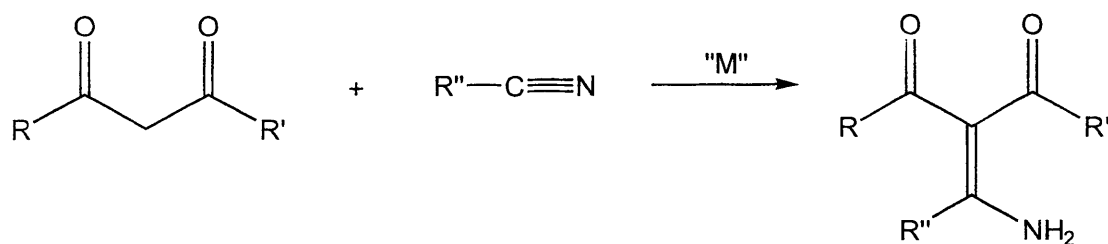
## 4. Carbon – carbon bond forming reactions catalysed by perfluoroalkylated metal complexes

### 4.1. Introduction

In recent years the implementation of fluoruous biphas technology for a range of carbon – carbon bond forming reactions has become a major endeavour for several authors in this expanding area of research (see Chapter 1). The main aims are to improve the economic and environmental factors to render existing methodologies (or novel regimes), more attractive to industry. The objective of the work described within this chapter is to investigate a carbon-carbon bond forming reaction that is catalysed by a recyclable fluoruous phase soluble catalyst. Furthermore, by building upon the data obtained from the sulfide oxidations, it is hoped that FRPSG can be used to recycle the catalyst.

#### 4.1.1. Carbon-carbon bond forming reactions between $\beta$ -dicarbonyls and nitriles

The metal catalysed carbon-carbon bond forming reaction between a 1,3-dicarbonyl compound and a nitrile species is somewhat unique.<sup>1</sup> The mechanism involves coordination of both species to the metal centre generating both the nucleophile and enhancing the electrophilicity of the nitrile (a more detailed account is given in section 4.3.1).<sup>2</sup> The general reaction scheme (**Scheme 4.1**) is very adaptable, tolerating a wide range of functionalities in both substrates. The products generated, unsaturated amino acid derivatives, are useful intermediates for the synthesis of amino acids and heterocycles.<sup>3</sup>



**Scheme 4.1**

Prior to the advent of the metal catalysed approach in the late seventies, the addition of protonated nucleophiles, such as 2,4-pentanedione, to Michael-type electrophiles and nitriles was kinetically disfavoured. Although the reactions could be promoted by the addition of base, the chemoselectivity obtained was quite poor.<sup>4</sup> However, upon coordination of the dicarbonyl substrate to a Lewis acidic metal centre, the nucleophilicity of the metallo-organic ring can be exploited (**Figure 4.1**).

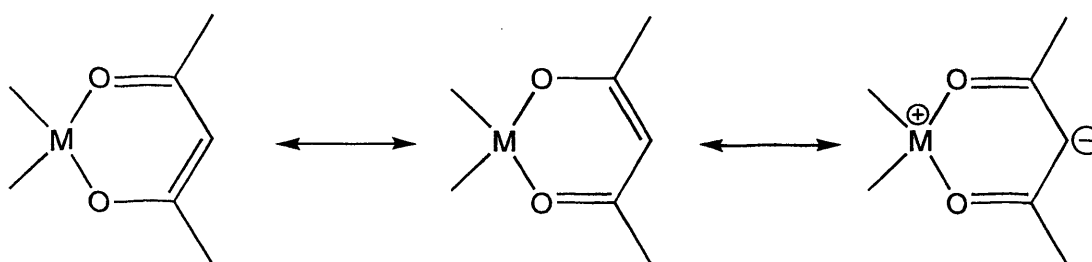


**Figure 4.1**

Several authors have investigated a variety of substitution reactions at the central methine carbon atom using a variety of electrophiles such as halogens, nitrates and isothiocyanate.<sup>5,6</sup> However, it was not until Eckberg *et al.* discovered that neutral electrophiles (Michael acceptors or nitriles) could be reacted to give insertion, rather than substitution, that the capacity for carbon-carbon bond formation was realised (**Figure 4.2**).<sup>7</sup>

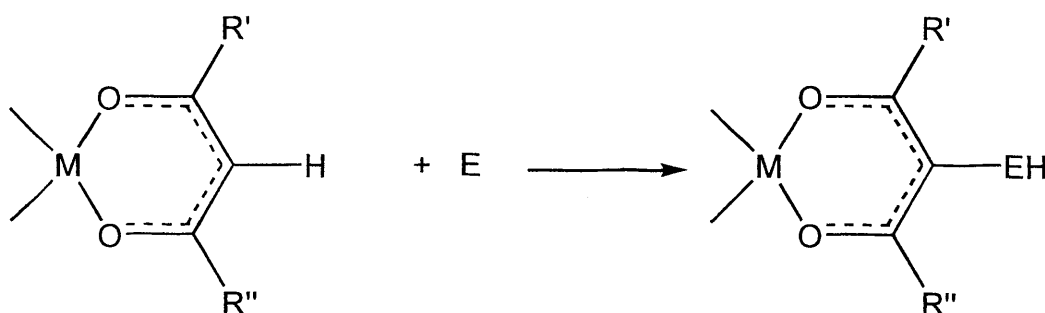
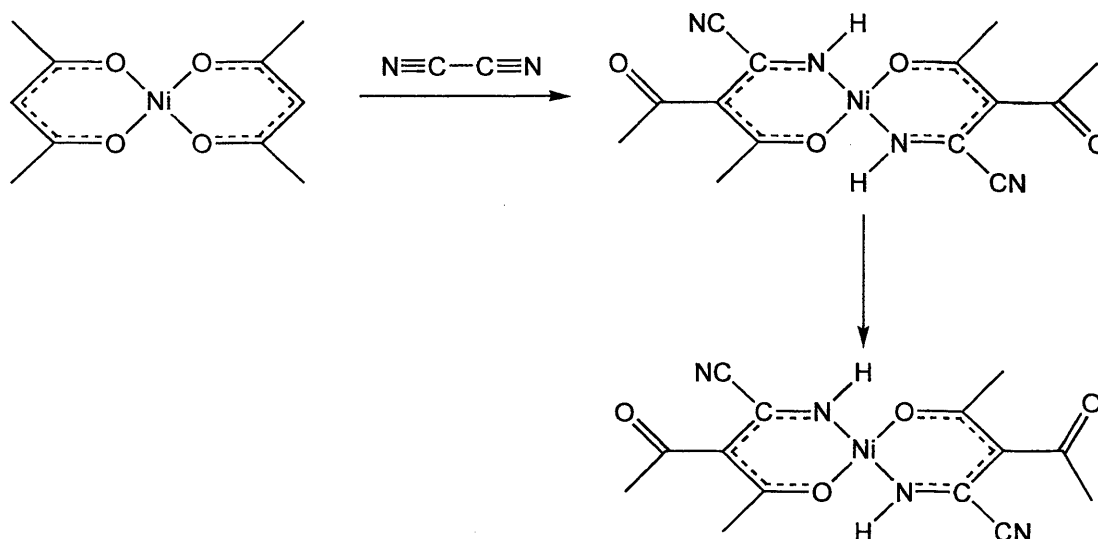


**Figure 4.2**

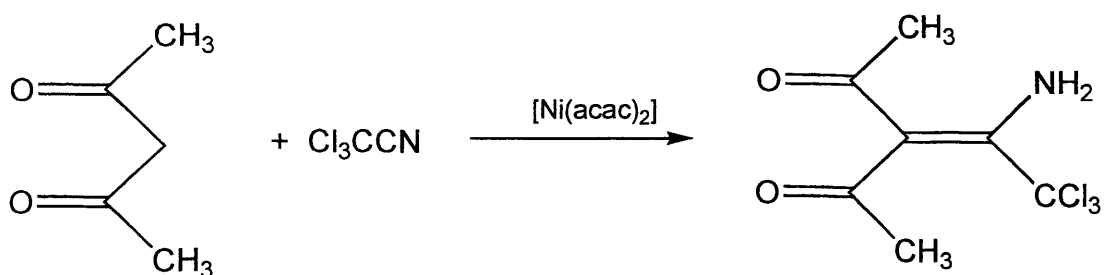
A variety of electrophiles were investigated with Corain *et al.* generating crystallographic evidence for the metal-assisted nucleophilic attack of 2,4-pentanedionato on cyanogen (**Scheme 4.2**).<sup>8</sup>



**Scheme 4.2**

Both isomers of the complex formed were analysed, with the only differences occurring at the orientation of the acetyl group with respect to the ‘NiNONO’ plane, and subsequently many insertion compounds were investigated in a similar fashion. The mechanism proposed, involves ring opening of the metallo-organic ring through dissociation of one of the oxygen donor atoms and concomitant end-on coordination of the nitrile *via* the nitrogen atom. This is followed by the metal-assisted nucleophilic attack of the central methine carbon atom at the electrophilic carbon of the coordinated cyanogen. The ligand / intermediate remains coordinated *via* the nitrogen atom as this is a better Lewis base than oxygen.<sup>8</sup>

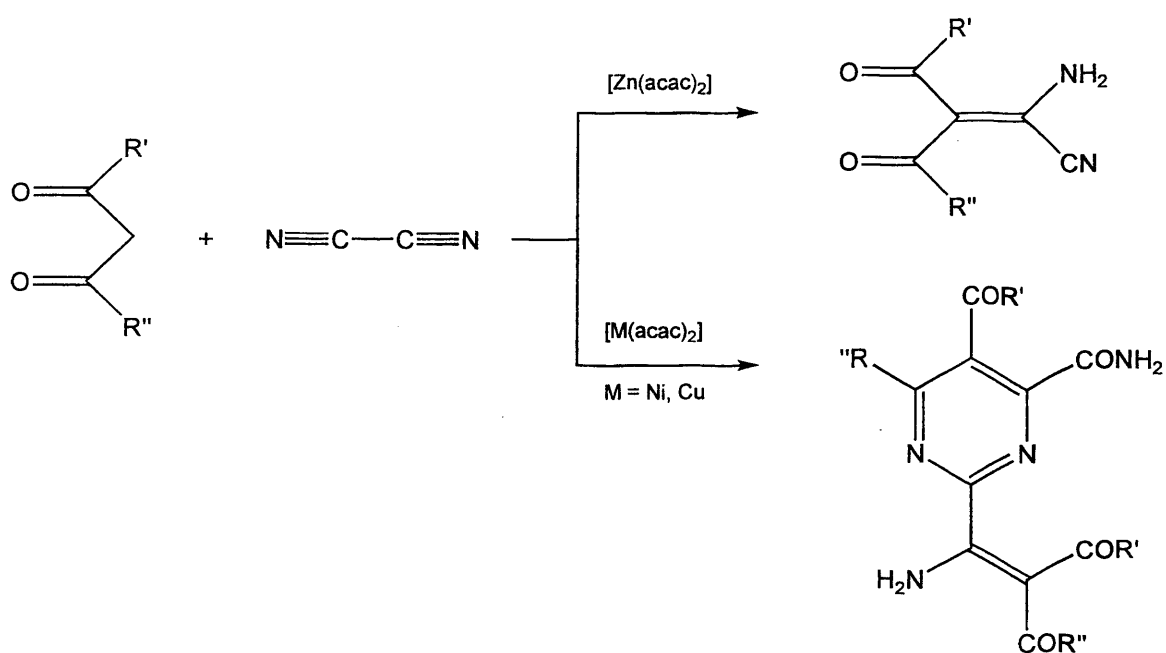
The progression to a catalytic reaction, resulting in the formation of a range of enaminedione compounds, was realised by Uehara *et al.* who reacted 2,4-pentanedione with trichloroacetonitrile in the presence of  $[\text{Ni}(\text{acac})_2]$  (**Scheme 4.3**).<sup>11</sup>



Scheme 4.3

Following this disclosure, the synthetic scope of the reaction was probed by Corain *et al.* revealing that a range of  $\beta$ -dicarbonyls were compatible with this approach including  $\beta$ -ketoesters,  $\beta$ -diesters and  $\beta$ -ketoamides.<sup>1</sup> The yields ranged from 60-90 %, although certain substrates required prolonged or slightly forcing conditions to achieve satisfactory levels of conversion. Furthermore, numerous metal complexes were found to be active catalysts for the reaction with copper, cobalt, manganese, zinc and nickel investigated.

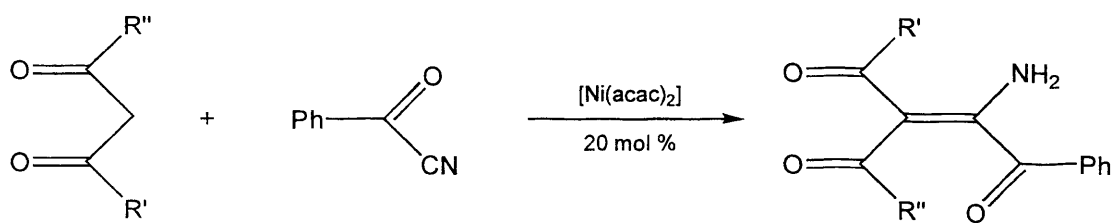
Although primarily Veronese, Corain and Basato have dominated this research, the systematic evaluation of a range of nitrile /  $\beta$ -dicarbonyl combinations was then analysed by numerous authors.<sup>1</sup> Overall, the strategy is very successful with the majority of the substrate pairings leading to the formation of enaminodiones. In certain cases, however, the enaminodione is directly converted into a cyclodimeric pyrimidine,<sup>10</sup> or a pyrrolic cycloisomer.<sup>11</sup> For example, the product formed in the addition of cyanogen to  $\beta$ -dicarbonyls, depends upon the catalyst used. Whilst [Zn(acac)<sub>2</sub>] leads to the formation of  $\beta$ -enaminodiones, the implementation of either [Ni(acac)<sub>2</sub>] or [Cu(acac)<sub>2</sub>] generates, chemospecifically, pyrimidines (Scheme 4.4).<sup>10</sup>



Scheme 4.4

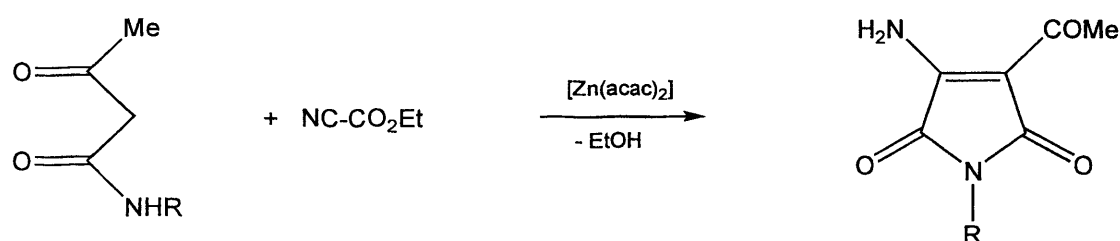
It is postulated that this alternative reactivity arises due to the ability of the copper and nickel metal centres to dimerise the coordinated addition product.

One particular combination where the unique nature of this methodology is highlighted, is in the coupling reaction between benzoyl cyanide and  $\beta$ -diketones.<sup>12</sup> Whereas a base catalysed approach would result in the nucleophilic attack at the carbonyl group with the C(O)-CN bond being broken, the utilisation of [Ni(acac)<sub>2</sub>] generates the  $\beta$ -enaminodione. The yields obtained are very high (73 – 87 %), but, a higher catalyst loading is required and the reactions are carried out in refluxing dichloroethane (Scheme 4.5).



Scheme 4.5

The addition of alkylcyanoformates to  $\beta$ -dicarbonyl compounds is known to proceed in the presence of metal halides (in certain cases coupled with organic bases), although the reaction is improved significantly by adopting the metal acetylacetonato catalysed approach.<sup>13</sup> In particular, the implementation of  $[\text{Zn}(\text{acac})_2]$  enables the reaction to be carried out under milder, cleaner conditions than the aforementioned approach.<sup>5</sup> The yields for the reactions are universally high with  $\beta$ -diketones,  $\beta$ -ketoesters and  $\beta$ -diesters yielding  $\beta$ -enaminodiones in high purity. For  $\beta$ -ketoamides the products obtained are cyclic amino amides, arising *via* a similar method to that described for cyanogen earlier (**Scheme 4.6**).

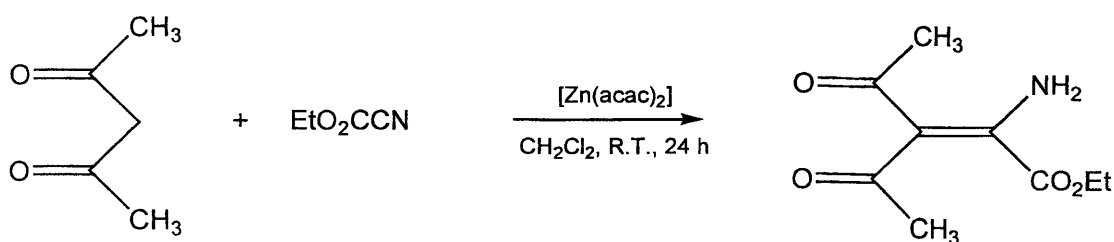
**Scheme 4.6**

Despite the effectiveness and versatility of this carbon-carbon bond forming regime, at the time of writing, there have been no attempts to either recover or recycle the catalytic species. Due to the toxicity of the nickel, copper and zinc salts used, the implementation of the reaction on a large scale would be compromised due to the health and environmental risks. As a consequence, a fluorosoluble analogue of these species may provide an alternative that can be easily recovered and hopefully recycled back into further reaction cycles. The remainder of this chapter describes the attempts to achieve these aims.

## 4.2. Enaminodione Reactions

### 4.2.1. Catalysis using fluorous derivatised $\beta$ -diketonates – ‘Preliminary investigations’

Initially, a relatively simple carbon-carbon bond forming reaction was chosen to determine the activity of the fluorinated  $\beta$ -diketonate complexes. The reaction between 2,4-pentanedione and ethyl cyanoformate (**Scheme 4.7**) was chosen due to the high level of conversion obtained when  $[\text{Zn}(\text{acac})_2]$  is used to catalyse the process at room temperature and this allowed for easy comparison with other catalysts under similar conditions.<sup>3</sup>



**Scheme 4.7**

The first catalyst analysed was the symmetrical zinc *bis*-1,1,1,2,2,3,3,4,4,5,5,6,6,-10,10,11,11,12,12,13,13,14,14,15,15,15-hexacosafuoro-pentadecane-7,9-dionate  $[\text{Zn}(\text{C}_6\text{F}_{13}/\text{C}_6\text{F}_{13})_2]$  (**IXb**), using the exact conditions employed by Veronese *et al.*<sup>3</sup> The result obtained suggested that the activity of the complex was comparable to that for zinc *bis*-acetylacetonato  $[\text{Zn}(\text{acac})_2]$  affording 67 % conversion to the enaminodione in comparison to an 85 % conversion for the non-fluorinated analogue. Following this result, the catalytic activity of the other three zinc  $\beta$ -diketonates (*i.e.* zinc *bis*-hexafluoroacetylacetonato  $[\text{Zn}(\text{hfacac})_2]$ , the unsymmetrical 1,1,1,5,5,6,6,7,7,8,8,9,9,-10,10,10-hexadecafluoro-decane-2,4-dionate  $[\text{Zn}(\text{CF}_3/\text{C}_6\text{F}_{13})_2]$  (**IXa**) and 1,1,1,2,2,3,3,4,4,5,5,6,6,7,7,-11,11,12,12,13,13,14,14,15,15,16,16,17,17,17-triacontafuorohepta-decane-8,10-dionate  $[\text{Zn}(\text{C}_7\text{F}_{15}/\text{C}_7\text{F}_{15})_2]$  (**IXc**) were analysed alongside  $[\text{Zn}(\text{acac})_2]$  and **IXb** for comparative purposes. At this stage, the main aim of the work was to establish the

activities of the catalysts, rather than separation and / or recovery. From this point on, all reactions were carried out in a Radleys Carousel Workstation to ensure that exactly the same conditions were employed for all the experiments (**Figure 4.3**).



**Figure 4.3**

The complexes were all dried under high vacuum before use and the reactions were carried out under anaerobic conditions using dry nitrogen and dry, degassed dichloromethane. The results obtained are shown in **Table 4.1** below.

**Table 4.1.** Catalysis of reaction between 2,4-pentanedione and ethyl cyanoformate

Catalyst	Mass of catalyst / mg	Yield / g	Yield / %
Zn(acac) <sub>2</sub>	26	1.763	88
Zn(hfacac) <sub>2</sub>	48	1.032	52
Zn(CF <sub>3</sub> /C <sub>6</sub> F <sub>13</sub> ) <sub>2</sub> ( <b>IXa</b> )	98	1.281	64
Zn(C <sub>6</sub> F <sub>13</sub> /C <sub>6</sub> F <sub>13</sub> ) <sub>2</sub> ( <b>IXb</b> )	148	1.724	86
Zn(C <sub>7</sub> F <sub>15</sub> /C <sub>7</sub> F <sub>15</sub> ) <sub>2</sub> ( <b>IXc</b> )	162	0.536	27

The five results clearly indicate that the complexes of the hexafluoroacetylacetonato and unsymmetrical ligand are poorer catalysts than either [Zn(acac)<sub>2</sub>] or [Zn(C<sub>6</sub>F<sub>13</sub>/C<sub>6</sub>F<sub>13</sub>)<sub>2</sub>], which both exhibit similar levels of activity. Unfortunately, the perfluoroheptyl derivatised complex (**IXc**), was not very soluble in dichloromethane, resulting in the poor conversion of 27 %. As mentioned earlier, the solubility of the perfluoroheptyl derivatised complexes is poor in virtually all solvents, even resulting in difficult characterisation (see Chapter 2). As a consequence, complex **IXc** was not analysed further for any catalytic reactions.

From these early results, attention was focussed upon the perfluorohexyl derivatised catalyst (**IXb**), with particular emphasis placed upon attaining reproducible results. Initially, this proved to be quite difficult to attain, with varying levels of conversion obtained using different batches of catalyst. However, it was determined that the increased Lewis acidity of the complex meant that more stringent drying conditions were required to remove water bound to the molecule. For this reason, the catalysts were thoroughly dried over silica gel under high vacuum for forty-eight hours prior to use. Once these problems had been surmounted, consistently high levels of activity were recorded and are detailed in **Table 4.2**.

**Table 4.2.** Catalysis of reaction between 2,4-pentanedione and ethyl cyanoformate

Catalyst	Mass of catalyst / mg	Yield / g	Yield / %
Zn(C <sub>6</sub> F <sub>13</sub> /C <sub>6</sub> F <sub>13</sub> ) <sub>2</sub>	148	1.853	93
Zn(C <sub>6</sub> F <sub>13</sub> /C <sub>6</sub> F <sub>13</sub> ) <sub>2</sub>	148	1.921	96
Zn(C <sub>6</sub> F <sub>13</sub> /C <sub>6</sub> F <sub>13</sub> ) <sub>2</sub>	148	1.724	86

These results clearly indicate the high activity of the catalyst with almost quantitative conversions observed. However, during the reaction undissolved solid was observed, indicating that there was possibly an excess of the zinc catalyst present. For this reason, it was decided to perform a series of tests to ascertain the amount of catalyst required to achieve a satisfactory level of conversion. **Table 4.3** details the results acquired where the mole percentage of (IXb) was lowered by 25% increments.

**Table 4.3.** 2,4-pentanedione and ethyl cyanoformate – catalyst loading experiments

Catalyst	Mass of catalyst / mg	Catalyst / mol %	Yield / g	Yield / %
Zn(C <sub>6</sub> F <sub>13</sub> /C <sub>6</sub> F <sub>13</sub> ) <sub>2</sub>	0	0.0	0.0*	-
Zn(C <sub>6</sub> F <sub>13</sub> /C <sub>6</sub> F <sub>13</sub> ) <sub>2</sub>	37	0.25	0.98	49
Zn(C <sub>6</sub> F <sub>13</sub> /C <sub>6</sub> F <sub>13</sub> ) <sub>2</sub>	74	0.50	1.26	63
Zn(C <sub>6</sub> F <sub>13</sub> /C <sub>6</sub> F <sub>13</sub> ) <sub>2</sub>	111	0.75	1.56	78
Zn(C <sub>6</sub> F <sub>13</sub> /C <sub>6</sub> F <sub>13</sub> ) <sub>2</sub>	148	1.00	1.92	96

\* - <sup>1</sup>H NMR spectrum exhibited only starting material

The results demonstrate that as the quantity of catalyst is increased, the amount of product formed also increases. Clearly, the optimal amount of catalyst required lies between 0.75 and 1.0 mol %, although further refinement was not made. The experiment carried out in the absence of any catalyst produces no enaminodione as indicated by the recovery of unreacted ethyl cyanoformate.

#### 4.2.2. Catalysis using perfluoroalkylated zinc $\beta$ -diketonates – ‘Recovery and Recycling’

Having determined the catalytic activity of the fluorinated zinc  $\beta$ -diketonate complexes (**IXa-c**), the next aim was to establish recovery and recycling procedures in order to produce an effective catalytic regime. After catalysing the reaction between 2,4-pentanedione and ethyl cyanofornate, the separation of the zinc catalyst from the enaminodione product was investigated by both solid / liquid and liquid / liquid extraction.

In a similar manner to the nickel-catalysed sulfide oxidations described in chapter 2, attempts were made to separate the fluorous zinc catalyst (**IXb**) from the final reaction mixture *via* filtration through a solid medium. At the end of the reaction, the crude reaction mixture was passed down a fluorous reverse phase silica gel column (Pasteur pipette column, approximately 8 cm in length, pre-eluted with dichloromethane). Owing to the almost slurry-like viscosity of the reaction mixture, care was needed to ensure the column did not become blocked by solid material and further dichloromethane was used to elute the remaining product ( $\sim 10 \text{ cm}^3$ ). A large percentage of the zinc complex was retained by the solid phase although small amounts of leaching were identified by the  $^{19}\text{F}$  NMR spectrum of the organic product eluted from the column. A similar result was obtained when Celite was employed to filter the catalyst from the reaction mixture, using the same procedure developed by Veronese for zinc *bis*-acetylacetonate.<sup>3</sup> However, whereas the catalyst could be removed from the FRPSG column by elution with diethyl ether, this was not possible for the Celite procedure.

At this early stage, an alternative means of separation was attempted using the more traditional liquid-liquid biphasic technique to extract the catalyst. Perfluoro-1,3-dimethylcyclohexane (PP3), which is immiscible with the reaction solvent (dichloromethane), was used to recover the catalyst in three separate, equal volume, extractions ( $3 \times 2 \text{ cm}^3$ ). Unfortunately, the partition of the product between the two phases was not totally efficient, with small amounts of the enaminodione product detected in the lower fluorous phase. In an attempt to reduce the level of enaminodione product entering the fluorous phase, the reaction was repeated, but at

the end of the reaction, the organic phase was diluted by a further 2 cm<sup>3</sup> of dichloromethane (taking the total volume to 4 cm<sup>3</sup>). Unfortunately, however, similar problems were encountered, even with a five-fold dilution of the dichloromethane phase indicated by the low product yields detailed in **Table 4.4** below.

**Table 4.4.** 2,4-pentanedione and ethyl cyanoformate – catalyst separation techniques

Catalyst	Separation Technique	Yield / g	Yield / %
Zn(C <sub>6</sub> F <sub>13</sub> /C <sub>6</sub> F <sub>13</sub> ) <sub>2</sub>	FRP	1.701	85
Zn(C <sub>6</sub> F <sub>13</sub> /C <sub>6</sub> F <sub>13</sub> ) <sub>2</sub>	FRP	1.878	94
Zn(C <sub>6</sub> F <sub>13</sub> /C <sub>6</sub> F <sub>13</sub> ) <sub>2</sub>	PP3	1.56	78
Zn(C <sub>6</sub> F <sub>13</sub> /C <sub>6</sub> F <sub>13</sub> ) <sub>2</sub>	PP3*	1.654	83

\* - Organic phase increased to 4 cm<sup>3</sup>

Although the yield of product recovered from the diluted extraction was slightly higher, attempts to recover the catalyst were hampered due to contamination by the organic product (a distinctive pale yellow colouration could be observed in the lower fluoros phase). Efforts were made to remove the product by washing with an organic solvent (chloroform), in which the catalyst is insoluble. Disappointingly, however, whilst this enabled the catalyst to be purified, the catalyst recovery remained low at approximately 75 %. This result indicated that the catalyst was not fully recovered from the reaction mixture in the initial extractions, a fact confirmed by the analysis of the <sup>19</sup>F NMR spectrum of the product, where six signals corresponding to the fluoros ponytail were identified. Due to these problems, liquid-liquid extraction was not investigated further for these reactions.

#### 4.2.3. Catalysis using perfluoroalkylated nickel $\beta$ -diketonates

The possibility of employing the analogous nickel complexes to effect the carbon-carbon bond forming reactions was postulated as an alternative to the zinc species, owing to their similar Lewis acid properties. It was also hoped that the efficient extraction using FRP silica gel, demonstrated for the sulfide oxidations, could be adapted to this reaction scheme. The initial investigation to ascertain the

activity of the nickel *bis*-1,1,1,2,2,3,3,4,4,5,5,6,6,10,10,11,11,12,12,13,13,14,14,15,-15,15-hexacosafuoro-pentadecane-7,9-dionate complex  $[\text{Ni}(\text{C}_6\text{F}_{13}/\text{C}_6\text{F}_{13})_2]$  (**VIIIb**), revealed that the species yielded conversions comparable to the zinc analogue (**XIb**). The same experimental procedure was employed to that described for the zinc experiments (**Scheme 4.7**), using a 1 mol % catalyst loading. However, in comparison to the zinc complex, the nickel catalyst was considerably less soluble in the dichloromethane reaction solvent, although upon addition of 2,4-pentanedione and ethyl cyanoformate, the complex dissolved producing a homogeneous green solution. After twenty-four hours, the distinctive yellow coloration of the enaminodione could be observed, indicating that reaction had occurred. The crude reaction mixture was passed down a FRPSG column, where the nickel catalyst was retained selectively, whilst the enaminodione product was eluted with further dichloromethane. Evaporation of the solvent yielded the pure product in 77 % yield. The reaction was repeated several times to establish reproducibility, the results of which are detailed in **Table 4.5** below.

**Table 4.5.** 2,4-pentanedione and ethyl cyanoformate – nickel catalysis

Catalyst	Mass of catalyst / mg	Yield / g	Percentage Yield
$\text{Ni}(\text{C}_6\text{F}_{13}/\text{C}_6\text{F}_{13})_2$	147	1.534	77
$\text{Ni}(\text{C}_6\text{F}_{13}/\text{C}_6\text{F}_{13})_2$	147	1.797	90
$\text{Ni}(\text{C}_6\text{F}_{13}/\text{C}_6\text{F}_{13})_2$	147	1.839	92

To ascertain the effectiveness of the nickel catalyst, in comparison to the zinc analogue, a similar series of experiments were carried out analysing the conversion obtained with 25 % increment catalyst loadings. The 0 % experiment was not repeated, although for comparative purposes, the 1 mol % run was probed alongside the three other experiments detailed in **Table 4.6** below.

**Table 4.6.** 2,4-pentanedione and ethyl cyanofornate – catalyst loading experiments

Catalyst	Mass of catalyst / mg	Catalyst / Mol %	Yield / g	Yield / %
Ni(C <sub>6</sub> F <sub>13</sub> /C <sub>6</sub> F <sub>13</sub> ) <sub>2</sub>	37	0.25	1.46	73
Ni(C <sub>6</sub> F <sub>13</sub> /C <sub>6</sub> F <sub>13</sub> ) <sub>2</sub>	74	0.50	1.64	82
Ni(C <sub>6</sub> F <sub>13</sub> /C <sub>6</sub> F <sub>13</sub> ) <sub>2</sub>	110	0.75	1.86	93
Ni(C <sub>6</sub> F <sub>13</sub> /C <sub>6</sub> F <sub>13</sub> ) <sub>2</sub>	147	1.00	1.84	92

The results clearly indicate that [Ni(C<sub>6</sub>F<sub>13</sub>/C<sub>6</sub>F<sub>13</sub>)<sub>2</sub>] is a more active catalyst than [Zn(C<sub>6</sub>F<sub>13</sub>/C<sub>6</sub>F<sub>13</sub>)<sub>2</sub>] due to the higher conversions obtained with only 0.25 and 0.5 mol % catalyst loadings (73 and 82 % compared to 49 and 63 % for the zinc analogue respectively). At three quarters of the original loading, the conversion is equal to the full 1 mol % result, suggesting that the optimal quantity is between 0.5 and 0.75 mol % based upon product formation, although further refinement was not made. For comparative purposes, especially for the alternative substrates (see section 4.3.), it was decided to perform future experiments with the 1 mol % loading, although on an industrial scale, the amount of catalyst could be reduced significantly, further enhancing the viability of this reaction. It is reasonable to postulate that this increased reactivity is due to the enhanced Lewis acidity of the fluorinated complex, imparted specifically by the long perfluoroalkyl tails. However, due to the eventual release of the coordinated enaminodione product, the Lewis acidity of the metal centre has to be finely balanced to enable the continuation of the catalytic cycle (see section 4.3.1). For [Zn(C<sub>6</sub>F<sub>13</sub>/C<sub>6</sub>F<sub>13</sub>)<sub>2</sub>], the Lewis acidity may be too powerful, thus retarding the activity, especially at lower catalyst loadings, (alternatively, the zinc species may be more susceptible to catalyst poisoning due to this increased Lewis acidity in particular, traces of water which may bind strongly, thus blocking the catalytic cycle).

Due to the high activity of [Ni(C<sub>6</sub>F<sub>13</sub>/C<sub>6</sub>F<sub>13</sub>)<sub>2</sub>], the three other nickel  $\beta$ -diketonate complexes were also examined in parallel investigations. In contrast to the analogous zinc complexes, [Ni(C<sub>6</sub>F<sub>13</sub>/CF<sub>3</sub>)<sub>2</sub>] and [Ni(hfacac)<sub>2</sub>] are both remarkably efficient catalysts for the reaction between 2,4-pentanedione and ethyl

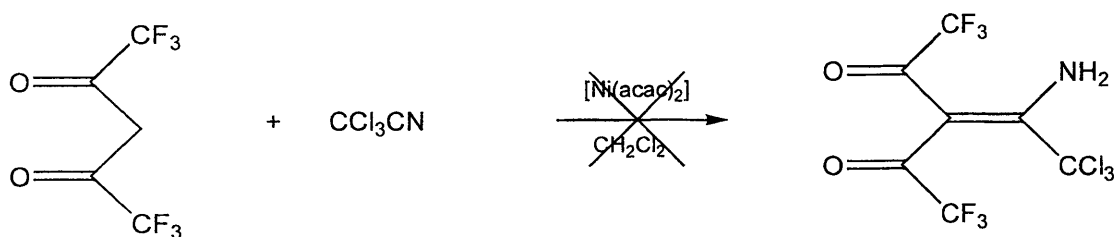
cyanofornate (**Table 4.7**). The most surprising distinction arose for the unsymmetrical complex (**VIIIa**), which afforded almost quantitative conversion. Significantly though, the reaction appeared to take place faster than when **VIIIb** was used, simply on the basis of the visual observation. In part, this prompted the detailed analysis of a series of ‘reaction profiles’ for a variety of substrate / catalyst combinations, which attempt to quantify this enhanced reactivity (see section 4.3.3.). Upon attempting to separate the unsymmetrical catalyst from the reaction mixture by using an FRPSG column, the leaching of the nickel species into the organic phase was clearly visible. However, a further investigation suggests that this poor retention is a result of the greater solubility of the unsymmetrical derivatised complex in dichloromethane. By simply stirring the catalyst together with the reagents in dichloromethane for 5 minutes, the separation was investigated before the reaction had begun to any extent. The result was analogous to that observed when the reaction had gone to completion, intimating that the retention on FRPSG is a balance of affinities between the solvent and solid phases.

**Table 4.7.** 2,4-pentanedione and ethyl cyanofornate – alternative nickel catalysts

Catalyst	Mass of catalyst / mg	Yield / g	Yield / %
Ni(acac) <sub>2</sub>	26	1.50	74
Ni(hfacac) <sub>2</sub>	47	1.37	68
Ni(C <sub>6</sub> F <sub>13</sub> /CF <sub>3</sub> ) <sub>2</sub> ( <b>VIIIa</b> )	97	1.97	99
Ni(C <sub>6</sub> F <sub>13</sub> /C <sub>6</sub> F <sub>13</sub> ) <sub>2</sub> ( <b>VIIIa</b> )	147	1.86	93

When [Ni(hfacac)<sub>2</sub>] and [Ni(acac)<sub>2</sub>] were investigated, as expected, neither complex could be retained by passing the reaction mixture down an FRPSG column. However, by implementing a slightly modified procedure to that described by Veronese *et al.*, [Ni(hfacac)<sub>2</sub>] could be removed *via* a Celite filtration.<sup>3</sup> However, once the product was removed, the catalyst could not be extracted from the solid media. Both complexes afforded excellent yields of the enaminodione product, although whilst [Ni(hfacac)<sub>2</sub>] was observed as a green band on the column, the [Ni(acac)<sub>2</sub>] filtration only resulted in a brownish residue on the Celite.

The inability to recover  $[\text{Ni}(\text{acac})_2]$  implies that the catalyst is expended during the reaction. Unfortunately, it was not possible to recover and hence characterise the small quantity of residue retained by the column. However, it is reasonable to assume that the initial acetylacetonato ligands of the nickel catalyst actually undergo reaction with ethyl cyanoformate in the first stage of the reaction in the same manner as the substrate  $\beta$ -diketone. Due to the fact that the cyanoformate is used in a 0.5 molar excess, it is unlikely that there will be any  $\beta$ -diketone to undergo a 'recombination' step to regenerate the catalyst. By analogy, it is reasonable to assume that a similar process would occur for the  $[\text{Zn}(\text{acac})_2]$  catalysed reaction, although in this case, the colour change is not so distinct. Whilst this is not, in any respect, deleterious for this reaction, for alternative  $\beta$ -dicarbonyl substrates the obvious problem arises of cross-coupled product from the ligands of the catalyst formed alongside the desired  $\beta$ -enaminodione. The advantage of the fluorinated catalysts, however, is that due to the electron withdrawing effect of the perfluoroalkyl moieties, the central intercarbonylic carbon atom is unable to function as a nucleophile, thus preventing reaction from occurring. This inertness was highlighted by Veronese who investigated the  $[\text{Ni}(\text{acac})_2]$  catalysed reaction between trichloroacetonitrile and 1,1,1,5,5,5-hexafluoro-2,4-pentanedione (**Scheme 4.8**).<sup>14</sup>



Scheme 4.8

To confirm that the chemistry of the highly fluorinated catalysts was similar, two experiments were performed that ruled out the possibility of any cross-coupled product. In the first test, no trace of reactivity was observed when  $[\text{Ni}(\text{C}_6\text{F}_{13}/\text{C}_6\text{F}_{13})_2]$  (**VIIIb**), was used to catalyse the reaction between 1,1,1,5,5,5-hexafluoro-2,4-pentanedione and ethyl cyanoformate (analogous to **Scheme 4.8**).

In a similar manner, when the same reaction was analysed using a vast surplus of VIIIb (4-fold excess), there was no evidence in either the  $^1\text{H}$  or  $^{19}\text{F}$  NMR spectra, of a cross-coupled compound arising from reaction of the fluorinated  $\beta$ -diketonate with the nitrile. These results suggest that for alternative substrates, the fluorinated catalysts will offer a cleaner more effective synthesis, as they are not incorporated into the reaction pathway.

Ultimately, the aim of analysing the nickel species was to produce an effective recycling regime for the fluorous catalysts. As described earlier, the symmetrical complex  $[\text{Ni}(\text{C}_6\text{F}_{13}/\text{C}_6\text{F}_{13})_2]$ , was readily separated from the reaction mixture by passing down a Pasteur pipette filled with approximately 8 cm of FRP silica gel. Significantly, no leaching was observed when the  $^{19}\text{F}$  NMR of the enaminedione product was analysed. Following these results, recovery and recycling were addressed using the same protocol as that used for the zinc system. Once the organic product had been eluted, passing diethyl ether down the column ( $15\text{ cm}^3$ ), enabled the metal complex to be removed, with no green coloration remaining on the column. For comparison, a reaction was carried out using standard silica gel to isolate the catalyst. Using this media, it was found that although separation could be achieved similarly to FRPSG, the catalyst could not be completely removed from the column. Once eluted from the FRPSG column, evaporation of the solvent yielded a green residue that unfortunately exhibited poor activity upon re-use. It was postulated that this decrease in activity was due to ether molecules coordinating to the metal centre and retarding the Lewis acidity of the complex. Initially, alternative solvents were employed in the column washing stage to overcome this problem including acetone, diisopropyl ether and ethyl ethanoate but in all cases the recovery was considerably lower than that obtained with diethyl ether. As a consequence, a 'washing' procedure was introduced into the catalytic regime to remove any last traces of the eluting solvent. By employing a hexane wash followed by a methanol wash, the catalyst was reconverted to a fine green powdery solid. Owing to the small quantities involved, the washes are performed *in situ* to minimise the loss of the catalyst. In order to ensure that the catalyst used for each cycle was analogous to the original (Run 1) catalyst, the recovered material was also dried under high vacuum for 24 hours between each cycle. These

refinements dramatically increased the turnover of the catalyst (see entries 1-3 in **Table 4.8** below).

**Table 4.8.** 2,4-pentanedione and ethyl cyanoformate – nickel recycling experiments

Run No.	Catalyst	Mass of catalyst recovered / mg	Yield / g	Percentage Yield
1	Ni(C <sub>6</sub> F <sub>13</sub> /C <sub>6</sub> F <sub>13</sub> ) <sub>2</sub>	152	1.83	91
2	Ni(C <sub>6</sub> F <sub>13</sub> /C <sub>6</sub> F <sub>13</sub> ) <sub>2</sub>	150	1.67	84
3	Ni(C <sub>6</sub> F <sub>13</sub> /C <sub>6</sub> F <sub>13</sub> ) <sub>2</sub>	149	1.64	82
4	Ni(C <sub>6</sub> F <sub>13</sub> /C <sub>6</sub> F <sub>13</sub> ) <sub>2</sub>	146	1.34	67
5	Ni(C <sub>6</sub> F <sub>13</sub> /C <sub>6</sub> F <sub>13</sub> ) <sub>2</sub>	137	1.04	52

Despite these enhancements, the catalytic activity dropped on Runs 4 and 5. Experimentally, the recovered catalyst became increasingly difficult to ‘wash’ in order to regenerate the powdery solid. This indicates that the reaction process is altering the catalyst. A possible explanation is that one of the fluorinated ligands is being exchanged for an acetylacetonato ligand (see first stage of proposed mechanism **Figure 4.4** overleaf).<sup>1,8</sup> As the reaction does not go to completion there will, inevitably, be a small percentage of the  $\beta$ -diketone substrate remaining, resulting in the formation of the heteroleptic complex [Ni(acac)/(C<sub>6</sub>F<sub>13</sub>/C<sub>6</sub>F<sub>13</sub>)]. Unfortunately, the retention of this species on the FRPSG column will not be as effective as for the homoleptic complex, resulting in the progressive loss of the catalyst. However, there are other factors that may result in a loss of catalyst integrity including; solvent coordination, cyanoformate coordination or even decomposition on the FRPSG column. Overall, these results clearly demonstrate the efficacy of this process with regard to catalyst recovery and re-use on a laboratory scale; the process has not been optimised and clearly the efficiency of the process could be improved on a larger scale by adjusting the stoichiometries to prevent the problem of excess reagents.

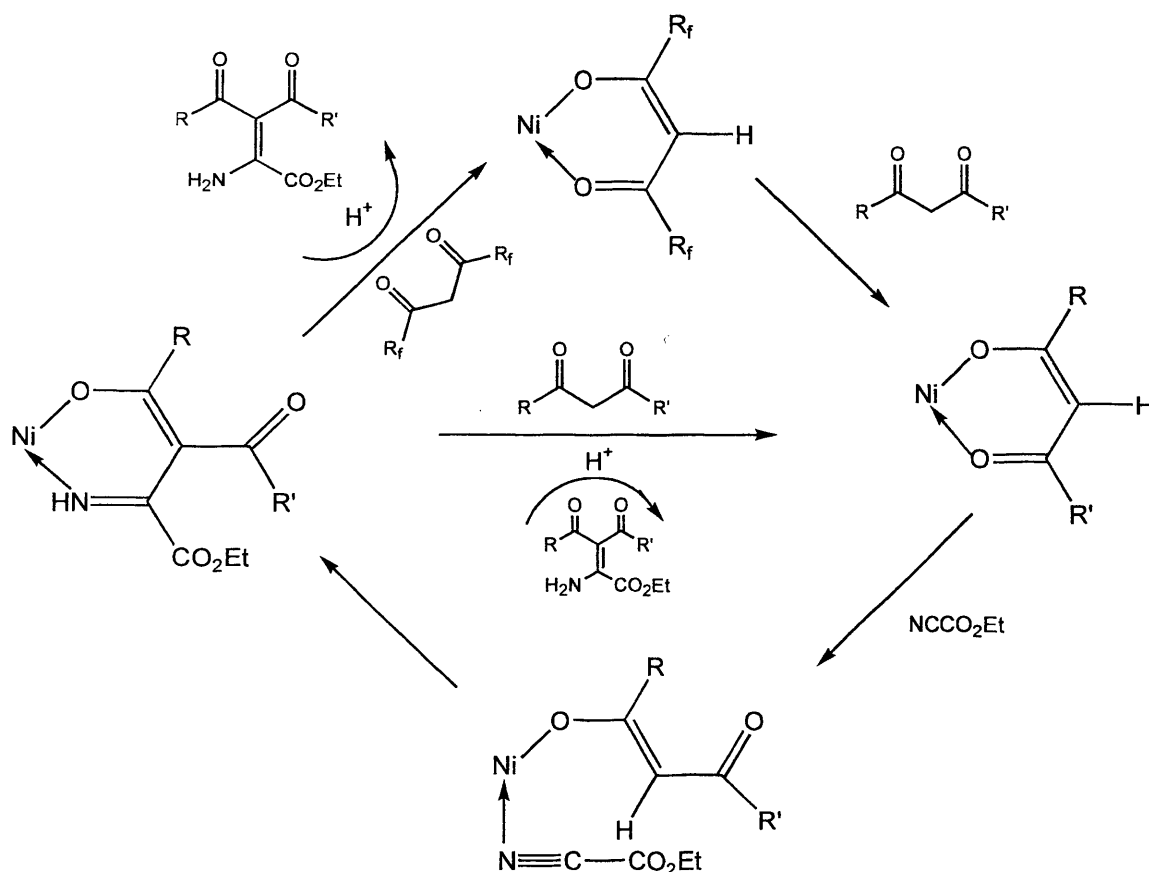
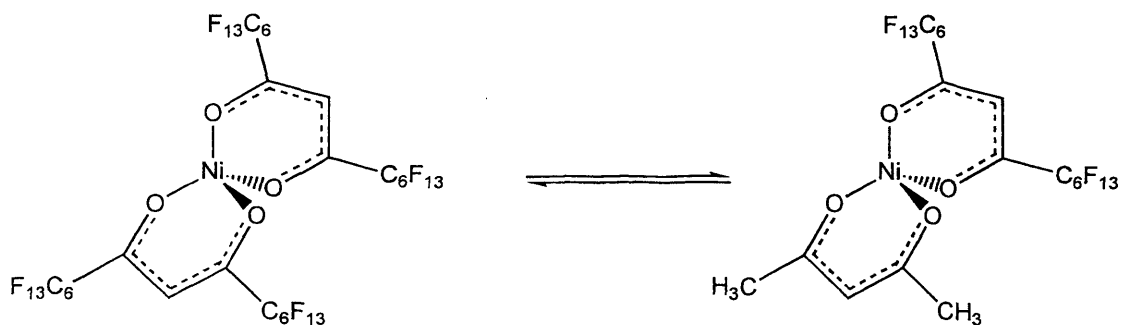


Figure 4.4

To test the effectiveness of the fluororous reverse phase silica gel as a means of removing the fluorinated catalysts, ICP mass spectrometry was carried out on the filtered products of three reactions catalysed by [Ni(CF<sub>3</sub>/C<sub>6</sub>F<sub>13</sub>)<sub>2</sub>] (**VIIIa**), [Ni(C<sub>6</sub>F<sub>13</sub>/C<sub>6</sub>F<sub>13</sub>)<sub>2</sub>] (**VIIIb**) and [Zn(C<sub>6</sub>F<sub>13</sub>/C<sub>6</sub>F<sub>13</sub>)<sub>2</sub>] (**XIb**). The Pasteur pipette dimensions and elution volumes were standardised to enable easy comparison. The analyses were carried out by GlaxoSmithKline laboratories, using a Jobin Yvon Ultima spectrometer (see Appendix 2). As expected, the leaching level for the unsymmetrical nickel catalyst (**VIIIa**) was very high (48 %), confirming that the molecule does not contain a sufficient degree of fluorination to be retained by the FRPSG column. Although significantly better, the result for the symmetrical nickel catalyst was quite disappointing at 7.5 % leaching. However, the result was rationalised when the percentage conversion was calculated for the reaction. Unfortunately, and somewhat inexplicably, the reaction had only reached 82 % conversion, and as a consequence, there will have been a considerable amount of

2,4-pentanedione remaining. Due to the exchange process occurring between this molecule and the fluorinated ligand, it is possible that a small quantity of the heteroleptic complex will be present (**Figure 4.5**). As the total fluorine content of this molecule is approximately equal to that of **VIIIa**, it is highly likely that this species generates the observed leaching.



**Figure 4.5**

This trend is confirmed by the leaching data obtained for the zinc analogue, **IXb**, that was significantly lower at only 4 %. For this particular reaction, the conversion was higher at 90 %, thus reducing the amount of heteroleptic complex and hence lowering the amount of zinc that leached down the fluorinated column. Unfortunately, it was not possible to repeat these analyses due to time constraints. However, the link between percentage conversion and the level of leaching observed is clearly apparent and it is regrettable that the system from an ‘ideal’ (i.e. >90 % conversion) could not have been analysed with the symmetrical nickel catalyst.

### 4.3. Catalysis using fluorinated derivatised $\beta$ -diketonates – ‘Alternative Substrates’

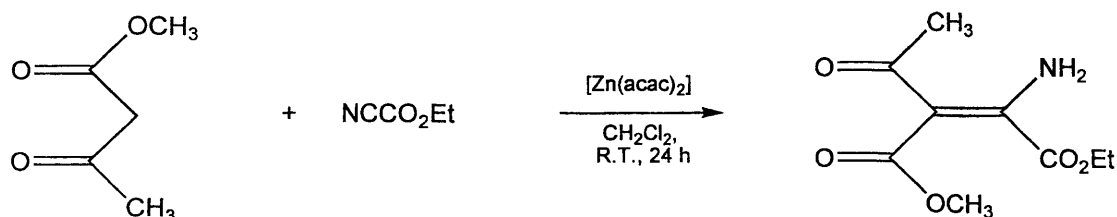
In order to evaluate the synthetic scope of the fluorinated catalysts and the novel separation and recycling regimes, a number of alternative substrates were investigated. In certain cases, the reactivity of the chosen substrate pairings were similar to 2,4-pentanedione / ethyl cyanoformate, although in other examples, the

compounds were specifically chosen due to their lower activity which meant that either forcing conditions or higher catalyst loadings had been employed previously.<sup>1</sup> It was hoped that this would provide a means of comparing the reactivity of the ‘fluorous’ approach to the conventional ‘[M(acac)<sub>2</sub>]’ approach. The following two sections delineate the various substrates analysed; section 4.3.2. describes alternative nitrile compounds, whilst the following section (4.3.1.) details the variation of the  $\beta$ -dicarbonyl component.

#### 4.3.1. Catalysis using fluorous derivatised $\beta$ -diketonates – ‘Alternative $\beta$ -dicarbonyls’

To fully analyse the extent of reactivity of the fluorous methodology, five further  $\beta$ -dicarbonyl compounds were chosen to investigate both steric and electronic effects, whilst also allowing comparison with literature sources.<sup>1</sup> To address the electronic effects, a ketoester (methylacetoacetate) and a diester (dimethyl malonate) were selected, whilst to analyse a combination of both mild electronic and steric effects, two further  $\beta$ -diketones were decided upon; benzoylacetone and dibenzoylmethane. Finally, to probe a  $\beta$ -dicarbonyl with severe steric effects, the bulky tertiary butyl substituted  $\beta$ -diketone (2,2,6,6-tetramethyl-3,5-heptanedione) was chosen.

Throughout the analysis of these alternative  $\beta$ -dicarbonyl substrates, the conditions employed were the same as those described for the 2,4-pentanedione / ethyl cyanofornate experiments described earlier. Rigorous drying procedures were also implemented for each new substrate due to the moisture sensitivity of the catalysts (see Chapter 6 for further details).<sup>3</sup> Furthermore, for ease of assessment between the reactions, the nitrile component was maintained as ethyl cyanofornate and due to the higher activity of the nickel catalysts, primarily [Ni(C<sub>6</sub>F<sub>13</sub>/ C<sub>6</sub>F<sub>13</sub>)<sub>2</sub>] was used, although throughout, comparison is made to the analogous zinc species (IXb). The first compound investigated, methylacetoacetate, gave a surprising result (Scheme 4.9). Although the literature reaction, catalysed by [Zn(acac)<sub>2</sub>], proceeds to 80 % conversion, the value obtained for the symmetrical nickel catalyst was considerably lower at only 9 %.



Scheme 4.9

All of the fluorinated catalysts gave low yields for this substrate; Table 4.9 summarises the results obtained. The high conversion obtained with [Zn(acac)<sub>2</sub>], whilst reassuring, casts a substantial doubt over the effectiveness of the fluorinated species. Overall, the zinc catalysts are better catalysts for this system, which is surprising when compared to the results observed for the 2,4-pentanedione reactions, where slightly higher reactivity was observed for the nickel species.

Table 4.9. Catalysis of reaction between methylacetoacetate and ethyl cyanoformate

Catalyst	Catalyst Loading / mol %	Mass of catalyst / mg	Conversion / %
Zn(acac) <sub>2</sub>	1	24	78
Zn(hfacac) <sub>2</sub>	1	45	~10 <sup>a</sup>
Zn(CF <sub>3</sub> /C <sub>6</sub> F <sub>13</sub> ) <sub>2</sub> (IXa)	1	91	~15 <sup>a</sup>
Zn(C <sub>6</sub> F <sub>13</sub> /C <sub>6</sub> F <sub>13</sub> ) <sub>2</sub> (IXb)	1	137	~20 <sup>a</sup>
Ni(acac) <sub>2</sub>	1	24	~30 <sup>a</sup>
Ni(hfacac) <sub>2</sub>	1	44	~4 <sup>a</sup>
Ni(CF <sub>3</sub> /C <sub>6</sub> F <sub>13</sub> ) <sub>2</sub> (VIIIa)	1	90	~20 <sup>a</sup>
Ni(C <sub>6</sub> F <sub>13</sub> /C <sub>6</sub> F <sub>13</sub> ) <sub>2</sub> (VIIIb)	1	137	~9 <sup>a</sup>

<sup>a</sup> Yields determined by <sup>1</sup>H NMR spectra

For the diester, dimethyl malonate no reactivity was observed with ethyl cyanoformate for any of the catalysts. However, this was rationalised to an extent, by the literature procedure described by Veronese *et al.* that required the harsher

conditions of refluxing chloroform for 5 hours, followed by 12 hours stirring at room temperature.<sup>3</sup> However, despite repeated attempts using these conditions, the reaction could not be achieved with any of the catalysts, including  $[\text{Zn}(\text{acac})_2]$ , which according to the literature should have resulted in a 73 % conversion.<sup>3</sup>

The lower reactivity of these substrates was attributed to two concurrent factors, centralising upon the key stages of the reaction mechanism (**Figure 4.6**).<sup>1,8</sup> As mentioned earlier, the first stage of the ' $[\text{M}(\text{acac})_2]$ ' catalysed approach will be the reaction between the coordinated ligand and the substrate nitrile, thus leaving a 'vacant site' for the substrate dicarbonyl to coordinate, enabling the reaction to continue. However, for the fluorinated catalysts, the first stage has to be an 'exchange' process between the fluorinated  $\beta$ -diketonate ligand and the substrate  $\beta$ -dicarbonyl. For this reason, the equilibrium process between the substrate dicarbonyl and the fluorous  $\beta$ -diketonate ligand was examined. This was achieved by analysing a stirred solution of  $[\text{Ni}(\text{C}_6\text{F}_{13}/\text{C}_6\text{F}_{13})_2]$  with each of the three dicarbonyl substrates in turn; 2,4-pentanedione, methylacetoacetate and dimethyl malonate, which were then analysed by mass spectroscopy. All three substrates generated a peak (100 %  $m/z$ ), due to the heteroleptic intermediate, indicating that exchange occurs in all three reactions. Unfortunately, however, the mass spectroscopy data does not give any indication as to the extent or relative rate of the exchange process occurring. However, some limited thermodynamic and kinetic parameters are available which provide an indication of the relative rates of ligand exchange. Veronese, proposes the following: "For copper (II) complexes, the coordinating affinity of the  $\beta$ -dicarbonyls in benzene decreases in the order dibenzoylmethane > acetylacetone > benzoylacetone >> ethyl acetoacetate > methyl acetoacetate".<sup>8</sup> A more general trend, can be described by classing the four groups into:  $\beta$ -diketones >  $\beta$ -ketoamides >  $\beta$ -ketoesters >  $\beta$ -diesters.<sup>1</sup>

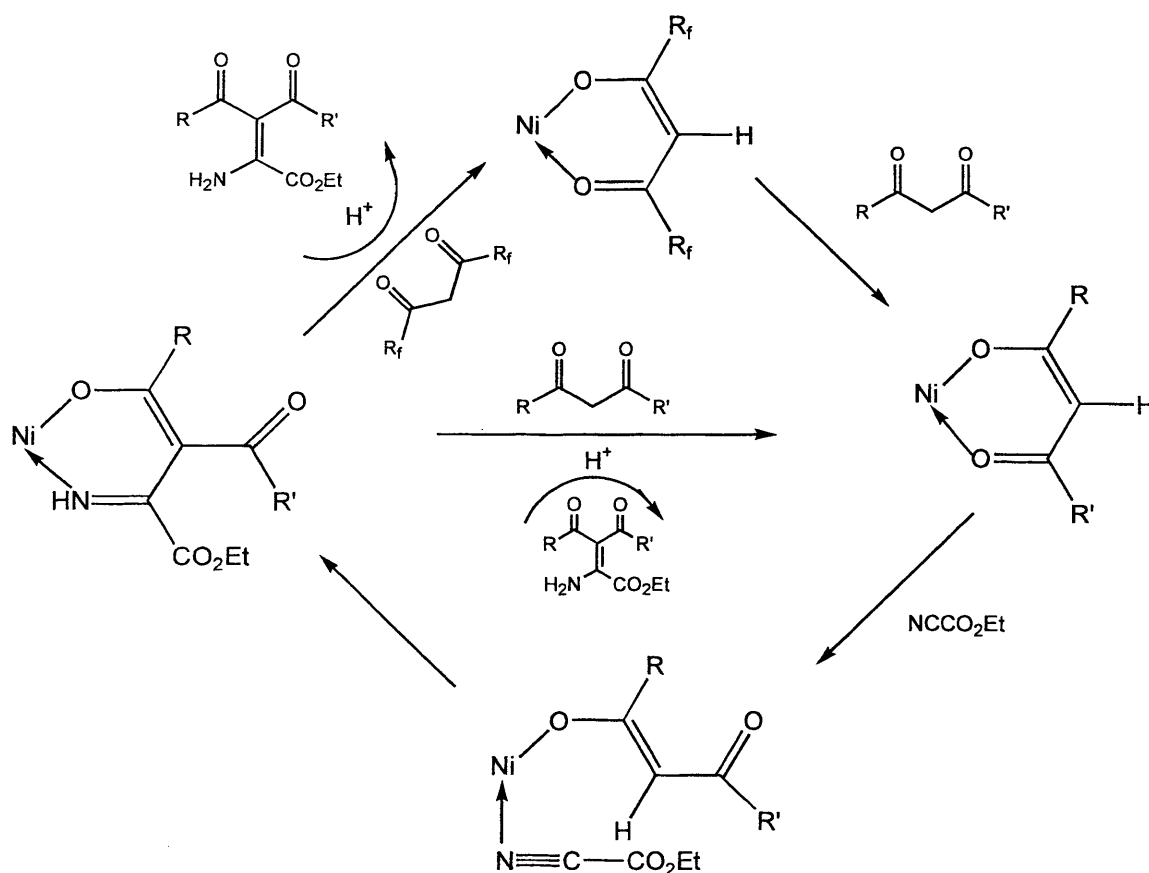


Figure 4.6

The second factor, which is intrinsically linked to the exchange process, regards the acidity of the substrate  $\beta$ -dicarbonyl. The initiation of the exchange step must begin with the dissociation of the fluorous ligand. Obviously, this process would be favoured in more acidic environments and thus explains why the reaction takes place for acetylacetone due to the comparatively low dissociation constant ( $\text{pK}_a = 9$ ).<sup>16</sup> The higher  $\text{pK}_a$ 's of the ketoester and diester (11 and 13 respectively) may preclude this dissociative step. As a consequence, the equilibrium occurring will be heavily biased towards the non-dissociated catalyst side thus preventing the catalytic cycle from beginning. Unfortunately, this reasoning implies that the fluorinated catalysts will only effect the carbon – carbon coupling reaction for  $\beta$ -dicarbonyls with a  $\text{pK}_a$  less than, or equivalent to, an alkyl  $\beta$ -diketone (*i.e.* 9). Unfortunately, the final stage of the reaction mechanism is also pH dependent. The coordinated enaminodionato intermediate is protonated by excess substrate  $\beta$ -

dicarbonyl, thus regenerating the active site of the catalyst. However, due to the electron withdrawing effect of the fluorinated  $\beta$ -diketonate of the catalyst, this coordination will be significantly enhanced, and as a consequence, the acidity of the substrate dicarbonyl becomes crucial with regard to liberating the final enaminedione product. Unfortunately, the higher pKa's of the diester and possibly the ketoester may prohibit this final stage, blocking the catalytic cycle.

Due to the fact that a higher rate of ligand exchange is observed with acetylacetone, it was postulated that a catalytic amount of this dicarbonyl compound might generate a small amount of the active heteroleptic intermediate that may promote the fluorous reaction with methylacetoacetate. It was hoped that this would initiate the catalytic cycle, thus enabling the ketoester to coordinate and react once the fluorous ligand had been exchanged (*i.e.* almost equivalent to generating a 'vacant site'). Unfortunately when the reaction was attempted, using 1 mol % acetylacetone and 1 mol % of the symmetrical fluorinated nickel catalyst **VIIIb**, the yield was, once again, very poor (10 %). Owing to the high reactivity of  $[\text{Zn}(\text{acac})_2]$  for this system (78 %), the symmetrical zinc catalyst (**IXb**), was investigated at elevated temperature, reproducing the literature conditions described for dimethyl malonate, a substrate that is reported to require more forcing conditions.<sup>3</sup> The reaction was carried out in dry chloroform at 60 °C, for 24 hours and resulted in 92 % conversion to the enaminedione. A similar procedure using **VIIIb**, resulted in a low level of conversion similar to that obtained for the room temperature reaction (~10 %). These reactions illustrate the comparatively lower activity of the fluorous  $\beta$ -diketonates in comparison to the literature standard of  $[\text{Zn}(\text{acac})_2]$ . Whereas the non-fluorous catalyst works at room temperature, the fluorous analogue requires the harsher conditions of refluxing chloroform to overcome an 'activation energy' associated with either the ligand exchange step or the final release of the product.

The poor activity of the catalysts was exacerbated when dimethyl malonate was investigated further. No reactivity was observed for  $[\text{Zn}(\text{acac})_2]$ , **VIIIb** or **IXb** when the reactions were performed in refluxing chloroform, even after twenty-four hours. Whilst the diesters are possibly the most difficult substrates to react (indicated by the low relative ability for ligand exchange), a satisfactory explanation

could not be derived, particularly regarding the inability to reproduce the literature precedent with  $[\text{Zn}(\text{acac})_2]$ .

The next substrate analysed was benzoylacetone. It was hoped that this  $\beta$ -diketone would exhibit intermediate reactivity between acetylacetone and methyl acetoacetate and the results confirmed this hypothesis. From **Table 4.10**, the higher reactivity of  $[\text{Zn}(\text{acac})_2]$  is clearly apparent. However, it is interesting to observe the comparatively high levels of reactivity attained with both the hexafluoroacetylacetonato and unsymmetrical derivatised catalysts for both zinc and nickel.

**Table 4.10.** Catalysis of reaction between benzoylacetone and ethyl cyanoformate

Catalyst	Catalyst Loading / mol %	Mass of catalyst / mg	Conversion / %
$\text{Zn}(\text{acac})_2$	1	20	87
$\text{Zn}(\text{hfacac})_2$	1	37	67 <sup>a</sup>
$\text{Zn}(\text{CF}_3/\text{C}_6\text{F}_{13})_2$ ( <b>IXa</b> )	1	75	54 <sup>a</sup>
$\text{Zn}(\text{C}_6\text{F}_{13}/\text{C}_6\text{F}_{13})_2$ ( <b>IXb</b> )	1	113	51 <sup>a</sup>
$\text{Ni}(\text{acac})_2$	1	20	51 <sup>a</sup>
$\text{Ni}(\text{hfacac})_2$	1	36	73 <sup>a</sup>
$\text{Ni}(\text{CF}_3/\text{C}_6\text{F}_{13})_2$ ( <b>VIIIa</b> )	1	74	70 <sup>a</sup>
$\text{Ni}(\text{C}_6\text{F}_{13}/\text{C}_6\text{F}_{13})_2$ ( <b>VIIIb</b> )	1	113	44 <sup>a</sup>

<sup>a</sup> Yields determined by <sup>1</sup>H NMR spectra

Disappointingly, however, the conversions for the two symmetrical catalysts (**VIIIb** and **IXb**) were both quite low at 44 % and 51 % respectively. The consequence of this poor reactivity was that a considerable amount of the heteroleptic complex remained present in the reaction mixture, leading to poor retention of the catalysts on the FRPSG column. Although the nickel catalyst (**VIIIb**) could be separated from the reaction mixture, the green ‘band’ travelled down the column considerably, indicating that leaching would eventually occur as the product was eluted. As a

consequence, recycling was not attempted for this substrate pairing. It may be possible to improve the overall yield of this reaction by using longer reaction times, alternative solvents and elevated reaction temperatures. However, due to time constraints and the overall aim of examining the activity of the fluorinated catalysts in comparison to their *protio* analogues, these refinements were not made.

The final two alternative  $\beta$ -dicarbonyl compounds analysed were both  $\beta$ -diketones, with progressively increasing steric bulk. The first compound, dibenzoylmethane, was chosen as a logical progression to benzoylacetone, containing two phenyl groups, thus increasing the steric bulk of the molecule. Once again, excellent conversions are reported for the  $[\text{Zn}(\text{acac})_2]$  catalysed process,<sup>3</sup> and this result was confirmed in the laboratory. However, upon analysis of the fluorinated catalysts, the conversions decreased significantly, echoing the trend observed for benzoylacetone (**Table 4.11**). In particular, the poor reactivity was most pronounced for the symmetrical nickel and zinc catalysts (**VIIIb** and **IXb**), where virtually no reactivity was observed, 20 % and 0 % respectively (the zinc reaction was repeated three times to confirm the inactivity of the catalyst for this system). From these results, it is obvious that the increase in steric bulk significantly decreases the rate of reactivity for the fully fluorinated symmetrical ligand-based catalysts. Undoubtedly, this effect arises due to a combination of the steric volume of both the substrate molecule and the fluorous ligand that imparts a powerful steric effect *via* the perfluorohexyl ponytails. This is supported by the results for all of the other fluorinated catalysts which demonstrate similar reactivity to each other, and also to the results obtained for benzoylacetone.

**Table 4.11.** Catalysis of reaction between dibenzoylmethane and ethyl cyanofornate

Catalyst	Catalyst Loading / mol %	Mass of catalyst / mg	Conversion / %
Zn(acac) <sub>2</sub>	1	16	86
Zn(hfacac) <sub>2</sub>	1	29	46 <sup>a</sup>
Zn(CF <sub>3</sub> /C <sub>6</sub> F <sub>13</sub> ) <sub>2</sub> ( <b>IXa</b> )	1	61	51 <sup>a</sup>
Zn(C <sub>6</sub> F <sub>13</sub> /C <sub>6</sub> F <sub>13</sub> ) <sub>2</sub> ( <b>IXb</b> )	1	91	0
Ni(acac) <sub>2</sub>	1	16	34 <sup>a</sup>
Ni(hfacac) <sub>2</sub>	1	29	64 <sup>a</sup>
Ni(CF <sub>3</sub> /C <sub>6</sub> F <sub>13</sub> ) <sub>2</sub> ( <b>VIIIa</b> )	1	60	64 <sup>a</sup>
Ni(C <sub>6</sub> F <sub>13</sub> /C <sub>6</sub> F <sub>13</sub> ) <sub>2</sub> ( <b>VIIIb</b> )	1	91	20 <sup>a</sup>

<sup>a</sup> Yields determined by <sup>1</sup>H NMR spectra

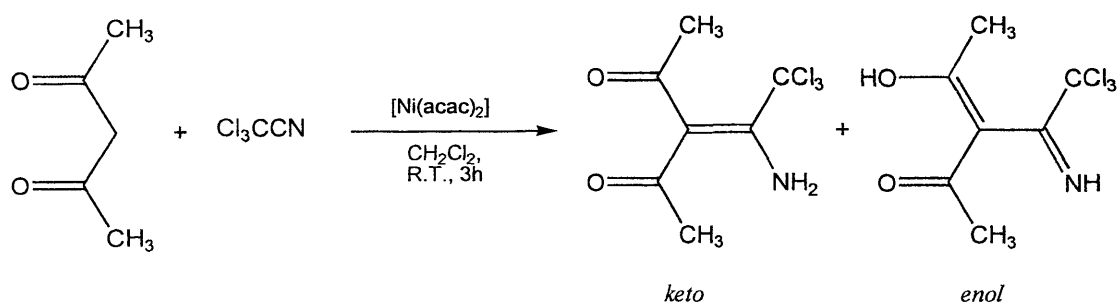
The results obtained for dibenzoylmethane, somewhat precluded the investigation of the tertiary butyl substituted  $\beta$ -diketone (2,2,6,6-tetramethyl-3,5-heptanedione) with ethyl cyanofornate, especially considering the literature precedent for this substrate which, for certain nitriles, can take up to 240 hours.<sup>14</sup> However, it was decided to perform a limited set of experiments with the symmetrical nickel catalyst (**VIIIb**) to confirm these predictions. At room temperature in dichloromethane and at 60 °C in refluxing chloroform, no reactivity was observed after 24 hours. The reaction at room temperature was left for 120 hours (5 days), after which time a small amount of a highly insoluble precipitate was observed (> 10 % yield). It was postulated that this material may have been a polymeric derivative of ethyl cyanofornate, but unfortunately the <sup>1</sup>H NMR spectrum of this material could not be obtained. For this species, it appears obvious that any exchange between the ligand and substrate is highly disfavoured due to severe steric crowding (**Figure 4.7**). Furthermore, the steric crowding of the heteroleptic intermediate would virtually prevent the coordination of the nitrile and the subsequent nucleophilic attack of the central intercarbonylic carbon atom.



the main aim was to evaluate the synthetic scope of the fluorinated catalysts, although due to the extensive investigations undertaken for the alternative  $\beta$ -dicarbonyl substrates, the emphasis of these experiments was to determine the reactivity of the symmetrical catalysts  $[\text{Ni}(\text{C}_6\text{F}_{13}/\text{C}_6\text{F}_{13})_2]$  and  $[\text{Zn}(\text{C}_6\text{F}_{13}/\text{C}_6\text{F}_{13})_2]$ , owing to their compatibility with the FRPSG methodology.

Three substrates were chosen; trichloroacetonitrile, malonitrile and benzoyl cyanide. The selection was based upon previously recorded reactivity; the first compound, trichloroacetonitrile was expected to exhibit comparable levels of activity to ethyl cyanoformate.<sup>1</sup> The second substrate, malonitrile, is comparatively less active, whilst the final nitrile compound, benzoyl cyanide is quite deactivated (see section 4.1.2.). By comparison to the literature sources, any increase (or decrease) in the catalytic activity of the fluorinated complexes will be highlighted as the series is transcended.

The literature preparation for the enaminodione formed between the reaction of trichloroacetonitrile and 2,4-pentanedione involves simply stirring the two reagents in dry dichloromethane for 3 hours. A variety of metal  $\beta$ -diketonate catalysts can be used, and very good yields are obtained, 72 % for  $[\text{Ni}(\text{acac})_2]$  (Scheme 4.10).<sup>14</sup>



Scheme 4.10

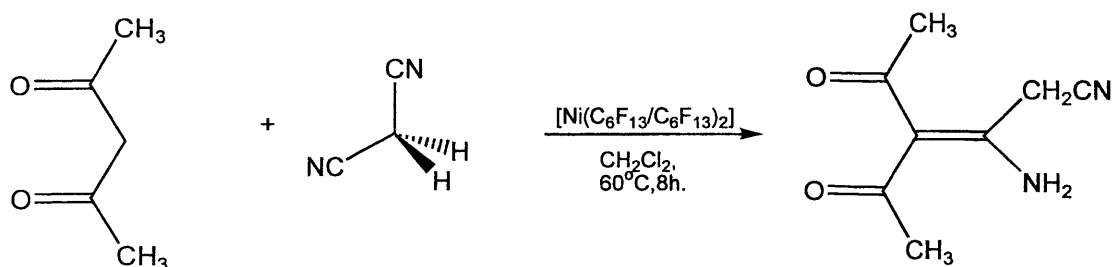
The reaction was investigated using the two symmetrical fluorinated catalysts (**IXb** and **VIIIb**), and, for comparison,  $[\text{Zn}(\text{acac})_2]$  and  $[\text{Ni}(\text{acac})_2]$ . In the literature, the reactions generate very viscous yellow oils which are dissolved in “Ligroin” (defined by Aldrich as a Mineral Spirit, b.p. 60 – 80 °C) and cooled to 0 °C for 5 hours to generate a white crystalline solid.<sup>14</sup> Surprisingly, this step of the procedure

proved to be crucial, as attempts to isolate the product by other crystallisation techniques resulted in the decomposition of the residue to a brown tar. However, overall the reaction proved to be very successful, with high yields for both fluorine catalysts (**Table 4.12**) and excellent separations on the FRPSG columns. This was indicated by the absence of any fluorine signals in the  $^{19}\text{F}$  NMR spectra of the product organic phase, although leaching data was not obtained due to time constraints. It would be reasonable to assume that the leaching data for this substrate pairing would be quite good, as the yields stated are isolated yields following crystallisation from Ligroin. The crude yields were virtually quantitative and following on from the discussion for the ethyl cyanoformate / 2,4-pentanedione leaching data, this high conversion would lead to low levels of the heteroleptic intermediate remaining in the reaction mixture. The narrow band on the FRPSG column observed for the fluorine nickel complex further substantiated this reasoning.

**Table 4.12.** Catalysis of reaction between 2,4-pentanedione and trichloroacetonitrile

Catalyst	Catalyst loading / mol %	Mass of catalyst / mg	Yield / g	Yield / %
Zn(acac) <sub>2</sub>	1	26	1.74	71
Zn(C <sub>6</sub> F <sub>13</sub> /C <sub>6</sub> F <sub>13</sub> ) <sub>2</sub> ( <b>IXb</b> )	1	148	1.83	75
Ni(acac) <sub>2</sub>	1	26	1.70	70
Ni(C <sub>6</sub> F <sub>13</sub> /C <sub>6</sub> F <sub>13</sub> ) <sub>2</sub> ( <b>VIIIb</b> )	1	147	1.62	66

As expected malonitrile (NCCH<sub>2</sub>CN), proved to be somewhat less reactive than trichloroacetonitrile. Initially, when the fluorinated catalysts were examined under room temperature conditions, no reactivity was observed (**Scheme 4.11**). In accordance with the literature procedure for this reaction, the experiments were repeated using refluxing chloroform for 8 hours.<sup>15</sup> The catalyst of choice for this system is [Ni(acac)<sub>2</sub>], and consequently only this catalyst and the fluorine analogue (**VIIIb**) were investigated. Also, the reactants were used at higher dilution, 1 mol dm<sup>-3</sup> (corresponding to 8 cm<sup>3</sup> rather than 2 cm<sup>3</sup> used previously), as an intractable tar-like material was generated at lower volumes.



Scheme 4.11

The reaction mixtures were passed down Celite and FRPSG columns accordingly, these were very difficult to perform due to an insoluble brown precipitate that blocked the pipettes. The orange solutions obtained were evaporated to dryness to yield orange solids, which when analysed by  $^1\text{H}$  NMR spectroscopy revealed the distinctive resonances for the enaminodione products, present as two isomeric keto-enol tautomers, with distinctive high chemical shifts for the enolic protons at  $\sim 16.5$   $\delta$  (Figure 4.8).<sup>15</sup>

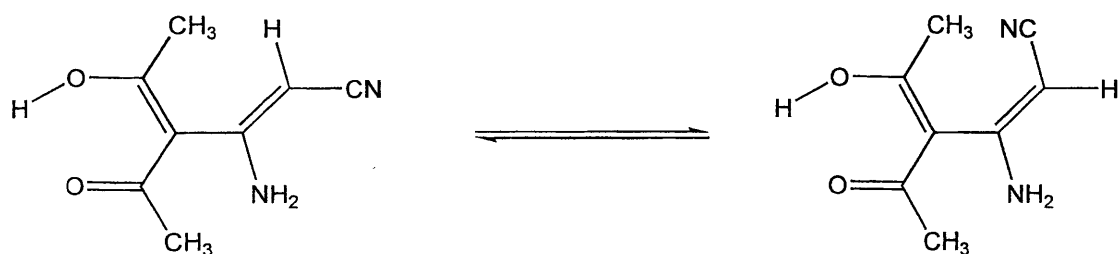


Figure 4.8

The yields achieved were quite respectable at 60 and 71 % for  $[\text{Ni}(\text{acac})_2]$  and **VIIIb** respectively. However, there was no trace of either catalyst remaining on the columns, although it is possible that they were contained within the intractable brown precipitate. Attempts were made to elute this material, but unfortunately this proved difficult and largely unsuccessful. Owing to these difficulties, the system was adjudged to be incompatible with the FRPSG regime and consequently the reaction was not pursued any further.

Although the literature procedure for the reaction between benzoyl cyanide and 2,4-pentanedione requires a 20 mol % [Ni(acac)<sub>2</sub>] catalyst loading, it was decided to investigate the fluorinated species at just 1 mol % to observe whether or not there was any conversion at all.<sup>14</sup> The reason for this choice, was that a 20 % molar equivalent of the fluorous nickel catalyst (**VIIIb**), would equate to 2.48 g, for a 1.95 g preparation of the enaminedione. Obviously the expense of the fluorous complex negated even attempting the reaction on this scale, however, for comparison the literature reaction was carried out using [Ni(acac)<sub>2</sub>], to give the product in 77 % yield (literature 73 %).<sup>14</sup> Unfortunately, little or no success was achieved with the 1 mol % loadings, even when the reactions were carried out in refluxing chloroform. The results are delineated in **Table 4.13** (C<sub>2</sub>H<sub>4</sub>Cl<sub>2</sub> = 1,2-dichloroethane).

**Table 4.13.** Catalysis of reaction between 2,4-pentanedione and benzoyl cyanide

Catalyst	Catalyst Loading / mol %	Temp / °C	Solvent	Conversion / %
Zn(acac) <sub>2</sub>	1	25	CH <sub>2</sub> Cl <sub>2</sub>	<5 <sup>a</sup>
Zn(C <sub>6</sub> F <sub>13</sub> /C <sub>6</sub> F <sub>13</sub> ) <sub>2</sub> ( <b>IXb</b> )	1	25	CH <sub>2</sub> Cl <sub>2</sub>	<5 <sup>a</sup>
Ni(acac) <sub>2</sub>	1	25	CH <sub>2</sub> Cl <sub>2</sub>	0
Ni(C <sub>6</sub> F <sub>13</sub> /C <sub>6</sub> F <sub>13</sub> ) <sub>2</sub> ( <b>VIIIb</b> )	1	25	CH <sub>2</sub> Cl <sub>2</sub>	0
Zn(acac) <sub>2</sub>	1	60	CHCl <sub>3</sub>	<5 <sup>a</sup>
Zn(C <sub>6</sub> F <sub>13</sub> /C <sub>6</sub> F <sub>13</sub> ) <sub>2</sub> ( <b>IXb</b> )	1	60	CHCl <sub>3</sub>	<5 <sup>a</sup>
Ni(C <sub>6</sub> F <sub>13</sub> /C <sub>6</sub> F <sub>13</sub> ) <sub>2</sub> ( <b>VIIIb</b> )	1	60	CHCl <sub>3</sub>	<5 <sup>a</sup>
Ni(acac) <sub>2</sub>	1	85	C <sub>2</sub> H <sub>4</sub> Cl <sub>2</sub>	0
Ni(acac) <sub>2</sub>	20	85	C <sub>2</sub> H <sub>4</sub> Cl <sub>2</sub>	77

<sup>a</sup> Yields determined by <sup>1</sup>H NMR spectra

The poor reactivity of this substrate was not unexpected although the low activity of **IXb** and **VIIIb** was very disappointing, once again indicating no improvement over the literature standard. As discussed earlier, however, the ability of the “M(acac)<sub>2</sub>” catalysts to function as the initial substrate molecule undoubtedly aids their activity.

Obviously, for this comparatively deactivated substrate pairing, the necessity for a ‘pre-formed’ nucleophile is more pronounced, resulting in the high catalyst loading and forcing conditions.

For the alternative nitrile substrates, the overall conclusion is that the activity of the catalysts is very similar to the standard organic catalysts ([Zn(acac)<sub>2</sub>] and [Ni(acac)<sub>2</sub>]). Unfortunately, no enhancement was observed for the comparatively de-activated substrate (benzoyl cyanide) and the malonitrile reaction proved to be too complicated to be compatible with the FRPSG methodology. However, for the trichloroacetonitrile reaction, the fluorous catalysts offered an effective, clean alternative with high yields and efficient separation.

#### 4.3.3. Catalysis using fluorous derivatised $\beta$ -diketonates – ‘Reaction Profiling’

The experiments described so far do not provide any information regarding the rate of activity observed with the different catalysts. For example, the reaction between ethyl cyanoformate and 2,4-pentanedione appears to proceed at a visibly faster rate with the unsymmetrical fluorous catalyst [Ni(CF<sub>3</sub>/C<sub>6</sub>F<sub>13</sub>)<sub>2</sub>] (**VIIIa**), rather than when the symmetrical analogue [Ni(C<sub>6</sub>F<sub>13</sub>/C<sub>6</sub>F<sub>13</sub>)<sub>2</sub>] (**VIIIb**) is used (see section 4.3.1.). It was also hoped that the analysis of the reaction profiles would confirm the contrast in reactivity between the fluorinated catalysts and the *protio* analogues by highlighting the initial exchange step for the fluorous complexes, as opposed to the almost instantaneous reactivity expected for the acetylacetonato complexes due to the ability of the ligand to act as a pre-formed nucleophile. To achieve these aims, the reactions between ethyl cyanoformate and two  $\beta$ -dicarbonyls were investigated; the first was simply the ‘standard’ reaction with 2,4-pentanedione that would enable a comparison to be made between the alternative catalysts due to the high levels of conversion observed. The second  $\beta$ -dicarbonyl analysed was benzoylacetone, which was chosen due to its intermediate activity observed with the fluorous catalysts. Also, however, for this substrate pairing, there is the possibility of forming two isomers of the final enaminodione product. Although there was no evidence for the formation of a second isomer when the products were analysed by <sup>1</sup>H NMR spectroscopy, it was hoped that the hplc chromatographic analysis, used to monitor product formation, would confirm this.

The analysis of the reaction profiles was achieved using the “DART” assembly at GlaxoSmithKline laboratories. Essentially this apparatus consists of a ReactArray™ reaction carousel, connected to a Gilson™ autosampler and an Agilent™ hplc spectrometer (**Figure 4.9**).



**Figure 4.9**

The reactions were sampled every two hours to monitor the conversion, which is detected by product formation as a function of peak area from the hplc trace (for the benzoylacetone reactions the conversions could also be followed by reagent consumption as the phenyl ring functions as a chromophore). A typical trace is shown overleaf (**Figure 4.10**), showing the reaction between ethyl cyanofornate and benzoylacetone, catalysed by  $[\text{Ni}(\text{CF}_3/\text{C}_6\text{F}_{13})_2]$ .

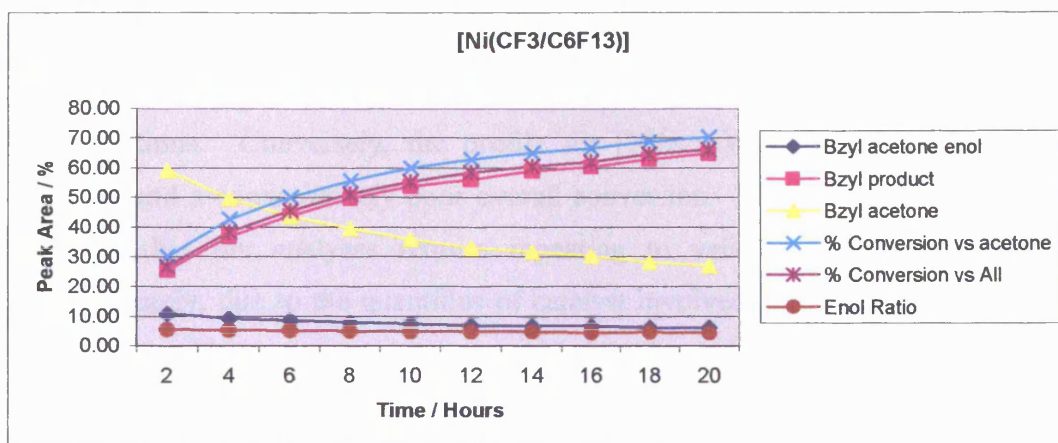
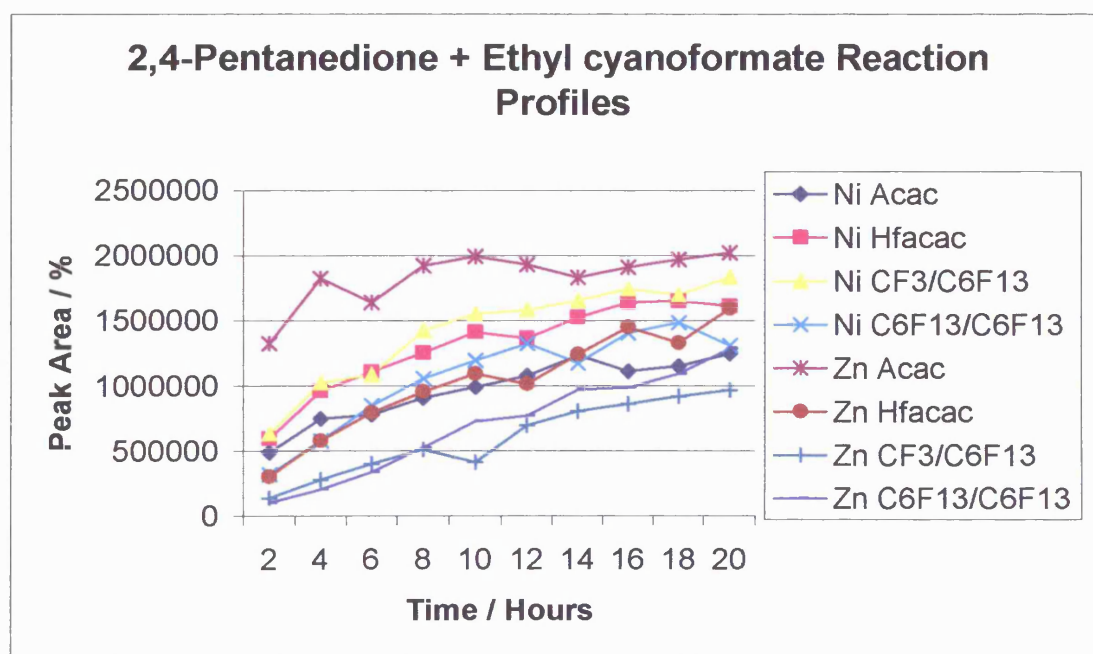


Figure 4.10

The reactions were carried out analogously to the laboratory procedures, maintaining the dry, anaerobic conditions throughout. However, due to the size of the reactor vessels and the depth of the sampling arm, the solution volume was increased by 1 cm<sup>3</sup> to 3 cm<sup>3</sup> (at the former volume, the reactions dried out, preventing sampling after approximately 10 hours). This change did not appear to affect the results, as the conversions extrapolated from the GC traces were comparable to the previous laboratory scale reactions. The reaction profiles for the 2,4-pentanedione / ethyl cyanoformate reactions are detailed in the chart shown overleaf (**Figure 4.11**). The individual traces, data tables and individual reaction profiles can be found on the accompanying CD-ROM. From the graph it can be observed that [Zn(acac)<sub>2</sub>] achieves the highest conversion, and as expected, the fastest initial rate of reaction. However, the visual observation that the unsymmetrical nickel catalyst (**VIIIa**), results in a more rapid conversion, in comparison to the other fluorinated species, is confirmed by the reaction profile that indicates a rapid increase in activity after two hours, *i.e.* after the initial exchange process has taken place. After fifteen hours the level of conversion is approximately equal to that of [Zn(acac)<sub>2</sub>] at the same point. The profiles also indicate the relatively slow conversions obtained with the two symmetrical fluoros complexes (**IXb** and **VIIIb**), although the nickel species is appreciably faster than the zinc analogue. As discussed earlier, these low initial rates may be a consequence of steric crowding during the initial exchange step. Both of the

hexafluoroacetylacetonato complexes generated surprisingly rapid conversions and to a certain extent, the zinc complex exhibited better reactivity than in the laboratory investigations. Conversely, the profile for  $[\text{Ni}(\text{acac})_2]$  revealed a slow rate of reaction and a comparatively poor overall conversion. These two results evidently indicate that the analyses require repeating to validate the trends observed. Unfortunately, due to the quantities of catalyst involved, and time constraints, this was not possible.

Fortunately, however, the trends observed for the 2,4-pentanedione reaction profiles were validated by the analogous investigation of the benzoylacetone / ethyl cyanoformate reactions (**Figure 4.12** overleaf).

**Figure 4.11**

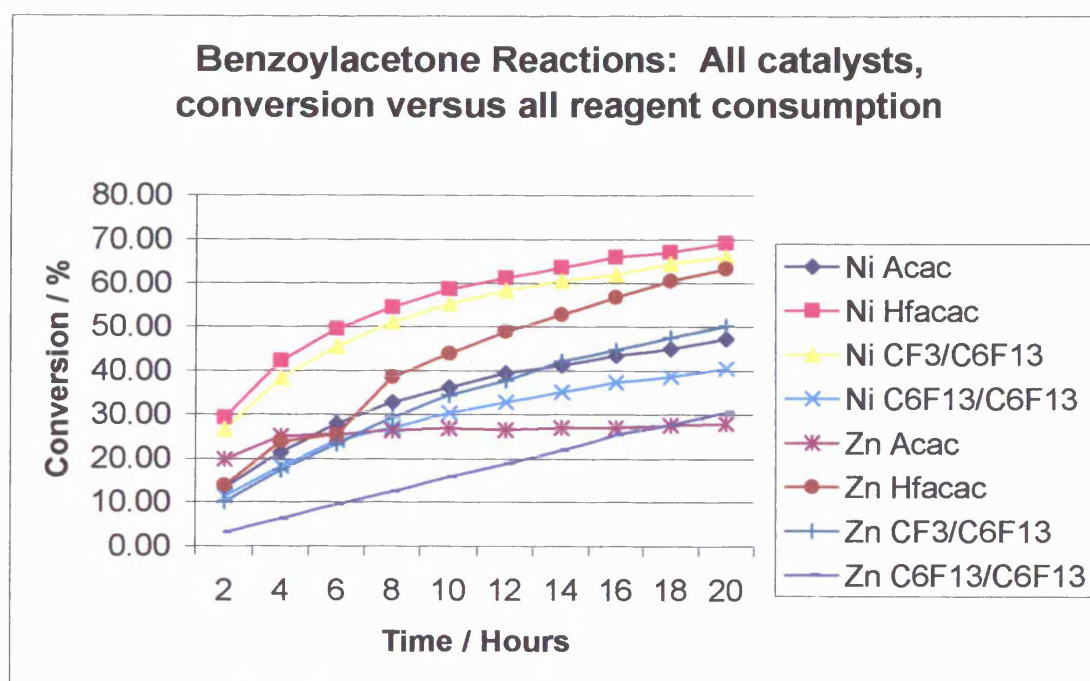
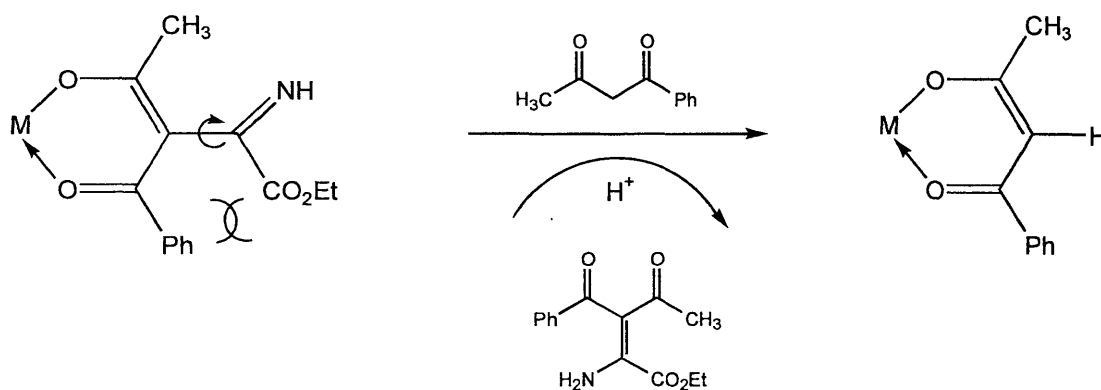


Figure 4.12

For this reaction, all of the catalysts have to undergo the initial exchange process between the coordinated ligands and the substrate benzoylacetone molecule. As a consequence, all of the profiles exhibit a ‘ramp’ shape, which contrasts directly to the profile observed when  $[\text{Zn}(\text{acac})_2]$  was used to catalyse the previous 2,4-pentanedione reaction. The activity of the catalysts correlates precisely over the two  $\beta$ -dicarbonyl substrates, with  $[\text{Ni}(\text{hfacac})_2]$  and the unsymmetrical nickel catalyst (**VIIIa**) attaining the fastest rates of reaction. Similarly, the two symmetrical catalysts appear to be initially retarded by the steric hindrance of the initial exchange step, before recovering to a reasonable rate of reaction. For this set of results, however, the profile generated by the  $[\text{Zn}(\text{acac})_2]$  catalysed reaction is clearly anomalous, as the overall conversion is very low, contrasting sharply to the result obtained from the laboratory investigations. Any number of factors could have contributed to this poor result, although a trace quantity of water in that specific reactor tube appears to be the most likely given the quality of the other data. Once again, it would have been beneficial to repeat these reaction profiles to eliminate error.

The other question that the reaction profile investigation addressed, was the possibility of forming two stereoisomers of the enaminodione product for the benzoylacetone reaction. Throughout the analysis of the GC traces, there was never any indication that a second isomer was formed; the peak generated by the product remained sharp and well defined during each reaction. Consequently, the mechanism proposed earlier must allow the more favoured, less sterically hindered isomer to form *via* free-rotation of the new carbon-carbon single bond of the coordinated enaminodionato intermediate (**Scheme 4.12**).



**Scheme 4.12**

#### 4.3.4. Catalysis using fluorinated $\beta$ -diketonates – ‘Conclusion’

The investigations described within this chapter have demonstrated the effectiveness and versatility of the fluorinated  $\beta$ -diketonate catalysts. In particular, the development of a novel means of catalyst recovery and recycling has been delineated. Unfortunately, due to the nature of the reaction, the effectiveness of this regime is dependent upon the extent of reaction, with almost complete conversion required to achieve effective recovery of the catalyst. The activity of the fluorinated catalysts was comparable, or even slightly better than the literature standard ([Zn(acac)<sub>2</sub>]) for the 2,4-pentanedione / ethyl cyanofornate pairing and for a range of nitrile substrates. Unfortunately, however, the yields were normally lower with the less reactive  $\beta$ -dicarbonyl substrates, such as the ketoesters. Overall, the

methodology clearly has potential, demonstrated by the low leaching levels of the fluorous catalysts, and for an optimised system the FRPSG approach represents an economically viable alternative to fluorous biphasic product / catalyst separation.

## 4.4. References for Chapter 4

- [1] B. Corain, M. Basato and A.C. Veronese, *J. Mol. Catal.*, 1993, **81**, 133.
- [2] F. D'Angeli, M. Basato, B. Corain, G. Valle, A.C. Veronese and G. Zanotti, *J. Org. Chem.*, 1984, **49**, 4696.
- [3] M. Basato, B. Corain, V. Gandolfi, B. Longato and A.C. Veronese, *J. Mol. Catal.*, 1989, **54**, 73.
- [4] J.H. Nelson, P.H. Howells, G.C. De Lullo and G.L. Landen, *J. Org. Chem.*, 1980, **45**, 1246.
- [5] J.P. Collman, *Angew. Chem. Int. Ed. Engl.*, 1965, **4**, 132.
- [6] P.R. Singh and R. Sahai, *Aust. J. Chem.*, 1970, **23**, 269.
- [7] R.P. Eckberg, J.H. Nelson, J.W. Kenney, P.H. Howells and R.A. Henry, *Inorg. Chem.*, 1977, **16**, 3128.
- [8] M. Basato, B. Corain and G. Zanotti, *J. Chem. Soc., Dalton Trans.*, 1988, 1213.
- [9] K. Uehara, Y. Ohashi and M. Tanaka, *Bull. Chem. Soc. Jpn.*, 1976, **49**, 1447.
- [10] M. Basato, B. Corain, A. Marcomini, G. Valle and G. Zanotti, *J. Chem. Soc., Perkin Trans. II*, 1984, 965.
- [11] M. Basato, R. Campostrini, B. Corain, B. Longato, S. Sitran, A.C. Veronese and G. Valle, *J. Chem. Soc., Perkin Trans. II*, 1985, 2019; M. Basato, R. Callegari, A.C. Veronese and G. Valle, *J. Chem. Soc., Perkin Trans. I*, 1994, 1779.
- [12] M. Basato, B. Corain, M. Cofler, A.C. Veronese and G. Zanotti, *J. Chem. Soc., Chem. Commun.*, 1984, 1593; M. Basato, U. Casellato, R. Graziani and A.C. Veronese, *J. Chem. Soc., Dalton Trans.*, 1992, 1193.
- [13] T. Iimori, Y. Nii, T. Izawa, S. Kobayashi and M. Ohno, *Tetrahedron Lett.*, 1979, **27**, 2525.
- [14] M. Basato, B. Corain, V. Gandolfi, C. Talmelli and A.C. Veronese, *J. Mol. Catal.*, 1986, **34**, 195.
- [15] M. Basato, R. Callegari, C.F. Morelli and A.C. Veronese, *J. Mol. Catal.*, 1997, **124**, 99; M. Basato, B. Corain, V. Gandolfi and A.C. Veronese, *J. Mol. Catal.*, 1986, **36**, 339.
- [16] J. M<sup>c</sup> Murry. *Organic Chemistry*, (3<sup>rd</sup> edition). Brooks / Cole. 1992.

## 5. Fluorinated Carboxylates

### 5.1. Introduction

#### 5.1.1. Carboxylate ligands

Carboxylate ligands, like the  $\beta$ -diketonates described in Chapter 2, are hard oxygen donor ligands that exhibit an extensive coordination chemistry to a wide range of metal centres.<sup>1</sup> Deprotonation of the parent carboxylic acid with a suitable base such as an alkali metal hydroxide, enables the anion to bind to the metal centre *via* several possible coordination modes; monodentate, bidentate or bridged geometries (Figure 5.1).<sup>2</sup>

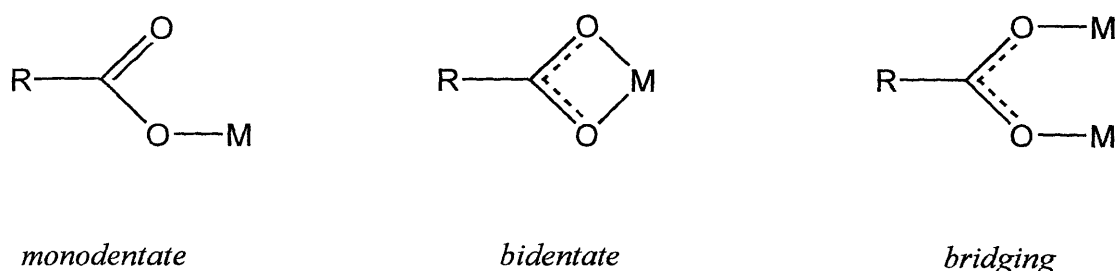


**Figure 5.1**

Examples of all three modes are well documented, although perhaps the most extensively investigated geometry is that of the bridging oxygen, where five different types of carboxylate bridge have been identified.<sup>3</sup>

The common, low molecular weight carboxylates formic acid, methanoic acid and ethanoic acid, form many stable coordination complexes that are used in large quantities on an industrial scale. In particular, the generation of ‘metal acetates’ accounts for a large percentage of the “millions of tonnes scale” production of ethanoic acid, with various applications from catalysis to extraction processes.<sup>3</sup> However, as the chain length of the carboxylate increases, the tendency to coordinate decreases due to the steric influence of the alkyl group. Overall, carboxylates are quite labile ligands, with many metal acetate complexes employed

as starting materials or catalyst precursors, for example palladium acetate, which is used commonly for both of these applications.<sup>4</sup>

### 5.1.2. Fluorinated Carboxylates

Fluorinated carboxylates exhibit similar coordination chemistry to their *protio* analogues, although the powerful electron withdrawing effect of the fluorinated group significantly alters both the synthesis of the complexes, and their subsequent reactivity. This is illustrated by the contrast in reactivity between acetic acid and trifluoroacetic acid. If the pKa's of the two carboxylic acids are compared, 4.72 and 0.23 respectively, the strength of the fluorinated acid is clearly apparent, approximately 33,000 times stronger (Figure 5.2).<sup>5</sup> This acidity is imparted by the stabilising effect of the fluorine atoms which withdraw electron density, thus stabilising the conjugate base by delocalising the negative charge. As a consequence, the fluorinated carboxylates are weaker ligands since this stabilising influence reduces the ability of the ligand to donate charge to the cationic metal centre. For this reason, the main use of fluorinated carboxylates is in catalytic cycles where a ligand is required to vacate a coordination position, thus allowing the substrate molecule to bind in the initial stage of the reaction.<sup>6</sup>

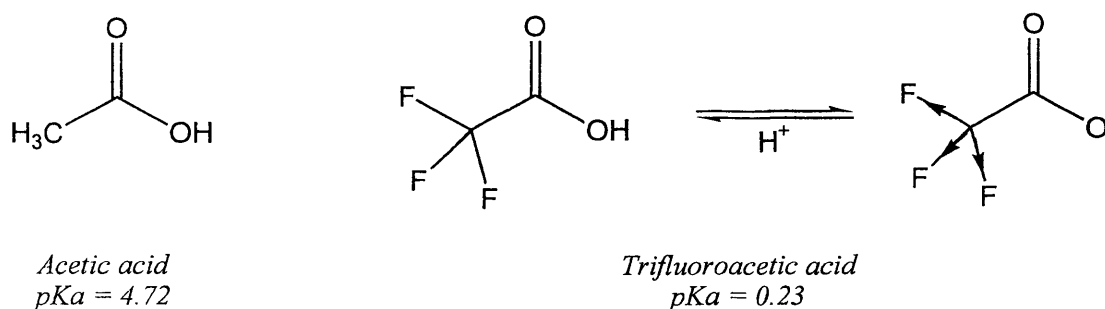
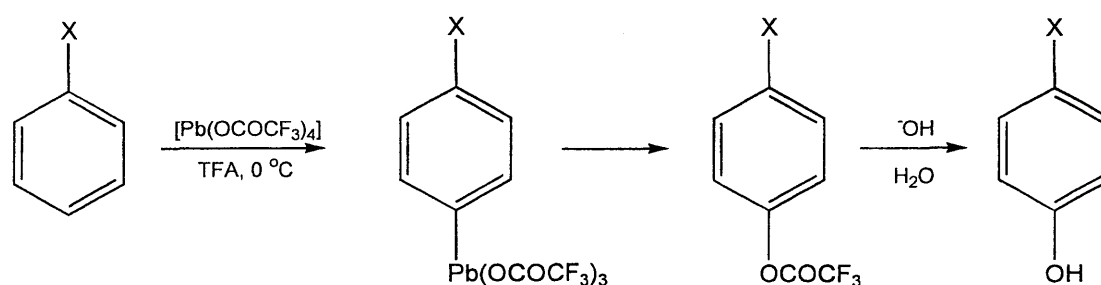


Figure 5.2

Unfortunately, this weak coordination imparts an inherent instability in many of the homoleptic complexes of trifluoroacetate, although the derivatives of most metals can be synthesised.<sup>7</sup> In many cases, a secondary electron donating ligand is required to stabilise the compound, for example tetrahydrofuran,<sup>8</sup> pyridine<sup>9</sup>

and dimethoxyethane<sup>6</sup> have all been used to stabilise zinc trifluoroacetate, whilst numerous hydrates of various metals have also been reported.<sup>7</sup> Stabilisation can also be achieved for certain trifluoroacetates by storing the complex in the presence of a small amount of trifluoroacetic acid. This is used for lead (IV) trifluoroacetate, an extremely reactive and moisture sensitive compound, which is also stored in the dark at 10 °C and in the absence of moisture.<sup>10</sup>

The applications of metal perfluoroacetate complexes are dominated by the trifluoroacetates, which are used as catalysts, catalyst precursors (see section 5.2.) and also as reagents, for example, in the trifluoroacetoxylation of various hydrocarbon species.<sup>10</sup> This final process arises due to the extreme reactivity of certain metal trifluoroacetates especially lead (IV) trifluoroacetate which is a very powerful oxidant and will react with inert species such as benzene, toluene and even heptane. Once formed, the trifluoroacetoxy substituted compounds can be hydrolysed under mild conditions to form the corresponding alcohols (**Scheme 5.1**).<sup>11</sup>



$X = H, Me, Et, i-Pr, t-Bu, F, Cl, Br$

**Scheme 5.1**

The investigation of longer chain perfluorinated carboxylates has only recently come to prominence with the development of fluorous biphasic catalysis. The coordination chemistry documented is as yet quite limited, with the investigation of various perfluorinated rhodium dimers dominating the research to date.<sup>12-15</sup> The complexes are quite easily prepared *via* ligand exchange with dirhodium tetraacetate  $[Rh_2(OAc)_4]$ , and in most cases the fluorinated carboxylic acids are commercially available. Numerous catalytic processes have been

investigated, details of which can be found in the following section (5.2.). Fish *et al.*, have also analysed perfluorinated carboxylates, although primarily, their intention was to utilise the ligand as a means of increasing the fluororous character of two metal perfluoroalkyl-substituted triazocyclononane complexes.<sup>16</sup>

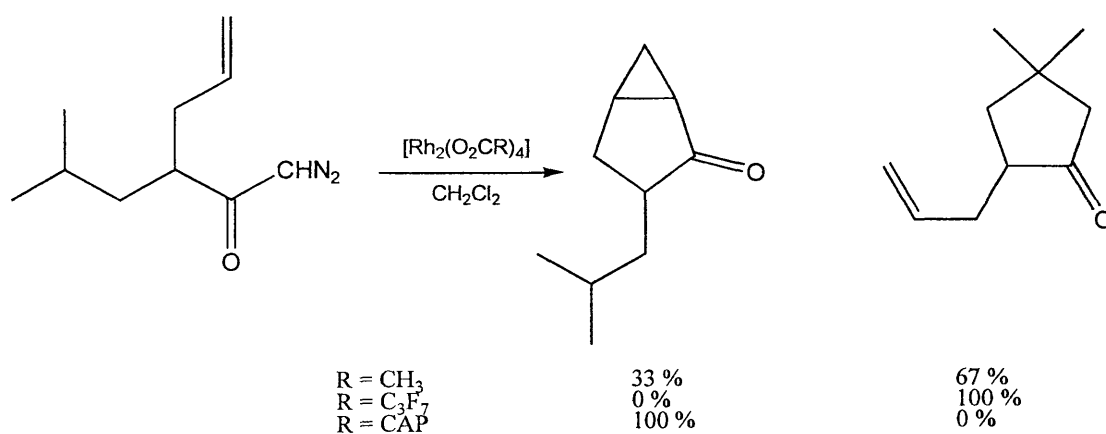
## 5.2. Catalysis using carboxylates

As expected, there are many catalytic applications of carboxylate compounds delineated throughout the literature. It would be neither appropriate nor valid to attempt to review these processes in this introduction, as the main aims of this work are to apply fluororous techniques to existing methodologies in order to render them more commercially viable and environmentally feasible on an industrial scale. However, it is necessary to describe the catalytic processes selected for investigation and also, to discuss the current status of the literature with regard to fluororous phase chemistry. Three catalytic systems have been chosen for investigation; dirhodium tetraacetate, cobalt acetate and manganese acetate. This chapter describes the evaluation of the fluororous analogues of these species as fluororous phase compatible catalysts. In particular, the aim was to utilise the FRPSG separation described in earlier chapters, in an attempt to reduce expenditure by moving away from traditional liquid-liquid fluororous biphasic separation.

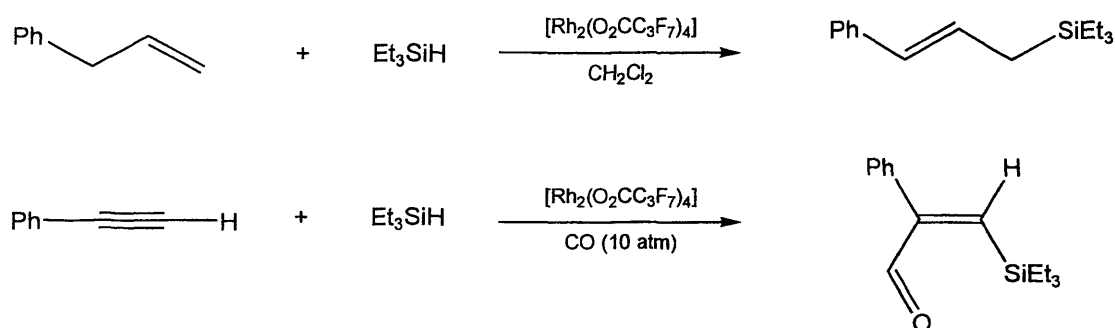
### 5.2.1. Dirhodium Tetraacetate

The dimeric rhodium carboxylates are an extremely versatile group of catalysts which have been investigated for a wide range of reactions.<sup>17</sup> The three commercially available dimers, dirhodium (II) tetraacetate ( $[\text{Rh}_2(\text{OAc})_4]$ ), dirhodium (II) tetrakis(trifluoroacetate) ( $[\text{Rh}_2(\text{tfa})_4]$ ), and dirhodium (II) tetrakis(perfluorobutyrate) ( $[\text{Rh}_2(\text{pfb})_4]$ ), all catalyse the carbenoid reactions of diazo compounds.<sup>17</sup> A wide range of substrates have been investigated, including many functionalities, from complex ring systems to unsaturated carbonyl moieties and amino groups. Significantly, the high activity of these catalysts has meant that only low catalyst loadings are required and in some cases dirhodium (II) tetraacetate can be used in amounts as low as 0.05 mol %.<sup>18</sup> The high levels of chemoselectivity

achievable with dirhodium (II) tetrakis(perfluorobutyrate) is another feature of these catalysts which has led to their extensive investigation over the past fifteen years. For example, dirhodium (II) tetrakis(perfluorobutyrate) has been shown to be highly selective in competitive intramolecular metal carbene transformations (**Scheme 5.2**).<sup>19</sup> It has been postulated by Doyle *et al.*, that the difference in selectivities observed between the fluorinated and non-fluorinated catalysts arises due to the alteration in charge localisation during the carbene transition state. Theoretical calculations on the probable carbene intermediates suggest that the higher positive charge on the carbene carbon for  $[\text{Rh}_2(\text{pfb})_4]$ , arising from the high electronegativity of the fluorine atoms, leads to C-H insertion over cyclopropanation.<sup>19</sup> Conversely, the lower positive charge associated with the “ $[\text{Rh}(\text{OAc})_4\text{Rh}=\text{CH}_2]$ ” intermediate results in the lower selectivity. The authors also calculated the values for a catalyst that selectively favours cyclopropanation ( $[\text{Rh}_2(\text{CAP})_4]$ , CAP = caprolactamate, a cyclic amide). As expected, the calculations revealed a very low charge localisation on the carbene carbon, consistent with the 100 % conversion to the cyclopropane derivative (**Scheme 5.2**).<sup>19</sup>

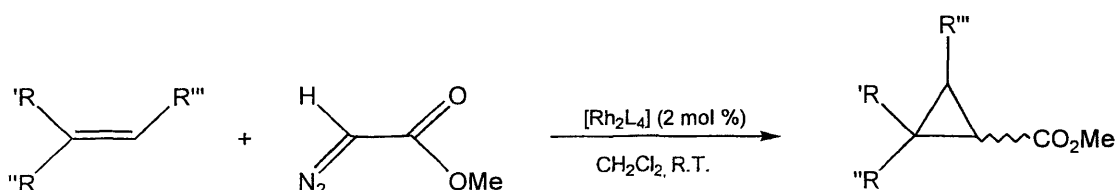
**Scheme 5.2**

Dirhodium (II) tetrakis(perfluorobutyrate) also catalyses the hydrosilylation of alkenes and alkynes and the silylcarbonylation of alkynes (**Scheme 5.3**).<sup>20</sup>



Scheme 5.3

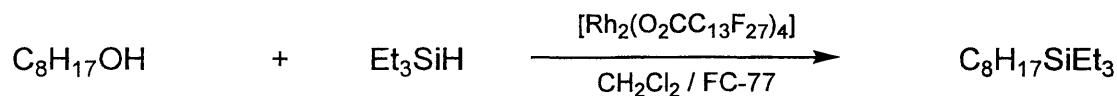
An extension of this work to the longer perfluoroalkyl chain rhodium dimers was reported during the course of this project by Endres and Maas, who analysed two species derived from perfluorohexyl and perfluoroheptyl substituted carboxylates ( $[\text{Rh}_2\text{L}_4]$ ,  $\text{L} = \text{O}_2\text{C-C}_6\text{H}_4\text{-4-C}_6\text{F}_{13}$  and  $\text{O}_2\text{CC}_7\text{F}_{15}$ ).<sup>12</sup> In the former case, an aromatic spacer group was incorporated to shield the metal atoms from the powerful electron withdrawing effect of the ponytails. The catalysts were investigated for the cyclopropanation of alkenes with methyl diazoacetate (Scheme 5.4).



Scheme 5.4

The catalytic system tolerated a variety of alkene substituents and yields of the cyclopropane product were generally high although not exceptional in comparison to those obtained with  $[\text{Rh}_2(\text{pfb})_4]$ . The reactions were carried out in dichloromethane and at the end of each cycle, the catalysts were extracted into PP3. Under these conditions, the catalysts could be reused three or four times with minimal losses in activity, however upon the application of a toluene / PP3 biphasic system, catalyst decomposition was encountered. In the case of the  $[\text{Rh}_2(\text{O}_2\text{C-C}_6\text{H}_4\text{-4-C}_6\text{F}_{13})_4]$  system, only 50 % recovery of the catalyst was possible.

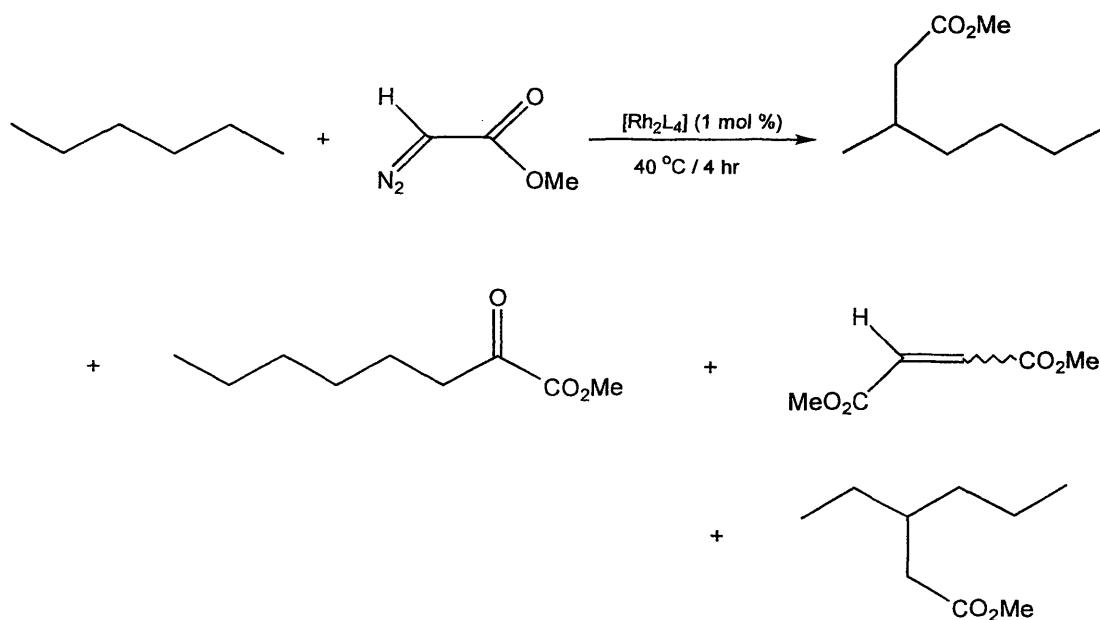
Following a similar approach, Biffis *et al.*, detailed the synthesis of two further fluoruous phase soluble rhodium carboxylate dimers; the perfluodecanoate and perfluorotetradecanoate derivatised species ( $[\text{Rh}_2\text{L}_4]$ ,  $\text{L} = \text{O}_2\text{CC}_9\text{F}_{19}$  and  $\text{O}_2\text{CC}_{13}\text{F}_{27}$ ).<sup>13</sup> In this work, the silylation of a variety of alcohols was investigated under standard organic and fluoruous biphasic conditions. Predictably, the activity of the fluoruous catalysts was considerably lower than that for the literature standard  $[\text{Rh}_2(\text{pfb})_4]$ , but only the perfluorotetradecanoate derivatised catalyst was sufficiently fluoruous phase soluble to offer viable fluoruous biphasic extraction – a somewhat surprising observation considering Endres and Maas’s success using the perfluoroheptyl derivatised rhodium dimer in a very similar system.<sup>12</sup> The authors investigated the silylation of 1-octanol using this catalyst in a dichloromethane / Fluoroinert® FC-77 (perfluorooctane(s)) biphasic (Scheme 5.5). Unfortunately, however, the reaction yield fell from 68 to 45 % after only three recycles, attributed by the authors to catalyst decomposition.



Scheme 5.5

Following on from their earlier paper, Endres and Maas extended the investigation of perfluorinated carboxylate rhodium dimers to species containing spacer groups in an attempt to shield the metal centres from the powerful electron withdrawing effect of the fluorinated moieties.<sup>14,15</sup> The authors detailed the synthesis and catalytic activity of a number of dimers containing alkyl spacer groups, including  $\text{CH}_2$ ,  $(\text{CH}_2)_2$  and  $(\text{CH}_2)_2\text{OCH}_2$ .<sup>14</sup> Overall, the introduction of the spacer groups dramatically reduced the fluoruous phase solubility of the complexes; only the methylene spacer derived dimer  $[\text{Rh}_2(\text{O}_2\text{CCH}_2\text{C}_6\text{F}_{13})_4]$ , was actually soluble in PP3. It appears likely that due to the insulating ability of the spacer groups, the polarity of the carboxylate head groups is such that repulsive interactions arise with the non-polar perfluorinated solvent molecules. All of the catalysts were investigated for the carbenoid C-H insertion reaction detailed in Scheme 5.6. The conversions obtained were relatively low and, unfortunately,

decreased as the size of the spacer group increased. More significantly, the catalysts were once again deleteriously affected by the catalytic cycle indicated by the fact that only 30 % recovery was possible for the fluororous soluble methylene spacer dimer  $[\text{Rh}_2(\text{O}_2\text{CCH}_2\text{C}_6\text{F}_{13})_4]$ .



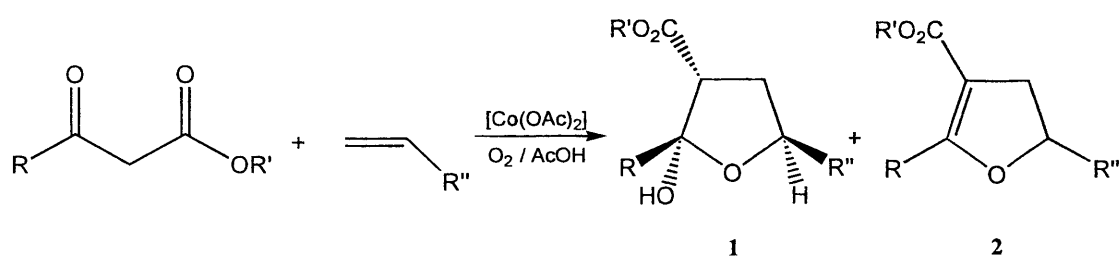
**Scheme 5.6**

Due to the low fluororous phase solubility encountered for the alkyl spacer carboxylate ligands, Endres and Maas hoped to increase the fluorophilicity of the rhodium dimers by synthesising two 3,5-*bis*-(perfluoroalkyl)benzoates.<sup>15</sup> By exploring the perfluorohexyl and perfluorooctyl derivatised systems, the total fluorine content was raised to 61 and 64 % respectively. Furthermore, both complexes were preferentially soluble in PP3, with no leaching detected when a variety of solvents were employed as the second organic phase. Unfortunately, however, the insolubility of the catalysts prevented them from dissolving in the substrate / dichloromethane phase, when investigated for the cyclopropanation of a variety of alkenes. As a consequence, the reactions were carried out in a hybrid organofluorine solvent (1,1,2-trichloro-1,1,2-trifluoroethane), followed by biphasic extraction of the catalyst using PP3 / dichloromethane. However, by employing a third solvent, the regime contradicts the underlying “environmentally friendly”

premise of fluorous biphasic catalysis as three solvents have replaced the original system, one of which is a banned chlorofluorocarbon. Furthermore, although the catalysts were effective for the cyclopropanation of styrene, 51 % of the perfluorohexyl species was lost after the fifth reaction cycle (38 % for the analogous perfluorooctyl system). The dimers were also evaluated for intermolecular and intramolecular carbenoid C-H insertion reactions, although similarly to the other fluorous species, degeneration of the active catalyst was observed after the first cycle.

### 5.2.2. Cobalt Acetate

Cobalt (II) acetate is a useful catalyst and reagent for a variety of synthetic transformations including carbon-carbon bond formation, functional group interconversions, oxidations, reductions and carbonylations.<sup>22</sup> Of the catalytic processes, the carbon-carbon bond forming reactions are particularly interesting due to the synthetic scope and stereoselectivity obtained.<sup>23</sup> A variety of 1,3-dicarbonyls can be added to terminal olefins, in the presence of acetic acid and oxygen, to yield substituted dihydrofurans (**Scheme 5.7**).



**Scheme 5.7**

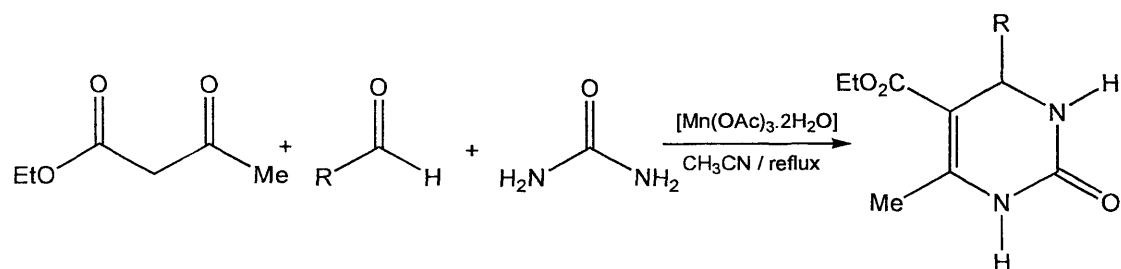
Only one diastereoisomer of the hemi-ketal (**1**), is formed during the reaction which, upon column chromatography, dehydrates to form the dihydrofuran (**2**), in moderate to good yield.<sup>24</sup> The system tolerates many functionalities in both substrate components, including cyclic dicarbonyls, conjugated olefins and sterically hindered substituents in both. Unfortunately, the “catalyst” loading is quite high, being used in an equimolar quantity to the dicarbonyl whilst the olefin is used in

vast excess. However, although it was hoped that this loading could be reduced, this should not pose a problem for the recyclable fluorinated derivatised analogue.

### 5.2.3. Manganese Acetate

Manganese (III) acetate  $[\text{Mn}(\text{OAc})_3]$  and oxo(trimanganese) heptaacetate  $[\text{Mn}_3\text{O}(\text{OAc})_7]$  are both extremely versatile oxidants, although in most cases, they are expended during the course of the reaction.<sup>25</sup> In a similar manner, manganese (III) acetate has been used for the aerobic epoxidation of unfunctionalised olefins.<sup>26</sup> Significantly, the reactions were optimised by carrying out the reactions in a perfluorinated solvent, FC75 (perfluoro-2-butyltetrahydrofuran), but once again, the process consumes the manganese acetate *via* a radical mechanism. Manganese (III) trifluoroacetate has also been employed as a reagent for the oxidation of saturated hydrocarbons.<sup>27</sup>

True catalytic reactions of manganese (III) acetate are consequently quite rare, although recently Kumar *et al.*, detailed the use of the complex as a catalyst for an efficient ‘one pot’ Biginelli reaction (**Scheme 5.8**).<sup>28</sup>



**Scheme 5.8**

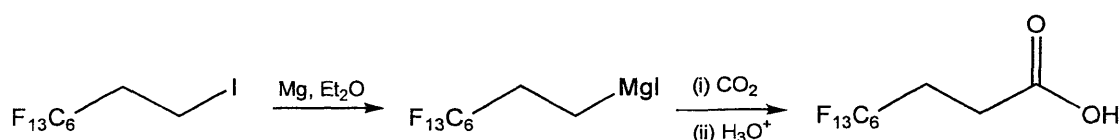
The reaction has been investigated with a wide range of aldehyde substrates, yielding universally high conversions in only two hours. The reaction mechanism proposed involves coordination of the ketoester to the manganese acetate, yielding the enolate which then reacts with a urea / aldehyde intermediate (acylimine). Unfortunately, the report does not detail the quantity of catalyst used, simply stating that ‘a catalytic amount’ was employed. Although the Biginelli reaction has been

investigated previously from a fluorous perspective, this was *via* fluorinated substrates rather than fluorinated catalysts.<sup>29</sup>

### 5.3. Ligand Synthesis and Coordination Chemistry

#### 5.3.1. Fluorinated Carboxylic Acids

Perfluoroalkyl carboxylic acids are amongst the most common commercially available fluorinated compounds, with chain lengths up to seventeen carbon atoms easily obtained.<sup>13</sup> For the three catalytic systems described, three fluorous carboxylic acids were chosen; the commercially available perfluoroheptanoic [ $C_6F_{13}CO_2H$ ] and perfluorononanoic [ $C_8F_{17}CO_2H$ ] acids, and for comparison, a ethylene spacer derived ligand, *2H,2H,3H,3H*-perfluorononanoic acid [ $C_6F_{13}CH_2CH_2CO_2H$ ]. This final carboxylic acid was prepared *via* carboxylation of the Grignard prepared from *1H,1H,2H,2H*-perfluorooctyl iodide (**Scheme 5.9**).<sup>30</sup>

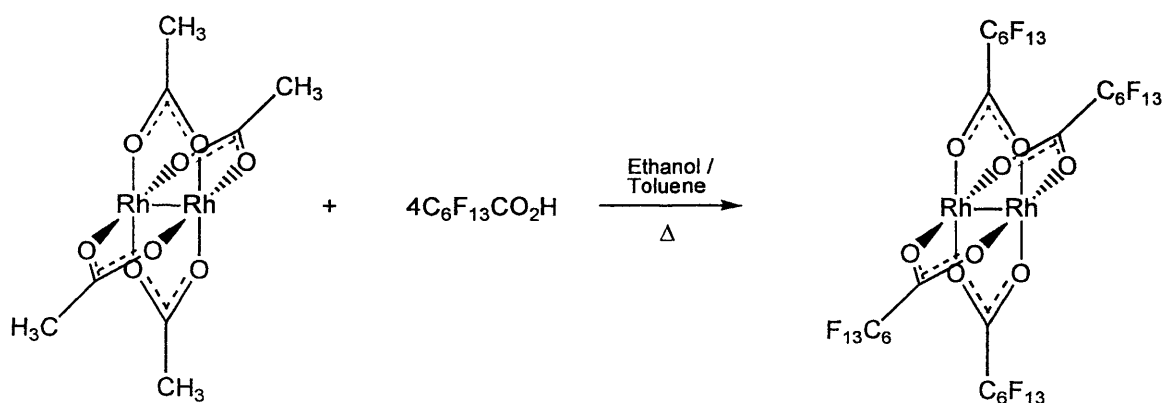


**Scheme 5.9**

Initially, the yield obtained from this reaction was quite low, with large amounts of *1H,1H,1H,2H,2H*-perfluorooctane generated due to the hydrolysis of the Grignard reagent. Previous synthetic procedures involving this intermediate have indicated that the reaction is fairly slow to initiate and also extremely moisture sensitive.<sup>31</sup> By following the method of Bhattacharyya *et al.* and also using dried carbon dioxide gas (rather than solid pellet form), the yield was raised considerably.<sup>31</sup> Characterisation data was in precise agreement with the literature account.<sup>30</sup>

### 5.3.2. Fluorous Carboxylate Rhodium Dimers

The syntheses of the perfluoroalkyl carboxylate dimers were attained *via* simple ligand exchange with dirhodium tetraacetate, following a similar procedure to that described by Bergbreiter, Morvant and Chen.<sup>32,12</sup> Essentially, the reaction proceeds as the liberated acetic acid is azeotropically distilled from the system by the refluxing ethanol / toluene mixture (**Scheme 5.10**).



**Scheme 5.10**

Both the perfluorohexyl and perfluorooctyl (**XIVa** and **XIVb** respectively), derivatised complexes were obtained as fine green powders in reasonable yield. Although both complexes are theoretically novel, they are analogous to the perfluoroheptyl and perfluorononyl derivatised systems prepared earlier and almost coincidentally to this work.<sup>12,13</sup> As a consequence, the characterisation data for the two complexes synthesised is comparable to the literature sources, with only the <sup>19</sup>F NMR revealing useful information. Unfortunately, elemental analysis could not be obtained for either complex due to the poor combustibility of the compounds.

In contrast, the rhodium dimer derived from the ethylene spacer carboxylate (**XIVc**), was prepared by reacting the sodium salt of the ligand with rhodium (III) chloride trihydrate.<sup>14</sup> According to the literature preparation of this compound, the earlier ligand exchange method fails due to the higher pK<sub>a</sub> of the ethylene spacer carboxylic acid. Whilst this is not surprising, it does serve to illustrate the

insulating effect of the ethylene spacer group on the fluororous ponytail. Eventually, the complex was obtained as a fine, bright-green powder, although the yield obtained (44 %) was slightly lower than that reported in the literature (53 %). Unfortunately, despite repeated attempts, the conversion could not be raised and during each reaction a considerable amount of rhodium metal was generated as a fine grey powder (a problem also encountered in the literature preparation). The characterisation data obtained for the compound, including  $^1\text{H}$  NMR,  $^{19}\text{F}$  NMR and mass spectrometry, was in agreement with the reported values.

Throughout the synthesis of the fluorinated rhodium dimers, attempts were made to obtain crystal structures of the compounds, in part due to the dearth of solid-state analysis of these compounds in the literature. Unfortunately, the complexes are quite insoluble in many common laboratory solvents, apart from Lewis basic species, which datively bind to the vacant sites of the rhodium metal centres. This behaviour was reported by Endres and Maas who reported the acetonitrile adduct of the perfluoroheptyl derivatised dimer.<sup>12</sup> For this reason, the three dimers were dissolved in a range of coordinating solvents, from simple ethers to aromatic amines. Of all the samples prepared, only the acetonitrile adduct of **XIVc** produced crystals suitable for X-ray analysis. To date, the solid-state structure shown in **Figure 5.3**, is the only example of a fluororous derivatised rhodium dimer, although there has been considerable interest in the study of donor ligands / solvent at the vacant sites of dirhodium tetraacetate.<sup>33</sup> The compound exists as two unique molecules differing by the unique orientation of the perfluoroalkyl chains, (the second molecule can be found on the accompanying CD-ROM., whilst a table of crystal data and structure refinements are given in Appendix 1). Both molecules are located on inversion centres with half of each molecule generated by symmetry (unlabelled). As expected the degree of thermal disorder increases as the perfluoroalkyl chain is transcended, indicated by the larger ellipsoids for the trifluoromethyl groups.

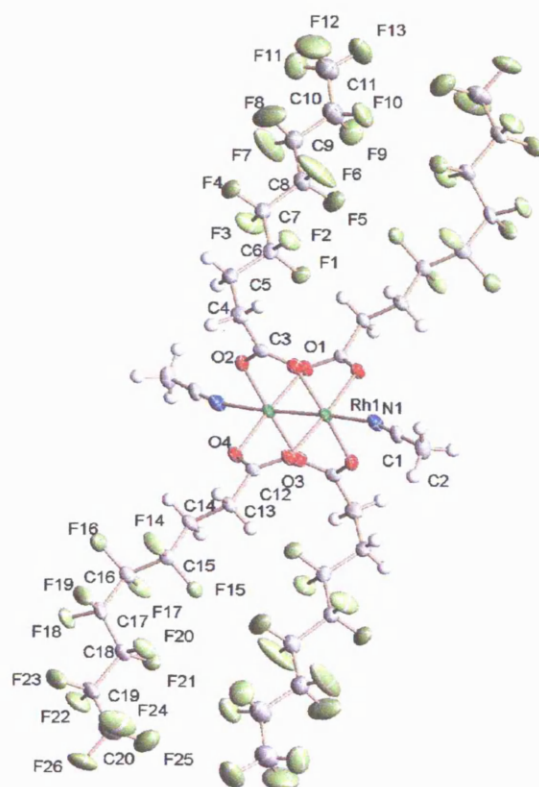


**Figure 5.3.** Crystal structure of  $[\text{Rh}_2(\text{O}_2\text{CCH}_2\text{CH}_2\text{C}_6\text{F}_{13})_4(\text{CH}_3\text{CN})_2]$  (**XIVc**)

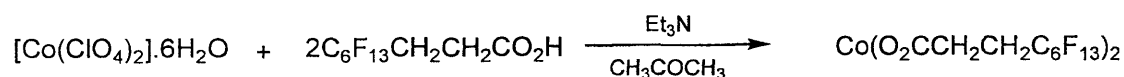
In comparison to a number of related rhodium dimers with coordinated molecules, the geometry of **XIVc** is very similar, with almost identical bond lengths for the Rh–Rh distances (**Table 5.1**).<sup>33</sup> It is interesting to observe that the bond lengths derived for **XIVc** are intermediate between the comparatively electron rich rhodium acetate dimer and the electron deficient trifluoroacetate analogue. Whilst the systems are not directly comparable, due to the variation in the lewis base used, this trend clearly represents the insulating influence of the ethylene spacer group that shields the powerful electron withdrawing effect of the perfluoroalkyl chains.

**Table 5.1.** Selected bond lengths of three carboxylate rhodium dimers

Bond	XIVc / Å	[Rh <sub>2</sub> (OAc) <sub>4</sub> (EtOH) <sub>2</sub> ] / Å <sup>34</sup>	[Rh(tfa) <sub>4</sub> (EtOH) <sub>2</sub> ] / Å <sup>33</sup>
Rh(1)-Rh(2)	2.3951(5)	2.3855(2)	2.396(2)
Rh(1)-O(1)	2.033(3)	2.039(3)	2.03(1)
Rh(1)-Lig(1)	2.230(3)	2.310(3)	2.28(1)

### 5.3.3. Fluorous Cobalt Carboxylates

The synthesis of the spacer derived fluorous carboxylate complex (**XVc**, **Scheme 5.11**) was achieved by employing a similar procedure to that described by Fish *et al.*, who prepared the perfluorooctyl derivatised species.<sup>16</sup> The compound was obtained as a fine lilac powder, similar to the parent cobalt acetate. Unfortunately, however, the complex was virtually insoluble in all common laboratory solvents, hampering many attempts at characterisation, especially NMR spectroscopy, which could not be obtained. Elemental analysis data was in agreement with the predicted values, whilst infrared spectroscopy revealed the coordinated carbonyl functionality.

**Scheme 5.11**

When a similar synthetic strategy was applied to the analogous non-spacer perfluorohexyl and perfluorooctyl carboxylate complexes (**XVa** and **XVb** respectively), very little reactivity was obtained. However, by exchanging the base used from triethylamine to potassium hydroxide, the yields increased to satisfactory levels. This is quite surprising as the pK<sub>a</sub>'s of the non-spacer acids are lower than the analogous spacer acid and therefore would be expected to be deprotonated by triethylamine. The difference in reactivity for potassium hydroxide must be attributed to the 'hardness' of the non-spacer carboxylic acids which consequently

react with the harder base.<sup>1</sup> Also, the driving force for the reaction is provided by the elimination of potassium perchlorate [KClO<sub>4</sub>], which was observed precipitating out of solution following the addition of the cobalt perchlorate. Both complexes were obtained as fine pink powders, which were comparatively more soluble than **XVc**. However, due to the paramagnetic metal centre (Co<sup>2+</sup>, d<sup>7</sup>), the <sup>19</sup>F NMR spectra were very badly distorted, although for **XVa**, the six broad resonances for the perfluorohexyl chain could be clearly recognised. Infrared analysis for both compounds revealed the shifted frequencies of the coordinated carbonyl groups. In comparison, the mass spectrometry data derived for these species was considerably more ambiguous, with a multitude of peaks that were not easily assigned. However, the traces were comparable, revealing similar fragmentation patterns, only differing by various factors of the difference in mass between the two complexes. The prominent peaks appear to correspond to hydrated dimers and trimers although the calculated masses are always marginally incorrect. The analysis was repeated to eliminate error, but the values were reproduced precisely.

In order to further characterise these molecules, attempts were made to obtain single crystals for X-ray analysis, but unfortunately, the complexes always precipitated out of solution as fine powders. However, recently, Tyrra *et al.*, have investigated a number of *bis*(dimethylamino-pyridine) adducts of trifluoroacetate complexes which provide suitable crystals for solid state analysis.<sup>35</sup> For this reason, the cobalt complexes were dissolved in a variety of coordinating solvents, following a similar approach to that employed for the fluorinated rhodium dimers. The pyridine adducts of both **XVa** and **XVb** yielded pink transparent crystals, but unfortunately only those of the perfluorooctyl species were of sufficient quality for X-ray analysis. The crystal structure (**Figure 5.4**), reveals that the disorder encountered previously for the perfluorohexyl derivatised species is exacerbated for the perfluorooctyl chain, to such an extent that the end of one of the chains could not be located. As a consequence, one carbon atom and seven fluorine atoms are missing from the structure. Attempts were made to model the system, but it was concluded that in this case the disorder was over more than two sites and, therefore, impossible to reproduce.

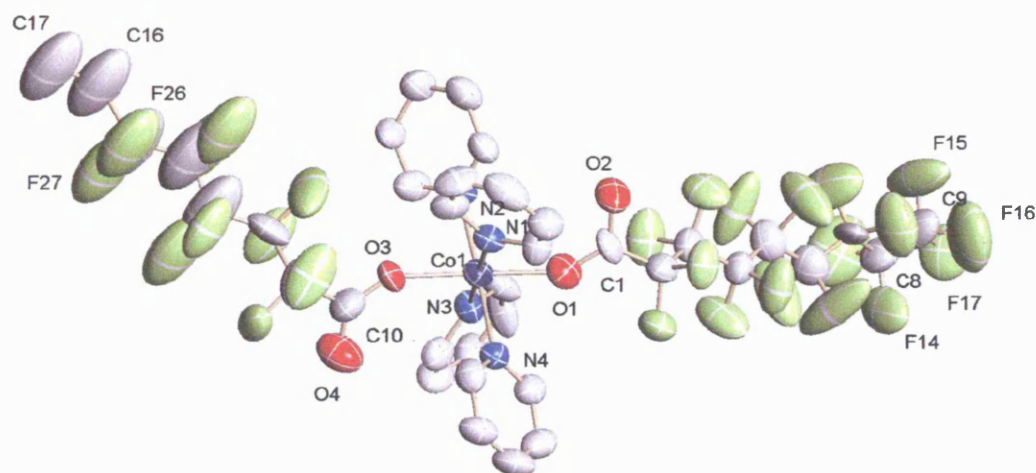


**Figure 5.4.** Crystal structure of  $[Co(O_2CC_8F_{17})_2(C_5H_5N)_4]$  (XVb)

The molecule adopts a distorted octahedral geometry with four equatorial pyridines and the two fluoros carboxylates bound axially to the metal centre. Significantly, the carboxylates are monodentate, with the carbonyl groups pointing away from the metal centre. This geometry is similar to that observed by Tyrre *et al.* for a range of similar metal trifluoroacetate amine adducts.<sup>35</sup> The Co-O bonds are equal and unremarkable, as are the Co-N bonds, unfortunately, the quality of the crystal structure prevents accurate comparison of the carbonyl bond lengths, negating the possibility of comparing the coordinated and non-coordinated species. The crystal packing diagram (**Figure 5.5**) reveals that the molecules align *via* the perfluoroalkyl chains in an almost ‘interlocked’ geometry. A table of crystal data and structure refinements are given in Appendix 1, whilst a complete collection of data for all the crystal structures contained in this thesis can be found on the accompanying CD-ROM.

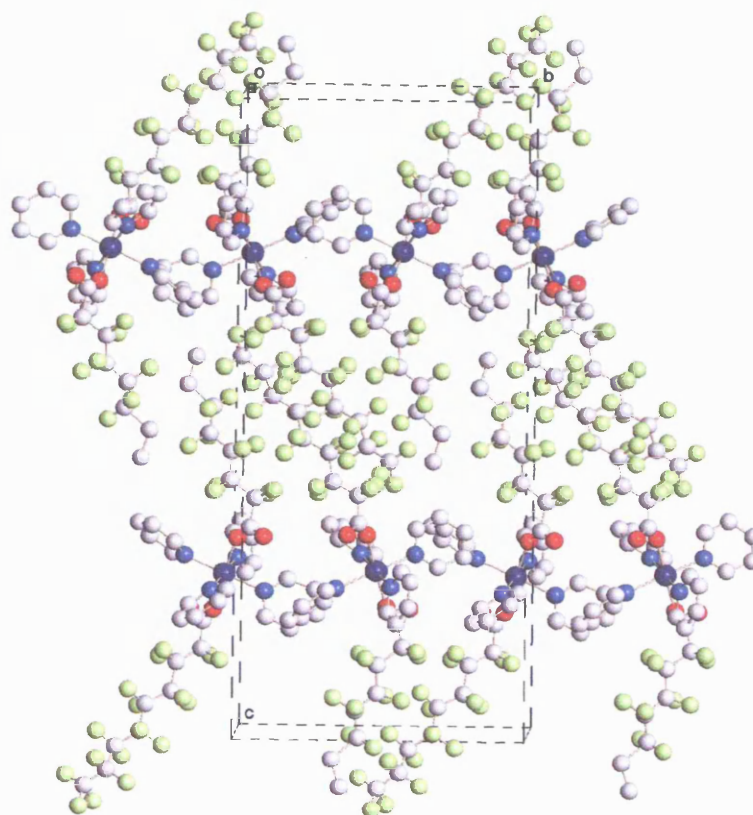


**Figure 5.5.** Crystal packing diagram of  $[\text{Co}(\text{O}_2\text{CC}_8\text{F}_{17})_2(\text{C}_3\text{H}_5\text{N})_4]$  (**XVb**)

#### 5.3.4. Fluorous Manganese Carboxylates

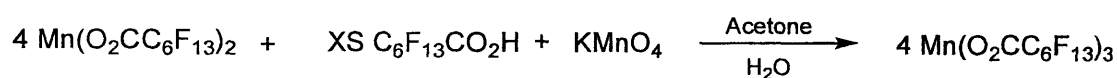
Unfortunately, the trends encountered for the cobalt complexes were mirrored in the synthesis of the analogous manganese species. The non-spacer perfluorohexyl and perfluorooctyl derivatised manganese (II) complexes (**XVIa** and **XVIb** respectively) were prepared following a similar route to that described for the corresponding cobalt complexes. Both were obtained as white solids in reasonable yields, although once again characterisation proved difficult due to the paramagnetism of the central manganese cation ( $\text{Mn}^{2+}$ ,  $d^5$ ). For **XVIa**, six broad resonances could be identified in the  $^{19}\text{F}$  NMR spectrum, but identically to the cobalt species, the  $^{19}\text{F}$  NMR spectrum of **XVIb** was heavily distorted with only four diffuse humps observed. The mass spectra of both complexes revealed an unusual,

yet distinctive pattern, similar to the analogous cobalt species. It appears likely that dimeric or even trimeric species are generated, although once again, the numbers do not correspond precisely to the calculated values. For comparison, the mass spectrum of commercially obtained manganese (III) acetate was examined. The trace revealed a very confusing pattern, with several high molecular weight ions although these could not be assigned. However, they did not correspond to dimeric or trimeric species and consequently did not reveal any distinct trends between the perfluoro- and *protio* analogues. Overall, it appears that these complexes do not exist as discrete monomeric species and that precise characterisation is not possible. Due to the degree of uncertainty regarding the exact formulation of these species, elemental analyses were not obtained.

The synthesis of the spacer fluorinated carboxylate manganese (II) complex (**XVIc**), was attained by the route described by Fish *et al.*, which was discussed earlier in the synthesis of **XVc**.<sup>16</sup> An extremely insoluble off-white material was obtained which was very difficult to characterise. The complex did not dissolve in any solvent system tested, even when gently warmed. As a consequence, no NMR spectroscopy data or mass spectrometry data could be obtained (the latter technique failing due to the insolubility of the compound in a variety of matrices). Only infrared analysis could be used to identify the carbonyl stretching frequency. Attempts were made to grow crystals of **XVIa** and **XVIb** from a variety of solvents including coordinating species, but unfortunately none of the crystals obtained were of sufficient quality to acquire crystallographic data.

In order to attempt the Biginelli reaction detailed earlier (see section 5.2.3.), the synthesis of the manganese (III) analogues needed to be accomplished to mimic the manganese (III) acetate that is used to mediate the reaction. It was also hoped that the manganese (III) species ( $\text{Mn}^{3+}$ ,  $d^6$ ), would be easier to characterise by NMR spectroscopy. Due to the absence of any commercially available manganese (III) starting materials, the synthesis of these compounds was attempted *via* two slightly unorthodox routes. The first strategy attempted was by simple ligand exchange from manganese (III) acetate, refluxing with an excess of the perfluorononanoic acid in acetic acid for two hours. After this time, an off-white powder was obtained, which when characterised revealed very similar trends to the data obtained for **XVIb**. In particular, the  $^{19}\text{F}$  NMR spectrum revealed the characteristically distorted

peaks of a paramagnetic species, whilst the mass spectrometry trace was almost identical. Numerous peaks were observed in the carbonyl region of the infrared spectrum, possibly indicating a mixture of products as well as starting material. The second approach was to react **XVIa** with an excess of perfluoroheptanoic acid in the presence of potassium manganate (VII), in order to effect the redox conversion of Mn(II) to Mn(III) (**Scheme 5.12**). A similar methodology has been used to synthesize manganese (III) acetylacetonate from manganese (II) chloride in the presence of acetylacetonate.<sup>36</sup>

**Scheme 5.12**

Unfortunately, when the reaction was attempted, a black solution was obtained upon the addition of the potassium permanganate and eventually a black tar-like material was yielded. The material was triturated in chloroform and hexane, but unfortunately, the product remained amorphous. Characterisation proved impossible due to the insolubility of the material in all common solvents. Following this result the synthesis of the manganese complexes was not pursued further and consequently, the catalytic procedures were not investigated.

Due to the difficulties encountered for the characterisation of the cobalt and manganese perfluorocarboxylates, it was decided to investigate the corresponding zinc complexes. It was hoped that informative NMR spectroscopy data could be generated, whilst the mass spectrometry data acquired could be compared to the confusing traces observed for the other two systems.

### 5.3.5. Fluorous Zinc Carboxylates

The synthesis of the perfluorohexyl and perfluorooctyl derivatised zinc carboxylates (**XVIIa** and **XVIIb** respectively) was achieved by reacting zinc dichloride with the appropriate ligand in the presence of potassium hydroxide (**Scheme 5.13**).



Scheme 5.13

Fine white powdery solids were obtained in good yield, which were soluble and thus easily characterised. Analysis by  $^{19}\text{F}$  NMR spectroscopy revealed the presence of the perfluoroalkyl tails, although the mass spectroscopy data for both species was uninformative with a variety of high mass ions that did not correspond to any obvious polymeric species. Furthermore, the traces did not show similar fragmentation patterns to either each other, or to those of the cobalt or manganese species. Fortunately, crystals of **XVIIa** revealed the solid-state structure of the molecule (**Figure 5.6**). A table of crystal data and structure refinements are given in Appendix 1, whilst a complete collection of data for all the crystal structures contained in this thesis can be found on the accompanying CD-ROM.

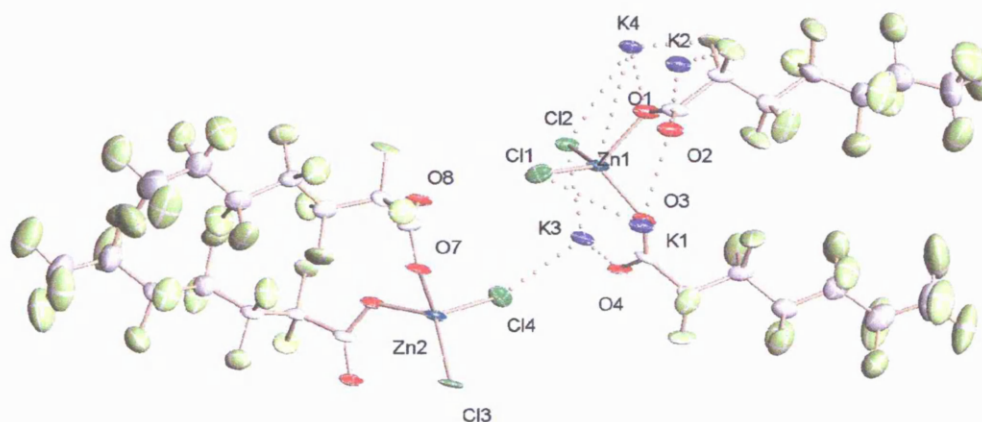


**Figure 5.6.** Crystal structure of perfluorohexyl derivatised carboxylate zinc species (“**XVIIa**”).

Unfortunately, the structure reveals that the carboxylate coordinates as a mixture of the free ligand and the potassium salt, furthermore, the chloride ions have remained attached to the central zinc atom, and are themselves bridging between molecules.

Similarly to the cobalt complex (XVb), the carboxylates bind *via* the monodentate coordination mode. However, a recent paper by Dell' Amico *et al.* that described the synthesis and characterisation of a variety of triflate and trifluoroacetate complexes of zinc, revealed that a complex extended bonding system can exist for these compounds.<sup>6</sup> The authors investigated a series of dimethoxyethane adducts that adopted *pseudo*-octahedral geometry in the solid state and existed as a polynuclear chain of molecules connected by bridging ligands.<sup>6</sup> To a certain extent, this unusual mixture of coordination does rationalise some of the earlier anomalous data, especially with regard to the mass spectrometry trace. Superficially, the structure shown represents a dimer, with four carboxylate ligands and two zinc metal centres, however, the additional potassium and chloride ions significantly increase the expected mass. In the mass spectrometry trace for this compound, there is a peak at 1820 Daltons, which is 60 Daltons less than the mass of the complex shown. The <sup>19</sup>F NMR data acquired for these complexes is also of little use as the perfluoroalkyl chains are equivalent due to the similar electronic environments of the coordinated carboxylate head groups.

Overall, with the exception of the dirhodium species, the investigation of the fluorinated carboxylate complexes has proved to be somewhat problematical due to the difficulty of precisely identifying the exact species present. The fact that the ligands appear to favour the monodentate coordination mode leads to a greater number of possible geometries than those possible for the bidentate bridging ligand modes, as illustrated by the rhodium dimers. Also, however, the ability of the potassium salt of the ligand to coordinate to the metal centres, further enhances the ambiguous chemistry of these ligands. As a consequence, the catalytic reactions investigated with the cobalt and manganese species are only preliminary (see section 5.4.2).

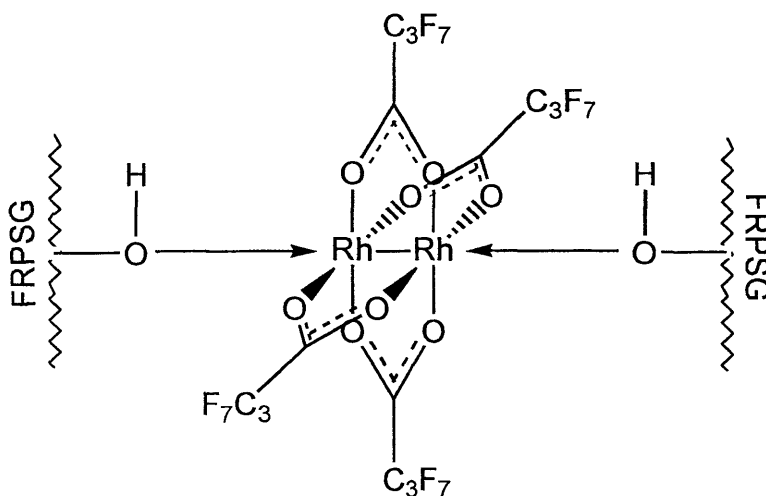
## 5.4. Catalysis Using Fluorinated Rhodium Carboxylates

### 5.4.1. Separation Science

Prior to the analysis of the fluorinated rhodium dimers for catalytic reactions, the separation science of the fluorous complexes was investigated and compared to the results obtained with the commercially available trifluoroacetate and heptafluorobutyrate analogues. It was found that the trifluoroacetate dimer had no solubility in the fluorous phase of a dichloromethane / perfluoro-1,3-dimethylcyclohexane biphasic system and was also not fluorous phase soluble in a comparable toluene biphasic system. As expected, the higher degree of fluorination rendered the heptafluorobutyrate dimer soluble in the fluorous phase, but unfortunately, not preferentially for either dichloromethane or toluene / PP3 biphasic systems. Similar to the literature findings, **XIVc** ( $[\text{Rh}_2(\text{O}_2\text{CCH}_2\text{CH}_2\text{C}_6\text{F}_{13})_4]$ ) exhibited very poor solubility in the fluorous phase, whilst the corresponding perfluoroalkyl dimers (**XIVa** and **XIVb**) were both preferentially fluorous phase soluble, with no leaching observed in either dichloromethane or toluene biphasic systems.<sup>13,14</sup> However, due to the failure of the liquid biphasic techniques described in the literature, the emphasis of the work described within this section was directed towards the FRPSG solid phase approach to catalyst recovery and reuse. For this reason, a detailed analysis of the retention of the fluorinated rhodium dimers on FRPSG was undertaken to assess the compatibility of this methodology.

The procedure used for the FRPSG testing was similar to that described for the fluorinated  $\beta$ -diketonates described in Chapter 2 (section 2.4). A Pasteur pipette containing FRPSG ( $6 \text{ cm}^3$ ) was pre-eluted with dichloromethane and then charged with a solution / suspension of the appropriate rhodium dimer (10 mg), also in dichloromethane. Dichloromethane was chosen for two reasons firstly, it is a non-coordinating solvent and secondly because it is the solvent of choice for many of the literature catalytic procedures. Predictably, the trifluoroacetate dimer did not possess a high enough degree of fluorination to be effectively retained by the column, with visible leaching observed as the solution was loaded on to the pipette. In contrast, the perfluorobutyrate dimer was effectively retained by the FRPSG column and furthermore, successive elutions with dichloromethane did not move the

discrete green band. However, the removal of the complex from the solid phase proved to be quite difficult, with only diethyl ether removing the majority of the material. A considerable volume was required to achieve ~ 70 % recovery and a brown residue remained on the column that could not be removed by any of the common laboratory solvents tested or by a number of fluorinated solvents. It was concluded from this experiment that the difficulty in recovering the dimer was due to coordination of free hydroxyls on the surface of the FRPSG that anchor the complexes to the surface (**Figure 5.7**). Unfortunately, although the silica is substituted with perfluoroalkyl moieties, there will inevitably be unreacted hydroxyls remaining.

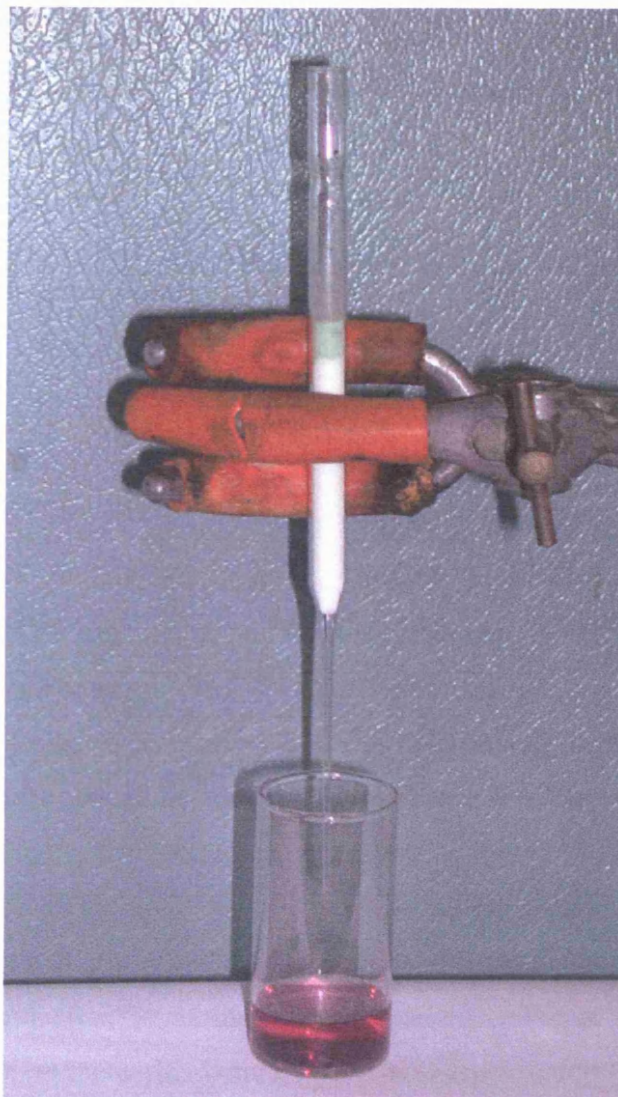


**Figure 5.7**

Unfortunately, this behaviour was echoed for the fluorous carboxylate rhodium dimers (**XIVa** and **XIVb**), with very low recovery when eluted by diethyl ether. In an attempt to prevent the irreversible binding of the rhodium dimers on the FRPSG, a number of solvent adducts of **XIVa** and **XIVb** were prepared. It was hoped that by ‘blocking’ the vacant sites on the rhodium atoms, the compounds could be eluted from the fluorous surface. The diethyl ether, THF and acetonitrile adducts were prepared for this purpose and of the three adducts the acetonitrile complex proved to be the most stable, being isolated as a fine powdery purple solid, whereas the ethereal adducts were obtained as slightly waxy materials. Unfortunately, however, when the adducts were loaded on to the FRPSG columns, they were not retained by

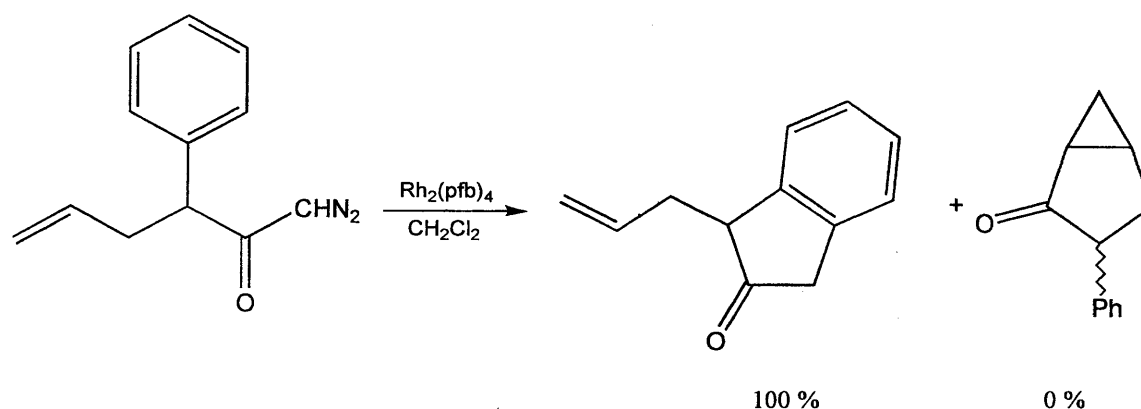
the solid phase. Furthermore, it became apparent that they degraded on the column, revealed by the fact that a green colouration of the free rhodium dimer remained on the silica. **Figure 5.8** shows the acetonitrile adduct of **XIVa** that passes straight through the column, whilst the liberated solvent-free dimer remains anchored at the top (green hue).

In direct contrast, however, the rhodium dimer of the spacer carboxylate was more compatible with the solid phase separation technique. The complex is soluble in dichloromethane allowing facile loading on to the column, where efficient retention is obtained even after subsequent elutions. Removal of the complex proved slightly more difficult, with only partial elution obtained with diethyl ether, although it was found that the remaining material could be eluted with acetone. Surprisingly, the dimer was recovered as a pink solution and subsequently a pink solid upon evaporation of the solvent mixture. However, when characterisation of the adduct was attempted by  $^1\text{H}$  NMR spectroscopy, the 'free' dimer was regenerated when the solid was dissolved in deuterated chloroform, indicated by a green precipitate at the base of the NMR tube. Although somewhat convoluted, this regime will hopefully provide an effective method of recycling the fluorous rhodium dimer (**XIVc**), without using any fluorinated solvents. As a consequence, the catalytic reactions were focussed upon this species and a comparison made to the literature standards.

**Figure 5.8**

#### 5.4.2. Catalytic Reactions

A relatively simple reaction was chosen to evaluate the fluorous catalysts and to test the applicability of the fluorous reverse phase silica gel methodology. The rhodium-catalysed decomposition of 1-diazo-3-phenyl-5-hexen-2-one was selected, as the reaction is reported to favour aromatic insertion (100 %) over cyclopropanation (0 %), when dirhodium heptafluorobutyrate (0.05 mol %) is used as the catalyst (**Scheme 5.14**).<sup>19</sup>



Scheme 5.14

The synthesis of the diazo compound was achieved by the literature reaction beginning with phenyl acetic acid.<sup>19</sup> Once characterised, the viscous yellow oil produced was subjected to reaction with dirhodium heptafluorobutyrate, in order to confirm the literature precedent. The reaction was carried out in dichloromethane and at the end of the process, the mixture was passed down a short (Pasteur pipette) fluoruous reverse phase silica gel column to remove the catalyst. The column was washed with further dichloromethane to remove the product and then followed by elution with diethyl ether to attempt to remove the catalyst. Unfortunately this proved impossible, as there was little trace of any green colouration on the column and due to the brown residue remaining, it was concluded that the catalyst had decomposed on the silica surface (see section 5.4.1.). The formation of the desired product, formed *via* aromatic substitution, was confirmed by NMR spectroscopy (94 % yield). Significantly, examination of the organic fractions by  $^{19}\text{F}$  NMR spectroscopy showed no trace of any fluorinated species.

The analogous reaction with the spacer carboxylate rhodium dimer (**XIVc**), was carried out under similar conditions. Unfortunately, the overall conversion was considerable lower than for the perfluorobutyrate dimer and the selectivity obtained was decreased, with traces of the cyclopropanation product visible in the  $^1\text{H}$  NMR spectrum (**Scheme 5.14**). The separation of the catalyst on the column was very effective, with no trace of any fluorinated species when the  $^{19}\text{F}$  NMR spectrum of the product was analysed. However, when the catalyst was eluted with acetone to

yield the pink intermediate, the corresponding solid could not be reconverted to a green powder as before. The solution was left standing for over two weeks without change. Attempts were made to employ this material for the catalytic reaction, but the activity obtained was minimal and the species could no longer be retained on the FRPSG column.

The disappointing activity of **XIVc** is undoubtedly due to the insulating effect of the spacer groups on the rhodium metal centres. When Endres and Maas examined a similar intramolecular C-H insertion reaction with the spacer carboxylate derived catalyst  $[\text{Rh}_2(\text{CH}_2\text{C}_6\text{F}_{13})_4]$ , efficient conversion could only be obtained by employing harsher conditions.<sup>14</sup> It is evident that the electron withdrawing effect of the perfluoroalkyl moieties is required to increase the electrophilicity of the complex which increases the positive charge on the carbene intermediate following the rationale described earlier in section 5.2.1. However, as the electrophilicity is raised, the species are more likely to bind irreversibly to the free hydroxyls present on the surface of the fluorosilica. Unfortunately the analysis indicates that a dichotomy exists between catalysts that are recyclable using FRPSG and those that are effective for the catalytic reactions.

## 5.5. Catalysis Using Fluorinated Cobalt Carboxylates

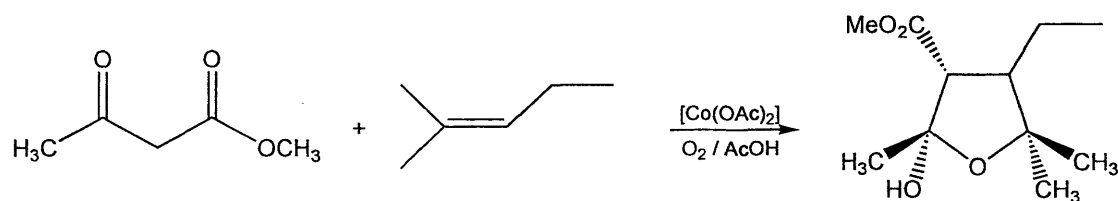
### 5.5.1. Separation Science

In a similar manner to the analysis of the fluorinated rhodium dimers, the retention of the fluorinated cobalt carboxylates by FRPSG was investigated prior to the catalytic investigations. The increased solubility of the non-spacer cobalt carboxylates (**XVa** and **XVb**), in comparison to either cobalt acetate or the spacer-derived analogue (**XVc**), was manifested in very poor retentions for both complexes on the fluorosilica. In comparison, the insolubility of **XVc** meant that a suitable solvent could not be found to efficiently load the complex on to the column. As a result, the powdery solid was introduced as a slurry to the top of the column. Predictably, once on the column, a variety of common laboratory solvent could not remove the complex, although slight recovery was recorded when hot methanol was used. Fluorous solvents and fluorosilica 'hybrid' solvents (benzotrifluoride,

trifluoroethanol) also had little effect and also prohibited the alternative liquid biphase approach.

### 5.5.2. Catalytic Reactions

Despite the poor compatibility of the fluorinated cobalt carboxylates with the fluorous separation regimes, it was decided to assess the catalytic activity of the complexes regardless of this setback. Although **XVc** could not be recovered from the FRPSG, the separation was very efficient, with no visible leaching. Following the earlier discussion (see section 5.2.2.), the reaction that was selected was the carbon-carbon bond forming reaction between methylacetoacetate and 2-methyl pentene (**Scheme 5.15**).<sup>23</sup>



**Scheme 5.15**

According to the literature, the reaction is reported to proceed to 68 % conversion although the exact conditions were poorly defined. As mentioned earlier, equimolar quantities of the catalyst were used to the dicarbonyl compound, whilst the alkene was used in vast excess. Unfortunately, the concentrations and temperature conditions were ambiguously described and for this reason a variety of test procedures were carried out to assess the reaction. At room temperature, the cobalt acetate was not soluble in acetic acid, although upon addition of the reagents, sparing solubility was observed. At elevated temperature (60 °C) the catalyst began to dissolve, although rapidly the solution turned black preventing further observation. The reaction was stirred under oxygen for a number of time durations, but unfortunately, even when the reaction was left overnight, the yields of the tetrahydrofuran product were very low, ranging from trace amounts to approximately 10% conversion. Attempts were made to improve the reaction by

drying the catalyst over silica gel under vacuum, using pre-dried methylacetoacetate and also by drying the acetic acid ( $\text{CrO}_3$ ). However, all of these proved fruitless with similarly poor conversions. For this reason and also due to the poor solubility of the fluorous catalyst (**XVc**), further analysis of this reaction was not undertaken.

## 5.6. Conclusions

The investigation of the perfluoroalkyl carboxylate rhodium dimers provided a logical extension to the literature discussions that were produced in parallel with the work described. Unfortunately, the implementation of solid phase fluorous extraction does not assist the recovery and recycling of these fragile catalysts and it appears likely that any developments in this area will focus upon developing the liquid biphasic approach, possibly through the continued investigation of the perfluoroalkyl benzoates.<sup>15</sup>

The difficulty of characterising the cobalt and manganese perfluorocarboxylates significantly hindered their investigation. In this regard, the choice of two paramagnetic metal centres hampered characterisation due to the inability to obtain NMR data, although the *protio* analogues offered the most versatile catalytic applications. Unfortunately, alternative methods of characterisation proved troublesome, with ambiguous mass spectrometry traces and uninformative infrared spectra. A further difficulty was imparted by the insolubility of these species, particularly those derived from the ethylene spacer ligand [ $\text{O}_2\text{CCH}_2\text{CH}_2\text{C}_6\text{F}_{13}$ ]. This also limited the catalytic investigations and it is difficult to envisage any future applications of these systems, unless alternative modifying agents are added such as the perfluoroalkyl-substituted triazocyclononane studied by Fish *et al.*<sup>16</sup>

## 5.7. References for Chapter 5

- [1] R.G. Pearson, *J. Am. Chem. Soc.*, 1963, **85**, 3533.
- [2] U. Casellato, P. Vigato and M. Vidali, *Coord. Chem. Rev.*, 1978, **26**, 85.
- [3] C. Oldham, 'Carboxylates, squarates and related species', 'Comprehensive Coordination Chemistry', G. Wilkinson, R.D. Gillard and J.A. M<sup>c</sup>Cleverty. Pergamon Press, Oxford.
- [4] H. Grennberg, 'Encyclopaedia of Reagents for Organic Synthesis', **6**, 3847. John Wiley & Sons, 1995.
- [5] J. M<sup>c</sup> Murry. 'Organic Chemistry', (third edition). 1992. Brooks / Cole.
- [6] D.B.D. Amico, D. Boschi, F. Calderazzo, L. Labella and F. Marchetti, *Inorg. Chim. Acta.*, 2002, **330**, 149.
- [7] M.J. Baillie, D.H. Brown, K.C. Moss and D.W.A. Sharp, *J. Chem. Soc.*, 1968, 3110.
- [8] F. Calderazzo, U. Englert, G. Pampaloni, V. Passarelli, G. Serni and R. Wang, *Can. J. Chem.*, 2001, **79**, 495.
- [9] S. Amasa, D.H. Brown and D.W.A. Sharp, *J. Chem. Soc.*, 1969, 2892.
- [10] Ž. Čeković and M.L. Mihailović, 'Encyclopaedia of Reagents for Organic Synthesis', **4**, 2959. John Wiley & Sons, 1995.
- [11] R.E. Partch, *J. Am. Chem. Soc.*, 1967, **89**, 3662.
- [12] A. Endres and G. Maas, *Tetrahedron Lett.*, 1999, **40**, 6365.
- [13] A. Biffis, E. Castello, M. Zecca and M. Basato, *Tetrahedron*, 2001, **57**, 10391.
- [14] A. Endres and G. Maas, *J. Organomet. Chem.*, 2002, **643-644**, 174.
- [15] A. Endres and G. Maas, *Tetrahedron*, 2002, **58**, 3999.
- [16] J.M. Vincent, A. Rabion, V.K. Yachandra and R.H. Fish, *Angew. Chem. Int. Ed. Engl.*, 1997, **36**, 2346; J.M. Vincent, A. Rabion, V.K. Yachandra and R.H. Fish, *Can. J. Chem.*, 2001, **79**, 888; J. Loiseau, E. Fouquet, R.H. Fish, J. Vincent and J. Verlhac, *J. Fluorine Chem.*, 2001, **108**, 195.
- [17] M.P. Doyle, 'Encyclopaedia of Reagents for Organic Synthesis', **2**, 2281 – 2293, John Wiley & Sons, 1995; M.P. Doyle, *Chem. Rev.* 1986, **86**, 919; A. Padwa and S.F. Hornbuckle, *Chem. Rev.* 1991, **91**, 263.
- [18] M.P. Doyle, D. van Leusen and W.H. Tamblyn, *Synthesis*, 1981, 787.

- [19] A. Padwa, D.J. Austen, A.T. Price, M.A. Semones, M.P. Doyle, M.N. Protopopova, R. Winchester and A. Tran, *J. Am. Chem. Soc.*, 1993, **115**, 8669.
- [20] M.P. Doyle, G.A. Devora and A.O. Nefedov, *Organometallics*, 1993, **12**, 11.
- [21] M.P. Doyle and M.S. Shanklin, *Organometallics*, 1992, **11**, 549.
- [22] M. Periasamy and M.L.N. Rao, 'Encyclopaedia of Reagents for Organic Synthesis', **2**, 1284. John Wiley & Sons, 1995.
- [23] J. Iqbal, T.K.P. Kumar and S. Manogaran, *Tetrahedron Lett.*, 1989, **30**, 4701. J. Iqbal, P. Tarakeshwar and S. Manogaran, *Tetrahedron*, 1991, **47**, 297.
- [24] J. Iqbal, B. Bhatia and N. Nayyar, *Tetrahedron*, 1991, **47**, 6468.
- [25] W.E. Fristad, J.R. Peterson, A.B. Ernst and G.B. Urbi, *Tetrahedron*, 1986, **42**, 3429. B.B. Snider, J.J. Patricia and S.A. Kates, *J. Org. Chem.*, 1988, **53**, 2137.
- [26] K.S. Ravikumar, F. Barbier, J-P. Bégué and D. Bonnet-Delpon, *Tetrahedron*, 1998, **54**, 7457.
- [27] S.R. Jones and J.M. Mellor, *J. Chem. Soc., Perkin Trans.*, 1977, 511.
- [28] K.A. Kumar, M. Kasthuraiah, C.S. Reddy and C.D. Reddy, *Tetrahedron Lett.*, 2001, **42**, 7873.
- [29] A. Studer, P. Jeger, P. Wipf and D.P. Curran, *J. Org. Chem.*, 1997, **62**, 2917.
- [30] A.M. Jouani, F. Szönyi and A. Cambon, *J. Fluorine Chem.*, 1992, **56**, 85.
- [31] P. Bhattacharyya, D. Gudmunsen, E.G. Hope, R.D.W. Kemmitt, D.R. Paige and A.M. Stuart, *J. Chem. Soc., Perkin Trans. I*, 1997, **1**, 3609.
- [32] D.E. Bergbreiter, M. Morvant and B. Chen, *Tetrahedron Lett.*, 1991, **32**, 2731.
- [33] M.A.S. Aquino and D.H. Macartnry, *Inorg. Chem.*, 1987, **26**, 2696. E.B. Boyar and S.D. Robinson, *Coord. Chem. Rev.*, 1983, **50**, 109.
- [34] F.A. Cotton, B.G. DeBoer, M.D. LaPrade, J.R. Pipal and D.A. Ucko, *Acta Crystallogr. Sect. B*, 1971, **27**, 1664.
- [35] W. Tyrra, D. Naumann and I. Pantenburg, *J. Fluorine Chem.*, 2003, **120**, 13.
- [36] M.N. Bhattacharjee, M.K. Chaudhuri and D.T. Khathing, *J. Chem. Soc., Dalton Trans.*, 1981, 669.

## 6. Experimental Procedures

### 6.1. General Experimental Procedures

#### 6.1.1. NMR spectroscopy

$^1\text{H}$ ,  $^{19}\text{F}\{^1\text{H}\}$ ,  $^{13}\text{C}\{^1\text{H}\}$  and  $^{31}\text{P}$  NMR spectra were recorded on Bruker DRX 400, Bruker AM 300 and Bruker ARX 250 spectrometers at the ambient temperature of the probe unless otherwise stated.  $^1\text{H}$  and  $^{13}\text{C}\{^1\text{H}\}$  NMR spectra were referenced internally using the residual *protio* solvent resonance relative to  $\text{SiMe}_4$  ( $\delta = 0$  ppm), whilst  $^{19}\text{F}$  NMR spectra were referenced to external  $\text{CFCl}_3$  ( $\delta = 0$  ppm), and  $^{31}\text{P}$  NMR spectra were referenced externally to 85 %  $\text{H}_3\text{PO}_4$  ( $\delta = 0$  ppm). All chemical shifts are quoted in  $\delta$  (ppm) and coupling constants in Hertz (Hz), using the high-frequency positive convention. The following spectrometer frequencies were used:

Bruker ARX 250 Spectrometer:	$^1\text{H}$ NMR spectra, 250.13 MHz, $^{19}\text{F}\{^1\text{H}\}$ NMR spectra, 235.34 MHz, $^{13}\text{C}\{^1\text{H}\}$ NMR spectra, 63 MHz $^{31}\text{P}$ NMR spectra, 101.26 MHz.
Bruker AM 300 Spectrometer:	$^1\text{H}$ NMR spectra, 301.37 MHz, $^{19}\text{F}\{^1\text{H}\}$ NMR spectra, 283.57 MHz, $^{31}\text{P}$ NMR spectra, 121.99 MHz.
Bruker DRX 400 Spectrometer:	$^1\text{H}$ NMR spectra, 400.13 MHz, $^{19}\text{F}\{^1\text{H}\}$ NMR spectra, 376.46 MHz.

The solvent most frequently used was deuterated chloroform ( $\text{CDCl}_3$ ). However, if this was not possible due to solubility problems, an alternative *deutero* solvent was employed and failing that, a common laboratory solvent (for example diethyl ether), was used with a sealed, deuterated benzene ( $\text{C}_6\text{D}_6$ ), capillary insert tube. Spectra of

air / moisture sensitive compounds were obtained by preparing the samples under an inert atmosphere in a dry-box using previously dried and freeze/pump/thaw degassed deuterated solvents. The solutions were then loaded into either a Young's NMR tube or a Teflon-sealed screw-cap NMR tube.

### 6.1.2. Infra-red Spectroscopy

Infrared spectra were recorded on a Digilab FTS-40 Fourier transform spectrometer and a Perkin Elmer spectrometer, both at  $4\text{ cm}^{-1}$  resolution (16 scans). Spectra for solids were recorded as Nujol mulls compressed between two sodium chloride discs or as a potassium bromide pressed disc, whilst those for oils were obtained as a thin films between the discs.

### 6.1.3. Mass Spectrometry

Electron impact (EI) and fast atom bombardment (FAB) mass spectra were recorded on a Kratos concept 1 H, double focussing, forward geometry mass spectrometer. 3-Nitrobenzyl alcohol was used as the matrix for the FAB spectra. Electrospray (ES) mass spectra were obtained on a Micromass Quattro LC spectrometer.

### 6.1.4. Elemental analysis

Elemental analyses were performed either by Butterworth Laboratories Ltd. or the Elemental Analysis Service at the University of North London.

### 6.1.5. X-Ray Crystallography

X-ray crystallographic data was collected on a Siemens P4 four circle diffractometer using a Mo K  $\alpha$  radiation source ( $\lambda = 0.7107\text{ \AA}$ ) or a Bruker Apex SMART 2000 diffractometer. Crystal data and structure refinements can be found in Appendix 1, whilst a complete collection of data for all the crystal structures contained in this thesis can be found in electronic format on the accompanying CD-ROM.

## 6.2. Anhydrous Solvents

Unless otherwise stated, dry solvents were used that had been freeze/pump/thaw degassed three times prior to their utilisation. The following literature drying techniques were employed:<sup>1</sup>

Diethyl Ether, 1,2-Dimethoxyethane, Hexane, Tetrahydrofuran;	Dried by heating to reflux over sodium metal (pressed into a wire) and benzophenone under an atmosphere of dry nitrogen for three days. Distilled from sodium benzophenone ketyl under nitrogen and transferred to a closed ampoule containing activated 4 Å molecular sieves.
Dichloromethane, 1,2-Dichloroethane, Chloroform, Ethyl acetate, PP3;	Dried refluxing over calcium hydride under an atmosphere of dry nitrogen for three days. Distilled from calcium hydride under nitrogen and then transferred to a closed ampoule containing activated 4 Å molecular sieves.
1,1,1-Trifluorotoluene	Dried by refluxing over phosphorus pentoxide under an atmosphere of dry nitrogen for three days. Distilled from phosphorus pentoxide and then transferred under nitrogen to a closed ampoule containing activated 4 Å molecular sieves.
Dimethyl Sulfoxide, Methanol	Purchased dry from Aldrich Chemical Co. and used as supplied.

### 6.3. Starting Materials and Reagents

Primarily, all chemicals were purchased from Aldrich Chemical Company and used as supplied – unless otherwise stated. However, most of the fluorinated compounds (including fluorinated carboxylic acids, esters and silanes) were purchased from Apollo Ltd. or Fluorochem Ltd. owing to the specialist nature of these reagents.

Fluorous reverse phase silica gel (FRPSG) was synthesised following the literature procedure described by Curran *et al.*<sup>2</sup> Flash chromatography grade silica (30 g) was dried at 120 °C under high vacuum for 14 hours, resulting in the removal of 6 cm<sup>3</sup> of water. The silica was then transferred to a 500 ml three-necked round bottomed flask, to which was added imidazole (9.5 g) and 1*H*,1*H*,2*H*,2*H*-perfluoro-octyldimethyl chlorosilane (50 g) as a solution in toluene (80 ml). Upon the addition of the chlorosilane, an exothermic reaction was observed. The mixture was then heated at 100 °C for 72 hours without stirring. The resulting fluorous reverse phase silica gel was then washed sequentially with toluene, methanol, methanol / water, tetrahydrofuran, diethyl ether and acetonitrile (50 ml each). A hexane wash (50 ml) was also incorporated to remove traces of the fluorinated silanol by-product. The white powdery solid obtained was then dried under high vacuum for 6 hours (51.8 g).

*Bis*-triphenylphosphine copper (I) nitrate was synthesised according to the literature procedure described by Cotton and Goodgame.<sup>3</sup>

The dimethoxyethane adduct of dioxomolybdenum (VI) dichloride [MoO<sub>2</sub>Cl<sub>2</sub>.dme] was prepared analogously to the route employed by Chiu *et al.*<sup>4</sup>

## 6.4. Laboratory Apparatus

### 6.4.1. Schlenk Line<sup>5</sup>

The manipulation of air and moisture sensitive compounds was carried out using a standard Schlenk line, thus ensuring anhydrous conditions throughout. Essentially, this apparatus consists of a glass dual manifold line connected to both a dry nitrogen supply and a vacuum pump (model: NGN PSR/2), which was protected by a liquid nitrogen cooled trap. The reaction vessels were connected to the line by thick walled Neoprene vacuum tubing, with the nitrogen / vacuum supplies controlled by ground glass Interkey or Young's greaseless taps. The Schlenk line was adapted to incorporate an oxygen inlet for the sulfide oxidation procedures. Prior to use of the line for this purpose, oxygen was flushed through the system for one hour. Upon completion of the oxidation reactions, nitrogen was flushed through the line for at least three hours to ensure that an inert atmosphere was replaced.

### 6.4.2. Glassware

The catalytic reactions were carried out in a Radley's Carousel Work Station, specifically in Radley's Carousel Reaction Tubes, which were evacuated and backfilled with nitrogen three times before use. The majority of the synthetic procedures were carried out in Pyrex glassware with Quickfit ground glass joints. For syntheses involving air and moisture sensitive components, the glassware was flame-dried under vacuum before use and upon cooling, backfilled with an atmosphere of dry nitrogen.

### 6.4.3. Faircrest Dry-box and Nitrogen Flush-box

The transferral of air and moisture sensitive compounds was carried out in either a Faircrest auto-recirculating positive pressure dry-box or a nitrogen positive pressure flush box. The nitrogen atmosphere of the Faircrest dry-box was maintained *via* circulation through columns of molecular sieves and manganese

dioxide that removed water and oxygen (< 5 ppm) respectively. A positive flow of dry nitrogen and an activated molecular sieve filter maintained the atmosphere of the nitrogen flush-box. However, the atmosphere was not as scrupulously dry as the Faircrest dry-box, and as a consequence, was only used for the rapid transferral of moderately sensitive materials.

## 6.5. Experimental Procedures

### 6.5.1. 3,3,4,4,5,5,6,6,7,7,8,8,8-Tridecafluoro-octan-2-one.

Methyl magnesium bromide (3.0 mol dm<sup>-3</sup> solution; 69 cm<sup>3</sup>, 0.206 moles) was added to diethyl ether (36 cm<sup>3</sup>) in a round bottomed flask under an atmosphere of dry nitrogen. A solution of perfluoroheptanoic acid (25 g, 0.069 moles), also in diethyl ether (23 cm<sup>3</sup>), was added dropwise over one hour to the stirred Grignard reagent. The reaction mixture was then refluxed for two hours. The reaction was then allowed to cool before being quenched with ice (62.5 g) followed by hydrochloric acid (6 M, 63 cm<sup>3</sup>). The aqueous layer was extracted with diethyl ether, (3 x 30 cm<sup>3</sup>) and the organic fractions combined. The yellow solution was then washed with a saturated solution of sodium chloride and then dried over magnesium sulfate. Evaporation of the diethyl ether produced a pale yellow, slightly viscous liquid. The crude product was distilled under vacuum (46 – 49 °C, 23.1 mmHg) to yield a clear colourless liquid (14.75 g, 59 %).

$\delta$  <sup>1</sup>H NMR (CDCl<sub>3</sub>) 2.45 [3H, s, CH<sub>3</sub>].

$\delta$  <sup>19</sup>F {<sup>1</sup>H} NMR (CDCl<sub>3</sub>) -81.44 [3F, t, <sup>4</sup>J<sub>FF</sub> 9.3 Hz, CF<sub>3</sub>], -120.90 [2F, t, <sup>4</sup>J<sub>FF</sub> 12.1 Hz, α-CF<sub>2</sub>], -122.90 [2F, um, CF<sub>2</sub>], -122.16 [2F, um, CF<sub>2</sub>], -124.09 [2F, um, CF<sub>2</sub>], -126.74 [2F, um, CF<sub>2</sub>].

$\delta$  <sup>13</sup>C NMR (CDCl<sub>3</sub>) 25.36 [s, CH<sub>3</sub>], 105 – 120 [um's, C<sub>6</sub>F<sub>13</sub>], 191.32 [t, <sup>2</sup>J<sub>CF</sub> 27.1 Hz, C=O].

*m/z* (ES) 362 ([M]<sup>+</sup>), 361 ([M-H]<sup>+</sup>), 319 ([C<sub>6</sub>F<sub>13</sub>]<sup>+</sup> 100%), 169 ([C<sub>3</sub>F<sub>7</sub>]<sup>+</sup>).

Infrared analysis: 1746 cm<sup>-1</sup> ν(C=O).

Elemental analysis. Found: C, 26.8; H, 0.9; N, <0.3; F, 68.7. C<sub>8</sub>H<sub>3</sub>OF<sub>13</sub> requires: C, 26.5; H, 0.8; N, 0.0; F, 68.2.

**6.5.2. 3,3,4,4,5,5,6,6,7,7,8,8,9,9,9-Pentadecafluoro-nonan-2-one.**<sup>6</sup>

Methyl magnesium bromide (3.0 mol dm<sup>-3</sup> solution; 48.3 cm<sup>3</sup>, 0.18 moles) was added to THF (65 cm<sup>3</sup>) in a round bottomed flask under an atmosphere of dry nitrogen. A solution of perfluorooctanoic acid (25 g, 0.060 moles), also in THF (31 cm<sup>3</sup>), was added dropwise over one hour to the stirred Grignard reagent. The reaction mixture was then refluxed for two hours. The resulting suspension was then allowed to cool before being quenched with ice (62.5 g) followed by hydrochloric acid (6 M, 63 cm<sup>3</sup>). The aqueous layer was extracted with diethyl ether (3 x 30 cm<sup>3</sup>) and the organic fractions combined. The yellow solution was then washed with a saturated solution of sodium chloride and then dried over magnesium sulfate. Evaporation of the diethyl ether produced a pale yellow, slightly viscous liquid. The crude product was distilled under vacuum (55 – 56 °C, 20 mmHg) to yield a clear colourless liquid (13.06 g, 52 %).

$\delta$  <sup>1</sup>H NMR (CDCl<sub>3</sub>) 2.4 [3H, s, CH<sub>3</sub>].

$\delta$  <sup>19</sup>F {<sup>1</sup>H} NMR (CDCl<sub>3</sub>) -81.41 [3F, t, <sup>4</sup>J<sub>FF</sub> 9.3 Hz, CF<sub>3</sub>], -120.86 [2F, t, <sup>4</sup>J<sub>FF</sub> 12.1 Hz,  $\alpha$ -CF<sub>2</sub>], -121.94 [2F, um, CF<sub>2</sub>], -122.56 [2F, um, CF<sub>2</sub>], -122.80 [2F, um, CF<sub>2</sub>], -122.84 [2F, um, CF<sub>2</sub>], -126.69 [2F, um, CF<sub>2</sub>].

*m/z* (ES) 413 ([MH]<sup>+</sup>), 393 ([M-F]<sup>+</sup>), 333 ([M-2F]<sup>+</sup> 100%), 150 ([C<sub>3</sub>F<sub>6</sub>]<sup>+</sup>), 69 ([CF<sub>3</sub>]<sup>+</sup>).

Infrared analysis: 1765 cm<sup>-1</sup>  $\nu$ (C=O).

**6.5.3. 1,1,1,5,5,6,6,7,7,8,8,9,9,10,10,10-Hexadecafluoro-decane-2,4-dione (V).**

Sodium ethoxide (1.03 g, 0.0152 moles) was placed into a 250 ml round bottomed flask containing diethyl ether (20 cm<sup>3</sup>) and stirred vigorously until dissolution had occurred, at which point the flask was cooled to 0 °C using an ice / salt bath. A solution of trifluoromethyl ethyl ester (1.64 cm<sup>3</sup>, 0.0138 moles), also in diethyl ether (5 cm<sup>3</sup>), was then added drop wise to the stirred solution. Following this a solution of tridecafluorohexyl methyl ketone (5 g, 0.0138 moles) in diethyl ether (5 cm<sup>3</sup>) was added dropwise over one hour. The reaction was maintained at 0 °C for 12 hours, after which time the reaction was stirred for 48 hours at room temperature. The

mixture was then hydrolysed by the addition of glacial ethanoic acid (1 g, 0.0166 moles) in deionised water (5 cm<sup>3</sup>), before the addition of copper (II) acetate (3.94 g, 0.0197 moles) also in deionised water (22 cm<sup>3</sup>), which generated an iridescent green colour. The ethereal layer was removed *in vacuo*, leaving the insoluble green copper complex in the aqueous layer. Suction filtration was used to remove the crystalline solid, which was washed with ice-cold water and light petroleum (40 – 60 °C), and dried under vacuum. The copper *bis*-1,1,1,5,5,6,6,7,7,8,8,9,9,10,10,10-hexadecafluoro-decane-2,4-dionate complex was then dissolved in diethyl ether (100 cm<sup>3</sup>) and hydrogen sulfide gas was then passed over the stirred solution for 25 minutes during which time the solution turned from green to dark black (CuS). The vessel was then flushed with nitrogen for one hour to remove the excess hydrogen sulfide. Evaporation of the diethyl ether followed by vacuum distillation (48 – 50 °C, 11.25 mmHg), afforded a pale yellow viscous oil (2.0 g, 32 %).

$\delta$  <sup>1</sup>H NMR (CDCl<sub>3</sub>) 6.25 [1H, s, C=C-H], 9.95 [1H, s, C-O-H] ∴ enol tautomer.

$\delta$  <sup>19</sup>F{<sup>1</sup>H} NMR (CDCl<sub>3</sub>) -76.93 [3F, s, α-CF<sub>3</sub>], -81.29 [3F, um, terminal CF<sub>3</sub>], -119.64 [2F, t, <sup>4</sup>J<sub>FF</sub> 11.3 Hz, α-CF<sub>2</sub>], -121.26 [2F, um, CF<sub>2</sub>], -122.73 [2F, um, CF<sub>2</sub>], -123.36 [2F, um, CF<sub>2</sub>], -126.76 [2F, um, CF<sub>2</sub>].

$\delta$  <sup>13</sup>C NMR (CDCl<sub>3</sub>) 95.51 [s, C=C], 105 – 121 [um's, C<sub>6</sub>F<sub>13</sub>], 117.45 [q, <sup>1</sup>J<sub>CF</sub> 281.3 Hz, CF<sub>3</sub>], 175.83 [q, <sup>2</sup>J<sub>CF</sub> 38.6 Hz, C=O (α-CF<sub>3</sub>)], 179.53 [t, <sup>2</sup>J<sub>CF</sub> 27.9 Hz, C=O (α-ponytail)].

*m/z* (ES) 458 ([M]<sup>+</sup>), 457 ([M-H]<sup>+</sup> 100 %), 439 ([M-F]<sup>+</sup>).

Infrared analysis: 1682 and 1622 cm<sup>-1</sup> ν(C=O) and ν(C-O-H) respectively.

Elemental analysis. Found: C, 25.9; H, 0.5; N, <0.3; F, 66.4. C<sub>10</sub>H<sub>2</sub>O<sub>2</sub>F<sub>16</sub> requires: C, 26.2; H, 0.4; N, 0.0; F, 66.4.

#### 6.5.4. 1,1,1,2,2,3,3,4,4,5,5,6,6,10,10,11,11,12,12,13,13,14,14,15,15,15-Hexacosafuoro-pentadecane-7,9-dione (IV).

Sodium ethoxide (1.24 g, 0.0182 moles) was placed into a round bottomed flask containing diethyl ether (20 cm<sup>3</sup>) and stirred vigorously under nitrogen, until dissolution had occurred, at which point the flask was cooled to 0 °C. A solution of ethyl perfluoroheptanoate (6.50 g, 0.017 moles), also in diethyl ether (5 cm<sup>3</sup>), was

then added dropwise to the stirred solution. Following this a solution of 3,3,4,4,5,5,6,6,7,7,8,8,8-tridecafluoro-octan-2-one (6.00 g, 0.017 moles) in diethyl ether (5 cm<sup>3</sup>) was added dropwise over one hour. The reaction was maintained at 0 °C for 12 hours, after which time the reaction was stirred for 48 hours at room temperature. The mixture was then hydrolysed by the addition of glacial ethanoic acid (1.2 g, 0.0199 moles) in deionised water (7 cm<sup>3</sup>), before the addition of copper (II) acetate (2.32 g, 0.0199 moles), also in deionised water (30 cm<sup>3</sup>). The ethereal layer was removed *in vacuo* using a nitrogen cooled pre-trap, leaving the insoluble green copper complex in the aqueous layer. Suction filtration was used to remove the crystalline solid, which was washed with ice-cold water and light petroleum (40 – 60 °C) until a fine green powder was obtained that was then dried under vacuum (9.10 g, 74 %). The copper *bis*-1,1,1,2,2,3,3,4,4,5,5,6,6,10,10,11,11,12,12,13,13,-14,14,15,15,15-hexacosafuoro-pentadecane-7,9-dionate complex was then dissolved in diethyl ether (100 cm<sup>3</sup>) in a three-necked round bottomed flask. Hydrogen sulfide gas was then passed over the stirred solution for 25 minutes during which time the solution turned from green to dark black (CuS). The vessel was then flushed with nitrogen for one hour to remove the excess hydrogen sulfide. Evaporation of the diethyl ether followed by vacuum distillation (52 – 55 °C, 15 mmHg), afforded a pale yellow viscous oil (3.36 g, 34 %).

$\delta$  <sup>1</sup>H NMR (CDCl<sub>3</sub>) 6.45 [1H, s, C=C-H], 9.2 [1H, s, C-OH] ∴ enol tautomer.

$\delta$  <sup>19</sup>F{<sup>1</sup>H} NMR (CDCl<sub>3</sub>) -81.28 [3F, t, <sup>4</sup>J<sub>FF</sub> 9.6 Hz, CF<sub>3</sub>], -120.30 [2F, t, <sup>4</sup>J<sub>FF</sub> 13.4 Hz, α-CF<sub>2</sub>], -122.07 [2F, um, CF<sub>2</sub>], -122.75 [2F, um, CF<sub>2</sub>], -123.21 [2F, um, CF<sub>2</sub>], -126.55 [2F, um, CF<sub>2</sub>].

$\delta$  <sup>13</sup>C NMR (d<sup>6</sup>-acetone) 98.31 [s, C=C], 105 – 121 [um's, C<sub>6</sub>F<sub>13</sub>], 176.07 [t, <sup>2</sup>J<sub>CF</sub> 27.2 Hz, C=O].

*m/z* (EI) 708 ([M]<sup>+</sup>), 689 ([M-F]<sup>+</sup>), 389 ([CO(CH<sub>2</sub>)COC<sub>6</sub>F<sub>12</sub>]<sup>+</sup> 100 %), 319 ([C<sub>6</sub>F<sub>13</sub>]<sup>+</sup>), 169 ([C<sub>3</sub>F<sub>7</sub>]<sup>+</sup>), 69 ([CF<sub>3</sub>]<sup>+</sup>).

Infrared analysis: 1663 and 1616 cm<sup>-1</sup> ν(C=O) and ν(C-OH) respectively.

Elemental analysis. Found: C, 25.1; H, 0.4; N, <0.3. C<sub>15</sub>H<sub>2</sub>O<sub>2</sub>F<sub>26</sub> requires: C, 25.4; H, 0.3; N, 0.0.

**6.5.5.** *1,1,1,2,2,3,3,4,4,5,5,6,6,7,7,11,11,12,12,13,13,14,14,15,15,16,16,17,17,17-Triacontafluoro-heptadecane-8,10-dione (I).*<sup>7</sup>

Sodium ethoxide (1.54 g, 0.022 moles) was placed into a round bottomed flask containing diethyl ether (17 cm<sup>3</sup>) and stirred vigorously under nitrogen, until dissolution had occurred. A solution of ethyl perfluorooctanoate (9.12 g, 0.021 moles), also in diethyl ether (5 cm<sup>3</sup>), was then added dropwise to the stirred solution. Following this a solution of pentadecafluorohexyl methyl ketone (8.50 g, 0.021 moles) in diethyl ether (5 cm<sup>3</sup>) was added dropwise over one hour. The reaction was then stirred for 50 hours at room temperature. The mixture was then hydrolysed by the addition of glacial ethanoic acid (1.8 g) in deionised water (10.5 cm<sup>3</sup>), before the addition of copper (II) acetate (3.47 g, 0.017 moles) also in deionised water (45 cm<sup>3</sup>). The ethereal layer was removed *in vacuo* using a nitrogen cooled pre-trap, leaving the insoluble green copper complex in the aqueous layer. Suction filtration was used to remove the crystalline solid, which was washed with ice-cold water and light petroleum (40 – 60 °C), until a fine powder was obtained, that was then dried under vacuum. The copper *bis*-1,1,1,2,2,3,3,-4,4,5,5,6,6,7,7,11,11,12,12,13,13,14,14,15,15,16,16,17,17,17-triacontafluoro-heptadecane-8,10-dionate complex was then dissolved in diethyl ether (100 cm<sup>3</sup>) in a three-necked round bottomed flask. Hydrogen sulfide gas was then passed over the stirred solution for 25 minutes during which time the solution turned from green to dark black (CuS). The vessel was then flushed with nitrogen for one hour to remove the excess hydrogen sulfide. Evaporation of the diethyl ether followed by vacuum distillation (20 mm Hg, 128 – 130 °C), afforded a cream coloured crystalline solid. The compound was then recrystallised from chloroform to yield a white solid (4.99 g, 30 %).

$\delta$  <sup>1</sup>H NMR (CDCl<sub>3</sub>) 6.45 [1H, s, C=C-H], ~ 6 - 9 (position variable) [1H, s, C-OH]  
∴ enol tautomer

$\delta$  <sup>19</sup>F{<sup>1</sup>H} NMR (CDCl<sub>3</sub>) -80.81 [3F, t, <sup>4</sup>J<sub>FF</sub> 9.8 Hz, CF<sub>3</sub>], -120.10 [2F, t, <sup>4</sup>J<sub>FF</sub> 12.2 Hz, α-CF<sub>2</sub>], -121.08 [2F, um, CF<sub>2</sub>], -121.64 [2F, um, CF<sub>2</sub>], -122.00 [2F, um, CF<sub>2</sub>], -122.37 [2F, um, CF<sub>2</sub>], -125.84 [2F, um, CF<sub>2</sub>].

$\delta$   $^{13}\text{C}$  NMR ( $\text{CDCl}_3$ ) 96.99 [s, C=C], 105 – 121 [ $\mu\text{m}'\text{s}$ ,  $\text{C}_7\text{F}_{15}$ ], 177.96 [t,  $^2J_{\text{CF}}$  28.3 Hz, C=O].

$m/z$  (ES) 808 ( $[\text{M}]^+$  100 %), 413 ( $[\text{C}_7\text{F}_{15}\text{CO}_2]^+$ ), 369 ( $[\text{C}_7\text{F}_{15}]^+$ ), 169 ( $[\text{C}_3\text{F}_7]^+$ ).

Infrared analysis: 1705, 1696, 1653 and 1617  $\text{cm}^{-1}$ .

**6.5.6. Copper bis(1,1,1,5,5,6,6,7,7,8,8,9,9,10,10,10-hexadecafluoro-decane-2,4-dionate) (VIa).**

1,1,1,5,5,6,6,7,7,8,8,9,9,10,10,10-hexadecafluoro-decane-2,4-dione (0.468 g,  $1.02 \times 10^{-3}$  moles) was dissolved in methanol ( $10 \text{ cm}^3$ ), to which sodium acetate (0.084 g,  $1.022 \times 10^{-3}$  moles) was added with stirring until dissolution had occurred. Copper (II) acetate (0.102 g,  $5.11 \times 10^{-4}$  moles) was dissolved in methanol ( $10 \text{ cm}^3$ ) and added dropwise to the stirred solution. The reaction mixture was stirred for 1 hour. The solvent was removed to yield the product as a pale green powdery solid, which was washed with hexane and dried *in vacuo* over silica gel (0.41 g, 82 %).

Infrared analysis: 1636  $\text{cm}^{-1}$ , 1527  $\text{cm}^{-1}$ .

Elemental analysis. Found: C, 23.9; H, 0.1.  $\text{CuC}_{20}\text{H}_2\text{O}_4\text{F}_{32}$  requires: C, 24.5; H, 0.2.

Crystals suitable for X-ray diffraction were grown by slow evaporation from an ether solution of the complex over a layer of chloroform. The crystals formed were actually the dihydrate resulting from exposure to the atmosphere.

**6.5.7. Copper bis(1,1,1,2,2,3,3,4,4,5,5,6,6,10,10,11,11,12,12,13,13,14,14,15,15,15-hexacosafuoro-pentadecane-7,9-dionate) (VIb).**

1,1,1,2,2,3,3,4,4,5,5,6,6,10,10,11,11,12,12,13,13,14,14,15,15,15-hexacosafuoro-pentadecane-7,9-dione (0.479 g,  $6.77 \times 10^{-4}$  moles) was dissolved in methanol ( $10 \text{ cm}^3$ ), to which sodium acetate (0.055 g,  $6.77 \times 10^{-4}$  moles) was added with stirring until dissolution had occurred. Copper (II) acetate (0.068 g,  $3.38 \times 10^{-4}$  moles) was dissolved in methanol ( $10 \text{ cm}^3$ ) and added dropwise to the stirred solution. The reaction mixture was stirred for 1 hour. A fine green powder formed, which was removed *via* suction filtration and dried *in vacuo* over silica gel (0.44 g, 88 %).

Infrared analysis: 1635  $\text{cm}^{-1}$ , 1527  $\text{cm}^{-1}$ .

Elemental analysis. Found: C, 22.9; H, 0.1.  $\text{CuC}_{30}\text{H}_2\text{O}_4\text{F}_{52}$  requires: C, 24.4; H, 0.1.

Crystals suitable for X-ray diffraction were grown by slow evaporation from an ether solution of the complex over a layer of chloroform. The crystals formed were actually the dihydrate resulting from exposure to the atmosphere.

**6.5.8.** *Copper bis(1,1,1,2,2,3,3,4,4,5,5,6,6,7,7,11,11,12,12,13,13,14,14,15,15,-16,16,17,17,17-triacontafluoro-heptadecane-8,10-dionate) (VIc).*

1,1,1,2,2,3,3,4,4,5,5,6,6,7,7,11,11,12,12,13,13,14,14,15,15,16,16,17,17,17-triacontafluoro-heptadecane-8,10-dione (0.482 g,  $5.96 \times 10^{-4}$  moles) was dissolved in methanol ( $10 \text{ cm}^3$ ), to which sodium acetate (0.055 g,  $5.96 \times 10^{-4}$  moles) was added with stirring until dissolution had occurred. Copper (II) acetate (0.060 g,  $2.98 \times 10^{-4}$  moles) was dissolved in methanol ( $10 \text{ cm}^3$ ) and added dropwise to the stirred solution. The reaction mixture was stirred for 1 hour. A fine green powder formed, which was removed *via* suction filtration and dried *in vacuo* over silica gel (0.39 g, 78 %).

Infrared analysis:  $1626 \text{ cm}^{-1}$ ,  $1528 \text{ cm}^{-1}$ .

Elemental analysis. Found: C, 22.4; H, 0.1.  $\text{CuC}_{34}\text{H}_2\text{O}_4\text{F}_{60}$  requires: C, 24.3; H, 0.1.

**6.5.9.** *Palladium bis(1,1,1,5,5,6,6,7,7,8,8,9,9,10,10,10-hexadecafluoro-decane-2,4-dionate) (VIIa).*

1,1,1,5,5,6,6,7,7,8,8,9,9,10,10,10-hexadecafluoro-decane-2,4-dione (0.359 g,  $7.85 \times 10^{-4}$  moles) was dissolved in 50:50 mixture of THF and dichloromethane ( $30 \text{ cm}^3$ ), to which palladium acetate (0.0881 g,  $3.92 \times 10^{-4}$  moles) was added. The reaction mixture was stirred for 1 hour, after which time the solvent was evaporated to yield a thick, black tar. The semi-solid was recrystallised from refluxing toluene and dried *in vacuo* over silica gel, to yield a powdery yellow solid (0.208 g, 52 %).

$\delta$   $^1\text{H}$  NMR ( $\text{CDCl}_3$ ) 6.4 [s, C-H].

$\delta$   $^{19}\text{F}\{^1\text{H}\}$  NMR ( $\text{CDCl}_3$ ) -73.42 [3F, s, *cis* / *trans*  $\text{CF}_3$ ], -73.56 [3F, s, *cis* / *trans*  $\text{CF}_3$ ], -81.18 [3F, t,  $^4J_{\text{FF}}$  11.3 Hz, *cis* / *trans* terminal  $\text{CF}_3$ ], -81.32 [3F, t,  $^4J_{\text{FF}}$  8.5 Hz,

*cis* / *trans* terminal CF<sub>3</sub>], -116.8 [2 x 2F, 2 x overlapping triplets, <sup>4</sup>J<sub>FF</sub> 12.8 Hz, α-CF<sub>2</sub>'s], -121.91 [4F, um, CF<sub>2</sub>'s], -122.29 [4F, um, CF<sub>2</sub>], -123.30 [4F, um, CF<sub>2</sub>], -126.60 [4F, um, CF<sub>2</sub>].

*m/z* (FAB) 1043 ([M+Na]<sup>+</sup>), 1020 ([M]<sup>+</sup>), 724 ([M+Na-C<sub>6</sub>F<sub>13</sub>]<sup>+</sup>).

Infrared analysis: 1598 cm<sup>-1</sup> ν(C=O).

Elemental analysis. Found: C, 22.9; H, 0.2. PdC<sub>20</sub>H<sub>2</sub>O<sub>4</sub>F<sub>32</sub> requires: C, 23.6; H, 0.2.

**6.5.10. Palladium bis(1,1,1,2,2,3,3,4,4,5,5,6,6,10,10,11,11,12,12,13,13,14,14,15,15,15-hexacosafuoro-pentadecane-7,9-dionate) (VIIb).**

1,1,1,2,2,3,3,4,4,5,5,6,6,10,10,11,11,12,12,13,13,14,14,15,15,15-hexacosafuoro-pentadecane-7,9-dione (0.373 g, 5.26 x 10<sup>-4</sup> moles) was dissolved in 50:50 mixture of THF and dichloromethane (30 cm<sup>3</sup>), to which palladium acetate (0.0591 g, 2.63 x 10<sup>-4</sup> moles) was added. The reaction mixture was stirred for 1 hour, during which time, the formation of a powdery, yellow / orange solid could be observed. The complex was isolated *via* suction filtration, washed with cold THF / dichloromethane and dried *in vacuo* (0.326 g, 81 %). (m.p. 114 – 116 °C).

δ <sup>1</sup>H NMR (CDCl<sub>3</sub>) 6.4 [s, C-H].

δ <sup>19</sup>F{<sup>1</sup>H} NMR (CDCl<sub>3</sub>) -81.31 [3F, t, <sup>4</sup>J<sub>FF</sub> 9.8 Hz, CF<sub>3</sub>], -116.76 [2F, t, <sup>4</sup>J<sub>FF</sub> 12.7 Hz, α-CF<sub>2</sub>], -121.81 [2F, um, CF<sub>2</sub>], -122.25 [2F, um, CF<sub>2</sub>], -123.28 [2F, um, CF<sub>2</sub>], -126.64 [2F, um, CF<sub>2</sub>].

*m/z* (FAB) 1517 ([M]<sup>+</sup>).

Infrared analysis: 1595 cm<sup>-1</sup> ν(C=O).

Elemental analysis. Found: C, 23.6; H, <0.3; N, <0.3. PdC<sub>30</sub>H<sub>2</sub>O<sub>4</sub>F<sub>52</sub> requires: C, 23.7; H, 0.1; N, 0.0.

**6.5.11. Palladium bis(1,1,1,2,2,3,3,4,4,5,5,6,6,7,7,11,11,12,12,13,13,14,14,15,15,16,16,17,17,17-triacontafuoro-heptadecane-8,10-dionate) (VIIc).<sup>8</sup>**

1,1,1,2,2,3,3,4,4,5,5,6,6,7,7,11,11,12,12,13,13,14,14,15,15,16,16,17,17,17-triacontafuoro-heptadecane-8,10-dione (0.470 g, 5.82 x 10<sup>-4</sup> moles) was dissolved

in 50:50 mixture of THF and dichloromethane (30 cm<sup>3</sup>), to which palladium acetate (0.065 g, 2.91 x 10<sup>-4</sup> moles) was added. The reaction mixture was stirred for 1 hour, during which time, the formation of a powdery, orange solid could be observed. The complex was isolated *via* suction filtration and washed with cold THF / dichloromethane (0.41 g, 82 %). (m.p. 114 – 117 °C).

$\delta$  <sup>19</sup>F{<sup>1</sup>H} NMR (C<sub>6</sub>D<sub>6</sub>) -81.24 [3F, t, <sup>4</sup>J<sub>FF</sub> 9.8 Hz, CF<sub>3</sub>], -117.17 [2F, um, α-CF<sub>2</sub>], -121.52 [2F, um, CF<sub>2</sub>], -121.97 [2F, um, CF<sub>2</sub>], -122.40 [2F, um, CF<sub>2</sub>], -123.13 [2F, um, CF<sub>2</sub>], -126.57 [2F, um, CF<sub>2</sub>].

*m/z* (FAB) 1721 ([M]<sup>+</sup>).

Infrared analysis: 1594 cm<sup>-1</sup> ν(C=O).

**6.5.12.** *Nickel bis(1,1,1,5,5,6,6,7,7,8,8,9,9,10,10,10-hexadecafluoro-decane-2,4-dionate) (VIIIa).*

1,1,1,5,5,6,6,7,7,8,8,9,9,10,10,10-hexadecafluoro-decane-2,4-dione (0.377 g, 8.22 x 10<sup>-4</sup> moles) was dissolved in methanol (25 cm<sup>3</sup>), to which sodium acetate (0.067 g, 8.22 x 10<sup>-4</sup> moles) was added with stirring until dissolution had occurred. Nickel dichloride hexahydrate (0.0977 g, 4.11 x 10<sup>-4</sup> moles) was dissolved in methanol (5 cm<sup>3</sup>) and added to the stirred solution. The reaction mixture was stirred for 1 hour and the solvent removed to give a pale green powdery solid that was washed with hexane and dried *in vacuo* over silica gel (0.34 g, 85 %). (m.p. 144 – 146 °C).

*m/z* (FAB) 974 ([MH]<sup>+</sup>).

Infrared analysis: 1639 cm<sup>-1</sup>, 1527 cm<sup>-1</sup>.

Elemental analysis. Found: C, 24.6; H, 0.2. NiC<sub>20</sub>H<sub>2</sub>O<sub>4</sub>F<sub>32</sub> requires: C, 24.7; H, 0.1.

**6.5.13.** *Nickel bis(1,1,1,2,2,3,3,4,4,5,5,6,6,10,10,11,11,12,12,13,13,14,14,15,15,15-hexacosafuoro-pentadecane-7,9-dionate) (VIIIb).*

Sodium acetate (0.0446 g, 5.43 x 10<sup>-4</sup> moles) was added to a stirred solution of 1,1,1,2,2,3,3,4,4,5,5,6,6,10,10,11,11,12,12,13,13,14,14,15,15,15-hexacosafuoro-pentadecane-7,9-dione (0.385 g, 5.42 x 10<sup>-4</sup> moles) which was dissolved in methanol (25 cm<sup>3</sup>). A solution of nickel dichloride hexahydrate (0.0645 g, 2.716 x

$10^{-4}$  moles) in methanol ( $5\text{ cm}^3$ ) was then added to the stirred solution. The reaction mixture was stirred for 1 hour and the solvent removed to give a pale green powdery solid that was washed with hexane and dried *in vacuo* over silica gel (0.37 g, 92 %). (m.p.  $146 - 147\text{ }^\circ\text{C}$ ).

$m/z$  (FAB) 1472 ( $[\text{M}]^+$ ), 1153 ( $[\text{M}-\text{C}_6\text{F}_{13}]^+$ ), 319 ( $[\text{C}_6\text{F}_{13}]^+$ ).

Infrared analysis:  $1638\text{ cm}^{-1}$ ,  $1528\text{ cm}^{-1}$ .

Elemental analysis. Found: C, 24.3; H, <0.3; N, <0.3.  $\text{NiC}_{30}\text{H}_2\text{O}_4\text{F}_{52}$  requires: C, 24.5; H, 0.1; N, 0.0.

**6.5.14.** Nickel bis(1,1,1,2,2,3,3,4,4,5,5,6,6,7,7,11,11,12,12,13,13,14,14,15,15,16,16,17,17,17-triacontafluoro-heptadecane-8,10-dionate) (**VIIIc**).<sup>9</sup>

Sodium acetate (0.049 g,  $5.98 \times 10^{-4}$  moles) was added to a stirred solution of 1,1,1,2,2,3,3,4,4,5,5,6,6,7,7,11,11,12,12,13,13,14,14,15,15,16,16,17,17,17-triacontafluoro-heptadecane-8,10-dione (0.483 g,  $5.98 \times 10^{-4}$  moles) which was dissolved in methanol ( $25\text{ cm}^3$ ). A solution of nickel dichloride hexahydrate (0.071 g,  $2.99 \times 10^{-4}$  moles) in methanol ( $5\text{ cm}^3$ ) was then added to the stirred solution. The reaction mixture was stirred for 1 hour, during which time, the formation of a powdery, apple green solid could be observed. The complex was isolated by suction filtration and washed with hexane, before drying *in vacuo* over silica gel (0.47 g, 94 %). (m.p.  $142 - 144\text{ }^\circ\text{C}$ ).

$m/z$  (FAB) 1672 ( $[\text{M}]^+$ ).

Infrared analysis:  $1638\text{ cm}^{-1}$ ,  $1533\text{ cm}^{-1}$ .

**6.5.15.** Zinc bis(1,1,1,5,5,6,6,7,7,8,8,9,9,10,10,10-hexadecafluoro-decane-2,4-dionate) (**IXa**).

Sodium hydroxide (0.033 g,  $8.17 \times 10^{-4}$  moles) was added to a stirred solution of 1,1,1,5,5,6,6,7,7,8,8,9,9,10,10,10-hexadecafluoro-decane-2,4-dione (0.374 g,  $8.17 \times 10^{-4}$  moles) dissolved in methanol ( $25\text{ cm}^3$ ). When dissolution was complete, zinc dichloride (0.0557 g,  $4.08 \times 10^{-4}$ ) was added and the reaction mixture stirred for two hours. After removing the solvent *in vacuo* the white powdery solid was dried under vacuum over silica gel (0.34 g, 85 %). (m.p.  $98 - 102\text{ }^\circ\text{C}$ ).

$\delta$   $^1\text{H}$  NMR ( $\text{CDCl}_3$ ) 6.15 [s, C-H].

$\delta$   $^{19}\text{F}\{^1\text{H}\}$  NMR ( $\text{C}_6\text{D}_6$ ) -76.24 [3F, s,  $\alpha\text{-CF}_3$ ], -81.77 [3F, t,  $^4J_{\text{FF}}$  10.0 Hz, terminal  $\text{CF}_3$ ], -120.01 [2F, t,  $^4J_{\text{FF}}$  13.5 Hz,  $\alpha\text{-CF}_2$ ], -122.07 [2F, um,  $\text{CF}_2$ ], -122.52 [2F, um,  $\text{CF}_2$ ], -123.28 [2F, um,  $\text{CF}_2$ ], -126.74 [2F, um,  $\text{CF}_2$ ].

$m/z$  (FAB) 979 ( $[\text{M}]^+$ ).

Infrared analysis:  $1645\text{ cm}^{-1}$ .

**6.5.16.** Zinc bis(1,1,1,2,2,3,3,4,4,5,5,6,6,10,10,11,11,12,12,13,13,14,14,15,15,15-hexacosafluoro-pentadecane-7,9-dionate) (**IXb**).

Sodium hydroxide (0.0325 g,  $5.41 \times 10^{-4}$  moles) was added to a stirred solution of 1,1,1,2,2,3,3,4,4,5,5,6,6,10,10,11,11,12,12,13,13,14,14,15,15,15-hexacosafluoro-pentadecane-7,9-dione (0.381 g,  $5.41 \times 10^{-4}$  moles) dissolved in methanol ( $25\text{ cm}^3$ ). When dissolution was complete, zinc dichloride (0.0368 g,  $2.70 \times 10^{-4}$ ) was added and the reaction mixture stirred for two hours. A white powdery solid was obtained *via* suction filtration, the complex was washed with methanol and dried *in vacuo* over silica gel (0.26 g, 74 %). (m.p.  $108 - 110\text{ }^\circ\text{C}$ ).

$\delta$   $^1\text{H}$  NMR ( $\text{CDCl}_3$ ) 5.3 [s, C-H]

$\delta$   $^{19}\text{F}\{^1\text{H}\}$  NMR ( $\text{C}_6\text{D}_6$ ) -81.80 [3F, t,  $^4J_{\text{FF}}$  10.1 Hz,  $\text{CF}_3$ ], -120.23 [2F, t,  $^4J_{\text{FF}}$  13.5 Hz,  $\alpha\text{-CF}_2$ ], -122.12 [2F, um,  $\text{CF}_2$ ], -122.63 [2F, um,  $\text{CF}_2$ ], -123.29 [2F, um,  $\text{CF}_2$ ], -126.73 [2F, um,  $\text{CF}_2$ ].

$m/z$  (FAB) 1002 ( $[\text{M}+\text{Na}]^+$ ), 979 ( $[\text{M}]^+$ ), 910 ( $[\text{M}-\text{CF}_3]^+$ ), 69 ( $[\text{CF}_3]^+$ ).

Infrared analysis:  $1646\text{ cm}^{-1}$   $\nu(\text{C}=\text{O})$ .

Elemental analysis. Found: C, 23.9; H, <0.3; N, <0.3.  $\text{ZnC}_{30}\text{H}_2\text{O}_4\text{F}_{52}$  requires: C, 24.4; H, 0.1; N, 0.0.

**6.5.17.** Zinc bis(1,1,1,2,2,3,3,4,4,5,5,6,6,7,7,11,11,12,12,13,13,14,14,15,15,16,16,-17,17,17-triacontafuoro-heptadecane-8,10-dionate) (**IXc**).

Sodium hydroxide (0.024 g,  $5.95 \times 10^{-4}$  moles) was added to a stirred solution of 1,1,1,2,2,3,3,4,4,5,5,6,6,7,7,11,11,12,12,13,13,14,14,15,15,16,16,17,17,17-triacontafuoro-heptadecane-8,10-dione (0.481 g,  $5.95 \times 10^{-4}$  moles) dissolved in

methanol (10 cm<sup>3</sup>). When dissolution was complete, zinc dichloride (0.041 g, 2.98 x 10<sup>-4</sup> moles) was added and the reaction mixture stirred for two hours. A white powdery solid was obtained *via* suction filtration, the complex was washed with methanol and dried *in vacuo* over silica gel (0.394 g, 79 %). (m.p. 116 – 118 °C).

$\delta$  <sup>19</sup>F{<sup>1</sup>H} NMR (C<sub>6</sub>D<sub>6</sub>) -82.91 [3F, t, <sup>4</sup>J<sub>FF</sub> 9.5 Hz, CF<sub>3</sub>], -121.38 [2F, um, CF<sub>2</sub>], -122.82 [2F, um, CF<sub>2</sub>], -123.50 [2F, um, CF<sub>2</sub>], -124.08 [2F, um, CF<sub>2</sub>], -124.72 [2F, um, CF<sub>2</sub>], -127.80 [2F, um, CF<sub>2</sub>].

*m/z* (FAB) 1680 ([M]<sup>+</sup>), 1660 ([M-HF]<sup>+</sup>).

Infrared analysis: 1642 cm<sup>-1</sup>  $\nu$ (C=O).

Elemental analysis. Found: C, 24.3; H, 0.1. ZnC<sub>34</sub>H<sub>2</sub>O<sub>4</sub>F<sub>60</sub> requires: C, 24.3; H, 0.1.

#### 6.5.18. Vanadyl bis(acetylacetonate) (**Xa**).<sup>10</sup>

To a stirred mixture of 2,4-pentanedione (0.402 g, 4.02 mmol) in methanol (10 cm<sup>3</sup>), vanadyl sulfate (0.33 g, 2.01 mmol) in water (8 cm<sup>3</sup>) was added. After stirring for ten minutes, sodium acetate (0.33 g, 4.02 mmol) was added and stirring continued for one hour. A blue solid was precipitated from the solution that was isolated by suction filtration and washed with methanol and water. After drying *in vacuo*, a blue / grey solid was obtained (0.41 g, 82 %).

Infrared analysis: 937 cm<sup>-1</sup>  $\nu$ (V=O).

#### 6.5.19. Vanadyl bis(hexafluoroacetylacetonate) (**Xb**).<sup>11</sup>

Vanadyl sulfate (4.6 g, 0.028 mol) was dissolved in water (2.5 cm<sup>3</sup>) and concentrated sulfuric acid (0.25 cm<sup>3</sup>) was added cautiously with stirring. Hexafluoroacetylacetonone (10 g, 0.05 moles) was then added forming a gold and blue biphasic. A saturated solution of sodium carbonate was then added until pH = 6 was achieved. The solution was then filtered yielding a pale green solid that was washed with two 1.5 cm<sup>3</sup> portions of benzene, prior to drying *in vacuo*. The yield obtained was very poor (< 15 mg).

$\delta$  <sup>1</sup>H NMR (CDCl<sub>3</sub>) 6.8 [1 H, s, C-H].

$\delta$   $^{19}\text{F}\{^1\text{H}\}$  NMR ( $\text{CDCl}_3$ ) -76.88 [s,  $\text{CF}_3$ ] - neither spectra exhibited the expected paramagnetism.

Infrared analysis: 985.9, 908.2  $\text{cm}^{-1}$   $\nu(\text{V}=\text{O})$ .

**6.5.20.** *Attempted synthesis of vanadyl bis(1,1,1,2,2,3,3,4,4,5,5,6,6,10,10,-11,11,12,12,13,13,14,14,15,15,15-hexacosafluoro-pentadecane-7,9-dionate) (Xc).*

To a stirred solution of 1,1,1,2,2,3,3,4,4,5,5,6,6,10,10,11,11,12,12,13,13,-14,14,15,15,15-hexacosafluoro-pentadecane-7,9-dione (0.478 g,  $6.75 \times 10^{-4}$  moles) in degassed methanol (10  $\text{cm}^3$ ), vanadyl sulfate (0.055 g,  $3.4 \times 10^{-4}$  moles) in degassed water (7.5  $\text{cm}^3$ ) was added. After stirring for 10 minutes, aqueous sodium acetate (0.055 g,  $6.75 \times 10^{-4}$  moles, degassed) was added over 10 minutes and stirring continued for one hour. A dark blue viscous oil was obtained which precipitated out of solution. The product was extracted with PP3 and the solvent removed *in vacuo* to yield a dark blue / black oil.

$\delta$   $^1\text{H}$  NMR ( $\text{CDCl}_3$ ) 6.45 [1H, s, C-H].

$\delta$   $^{19}\text{F}\{^1\text{H}\}$  NMR ( $\text{CDCl}_3$ ) -81.24 [3F, t,  $^4J_{\text{FF}}$  9.4 Hz, terminal  $\text{CF}_3$ ], -121.09 [2F, t,  $^4J_{\text{FF}}$  12.52 Hz,  $\alpha\text{-CF}_2$ ], -122.04 [2F, um,  $\text{CF}_2$ ], -122.43 [2F, um,  $\text{CF}_2$ ], -123.21 [2F, um,  $\text{CF}_2$ ], -126.59 [2F, um,  $\text{CF}_2$ ] - neither spectra exhibited the expected paramagnetism.

$m/z$  (FAB) 1481 ( $[\text{M}]^+$ ), 1162 ( $[\text{M}-\text{C}_6\text{F}_{13}]^+$ ).

**6.5.21.** *Dioxobis(acetylacetonate) molybdenum (VI) (XIa).*<sup>12</sup>

Sodium molybdate dihydrate (4.85 g, 0.02 moles) was dissolved in deionised water (50  $\text{cm}^3$ ) and hydrochloric acid (6 M) was added until pH = 1 was achieved. At this point 2,4-pentanedione (6  $\text{cm}^3$ , 0.06 moles) was added dropwise with rapid stirring. The yellow solid formed was isolated by suction filtration and washed with a cold solution of 2,4-pentanedione and ethanol (50 : 50, 10  $\text{cm}^3$ ) prior to drying *in vacuo*.

$\delta$   $^1\text{H}$  NMR ( $\text{CDCl}_3$ ) 2.3 [6H, s,  $\text{CH}_3$ ], 6.00 [1H, s, C-H].

**6.5.22.** *Attempted synthesis of Dioxobis(hexafluoroacetylacetonate) molybdenum (VI) (XIb).*

Sodium molybdate (2.43 g, 0.01 moles) was dissolved in water (25 cm<sup>3</sup>) and hydrochloric acid (6 M) was added until the solution reached pH 1. Hexafluoroacetylacetonate (6.13 g, 0.03 moles) was then added to the solution with vigorous stirring to disrupt the biphasic mixture. A colourless, cloudy solution formed which yielded a white solid *via* suction filtration. Unfortunately, the compound isolated was the tetraol (CF<sub>3</sub>C(OH)<sub>2</sub>CH<sub>2</sub>C(OH)<sub>2</sub>CF<sub>3</sub>), formed *via* the hydrolysis of hexafluoroacetylacetonate.

$\delta$  <sup>1</sup>H NMR (d<sup>6</sup>-acetone) 2.1 [s, CH<sub>2</sub>], 7.1 [br s, OH].

$\delta$  <sup>19</sup>F{<sup>1</sup>H} NMR (d<sup>6</sup>-acetone) -86.97 [s, CF<sub>3</sub>].

**6.5.23.** *Dioxobis(1,1,2,2,3,3,4,4,5,5,6,6,10,10,11,11,12,12,13,13,14,14,15,15,15-hexacosafuoro-pentadecane-7,9-dionate) molybdenum (VI) (XIc).*

To a stirred solution of 1,1,1,2,2,3,3,4,4,5,5,6,6,10,10,11,11,12,12,13,13,-14,14,15,15,15-hexacosafuoro-pentadecane-7,9-dione (0.459 g, 6.48 x 10<sup>-4</sup> moles) in THF (10 cm<sup>3</sup>), was added potassium hydroxide (0.036 g, 6.48 x 10<sup>-4</sup> moles). Once dissolution had occurred, the mixture was added to a solution of MoO<sub>2</sub>Cl<sub>2</sub>.dme (0.094 g, 3.25 x 10<sup>-4</sup> moles), also in THF (5 cm<sup>3</sup>). The dark yellow solution was stirred vigorously for 2 hours. After this period of time, the solvent was removed *in vacuo* during which time, as the final traces of THF were removed, the residue turned turquoise blue.

$\delta$  <sup>1</sup>H NMR (d<sup>6</sup>-acetone) 6.2 [s, C-H].

$\delta$  <sup>19</sup>F{<sup>1</sup>H} NMR (d<sup>4</sup> MeOH) -80.79 [3F, t, <sup>4</sup>J<sub>FF</sub> 10.1 Hz, CF<sub>3</sub>], -119.24 [2F, t, <sup>4</sup>J<sub>FF</sub> 12.8 Hz, α-CF<sub>2</sub>], -121.01 [2F, um, CF<sub>2</sub>], -121.55 [2F, um, CF<sub>2</sub>], -122.42 [2F, um, CF<sub>2</sub>], -125.83 [2F, um, CF<sub>2</sub>].

*m/z* (FAB) 1542 ([M]<sup>+</sup>), 1524 ([M-H<sub>2</sub>O]<sup>+</sup>), 1508 ([M-H<sub>2</sub>O<sub>2</sub>]<sup>+</sup>), 1470 ([MoC<sub>30</sub>O<sub>4</sub>F<sub>50</sub>]<sup>+</sup>).

Elemental analysis. Found: C, 23.4; H, 0.2. MoC<sub>30</sub>H<sub>2</sub>O<sub>6</sub>F<sub>52</sub> requires: C, 23.3; H, 0.1.

**6.5.24. Copper bis(triphenylphosphine)(1,1,1,2,2,3,3,4,4,5,5,6,6,10,10,11,11,12,12-13,13,14,14,15,15,15-hexacosafluoro-pentadecane-7,9-dionate) (XIIa).**

1,1,1,2,2,3,3,4,4,5,5,6,6,10,10,11,11,12,12,13,13,14,14,15,15,15-hexacosafluoro-pentadecane-7,9-dione (0.219 g,  $3.09 \times 10^{-4}$  moles) was dissolved in methanol (20 cm<sup>3</sup>), to which sodium hydroxide (0.0185 g,  $3.09 \times 10^{-4}$  moles) was added with stirring until dissolution had occurred. Cu<sup>I</sup>(PPh<sub>3</sub>)<sub>2</sub>NO<sub>3</sub> (0.201 g,  $3.09 \times 10^{-4}$  moles) was then added; immediately an orange / red solid began to precipitate out of solution. After stirring for 30 minutes, the solid was isolated by suction filtration, washed with methanol and dried *in vacuo* over silica gel (0.38 g, 95 %). (m.p. 122 – 124 °C).

$\delta$  <sup>1</sup>H NMR (CDCl<sub>3</sub>) 5.65 [1H, s, C-H], 7.10 – 7.40 [30H, s, PPh<sub>3</sub>].

$\delta$  <sup>19</sup>F{<sup>1</sup>H} NMR (CDCl<sub>3</sub>) -81.23 [3F, t, <sup>4</sup>J<sub>FF</sub> 9.7 Hz, CF<sub>3</sub>], -119.91 [2F, t, <sup>4</sup>J<sub>FF</sub> 13.0 Hz, α-CF<sub>2</sub>], -122.20 [2F, um, CF<sub>2</sub>], -122.80 [2F, um, CF<sub>2</sub>], -123.26 [2F, um, CF<sub>2</sub>], -126.57 [2F, um, CF<sub>2</sub>].

$\delta$  <sup>31</sup>P {<sup>1</sup>H} NMR (CDCl<sub>3</sub>) -3.20 [s, PPh<sub>3</sub>].

Infrared analysis: 1646 cm<sup>-1</sup> ν(C=O).

Elemental analysis. Found: C, 47.3; H, 2.4. CuC<sub>51</sub>H<sub>31</sub>O<sub>2</sub>F<sub>26</sub>P<sub>2</sub> requires: C, 47.3; H, 2.4.

**6.5.25. Copper bis(triphenylphosphine)(1,1,1,2,2,3,3,4,4,5,5,6,6,7,7,11,11,12,12,-13,13,14,14,15,15,16,16,17,17,17-triacontafuoro-heptadecane-8,10-dionate) (XIIb).**

1,1,1,2,2,3,3,4,4,5,5,6,6,7,7,11,11,12,12,13,13,14,14,15,15,16,16,17,17,17-triacontafuoro-heptadecane-8,10-dione (0.289 g,  $3.58 \times 10^{-4}$  moles) was dissolved in methanol (20 cm<sup>3</sup>), to which sodium hydroxide (0.021 g,  $3.58 \times 10^{-4}$  moles) was added with stirring until dissolution had occurred. Cu<sup>I</sup>(PPh<sub>3</sub>)<sub>2</sub>NO<sub>3</sub> (0.233 g,  $3.58 \times 10^{-4}$  moles) was then added; immediately an orange / red solid began to precipitate out of solution. After stirring for 30 minutes, the solid was isolated by suction filtration, washed with methanol and dried *in vacuo* over silica gel (0.46 g, 92 %). (m.p. 126 – 127 °C).

$\delta$   $^1\text{H}$  NMR ( $\text{CDCl}_3$ ) 5.91 [1H, s, C-H], 7.20 – 7.50 [30H, s,  $\text{PPh}_3$ ].

$\delta$   $^{19}\text{F}\{^1\text{H}\}$  NMR ( $\text{CDCl}_3$ ) -81.25 [3F, t,  $^4J_{\text{FF}}$  9.3 Hz,  $\text{CF}_3$ ], -119.93 [2F, t,  $^4J_{\text{FF}}$  11.8 Hz,  $\alpha\text{-CF}_2$ ], -122.00 [2F, um,  $\text{CF}_2$ ], -122.50 [2F, um,  $\text{CF}_2$ ], -122.27 [2F, um,  $\text{CF}_2$ ], -123.18 [2F, um,  $\text{CF}_2$ ], -126.57 [2F, um,  $\text{CF}_2$ ].

$\delta$   $^{31}\text{P}\{^1\text{H}\}$  NMR ( $\text{CDCl}_3$ ) -3.4 [s,  $\text{PPh}_3$ ].

Infrared analysis:  $1646.3\text{ cm}^{-1}$   $\nu(\text{C}=\text{O})$ .

$m/z$  (FAB) 1395 ( $[\text{M}]^+$ ).

Elemental analysis. Found: C, 45.5; H, 2.2.  $\text{CuC}_{53}\text{H}_{31}\text{O}_2\text{F}_{30}\text{P}_2$  requires: C, 45.6; H, 2.2.

Crystals of (**XIIIb**) suitable for X-ray diffraction were grown by slow evaporation from acetone.

**6.5.26.** *Attempted synthesis of rhodium dichloride pentamethylcyclopentadienyl-(1,1,1,2,2,3,3,4,4,5,5,6,6,10,10,11,11,12,12,13,13,14,14,15,15,15-hexacosafluoropentadecane-7,9-dionate) (XIIIa).*

Sodium hydroxide (0.0236 g,  $5.41 \times 10^{-4}$  moles) was added to a stirred solution of 1,1,1,2,2,3,3,4,4,5,5,6,6,10,10,11,11,12,12,13,13,14,14,15,15,15-hexacosafluoropentadecane-7,9-dionate (0.381 g,  $5.41 \times 10^{-4}$  moles) dissolved in methanol (25  $\text{cm}^3$ ). When complete dissolution had occurred, the solvent was removed *in vacuo*. The solid was then redissolved in dichloromethane (15  $\text{cm}^3$ ), and a solution of  $[\text{Rh}_2\text{Cl}_4\text{Cp}^*_2]$  (0.122 g,  $1.968 \times 10^{-4}$  moles) in dichloromethane (10  $\text{cm}^3$ ) was added. The reaction mixture was stirred for three hours, before the solvent was evaporated to yield an orange tar-like semi-solid, (0.38 g, 95 %).

$\delta$   $^1\text{H}$  NMR ( $\text{CDCl}_3$ ) 1.6 – 1.8 [4 x  $\text{Cp}^*$  signals], 5.7 – 5.9 [2 (maybe 3), C=C-H].

$\delta$   $^{19}\text{F}\{^1\text{H}\}$  NMR ( $\text{CDCl}_3$ ) -81.24 [3F, t,  $^4J_{\text{FF}}$  9.77 Hz,  $\text{CF}_3$ ], -81.40 [3F, t,  $^4J_{\text{FF}}$  10.03 Hz,  $\text{CF}_3$ ], -116.65 – -126.67 [multiple unresolved multiplets].

**6.5.27.** *General procedure for nickel catalysed sulfide (thioanisole) oxidations.*<sup>13</sup>

Thioanisole (0.53  $\text{cm}^3$ ,  $4.5 \times 10^{-3}$  moles), isobutyraldehyde (0.66  $\text{cm}^3$ , 0.07 moles) and  $[\text{Ni}(\beta\text{-diketonate})_2]$  (“x” moles) are dissolved in dry, degassed ethyl ethanoate

(3 cm<sup>3</sup>) and stirred vigorously under an atmosphere of oxygen for 16 hours at 60 °C. The solvent is then removed in *vacuo*, the residue dissolved in dichloromethane (~ 3 cm<sup>3</sup>) and the solution is then passed down a short (Pasteur pipette) column of FRP silica gel. The column is eluted with further dichloromethane to elute the sulfoxide, and the solution dried over anhydrous magnesium sulfate. Evaporation of the solvent affords a slightly viscous colourless oil.

$\delta$  <sup>1</sup>H NMR (CDCl<sub>3</sub>) Sulfide: 2.4 [3H, s, CH<sub>3</sub>], 7.1 [5H, um, Ph]. Sulfoxide: 2.65 [3H, s, CH<sub>3</sub>], 7.45 [5H, um, Ph]. Sulfone: 3.0 [3H, s, CH<sub>3</sub>], 7.6 [5H, um, Ph].

*m/z* (ES) 157 ([CH<sub>3</sub>SO<sub>2</sub>Ph]<sup>+</sup>), 141 ([CH<sub>3</sub>SOPh]<sup>+</sup>), 124 ([CH<sub>3</sub>SPh]<sup>+</sup>).

#### 6.5.28. General procedure for molybdenum catalysed alcohol oxidations.<sup>14</sup>

3-methyl-2-buten-1-ol (1 g, 0.012 moles), was added to a stirred solution of the appropriate dioxobis( $\beta$ -diketonate) molybdenum (5 mol %) in DMSO (33 cm<sup>3</sup>, 40 equiv) over activated 4Å molecular sieves. The reaction was stirred at 100 °C for seven hours. Following this period, the mixture was poured into a separating funnel containing water (25 cm<sup>3</sup>) and diethyl ether (25 cm<sup>3</sup>). The aqueous layer was extracted three times with diethyl ether (25 cm<sup>3</sup>) and the combined extracts were washed with a saturated sodium chloride solution before being dried over magnesium sulfate. The aldehyde / alcohol mixture was obtained as a light brown oil in quantitative yield.

$\delta$  <sup>1</sup>H NMR (CDCl<sub>3</sub>) Aldehyde: 1.9 [3H, s, CH<sub>3</sub>], 2.1 [3H, s, CH<sub>3</sub>], 5.85 [1H, d, <sup>3</sup>J<sub>HH</sub> 9.0 Hz, C=C-H], 9.9 [1H, d, <sup>3</sup>J<sub>HH</sub> 9.1 Hz, CHO]. Alcohol: 1.65 [3H, s, CH<sub>3</sub>], 1.75 [3H, s, CH<sub>3</sub>], 4.1 [2H, d, <sup>3</sup>J<sub>HH</sub> 6.8 Hz, CH<sub>2</sub>], 5.35 [1H, t, <sup>3</sup>J<sub>HH</sub> 7.0 Hz, C=C-H].

#### 6.5.29. Enaminodione procedures: 2,4-Pentanedione and Ethyl Cyanoformate.<sup>15</sup>

To a solution of 2,4-pentanedione (1 g, 0.01 moles), in dichloromethane (2 cm<sup>3</sup>), ethyl cyanoformate (1.48 g, 0.015 moles) and the appropriate Zn/Ni  $\beta$ -diketonate catalyst (1 mol %) were added. The mixture was then stirred under nitrogen for 24 hours. Following this period, the suspension was then filtered through either celite or FRP silica gel and washed with further dichloromethane, to yield a clear filtrate,

which was evaporated to yield the  $\beta$ -enamino- $\beta$ -ethoxycarbonyl-diketone as a pale cream, crystalline solid.

$\delta$   $^1\text{H}$  NMR ( $\text{CDCl}_3$ , 263K) 1.3 [3H, t,  $^3J_{\text{HH}}$  7.0 Hz,  $\text{OCH}_2\text{CH}_3$ ], 2.2 [3H, s,  $\text{C}(\text{O})\text{CH}_3$ ], 2.4 [3H, s,  $\text{C}(\text{O})\text{CH}_3$ ], 4.35 [2H, quartet,  $^3J_{\text{HH}}$  7.0 Hz,  $\text{OCH}_2$ ], 6.1 [1H, br s, NH], 10.0 [1H, br s, NH].

$m/z$  (ES) 199 ( $[\text{M}]^+$ ).

#### 6.5.30. Enaminodione procedures: Methylacetoacetate and Ethyl Cyanoformate.<sup>15</sup>

To a solution of methylacetoacetate (1.08 g,  $9.29 \times 10^{-3}$  moles) in dichloromethane ( $2 \text{ cm}^3$ ), ethyl cyanoformate (1.38 g, 0.014 moles) and the appropriate Zn/Ni  $\beta$ -diketonate catalyst (1 mol %) were added. The mixture was then stirred under nitrogen for 24 hours. Following this period, the suspension was then filtered through either celite or FRP silica gel and washed with further dichloromethane, to yield a clear filtrate, which was evaporated to yield the  $\beta$ -enamino- $\beta$ -ethoxycarbonyl-ketoester as a white, crystalline solid.

$\delta$   $^1\text{H}$  NMR ( $\text{CDCl}_3$ ) 1.5 [3H, t,  $^3J_{\text{HH}}$  7.0 Hz,  $\text{OCH}_2\text{CH}_3$ ], 2.5 [3H, s,  $\text{C}(\text{O})\text{CH}_3$ ], 3.85 [3H, s,  $\text{OCH}_3$ ], 4.5 [2H, quartet,  $^3J_{\text{HH}}$  7.0 Hz,  $\text{OCH}_2$ ], 6.2 [1H, br s, NH], 10.5 [1H, br s, NH].

$m/z$  (ES) 215 ( $[\text{M}]^+$ ).

#### 6.5.31. Enaminodione procedures: Dimethylmalonate and Ethyl Cyanoformate.<sup>15</sup>

To a solution of dimethylmalonate (1.14 g,  $8.65 \times 10^{-3}$  moles) in dichloromethane ( $2 \text{ cm}^3$ ), ethyl cyanoformate (1.29 g, 0.013 moles) and the appropriate Zn/Ni  $\beta$ -diketonate catalyst (1 mol %) were added. The mixture was then stirred under nitrogen for 24 hours. Following this period, the suspension was then filtered through either celite or FRP silica gel and washed with further dichloromethane. Unfortunately, no product was observed with any of the catalysts or under any of the conditions examined (see Chapter 4, section 4.3.1).

**6.5.32. Enaminodione procedures: Benzoylacetone and Ethyl Cyanoformate.**<sup>15</sup>

To a solution of benzoylacetone (1.24 g,  $7.65 \times 10^{-3}$  moles) in dichloromethane (2 cm<sup>3</sup>), ethyl cyanoformate (1.14 g, 0.011 moles) and the appropriate Zn/Ni  $\beta$ -diketonate catalyst (1 mol %) were added. The mixture was then stirred under nitrogen for 24 hours. Following this period, the suspension was then filtered through either celite or FRP silica gel and washed with further dichloromethane to yield a clear filtrate, which was evaporated to yield the  $\beta$ -enamino- $\beta$ -ethoxycarbonyl-diketone as a pale cream, crystalline solid. The product could be purified by column chromatography (30 % ethyl ethanoate / 70 % 40-60 °C light petroleum).

$\delta$  <sup>1</sup>H NMR (CDCl<sub>3</sub>) 1.1 [3H, t, <sup>3</sup>J<sub>HH</sub> 7.1 Hz, OCH<sub>2</sub>CH<sub>3</sub>], 2.25 [3H, s, C(O)CH<sub>3</sub>], 4.2 [2H, quartet, <sup>3</sup>J<sub>HH</sub> 7.1 Hz, OCH<sub>2</sub>], 6.5 [1H, br s, NH], 7.6 – 8.2 [5H, um, phenyl], 10.0 [1H, br s, NH].

*m/z* (ES) 261 ([M]<sup>+</sup>).

**6.5.33. Enaminodione procedures: Dibenzoylmethane and Ethyl Cyanoformate.**<sup>15</sup>

To a solution of dibenzoylmethane (1.39 g,  $6.18 \times 10^{-3}$  moles) in dichloromethane (2 cm<sup>3</sup>), ethyl cyanoformate (0.92 g,  $9.28 \times 10^{-3}$  moles) and the appropriate Zn/Ni  $\beta$ -diketonate catalyst (1 mol %) were added. The mixture was then stirred under nitrogen for 24 hours. Following this period, the suspension was then filtered through either celite or FRP silica gel and washed with further dichloromethane, to yield a clear filtrate, which was evaporated to yield the  $\beta$ -enamino- $\beta$ -ethoxycarbonyl-diketone as a pale cream, crystalline solid.

$\delta$  <sup>1</sup>H NMR (CDCl<sub>3</sub>) 1.1 [3H, t, <sup>3</sup>J<sub>HH</sub> 6.0 Hz, CH<sub>3</sub>], 4.2 [2H, quartet, <sup>3</sup>J<sub>HH</sub> 6.0 Hz, CH<sub>2</sub>], 7.2 – 8.1 [10H, um, phenyl], 8.3 [2H, br s, NH<sub>2</sub>].

*m/z* (ES) 325 ([MH]<sup>+</sup>), 324 ([M]<sup>+</sup>) 100 %.

**6.5.34. Enaminodione procedures: Tetramethyl-3,5-heptanedione and Ethyl Cyanoformate.**<sup>15</sup>

To a solution of tetramethyl-3,5-heptanedione (1.3 g,  $7.06 \times 10^{-3}$  moles), in dichloromethane (2 cm<sup>3</sup>), ethyl cyanoformate (1.05 g, 0.011 moles) and [Ni(C<sub>6</sub>F<sub>13</sub>/C<sub>6</sub>F<sub>13</sub>)<sub>2</sub>] (0.104 g,  $7.05 \times 10^{-5}$  moles) were added. The mixture was then stirred under nitrogen for 24 (and later 120) hours. Following this period, the suspension was then filtered through FRP silica gel and washed with further dichloromethane, to yield a clear yellow filtrate. Unfortunately, no product was generated, apart from a small amount of an intractable (possibly polymeric) material that could not be characterised.

**6.5.35. Enaminodione procedures: 2,4-Pentanedione and Benzoyl cyanide.**<sup>15</sup>

To a solution of 2,4-pentanedione (0.84 g,  $8.39 \times 10^{-3}$  moles) in dichloromethane (2 cm<sup>3</sup>), benzoyl cyanide (1.11 g,  $8.43 \times 10^{-3}$  moles) and the appropriate Zn/Ni  $\beta$ -diketonate catalyst (1 mol %) were added. The mixture was then stirred under nitrogen for 24 hours. Following this period, the suspension was then filtered through either celite or FRP silica gel and washed with further dichloromethane to yield a clear filtrate. Upon evaporation of the solvent, a small amount of 1-amino-1-benzoyl-2,2-diacylethene was obtained (see Chapter 4, section 4.3.2.).

$\delta$  <sup>1</sup>H NMR (CDCl<sub>3</sub>) 2.35 [3H, s, CH<sub>3</sub>], 2.7 [3H, s, CH<sub>3</sub>], 6.5 [1H, br s, NH], 7.2 – 7.9 [5H, um, phenyl], 11.3 [1H, br s, NH].

*m/z* (ES) 231 ([M]<sup>+</sup>), 230 ([M - H]<sup>+</sup>), 214 ([M - NH<sub>2</sub>]<sup>+</sup>).

**6.5.36. Enaminodione procedures: 2,4-Pentanedione and Malonitrile.**<sup>16</sup>

To a solution of 2,4-pentanedione (0.794 g,  $7.94 \times 10^{-3}$  moles) in chloroform (8 cm<sup>3</sup>), malonitrile (1.48 g, 0.015 moles) and the appropriate Zn/Ni  $\beta$ -diketonate catalyst (1 mol %) were added. The mixture was then stirred at reflux, under nitrogen for 8 hours. Following this period, the suspension was then filtered through either celite or FRP silica gel and washed with dichloromethane to yield an

orange filtrate, which was evaporated to yield the  $\beta$ -cyanomethylene- $\beta$ -enaminodione as an orange, crystalline solid.

$\delta$   $^1\text{H}$  NMR ( $\text{CDCl}_3$ ) two isomeric ketoenol tautomers, 'isomer 1': 2.05 [6H, s, 2 x  $\text{CH}_3$ ], 3.8 [1H, s, CH], 5.2 [2H, br s, NH], 16.5 [1H, br s, OH], 'isomer 2': 2.1 [6H, s, 2 x  $\text{CH}_3$ ], 3.65 [1H, s, CH], 4.8 [2H, br s, NH], 16.5 [1H, br s, OH].

$m/z$  (ES) 165 ( $[\text{M}-\text{H}]^+$ ) 149 ( $[\text{M}-\text{NH}_3]^+$ ).

#### 6.5.37. Enaminodione procedures: 2,4-Pentanedione and Trichloroacetonitrile.<sup>17</sup>

To a solution of 2,4-pentanedione (1.00 g, 0.01 moles) in dichloromethane (2  $\text{cm}^3$ ), trichloroacetonitrile (2.16 g, 0.015 moles) and the appropriate Zn/Ni  $\beta$ -diketonate catalyst (1 mol %) were added. The mixture was then stirred under nitrogen for 4 hours. Following this period, the suspension was then filtered through either celite or FRP silica gel and washed with further dichloromethane to yield a clear filtrate that was evaporated to yield a yellow residue, which was dissolved in Ligroin. After 5 hours at 0  $^\circ\text{C}$ , the  $\beta$ -trichloromethylenaminodione was collected by suction filtration, as a pale cream, crystalline solid (m.p. 56 – 57  $^\circ\text{C}$ ).

$\delta$   $^1\text{H}$  NMR ( $\text{CDCl}_3$ ) two isomeric keto-enol tautomers, keto isomer: 2.2 [3H, s,  $\text{CH}_3$ ], 2.75 [3H, s,  $\text{CH}_3$ ], 8.7 [2H, br s,  $\text{NH}_2$ ]; enol isomer: 2.1 [3H, s,  $\text{CH}_3$ ], 2.75 [3H, s,  $\text{CH}_3$ ], 10.5 [1H, br s, NH], 16.6 [1H, br s, OH].

$m/z$  (ES) 248 / 246 / 244 ( $[\text{M}]^+$ ), 210 ( $[\text{M}-\text{Cl}]^+$ ), 174 ( $[\text{M}-2\text{Cl}]^+$ ).

#### 6.5.38. 2H,2H,3H,3H-perfluorononanoic acid, $\text{C}_6\text{F}_{13}\text{CH}_2\text{CH}_2\text{CO}_2\text{H}$ .<sup>18,19</sup>

A solution of  $\text{CF}_3(\text{CF}_2)_5\text{CH}_2\text{CH}_2\text{I}$  (11.85 g, 0.025 moles) in diethyl ether (35  $\text{cm}^3$ ) was added dropwise to a stirred suspension of magnesium turnings (0.720 g, 0.03 moles) also in diethyl ether (7.5  $\text{cm}^3$ ) containing two drops of 1,2-dibromoethane. The reaction spontaneously refluxed during the addition, after which, the reaction was refluxed for two further hours. The reaction was allowed to cool before dry carbon dioxide was bubbled through the solution for two hours. The reaction was quenched with hydrochloric acid (6 M, 60  $\text{cm}^3$ ) and extracted three times with diethyl ether (3 x 50  $\text{cm}^3$ ). The combined organic extracts were then extracted with

a solution of sodium hydroxide (6 M, 3 x 100 cm<sup>3</sup>) to generate the sodium salt of the carboxylic acid. The solution was heated to 100 °C for 10 minutes to remove any volatile organic components, before being acidified with concentrated hydrochloric acid to liberate the free fluorinated carboxylic acid. The white crystalline solid was collected by suction filtration, washed with water and dried thoroughly prior to recrystallisation from toluene (5.23 g, 53 %).

$\delta$  <sup>1</sup>H NMR (CDCl<sub>3</sub>) 2.35 [2H, um, CH<sub>2</sub>-CO<sub>2</sub>H], 2.75 [2H, um, CF<sub>2</sub>-CH<sub>2</sub>].

$\delta$  <sup>19</sup>F{<sup>1</sup>H} NMR (CDCl<sub>3</sub>) -81.25 [3F, t, <sup>4</sup>J<sub>FF</sub> 9.7 Hz, CF<sub>3</sub>], -115.18 [2F, um, α-CF<sub>2</sub>], -122.33 [2F, um, CF<sub>2</sub>], -123.31 [2F, um, CF<sub>2</sub>], -123.95 [2F, um, CF<sub>2</sub>], -126.54 [2F, um, CF<sub>2</sub>].

m/z (ES) 392 ([M]<sup>+</sup>), 391 ([M-H]<sup>+</sup>).

Infrared analysis: 1723 cm<sup>-1</sup> ν(C=O).

**6.5.39.** *Preparation of tetrakis(μ-perfluoroheptanato-O:O') dirhodium [Rh<sub>2</sub>(O<sub>2</sub>CC<sub>6</sub>F<sub>13</sub>)<sub>4</sub>], (XIVa).*<sup>20</sup>

A solution of perfluoroheptanoic acid (0.66 g, 1.81 mmol) in toluene (7 cm<sup>3</sup>) was placed in a 100 cm<sup>3</sup> three-necked round bottomed flask equipped with a dropping funnel and a Dean-Stark trap and was heated to 105 °C. A solution of [Rh<sub>2</sub>(OAc)<sub>4</sub>] (0.21 g, 0.48 mmol) in ethanol (15 cm<sup>3</sup>) was then added dropwise over ten minutes to the stirred toluene solution. The ethanol and liberated acetic acid were distilled from the reaction leaving a green residue which was dissolved in hexane (10 cm<sup>3</sup>) and cooled to 0 °C. The precipitated green powder was collected by suction filtration, dissolved in the minimum amount of toluene and left overnight at -20 °C. The precipitate was recovered by suction filtration, washed with ice-cold hexane and dried in a vacuum oven at 90 °C to yield **XIVa** as a fine green powder (0.17 g, 22 %). (m.p. decomposition ~250 °C).

$\delta$  <sup>19</sup>F{<sup>1</sup>H} NMR (C<sub>6</sub>D<sub>6</sub>) -81.73 [3F, um, CF<sub>3</sub>], -117.45 [2F, um, α-CF<sub>2</sub>], -122.00 [2F, um, CF<sub>2</sub>], -123.36 [2F, um, CF<sub>2</sub>], -123.52 [2F, um, CF<sub>2</sub>], -126.74 [2F, um, CF<sub>2</sub>].

Infrared analysis: 1634 cm<sup>-1</sup> ν(C=O).

**6.5.40.** Preparation of tetrakis( $\mu$ -perfluorononanoato-*O:O'*) dirhodium  $[Rh_2(O_2CC_8F_{17})_4]$ , (**XIVb**).<sup>20</sup>

A solution of perfluorononanoic acid (0.84 g, 1.81 mmol) in toluene (7 cm<sup>3</sup>) was placed in a 100 cm<sup>3</sup> three-necked round bottomed flask equipped with a dropping funnel and a Dean-Stark trap and heated to 105 °C. A solution of Rh<sub>2</sub>(OAc)<sub>4</sub> (0.21 g, 0.48 mmol) in ethanol (15 cm<sup>3</sup>) was then added dropwise over ten minutes to the stirred toluene solution. The ethanol and liberated acetic acid were distilled from the reaction leaving a green residue which was dissolved in hexane (10 cm<sup>3</sup>) and cooled to 0 °C. The precipitated green powder was collected by suction filtration, dissolved in the minimum amount of toluene and left overnight at -20 °C. The precipitate was recovered by suction filtration, washed with ice-cold hexane and dried in a vacuum oven at 90 °C to yield **XIVb** as a fine green powder (0.12 g, 12 %). (m.p. decomposition ~ 250 °C).

$\delta$  <sup>19</sup>F{<sup>1</sup>H} NMR (C<sub>6</sub>D<sub>6</sub>) -81.71 [3F, um, CF<sub>3</sub>], -117.53 [2F, um,  $\alpha$ -CF<sub>2</sub>], -122.06 [4F, um, CF<sub>2</sub>], -123.39 [2F, um, CF<sub>2</sub>], -123.64 [4F, um, CF<sub>2</sub>], -125.85 [2F, um, CF<sub>2</sub>].

Infrared analysis: 1642 cm<sup>-1</sup>  $\nu$ (C=O).

**6.5.41.** Preparation of tetrakis[ $\mu$ -3-(perfluorohexyl)propionato-*O:O'*] dirhodium  $[Rh_2(O_2CCH_2CH_2C_6F_{13})_4]$ , (**XIVc**).<sup>21</sup>

A solution of 2*H*,2*H*,3*H*,3*H*-perfluorononanoic acid (0.32 g, 0.8 mmol) and sodium hydroxide (33 mg, 0.8 mmol) in ethanol (60 cm<sup>3</sup>) was added to a stirred solution of [RhCl<sub>3</sub>.3H<sub>2</sub>O] (54 mg, 0.2 mmol) in refluxing ethanol (20 cm<sup>3</sup>). After refluxing for 10 minutes a dark green / grey solution was formed, which was allowed to cool to room temperature. A dark green powder was isolated by suction filtration that was then dissolved in hot ethanol and filtered to remove a grey powder (rhodium). The solution was concentrated and cooled in an ice bath to yield a vivid green powder that was collected by suction filtration and washed with the minimum amount of ice-cold ethanol. The complex was then dried *in vacuo* over silica gel (80 mg, 44 %). (m.p. decomposition ~ 250 °C).

$\delta$   $^1\text{H}$  NMR ( $d^4$  MeOH) poor solubility, 2.4 [um,  $(\text{CH}_2)_2$ ].

$\delta$   $^{19}\text{F}\{^1\text{H}\}$  NMR ( $\text{C}_6\text{D}_6$ ) -81.77 [3F, t,  $^4J_{\text{FF}}$  9.6 Hz,  $\text{CF}_3$ ], -115.53 [2F, um,  $\alpha\text{-CF}_2$ ], -122.36 [2F, um,  $\text{CF}_2$ ], -123.40 [2F, um,  $\text{CF}_2$ ], -124.17 [2F, um,  $\text{CF}_2$ ], -126.76 [2F, um,  $\text{CF}_2$ ].

$m/z$  (FAB) 1770 ( $[\text{MH}]^+$ ).

Crystals of the acetonitrile adduct of **XIVc**, suitable for X-ray diffraction, were grown by dissolving the dimer in acetonitrile and allowing the solvent to slowly evaporate.

#### 6.5.42. Preparation of cobalt (II) bis(perfluoroheptanate) [ $\text{Co}(\text{O}_2\text{CC}_6\text{F}_{13})_2$ ] (**XVa**).

Perfluoroheptanoic acid (1.019 g,  $2.8 \times 10^{-3}$  moles) was dissolved in acetone ( $5 \text{ cm}^3$ ) to which potassium hydroxide (0.157 g,  $2.8 \times 10^{-3}$  moles) was added. Once dissolved, cobalt perchlorate [ $\text{Co}(\text{ClO}_4)_2 \cdot 6\text{H}_2\text{O}$ ] (0.501 g,  $1.37 \times 10^{-3}$  moles), also dissolved in acetone ( $5 \text{ cm}^3$ ), was added dropwise to the stirred solution. The solution immediately turned pink and cloudy due to the liberation of potassium perchlorate ( $\text{KClO}_4$ ). Removal of this solid yielded a pink solution which was evaporated to leave a bright pink residue. Trituration of this material in chloroform for one hour yielded a pink solid that was collected by suction filtration (0.98 g, 91 %). (m.p. 119 – 124 °C).

$\delta$   $^{19}\text{F}\{^1\text{H}\}$  NMR ( $d^6$ -acetone), paramagnetic, -80.38 [3F, um,  $\text{CF}_3$ ], -114.70 [2F, um,  $\text{CF}_2$ ], -118.66 [2F, um,  $\text{CF}_2$ ], -119.98 [2F, um,  $\text{CF}_2$ ], -121.45 [2F, um,  $\text{CF}_2$ ], -125.24 [2F, um,  $\text{CF}_2$ ].

$m/z$  (FAB) 1801, 1648, 1282, 935, 541.

Infrared analysis:  $1652 \text{ cm}^{-1}$   $\nu(\text{C}=\text{O})$ .

#### 6.5.43. Preparation of cobalt (II) bis(perfluorononanate) [ $\text{Co}(\text{O}_2\text{CC}_8\text{F}_{17})_2$ ] (**XVb**).

Perfluorononanoic acid (1.30 g,  $2.8 \times 10^{-3}$  moles) was dissolved in acetone ( $5 \text{ cm}^3$ ) to which potassium hydroxide (0.157 g,  $2.8 \times 10^{-3}$  moles) was added. Once dissolved, cobalt perchlorate [ $\text{Co}(\text{ClO}_4)_2 \cdot 6\text{H}_2\text{O}$ ] (0.501 g,  $1.37 \times 10^{-3}$  moles), also dissolved in acetone ( $5 \text{ cm}^3$ ), was added dropwise to the stirred solution. The

solution immediately turned pink and cloudy due to the liberation of potassium perchlorate ( $\text{KClO}_4$ ). Removal of this solid yielded a pink solution which was evaporated to leave a bright pink residue. Trituration of this material in chloroform for one hour yielded a pink solid that was collected by suction filtration (1.26 g, 93 %). (m.p. 147 – 150 °C).

$m/z$  (FAB) 2201, 2048, 1582, 1135, 641.

Infrared analysis:  $1650\text{ cm}^{-1}$   $\nu(\text{C}=\text{O})$ .

Crystals suitable for X-ray diffraction, of the pyridine adduct of **XVb** were grown by dissolving the complex in pyridine and allowing the solvent to slowly evaporate.

**6.5.44.** *Preparation of cobalt (II) bis(2H,2H,3H,3H-perfluorononanoate)*  
*[Co(O<sub>2</sub>CCH<sub>2</sub>CH<sub>2</sub>C<sub>6</sub>F<sub>13</sub>)<sub>2</sub>] (XVc).<sup>22</sup>*

A solution of 2H,2H,3H,3H-perfluorononanoic acid (0.55 g,  $1.4 \times 10^{-3}$  moles) and triethylamine (0.20 cm<sup>3</sup>,  $1.4 \times 10^{-3}$  moles) dissolved in acetone (15 cm<sup>3</sup>) was added dropwise to a stirred solution of cobalt perchlorate (0.25 g,  $7.0 \times 10^{-4}$  moles) in acetone (30 cm<sup>3</sup>). The pink solution formed was stirred for one hour, during which time the formation of a purple precipitate was observed. The solid was collected by suction filtration and washed three times with acetone (0.47 g, 81 %). (m.p. decomposition ~ 180 °C).

Infrared analysis:  $1725\text{ cm}^{-1}$   $\nu(\text{C}=\text{O})$ .

Elemental analysis. Found: C, 24.8; H, 0.8.  $\text{CoC}_{18}\text{H}_8\text{O}_4\text{F}_{26}$  requires: C, 24.7; H, 1.3.

**6.5.45.** *Preparation of manganese (II) bis(perfluoroheptanoate)*  
*[Mn(O<sub>2</sub>CC<sub>6</sub>F<sub>13</sub>)<sub>2</sub>] (XVIa).*

Perfluoroheptanoic acid (1.019 g,  $2.8 \times 10^{-3}$  moles) was dissolved in acetone (5 cm<sup>3</sup>) to which potassium hydroxide (0.157 g,  $2.8 \times 10^{-3}$  moles) was added. Once dissolved, manganese perchlorate [ $\text{Mn}(\text{ClO}_4)_2 \cdot 6\text{H}_2\text{O}$ ] (0.496 g,  $1.37 \times 10^{-3}$  moles), also dissolved in acetone (5 cm<sup>3</sup>), was added dropwise to the stirred solution. After stirring for two hours, the precipitated  $\text{KClO}_4$  was removed by suction filtration to leave a colourless solution. The solvent was removed to yield a cream coloured

residue which was triturated in chloroform for one hour to yield a white solid that was collected by suction filtration (0.91 g, 85 %). (m.p. 113 – 115 °C).

$m/z$  (FAB) 1789, 1636, 1292, 948, 604, 511, 260.

Infrared analysis:  $1676\text{ cm}^{-1}$   $\nu(\text{C}=\text{O})$ .

**6.5.46. Preparation of manganese (II) bis(perfluorononanoate)  $[\text{Mn}(\text{O}_2\text{CC}_8\text{F}_{17})_2]$  (XVIb).**

Perfluorononanoic acid (1.30 g,  $2.8 \times 10^{-3}$  moles) was dissolved in acetone ( $5\text{ cm}^3$ ) to which potassium hydroxide (0.157 g,  $2.8 \times 10^{-3}$  moles) was added. Once dissolved, manganese perchlorate  $[\text{Mn}(\text{ClO}_4)_2 \cdot 6\text{H}_2\text{O}]$  (0.496 g,  $1.37 \times 10^{-3}$  moles), also dissolved in acetone ( $5\text{ cm}^3$ ), was added dropwise to the stirred solution. After stirring for two hours, the precipitated  $\text{KClO}_4$  was removed by suction filtration to leave a colourless solution. The solvent was removed to yield a cream coloured residue which was triturated in chloroform for one hour to yield a white solid that was collected by suction filtration (1.17 g, 87 %). (m.p. 162 – 165 °C).

$m/z$  (FAB) 2189, 2036, 1592, 1148, 704, 260.

Infrared analysis:  $1670\text{ cm}^{-1}$   $\nu(\text{C}=\text{O})$ .

**6.5.47. Preparation of manganese (II) 2H,2H,3H,3H-perfluorononanoate  $[\text{Mn}(\text{O}_2\text{CCH}_2\text{CH}_2\text{C}_6\text{F}_{13})_2]$  (XIVc).<sup>22</sup>**

A solution of 2H,2H,3H,3H-perfluorononanoic acid (0.55 g,  $1.4 \times 10^{-3}$  moles) and triethylamine ( $0.20\text{ cm}^3$ ,  $1.4 \times 10^{-3}$  moles) dissolved in acetone ( $15\text{ cm}^3$ ) was added dropwise to a stirred solution of manganese perchlorate (0.25 g,  $7.0 \times 10^{-4}$  moles) in acetone ( $30\text{ cm}^3$ ). The beige solution formed was stirred overnight, resulting in a sticky off-white residue that precipitated out of solution. The solvent was removed *in vacuo* and the beige residue was triturated in chloroform for two hours. The solid was collected by suction filtration (0.28 g, 48 %). (m.p. decomposition  $\sim 170\text{ }^\circ\text{C}$ ).

Infrared analysis:  $1715\text{ cm}^{-1}$   $\nu(\text{C}=\text{O})$ .

**6.5.48.** *Attempted synthesis of manganese (III) tris(perfluorononanoate) [Mn(O<sub>2</sub>CC<sub>8</sub>F<sub>17</sub>)<sub>3</sub>] - ligand exchange method.*

Perfluorononanoic acid (5.71 g, 0.012 moles) was dissolved in acetic acid (20 cm<sup>3</sup>) to which was added manganese (III) acetate (1.0 g, 3.7 × 10<sup>-3</sup> moles). The mixture was refluxed for two hours, after which time the acetic acid was distilled off to leave a beige residue. The product was triturated in chloroform for one hour to yield an off-white solid that was collected by suction filtration.

*m/z* (FAB) 2189, 2036, 1570, 1148, 704, 260.

Infrared analysis: 1650, 1671, 1725 cm<sup>-1</sup> ν(C=O).

**6.5.49.** *Attempted synthesis of manganese (III) tris(perfluoroheptanoate) [Mn(O<sub>2</sub>CC<sub>6</sub>F<sub>13</sub>)<sub>3</sub>] - oxidation method.*

Perfluoroheptanoic acid (1.00 g) was added to a stirred solution of [Mn(O<sub>2</sub>CC<sub>6</sub>F<sub>13</sub>)<sub>2</sub>] (0.5 g, 6.4 × 10<sup>-4</sup> moles) in acetone (10 cm<sup>3</sup>). Potassium permanganate (0.025 g, 1.6 × 10<sup>-4</sup> moles) was then added, before the addition of five drops of water to dissolve the oxidising agent. The purple solution produced gradually turned black and the reaction was left to stir overnight. The acetone was removed *in vacuo* to leave a black residue that was triturated in chloroform for one hour although the solid remained tar-like. Trituration was attempted in hexane with similar results. The black tar was completely insoluble in all the solvent systems that were attempted negating characterisation.

**6.5.50.** *Preparation of zinc (II) bis(perfluoroheptanoate) [Zn(O<sub>2</sub>CC<sub>6</sub>F<sub>13</sub>)<sub>2</sub>] (XVIIa).*

Perfluoroheptanoic acid (1.019 g, 2.8 × 10<sup>-3</sup> moles) was dissolved in acetone (5 cm<sup>3</sup>) to which potassium hydroxide (0.157 g, 2.8 × 10<sup>-3</sup> moles) was added. Once dissolved, zinc chloride (0.187 g, 1.37 × 10<sup>-3</sup> moles), also dissolved in acetone (5 cm<sup>3</sup>), was added dropwise to the stirred solution. The solvent was removed *in vacuo* to yield a white semi solid. Trituration of this material in chloroform for one hour yielded a white solid that was collected by suction filtration (0.99 g, 92 %). (m.p. 203 – 208 °C).

$\delta$   $^{19}\text{F}\{^1\text{H}\}$  NMR ( $\text{CDCl}_3$ ) -80.90 [3F, t,  $^4J_{\text{FF}}$  9.6 Hz,  $\text{CF}_3$ ], -116.30 [2F, t,  $^4J_{\text{FF}}$  11.5 Hz,  $\alpha\text{-CF}_2$ ], -121.39 [2F, um,  $\text{CF}_2$ ], -122.13 [2F, um,  $\text{CF}_2$ ], -122.53 [2F, um,  $\text{CF}_2$ ], -125.90 [2F, um,  $\text{CF}_2$ ].

$m/z$  (ES) 827 ( $[\text{M}+2\text{H}_2\text{O}]^+$ ).

Infrared analysis:  $1707\text{cm}^{-1}$   $\nu(\text{C}=\text{O})$ .

Crystals of (XVIIa) suitable for X-ray diffraction were grown by slow evaporation from chloroform.

#### 6.5.51. Preparation of zinc (II) bis(perfluorononanoate) [ $\text{Zn}(\text{O}_2\text{CC}_8\text{F}_{17})_2$ ] (XVIIb).

Perfluorononanoic acid (1.30 g,  $2.8 \times 10^{-3}$  moles) was dissolved in acetone ( $5 \text{ cm}^3$ ) to which potassium hydroxide (0.157 g,  $2.8 \times 10^{-3}$  moles) was added. Once dissolved, zinc chloride (0.187 g,  $1.37 \times 10^{-3}$  moles), also dissolved in acetone ( $5 \text{ cm}^3$ ), was added dropwise to the stirred solution. The solvent was removed *in vacuo* to yield a white semi solid. Trituration of this material in chloroform for one hour yielded a white solid that was collected by suction filtration (1.19 g, 88 %). (m.p.  $196 - 199^\circ\text{C}$ ).

$\delta$   $^{19}\text{F}\{^1\text{H}\}$  NMR ( $\text{CDCl}_3$ ) -80.84 [3F, t,  $^4J_{\text{FF}}$  9.9 Hz,  $\text{CF}_3$ ], -116.30 [2F, um,  $\text{CF}_2$ ], -121.15 [2F, um,  $\text{CF}_2$ ], -121.58 [4F, um,  $\text{CF}_2$ ], -122.30 [4F, um,  $\text{CF}_2$ ], -125.88 [2F, um,  $\text{CF}_2$ ].

Infrared analysis:  $1691\text{cm}^{-1}$   $\nu(\text{C}=\text{O})$ .

#### 6.5.52. Synthesis of 1-diazo-3-phenyl-5-hexen-2-one.<sup>23</sup>

The synthesis of the diazo compound was carried out following the literature procedure and the characterisation data were in agreement with the recorded values.

$\delta$   $^1\text{H}$  NMR ( $\text{CDCl}_3$ ) 2.45 [1H, ddd], 2.9 [1H, ddd], 3.55-3.65 [1H, um], 4.95-5.10 [2H, um], 5.15 [1H, s], 5.60-5.80 [1H, um], 7.2-7.4 [5H um, Ph].

Electrospray mass spectrum  $m/z$  199 ( $[\text{M}-\text{H}]^+$ ) (100 %).

**6.5.53.** *Transition metal catalysed decomposition of 1-diazo-3-phenyl-5-hexen-2-one using  $[Rh_2(O_2CC_3F_7)_4]$ .*<sup>23</sup>

A solution containing 1-diazo-3-phenyl-5-hexen-2-one (0.17 g,  $8.5 \times 10^{-4}$  moles) in dichloromethane (50 cm<sup>3</sup>), was treated with rhodium (II) perfluorobutyrate (0.005 g,  $4.73 \times 10^{-6}$  moles). The mixture was allowed to stir at room temperature for 30 minutes and was then concentrated under reduced pressure. The mixture was then passed through a column of fluorosilica reverse phase silica gel. A light brown solution was obtained which produced a yellow / light brown oil. Further dichloromethane was used to elute the product, followed by diethyl ether in an attempt to remove the catalyst from the column (see Chapter 5, section 5.4). 1,3-dihydro-1-(2-propenyl)-2H-inden-2-one was obtained in virtually quantitative yield (94 %) as a light brown oil.

$\delta$  <sup>1</sup>H NMR (CDCl<sub>3</sub>) 2.4-2.6 [2H, um], 3.45-3.6 [3H, um], 4.95-5.1 [2H um], 5.65-5.8 [1H, um], 7.2-7.4 [4H, um, Ph].

Electrospray mass spectrum m/z 172 ([M]<sup>+</sup>), 171 ([M-H]<sup>+</sup>) (100 %).

**6.5.54.** *Transition metal catalysed decomposition of 1-diazo-3-phenyl-5-hexen-2-one using  $[Rh_2(O_2CCH_2CH_2C_6F_{13})_4]$ .*<sup>23</sup>

A solution containing 1-diazo-3-phenyl-5-hexen-2-one (0.17 g,  $8.5 \times 10^{-4}$  moles) in dichloromethane (50 cm<sup>3</sup>), was treated with  $[Rh_2(O_2CCH_2CH_2C_6F_{13})_4]$  (0.008 g,  $4.73 \times 10^{-6}$  moles). The mixture was allowed to stir at room temperature for 30 minutes and was then concentrated under reduced pressure. The mixture was then passed through a column of fluorosilica reverse phase silica gel. A light brown solution was obtained which produced a yellow / light brown oil. Further dichloromethane was used to elute the product, followed by acetone to remove the catalyst (pink solution) from the column (see Chapter 5, section 5.4.2.). Evaporation of the dichloromethane yielded a gold coloured liquid in virtually quantitative yield. However, a significant amount of starting material remained and 3-phenylbicyclo[3.1.0]hexan-2-one was formed alongside the desired product due to cyclopropanation also occurring.

$\delta$   $^1\text{H}$  NMR ( $\text{CDCl}_3$ ) aromatic insertion product (1,3-dihydro-1-(2-propenyl)-2*H*-inden-2-one) – see 6.5.52 above. Cyclopropanation product (3-phenylbicyclo[3.1.0]hexan-2-one), 1.0 [1H, um], 1.15-1.20 [1H, um], 2.1-2.2 [1H, um], 2.35-2.4 [1H, um], 2.7 [1H, um], 3.5 [1H, um], 7.25-7.3 [5H, um, Ph].

Electrospray mass spectrum  $m/z$  172 ( $[\text{M}]^+$ ), 171 ( $[\text{M}-\text{H}]^+$ ) (100 %).

## 6.6. References for Chapter 6

- [1] D.D. Perrin and W.L.F. Armarego. 'Purification of Laboratory Chemicals' (third edition). 1988. Pergamon Press, Oxford
- [2] F.A. Cotton and D.M.L. Goodgame, *J. Chem. Soc.*, 1960, 5267.
- [3] S. Kainz, Z. Luo, D.P. Curran and W. Leitner, *Synthesis*, 1998, 1425; D.P. Curran, *Green Chemistry*, 2001, **3**, G3.
- [4] H.T. Chiu, Y.P. Chen, S.H. Chuang, J.S. Jen, G.H. Lee and S.M. Peng, *J. Chem. Soc., Chem. Commun.*, 1996, 139.
- [5] Protocol, Fluorine Laboratory, University of Leicester, 1998.
- [6] A. Kondo and S. Iwatsuki, *J. Fluorine Chem.*, 1984, **26**, 59.
- [7] A.E. Pedler, R.C. Smith and J.C. Tatlow, *J. Fluorine Chem.*, 1971 / 72, **1**, 433.
- [8] B. Betzemeier, F. Lhermitte and P. Knochel, *Tetrahedron Lett.*, 1998, 6667.
- [9] I. Klement, H. Lutjens and P. Knochel, *Angew. Chem. Int. Ed. Engl.*, 1997, **36**, 1454.
- [10] E. Hata, T. Takai, T. Yamada and T. Mukaiyama, *Chem. Lett.*, 1994, 1849.
- [11] R.L. Carlin and F.A. Walker, *J. Am. Chem. Soc.*, 1965, **87**, 2128.
- [12] H. Gehrke (Jnr.) and J. Veal, *Inorg. Chim. Acta.*, 1969, **3:4**, 623.
- [13] S. Vincent, C. Lion, M. Hedayatullah, A. Challier, G. Delmas and G. Magnaud, *Phosphorous, Sulfur and Silicon*, 1994, **92**, 189.
- [14] C.Y. Lorber, I. Pauls and J.A. Osborn, *Bull. Soc. Chim. Fr.*, 1996, 133, 755.
- [15] M. Basato, B. Corain, V. Gandolfi, B. Longato and A.C. Veronese, *J. Mol. Catal.*, 1989, **54**, 73.
- [16] M. Basato, R. Callegari, C.F. Morelli and A.C. Veronese, *J. Mol. Catal.*, 1997, **124**, 99; M. Basato, B. Corain, V. Gandolfi and A.C. Veronese, *J. Mol. Catal.*, 1986, **36**, 339.
- [17] M. Basato, B. Corain, V. Gandolfi, C. Talmelli and A.C. Veronese, *J. Mol. Catal.*, 1986, **34**, 195.
- [18] A.M. Jouani, F. Szönyi and A. Cambon, *J. Fluorine Chem.*, 1992, **56**, 85.
- [19] P. Bhattacharyya, D. Gudmunsen, E.G. Hope, R.D.W. Kemmitt, D.R. Paige and A.M. Stuart, *J. Chem. Soc., Perkin Trans. 1*, 1997, **1**, 3609.

- [20] D.E. Bergbreiter, M. Morvant and B. Chen, *Tetrahedron Lett.*, 1991, **32**, 2731.
- [21] A. Endres and G. Maas, *J. Organomet. Chem.*, 2002, **643-644**, 174.
- [22] J.M. Vincent, A. Rabion, V.K. Yachandra and R.H. Fish, *Can. J. Chem.*, 2001, **79**, 888.
- [23] A. Padwa, D.J. Austen, A.T. Price, M.A. Semones, M.P. Doyle, M.N. Protopopova, R. Winchester and A. Tran, *J. Am. Chem. Soc.*, 1993, **115**, 8669.

## Appendix 1 – Crystallographic Data and Structure Refinements

Table 1. Crystallographic data and structure refinement for C<sub>6</sub>F<sub>13</sub>C(CH<sub>3</sub>)OH.

Identification code	2069	
Empirical formula	C <sub>9</sub> H <sub>7</sub> F <sub>13</sub> O	
Formula weight	378.15	
Temperature	200(2) K	
Wavelength	0.71073 Å	
Crystal system	Triclinic	
Space group	P(-)1	
Unit cell dimensions	a = 6.594(3) Å	α = 69.63(5)°.
	b = 15.444(10) Å	β = 84.77(4)°.
	c = 21.429(12) Å	γ = 85.08(5)°.
Volume	2034(2) Å <sup>3</sup>	
Z	6	
Density (calculated)	1.852 Mg/m <sup>3</sup>	
Absorption coefficient	0.239 mm <sup>-1</sup>	
F(000)	1116	
Crystal size	0.70 x 0.24 x 0.18 mm <sup>3</sup>	
Theta range for data collection	2.00 to 25.00°.	
Index ranges	-7 ≤ h ≤ 0, -17 ≤ k ≤ 17, -25 ≤ l ≤ 25	
Reflections collected	7337	
Independent reflections	6943 [R(int) = 0.0379]	
Completeness to theta = 25.00°	96.9 %	
Absorption correction	Psi scan	
Max. and min. transmission	0.99 and 0.83	
Refinement method	Full-matrix least-squares on F <sup>2</sup>	
Data / restraints / parameters	6943 / 0 / 607	
Goodness-of-fit on F <sup>2</sup>	1.354	
Final R indices [I > 2σ(I)]	R1 = 0.1192, wR2 = 0.3396	
R indices (all data)	R1 = 0.1676, wR2 = 0.3852	
Largest diff. peak and hole	1.871 and -0.751 e.Å <sup>-3</sup>	

Table 2. Crystallographic data and structure refinement for [Cu(CF<sub>3</sub>/C<sub>6</sub>F<sub>13</sub>)<sub>2</sub>] (VIa)

Identification code	2013	
Empirical formula	C <sub>20</sub> H <sub>6</sub> F <sub>32</sub> O <sub>6</sub> Cu	
Formula weight	1013.78	
Temperature	150(2) K	
Wavelength	0.71073 Å	
Crystal system	Monoclinic	
Space group	P2(1)/n	
Unit cell dimensions	a = 13.917(7) Å	α = 90°.
	b = 5.375(3) Å	β = 103.704(8)°.
	c = 20.678(11) Å	γ = 90°.
Volume	1502.7(13) Å <sup>3</sup>	
Z	2	
Density (calculated)	2.240 Mg/m <sup>3</sup>	
Absorption coefficient	0.966 mm <sup>-1</sup>	
F(000)	982	
Crystal size	0.32 x 0.09 x 0.08 mm <sup>3</sup>	
Theta range for data collection	1.60 to 25.00°.	
Index ranges	-16 ≤ h ≤ 16, -6 ≤ k ≤ 6, -24 ≤ l ≤ 24	
Reflections collected	7865	
Independent reflections	2651 [R(int) = 0.0674]	
Completeness to theta = 25.00°	99.6 %	
Absorption correction	Empirical	
Max. and min. transmission	0.928 and 0.41	
Refinement method	Full-matrix least-squares on F <sup>2</sup>	
Data / restraints / parameters	2651 / 0 / 277	
Goodness-of-fit on F <sup>2</sup>	1.043	
Final R indices [I > 2σ(I)]	R1 = 0.0594, wR2 = 0.1501	
R indices (all data)	R1 = 0.0807, wR2 = 0.1578	
Largest diff. peak and hole	0.767 and -1.202 e.Å <sup>-3</sup>	

Table 3. Crystallographic data and structure refinement for [Cu(C<sub>6</sub>F<sub>13</sub>/C<sub>6</sub>F<sub>13</sub>)<sub>2</sub>] (VIb)

Identification code	1032	
Empirical formula	C <sub>30</sub> H <sub>6</sub> Cu F <sub>52</sub> O <sub>6</sub>	
Formula weight	1513.89	
Temperature	160(2) K	
Wavelength	0.71073 Å	
Crystal system	Monoclinic	
Space group	P2/c	
Unit cell dimensions	a = 14.6481(10) Å	α = 90°.
	b = 5.5300(4) Å	β =
	c = 28.947(2) Å	γ = 90°.
Volume	2335.5(3) Å <sup>3</sup>	
Z	2	
Density (calculated)	2.153 Mg/m <sup>3</sup>	
Absorption coefficient	0.719 mm <sup>-1</sup>	
F(000)	1462	
Crystal size	0.30 x 0.14 x 0.12 mm <sup>3</sup>	
Theta range for data collection	1.40 to 26.00°.	
Index ranges	-18 ≤ h ≤ 18, -6 ≤ k ≤ 6, -35 ≤ l ≤ 35	
Reflections collected	17270	
Independent reflections	4591 [R(int) = 0.0237]	
Completeness to theta = 26.00°	100.0 %	
Absorption correction	Empirical	
Max. and min. transmission	0.93 and 0.83	
Refinement method	Full-matrix least-squares on F <sup>2</sup>	
Data / restraints / parameters	4591 / 0 / 565	
Goodness-of-fit on F <sup>2</sup>	1.044	
Final R indices [I > 2σ(I)]	R1 = 0.0453, wR2 = 0.1214	
R indices (all data)	R1 = 0.0568, wR2 = 0.1281	
Largest diff. peak and hole	0.697 and -0.357 e.Å <sup>-3</sup>	

Table 4. Crystallographic data and structure refinement for [Cu(PPh<sub>3</sub>)<sub>2</sub>(C<sub>7</sub>F<sub>15</sub>/C<sub>7</sub>F<sub>15</sub>)] (XIIb)

Identification code	2119	
Empirical formula	C <sub>53</sub> H <sub>31</sub> Cu F <sub>30</sub> O <sub>2</sub> P <sub>2</sub>	
Formula weight	1395.26	
Temperature	150(2) K	
Wavelength	0.71073 Å	
Crystal system	Monoclinic	
Space group	C2/c	
Unit cell dimensions	a = 36.7726(17) Å	α = 90°.
	b = 13.2221(5) Å	β =
	93.7290(10)°.	
	c = 22.5317(9) Å	γ = 90°.
Volume	10932.0(8) Å <sup>3</sup>	
Z	8	
Density (calculated)	1.695 Mg/m <sup>3</sup>	
Absorption coefficient	0.603 mm <sup>-1</sup>	
F(000)	5552	
Crystal size	0.32 x 0.29 x 0.15 mm <sup>3</sup>	
Theta range for data collection	1.64 to 25.00°.	
Index ranges	-42 ≤ h ≤ 43, -15 ≤ k ≤ 15, -26 ≤ l ≤ 26	
Reflections collected	38861	
Independent reflections	9618 [R(int) = 0.0284]	
Completeness to theta = 25.00°	99.9 %	
Absorption correction	Empirical	
Max. and min. transmission	0.746 and 0.655	
Refinement method	Full-matrix least-squares on F <sup>2</sup>	
Data / restraints / parameters	9618 / 0 / 862	
Goodness-of-fit on F <sup>2</sup>	1.061	
Final R indices [I > 2σ(I)]	R1 = 0.0515, wR2 = 0.1351	
R indices (all data)	R1 = 0.0619, wR2 = 0.1417	
Largest diff. peak and hole	1.131 and -0.604 e.Å <sup>-3</sup>	

Table 5. Crystal data and structure refinement for  $[\text{Rh}_2(\text{O}_2\text{CCH}_2\text{CH}_2\text{C}_6\text{F}_{13})_4(\text{CH}_3\text{CN})_2]$  (XIVc)

Identification code	2185	
Empirical formula	C40 H22 F52 N2 O8 Rh2	
Formula weight	1852.42	
Temperature	150(2) K	
Wavelength	0.71073 Å	
Crystal system	Triclinic	
Space group	P-1	
Unit cell dimensions	a = 9.7968(6) Å	α =
84.3220(10)°.	b = 12.9856(7) Å	β =
86.4930(10)°.	c = 23.2694(13) Å	γ =
87.9440(10)°.		
Volume	2938.9(3) Å <sup>3</sup>	
Z	2	
Density (calculated)	2.093 Mg/m <sup>3</sup>	
Absorption coefficient	0.778 mm <sup>-1</sup>	
F(000)	1796	
Crystal size	0.33 x 0.33 x 0.14 mm <sup>3</sup>	
Theta range for data collection	1.58 to 26.00°.	
Index ranges	-11 ≤ h ≤ 12, -16 ≤ k ≤ 16, -28 ≤ l ≤ 28	
Reflections collected	22828	
Independent reflections	11365 [R(int) = 0.0423]	
Completeness to theta = 26.00°	98.4 %	
Absorption correction	Empirical	
Max. and min. transmission	0.894 and 0.585	
Refinement method	Full-matrix least-squares on F <sup>2</sup>	
Data / restraints / parameters	11365 / 0 / 939	
Goodness-of-fit on F <sup>2</sup>	1.045	
Final R indices [I > 2σ(I)]	R1 = 0.0473, wR2 = 0.1330	
R indices (all data)	R1 = 0.0532, wR2 = 0.1377	
Largest diff. peak and hole	2.042 and -0.829 e.Å <sup>-3</sup>	

Table 6. Crystal data and structure refinement for [Co(O<sub>2</sub>CC<sub>8</sub>F<sub>17</sub>)<sub>2</sub>(NC<sub>5</sub>H<sub>5</sub>)<sub>4</sub>] (XVb)

Identification code	2161	
Empirical formula	C <sub>38</sub> H <sub>20</sub> Co F <sub>34</sub> N <sub>4</sub> O <sub>4</sub>	
Formula weight	1301.51	
Temperature	150(2) K	
Wavelength	0.71073 Å	
Crystal system	Orthorhombic	
Space group	P2(1)2(1)2(1)	
Unit cell dimensions	a = 10.1410(5) Å	α = 90°.
	b = 14.3325(7) Å	β = 90°.
	c = 32.8490(15) Å	γ = 90°.
Volume	4774.5(4) Å <sup>3</sup>	
Z	4	
Density (calculated)	1.811 Mg/m <sup>3</sup>	
Absorption coefficient	0.538 mm <sup>-1</sup>	
F(000)	2564	
Crystal size	0.33 x 0.16 x 0.09 mm <sup>3</sup>	
Theta range for data collection	2.36 to 25.00°.	
Index ranges	-12 ≤ h ≤ 12, -17 ≤ k ≤ 17, -39 ≤ l ≤ 38	
Reflections collected	34708	
Independent reflections	8350 [R(int) = 0.0615]	
Completeness to theta = 25.00°	99.4 %	
Absorption correction	Empirical	
Max. and min. transmission	0.86 and 0.75	
Refinement method	Full-matrix least-squares on F <sup>2</sup>	
Data / restraints / parameters	8350 / 0 / 556	
Goodness-of-fit on F <sup>2</sup>	1.069	
Final R indices [I > 2σ(I)]	R1 = 0.1286, wR2 = 0.3237	
R indices (all data)	R1 = 0.1682, wR2 = 0.3493	
Absolute structure parameter	0.08(5)	
Largest diff. peak and hole	1.451 and -0.656 e.Å <sup>-3</sup>	

Table 7. Crystal data and structure refinement for  $[\text{Zn}(\text{O}_2\text{CC}_6\text{F}_{13})_2]$  (XVIIa)

Identification code	2135	
Empirical formula	C14 Cl2 F26 K2 O4 Zn	
Formula weight	940.61	
Temperature	150(2) K	
Wavelength	0.71073 Å	
Crystal system	Triclinic	
Space group	P-1	
Unit cell dimensions	a = 10.1732(18) Å	$\alpha = 82.213(3)^\circ$ .
	b = 11.190(2) Å	$\beta = 83.775(3)^\circ$ .
	c = 24.911(4) Å	$\gamma = 89.794(3)^\circ$ .
Volume	2792.9(9) Å <sup>3</sup>	
Z	4	
Density (calculated)	2.237 Mg/m <sup>3</sup>	
Absorption coefficient	1.568 mm <sup>-1</sup>	
F(000)	1808	
Crystal size	0.39 x 0.36 x 0.04 mm <sup>3</sup>	
Theta range for data collection	1.66 to 25.00°.	
Index ranges	-12 ≤ h ≤ 12, -13 ≤ k ≤ 13, -29 ≤ l ≤ 29	
Reflections collected	19535	
Independent reflections	9671 [R(int) = 0.0811]	
Completeness to theta = 25.00°	98.5 %	
Absorption correction	Empirical	
Max. and min. transmission	0.928 and 0.611	
Refinement method	Full-matrix least-squares on F <sup>2</sup>	
Data / restraints / parameters	9671 / 0 / 871	
Goodness-of-fit on F <sup>2</sup>	0.996	
Final R indices [I > 2σ(I)]	R1 = 0.0939, wR2 = 0.2160	
R indices (all data)	R1 = 0.1580, wR2 = 0.2461	
Largest diff. peak and hole	1.810 and -1.195 e.Å <sup>-3</sup>	

## Appendix 2 – ICP Data

### Zn and Ni by ICP Spectroscopy

**Date:** 04-Aug-2003      **Lab 6-102 / Tonbridge**

**Sample originator:**      **B.Croxtall**

**Analyst:** Martin Teasdale

The samples below were submitted for Zn and Ni content.

#### Experimental

This experiment had COSSH assessment GA1. The method in report SM39a (M00167-01) was followed to prepare the samples. A Mettler Toledo balance (AT262 Delta serial no.1116511239) was used to accurately weigh the samples. The samples were acid digested in 3 ml Romil ultra pure nitric acid using a microwave method (ramp to 170C and hold for 12 min) on a Milestone Ethos Plus microwave digestion oven. The solutions was made up with pure Elga water. A Jobin Yvon Ultima spectrometer was used with the following variables:-

Mass /g	0.03	Acid Strength / %	15
Volume / ml	10	Glass or Plastic Flasks	plastic
Dilution	none	ICP Method	HM 19/3/02
Nebuliser Gas/ Bar	3	Original Weights LNB	MT101892-200
Sheath Gas / L min <sup>-1</sup>	0.2	Replicates	1
Nebuliser	cyclone	Data Box	S5383
Standards / ppm	0 ,0.4, 1, 2	Sample flow / ml min <sup>-1</sup>	1.0
Plasma gas / L min <sup>-1</sup>	12	Nitrogen purge/ L min <sup>-1</sup>	3
Power / W	1000	LNB ref	MT101892-009

**Limit of Detection** < 1 ppm in the sample

#### Results (ppm)

Sample	Ni (ug/g)	Zn (ug/g)	Ref
Chloromethane	-	<0.1	A1
Zn salt	-	160	A2
Ni salt	350	-	A3

## **Appendix 3 – Courses, Lectures and Conferences Attended**

### ***Courses***

The following courses have been undertaken as part of the post-graduate studies

CH314 – Bioinorganic Chemistry - Pass

CH414 – Fluorine Chemistry – Pass

CH416 – Metalloenzyme Chemistry – Pass

CH501 – Postgraduate Lecture course:-

NMR Techniques I – NMR Techniques and Interpretation

NMR Techniques II – 2D NMR Techniques

NMR Techniques III - the nOe effect

Chemdraw, Molecular Modelling and Presentation

Beilstein, Crossfire and BIDS

Use of the Library

Endnote

Advanced Scientific Writing

NMR Data Presentation

A Course for Demonstrators

### Lectures Attended

18.10.1999	<i>Literature Session</i>	Dr. E. Raven
25.10.1999	<i>Literature Session</i>	Mr. R. Nasser Mr. A. Davenport
01.11.1999	<i>Coordination Chemistry at Work: Ligand Design For Surface Engineering</i>	Prof. P. Tasker University of Edinburgh
08.11.1999	<i>Polynuclear and Polymeric Architectures in the Group I and Group II Coordination Chemistry of Phenolate Ligands</i>	Dr. J. D. Crane University of Hull
15.11.1999	<i>Polymer Supported Asymmetric Alkene Epoxidation Catalysts</i>	Prof. D. C. Sherrington University of Strathclyde
22.11.1999	<i>Literature Session</i>	Miss C. Ackroyd Mr. C. Davies Mr. T. Reeve
06.12.1999	<i>Literature Session</i>	Mr. D. R. W. Wood
13.12.1999	<i>Study of E. Coli Flavodoxin NADP<sup>+</sup> Reductase</i>	Dr. C. Leadbeater
10.01.2000	<i>Computer-Aided Learning in Chemistry</i>	Dr. S. Walker
17.01.2000	<i>Literature Session</i>	Miss J. Fawcett Mr. L. Lad
24.01.2000	<i>Literature Session</i>	Mr. J. Sherrington
31.01.2000	<i>Literature Session</i>	Mr. M. Hanton Miss N. Patel
07.02.2000	<i>Structural Systematics in Inorganic Chemistry</i>	Prof. A. G. Orpen
14.02.2000	<i>Reactions of R<sub>2</sub>P(E)NHP(E')R'<sub>2</sub> (E, E' = O, S, Se)</i>	Dr. D. J. Birdsall
21.02.2000	<i>Preparative and Mechanistic Studies of Hydrogenation and Transfer Hydrogenation</i>	Dr. S. Lange
28.02.2000	<i>1<sup>st</sup> Year Outlines</i>	Miss N. Patel Mr. M. Hanton Mr. J. Sherrington
06.03.2000	<i>Synthetic Challenges in Polyoxometallate and Metal Alkoxide Chemistry</i>	Dr. R. J. Errington University of Newcastle
13.03.2000	<i>Chalcogen-Nitrogen Chemistry; from the sublime to the ridiculous</i>	Dr. P. Kelly University of Loughborough
20.03.2000	<i>3<sup>rd</sup> Year Project Presentations</i>	Various
03.04.2000	<i>Molecules with Moving Parts: The Race for Molecular Machinery</i>	Prof. D. Leigh University of Warwick
03.04.2000	<i>Porphyrin-Stoppered Rotaxanes as Models of the</i>	Prof. J. P. Sauvage

	<i>Photosynthetic Reaction Centre</i>	Univerité Louis Pasteur
15.05.2000	<i>2<sup>nd</sup> Year Progress</i>	Mr. D. R. W. Wood
22.05.2000	<i>Probing Reaction Mechanisms in Conventional and Supercritical Fluids by Fast and Ultrafast Time-resolved Infrared Spectroscopy: from Organometallic Noble Gas Complexes to CO<sub>2</sub> Activation</i>	Dr. M. George University of Nottingham
05.06.2000	<i>Coordination of Mono and Hybrid Multidentate Phosphine Ligands in Platinum Group Metals</i>	Mr. R. Nassar
19.06.2000	<i>Catalytic Mechanism of Ascorbate Peroxidase</i>	Mr. L. Lad
26.06.2000	<i>Synthesis of Transition Metal Half Sandwich Complexes of Oxazolines / Imidazolines and their Applications in Asymmetric Catalysis</i>	Mr. A. Davenport
16.10.2000	<i>Literature Session</i>	Dr. G. Solan Dr. P. W. Dyer
23.10.2000	<i>Literature Session</i>	Ms. N. Patel Mr. M. Hanton
13.11.2000	<i>Literature Session</i>	Mr. T. Woodcock Mr. S. Hilton
20.11.2000	<i>One Armed Bandits: Studying the Effects of Functionalising Classical Ligands in Coordination and Organometallic Chemistry</i>	Dr. P. C. McGowan University of Leeds
27.11.2000	<i>Ligand Field Theory in the New Millennium: Is there Life After Density Functional Theory?</i>	Dr. R. Deeth University of Warwick
11.12.2000	<i>Anions as Templating Agents in Coordination Chemistry</i>	Dr R. Villar-Compte Imperial College
22.01.2001	<i>Literature Session</i>	Mr. C. Davies Mr. J. Sherrington Mr. T. Reeve
29.01.2001	<i>If You Can See It It's Not The Catalyst – Or Is It? NMR Techniques For Monitoring Catalytic Reactions</i>	Dr. J. Iggo University of Liverpool
05.02.2001	<i>Inverse Crown Ether Complexes and Related Mixed-Metal Macrocycles of the s-Block</i>	Prof. R. E. Mulvey University of Strathclyde
12.02.2001	<i>Literature Session</i>	Mr. A. West Miss R. Chaggar Mr. R. Chester
19.02.2001	<i>Developing New Routes for Quantum Dot Synthesis</i>	Prof. P. O'Brien University of Manchester

26.02.2001	<i>1<sup>st</sup> Year Outlines</i>	Mr. C. Davies Ms. S. Kandola Mr. T. Reeve Mr. S. Suhard
05.03.2001	<i>Tinkering With Proteins: The How's and Whys</i>	Dr. M. Mewies University of Leicester
12.03.2001		Dr. M. Willis University of Bath
19.03.2001	<i>3<sup>rd</sup> Year B.Sc. Project Presentations</i>	Various
21.03.2001	<i>1<sup>st</sup> Tim Norwood Memorial Lecture – Magnetic Resonance at the Interface Between Chemistry and Medicine</i>	Prof. L. D. Hall University of Cambridge
26.03.2001	<i>Literature Session</i>	Mr. B. Croxtall Mr. D. Wood Mr. S. Suhard
14.05.2001	<i>Zirconacycles in Phosphine Synthesis: Coordination Chemistry and Applications in Platinum Group-catalysed Carboxylation of Olefins and Ethylene Polymerisation</i>	Dr. S. Doherty <i>Queen's University Belfast</i>
04.06.2001	<i>Literature Session</i>	Ms. S. Kandola Mr. T. Reeve
11.06.2001	<i>2<sup>nd</sup> Year Talks</i>	Mr. B. Croxtall Mr. M. Hanton
18.06.2001	<i>2<sup>nd</sup> Year Talks</i>	Ms. N. Patel Mr. J. Sherrington
25.06.2001	<i>3<sup>rd</sup> Year Talk</i>	Mr. D. R. W. Wood
01.10.2001	<i>Enabling Technologies for Biology and Medicine Arising From Endeavours in Total Synthesis</i>	Prof. K. C. Nicolaou <i>Scripps Research Institute</i>
04.10.2001	<i>Basic Instinct: New Synthetic Adventures with Chiral Bases</i>	Dr. P. O'Brien <i>University of York</i>
10.10.2001	<i>Stable Carbenes and Diradicals: New Stabilisation and Bonding Modes</i>	Dr. D. Bourrison <i>Université Paul Sabatier, Toulouse, France</i>
15.10.2001	<i>Introductory Session</i>	Dr. P. Dyer <i>University of Leicester</i>
22.10.2001	<i>Sex and Bugs and Rock 'N' Roll</i>	Dr. A. Hooper <i>Institute of Arable Crops Research, Rothamstead</i>

29.10.2001	<i>Literature Session</i>	Ms. N. Patel Mr. M. Hanton
05.11.2001	<i>Literature Session</i>	Mr. P. Griffith Mr. D. Harding
14.11.2001	<i>Designing Catalysts for Polymer Synthesis</i> <i>RSC Joseph Chatt Lecture</i>	Prof. V.C. Gibson <i>Imperial College</i>
26.11.2001	<i>Literature Session</i>	Mr. G. Barth Mr. M. Dix
03.12.2001	<i>Organometallic Synthesis, Catalysis and Green</i> <i>Chemistry Research in Leicester</i>	Dr. G. Solan Dr. P. Dyer <i>University of Leicester</i>
10.12.2001	<i>The Electronic Structure of the Active Sites of</i> <i>Molybdoenzymes</i>	Dr. J. McMaster <i>University of Nottingham</i>
21.01.2002	<i>Literature Session</i>	Mr. C. Davies Mr. J. Sherrington Mr. T. Reeve
28.01.2002	<i>The Application of Very Low Temperature</i> <i>Crystallography to Chemical Problems</i>	Prof. J. Howard <i>University of Durham</i>
04.02.2002	<i>1<sup>st</sup> Year Outlines</i>	Miss A. Hickman Miss K. Sharpe Mr. J. Pelletier
11.02.2002	<i>High Activity Catalysts for C-C Bond Formation</i>	Dr. R. Bedford <i>University of Exeter</i>
18.02.2002	<i>1<sup>st</sup> Year Outlines</i>	Mr. A. West Miss R. Chaggar Mr. O. Duaij
25.02.2002	<i>The New World of Phospha-Organometallic</i> <i>Chemistry</i>	Prof. J. Nixon <i>University of Sussex</i>
04.03.2002	<i>Compounds with Novel Boron-containing</i> <i>Ligands: Transition Metal Complexes of Boron</i> <i>and [1]Bora-metallocenophanes</i>	Dr. H. Braunschweig <i>Imperial College</i>
11.03.2002	<i>Literature Session</i>	Mr. S. Suhard Miss S. Kandola
18.03.2002	<i>Inorganic Chemistry Research at Leicester</i>	Dr. D. Davies Dr. E. Raven <i>University of Leicester</i>
29.04.2002	<i>Literature Session</i>	Mr. A. West Mr. J. Pelletier Miss A. Hickman

08.05.2002 *Ferrocene Ligand Design*

Dr. N. Long

*Imperial College*

27.05.2002 *3<sup>rd</sup> Year Talk*

Mr. M. Hanton

*University of Leicester*

10.06.2002 *3<sup>rd</sup> Year Talk*

Miss N. Patel

*University of Leicester*

17.06.2002 *3<sup>rd</sup> Year Talk*

Mr. J. Sherrington

## Conferences Attended and Presentations

“Synthesis and Catalysis Symposium” – University of Sheffield

“Inorganic Chemistry at the Heart of England” – University of Wolverhampton – 07.04.00

**Poster** – Perfluoroalkyl-Derivatised  $\beta$ -diketonate Ligands; Synthesis and Coordination Chemistry.

B. Croxtall, E. G. Hope, A. M. Stuart.

“Green Chemistry Symposium” – University of Leicester – 24.05.00

“International Fluorine Conference” – University of Durham – 16.07.00 – 21.07.00

**Poster** – Perfluoroalkyl-Derivatised  $\beta$ -diketonate Ligands; Synthesis and Coordination Chemistry.

B. Croxtall, E. G. Hope, A. M. Stuart. (Updated)

**Poster** – Ortho-Perfluoroalkyl Substituted Triarylphosphine Ligands; Synthesis and Coordination Chemistry. B. Croxtall, E. G. Hope, A. M. Stuart.

“RSC Annual Conference 2001” Birmingham I.C.C. 30.07.01 – 02.08.01.

**Talk:-** “Perfluoroalkyl-derivatised beta-diketonate ligands; synthesis, coordination chemistry and catalysis” B. Croxtall, E.G. Hope and A.M. Stuart.

“RSC Fluorine Subject Group Postgraduate Meeting” – University of Leicester - 05.09.2001.

“Fluorine in Organic Chemistry” – SCI, London – 08.11.01.

“A Symposium for Final Year CASE Students” – GlaxoSmithkline, Tunbridge Wells - 04.09.02.

**Talk:-**“The Synthesis, Coordination Chemistry and Catalysis of Perfluoroalkyl-Derivatised beta-Diketonate Ligands” B. Croxtall, E.G. Hope and A.M. Stuart.